# Molecular and Cellular Aspects of the SREBP Pathway

A thesis submitted to the National University of Ireland, Cork, in fulfilment of the requirements for the degree of

**Doctor of Philosophy**

by

**Katherine Barriscale, BSc.**


**School of Biochemistry and Cell Biology,**
**University College Cork**

**April 2014**

**Supervisor: Professor Tommie V. McCarthy**

**Head of Department: Professor David Sheehan**

**Acknowledgements**

Firstly, I must thank my supervisor Professor Tommie McCarthy, for sharing his knowledge and wisdom of the sciences with me, and for his dedicated supervision and patience over the past four years. I could not have asked for a better supervisor.

My fellow lab members and friends, Steph, Sharon, Kai and Michael, thank you for bringing normality to the crazy days full of science related "plot twists" and always helping me to see a bright side to a negative result. I am also grateful to the many others who have shared their know-how with me and helped me along my PhD journey; Noreen, Pat, Jenny and Trish; members of the Atkins/Baranov labs; and also Dr. Emilie Tresse and Dr. Pat Kiely for providing the peptide arrays and sharing their insight on protein-protein interactions.

I am grateful to the PhD Scholars Programme in Cancer Biology and the Health Research Board for giving me the opportunity to pursue and expand my interest, knowledge and expertise in the biological sciences and to explore and develop my passion for research. I am also grateful to Dr. Kellie Dean, my thesis committee members Professor Rosemary O' Connor and Dr. Orla Barry, and the external examiners Professor Gerard Evan, Dr. Helke Hillebrand, Professor Donald McDonnell and Professor Kevin Sullivan, all of whom took the time to share their knowledge and offer guidance and direction throughout the course of my PhD.

I want to thank my friends Lorna, Katy, Carol and Ruth for always being there and reminding me of a world outside of my research. Dr. Kerry, we navigated our way through the PhD experience together. I must not forget to thank Keenan, a dear family friend. You told us that from a very young age you believed we would do well academically; I hope that in some way I have lived up to this expectation.

Most of all I must thank my family. Mum and Dad, thank you for the love, support and guidance that only parents can provide, and thank you for always asking how things were going and never looking disinterested when I gave a ten minute reply. Nicole, you are the best big sister a girl could ask for and I always knew that you were only a phone call away to bring support and laughter, as well as constant assurance that I would get there in the end. Sara, I am so proud of everything that *you* have achieved over the last four years, you have grown so much. Thank you all for just being you.

I must also thank the new family I gained during my PhD, who I will collectively and affectionately refer to as "The Walshs". Not to forget Mr B. Tholamew and Ms L. Spy. I finally want to thank my husband, Christopher. Although I am delighted to never have to hear the words "how's the thesis going" again, I must thank you for listening to my incessant scientific ramblings at the end of each day and for refusing to let me panic as the end was drawing near. You are my rock, my best friend and my love. You inspire me to be the best that I can be and I truly could not have done this without you.

*To Mary and Gerard Barriscale, forever in my heart*

# Table of Contents

# Declaration

This thesis has not been submitted in whole or in part to this or any other university for any degree and is, unless otherwise stated, the original work of the author.

Signed: _____

Katherine Barriscale

# Abstract

The SREBP (sterol response element binding proteins) transcription factors are central to regulating *de novo* biosynthesis of cholesterol and fatty acids. The SREBPs are regulated by retention or escape from the ER to the Golgi where they are proteolytically cleaved into active forms. The SREBP cleavage activating protein (SCAP) and the INSIG proteins are essential in this regulatory process. The aim of this thesis is to further characterise the molecular and cellular aspects surrounding regulation of SREBP processing.

SREBP and SCAP are known to interact via their carboxy-terminal regulatory domains (CTDs) but this interaction is poorly characterised. Significant steps were achieved in this thesis towards specific mapping of the interaction site. These included cloning and over expression and partial purification of tagged SREBP1 and SREBP2 CTDs and probing of a SCAP peptide array with the CTDs. Results from the SREBP2 probing were difficult to interpret due to insolubility issues with the protein, however, probing with SREBP1 revealed five potential binding sites which were detected reproducibly. Further research is necessary to overcome SREBP2 insolubility issues and to confirm the identified SREBP1 interaction site(s) on SCAP.

INSIG1 has a central role in regulating SREBP processing and in regulating stability of 3-hydroxy-3-methylglutaryl coenzyme A reductase (HMGCR), a rate limiting enzyme in cholesterol biosynthesis. There are two protein isoforms of human INSIG1 produced through the use of two in-frame alternative start sites. Bioinformatic analysis indicated that the presence of two in-frame start sites within

the 5-prime region of INSIG1 mRNA is highly conserved and that production of two isoforms of INSIG1is likely a conserved event. Functional differences between these two isoforms were explored. No difference in either the regulation of SREBP processing or HMGCR degradation between the INSIG1 isoforms was observed and the functional significance of the two isoforms is as yet unclear.

The final part of this thesis focused on enhancing the cytotoxicity of statins by targeted inhibition of SREBP processing by oxysterols. Statins have significant potential as anti-cancer agents as they inhibit the activity of HMGCR leading to a deficiency in mevalonate which is essential for cell survival. The levels of HMGCR fluctuate widely due to cholesterol feedback of SREBP processing. The relationship between sterol feedback and statin mediated cell death was investigated in depth in HeLa cells. Down regulation of SREBP processing by sterols significantly enhanced the efficacy of statin mediated cell death. Investigation of sterol feedback in additional cancer cell lines showed that sterol feedback was absent in cell lines A-498, DU-145, MCF-7 and MeWo but was present in cell lines HT-29, HepG2 and KYSE-70. In the latter inhibition of SREBP processing using oxysterols significantly enhanced statin cytotoxicity. The results indicate that this approach is valid to enhance statin cytotoxicity in cancer cells, but may be limited by deregulation of SREBP processing and off target effects of statins, which were observed for some of the cancer cell lines screened.

# Abbreviations

| | |
|---|---|
| 19-OHC | 19-hydroxycholesterol |
| 25-OHC | 25-hydroxycholesterol |
| AML | Acute myeloid leukaemia |
| ANOVA | Analysis of variance |
| Apaf1 | Apoptotic protease activating factor 1 |
| AR | Androgen receptor |
| BLAST | Basic local alignment search tool |
| BSA | Bovine serum albumin |
| cDNA | Complementary DNA |
| CHAPS | 3-[(3-Cholamidopropyl)dimethylammonio]-1- propanesulfonate |
| CKI | Cyclin-dependent kinase inhibitors |
| CMV | Cytomegalovirus |
| CTD | Carboxy-terminal domain |
| DLR | Dual luciferase reporter |
| DMSO | Dimethyl sulfoxide |
| DNA | Deoxyribonucleic acid |
| DTT | Dithiothreitol |
| ECL | Enhanced chemiluminescence |
| ED50 | Effective dose to reduce cell viability to 50% |
| EDTA | Ethylenediaminetetraacetic acid |
| eIFs | Eukaryotic initiation factors |
| ER | Endoplasmic reticulum |
| EtOH | Ethanol |
| EV | Empty vector |
| FACS | Fluorescence assisted cell sorting |

| | |
|---|---|
| FASN | Fatty acid synthase |
| FBS | Foetal bovine serum |
| FF | Firefly luciferase |
| FPLC | Fast protein liquid chromatography |
| FS | Media containing FBS |
| G-418 | Geneticin |
| GFP | Green fluorescent protein |
| GLuc | Gaussia luciferase |
| GLuc | Gaussia luciferase |
| GST | Glutathione-S-transferase |
| HA | Haemaglutenin |
| HeLa-PHGL | HeLa promoter HMGCR gaussia luciferase (stable cell line) |
| His | Histidine |
| HMGCR | 3-hydroxy-3-methylglutaryl-Coenzyme A reductase receptor |
| HRP | Horseradish peroxidase |
| IBs | Inclusion bodies |
| INSIG1 | Insulin induced gene 1 |
| IPTG | Isopropyl β-D-1-thiogalactopyranoside |
| IR | Infrared |
| kDa | Kilo-daltons |
| LB | Luria broth |
| LDLR | Low density lipoprotein receptor |
| LDS | Lipid depleted serum |
| MEGA | Molecular evolutionary genetics analysis |
| MELADL | Hexapeptide sequence in SCAP (methionine-glutamic acid-leucine-alanine-aspartic acid-leucine) |
| mRNA | Messenger RNA |

| | |
|---|---|
| MTT | 3-(4,5-dimethylthiazol-2-yl)-2,5-diphenyltetrazolium bromide |
| MβCD | Methyl-β-cyclodextrin |
| NADPH | Nicotinamide adenine dinucleotide phosphate |
| NCBI | National Centre of Bioinformatics |
| NF-Y | Nuclear factor Y |
| NP-40 | Nonyl phenoxypolyethoxylethanol |
| nSREBP | N-terminal (amino-terminal) of SREBP |
| NTD | Amino terminal domain |
| O.D. | Optical density |
| P/S | Penicillin/Streptomycin |
| P4 | Progesterone |
| P450 | Cytochrome P450 |
| PAGE | Polyacrylamide gel electrophoresis |
| PAIR-BP | Plasminogen activator inhibitor 1 RNA binding protein |
| PBS | Phosphate buffered saline |
| PCR | Polymerase chain reaction |
| PGRMC1 | Progesterone receptor membrane component 1 |
| PI | Propidium iodide |
| PM | Plasma membrane |
| PMSF | Phenylmethylsulfonyl fluoride |
| PPAR | Peroxisome proliferator-activated receptor |
| PR | Progesterone receptor |
| PUFA | Poly unsaturated fatty acid |
| RACK1 | Receptor for Activated C Kinase 1 |
| RIPA | Radio immunoprecipitation Assay |
| RL | Renilla luciferase |
| RNA | Ribonucleic acid |

| | |
|---|---|
| RT | Room temperature |
| SCAP | SREBP cleavage activating protein |
| SD | Standard deviation |
| SDM | Site-directed mutagenesis |
| SDS | Sodium dodecyl sulphate |
| SIGCs | Spontaneously immortalised granulosa cells |
| SMART | Simple Modular Architecture Research Tool |
| Sp1 | Ubiquitous transcription factor |
| SRE | Sterol response element |
| SREBP | Sterol regulatory element binding protein |
| SSLR | Single secreted luciferase reporter |
| SV4 | Simian virus 40 |
| TBS | Tris buffered saline |
| Tcf/Lef | T-cell factor-1/ lymphoid enhancing factor-1 |
| TF | Transcription factor |
| TK | Thymidine kinase |
| TM | Transmembrane |
| WD40 | Tryptophan Aspartate 40 |
| WT | Wild type |

# Chapter 1
General Introduction

***Cholesterol***

Cholesterol is a vital component within the cell. Membrane lipid rafts contain high concentrations of cholesterol and are required to maintain membrane structure and fluidity (Ikonen 2008). Lipid rafts also function as an anchor for glycosylphosphatidylinisotol (GPI)-modified signalling molecules, as well as being sites for protein endocytosis (Simons & Toomre 2000; Simons & Ikonen 2000). Membranes deplete of cholesterol can display defective membrane receptor trafficking through inability of clathrin to induce membrane curvature (Rodal et al. 1999; Subtil et al. 1999). Cholesterol is also a precursor molecule for oxysterols and bile acids which have signalling roles within the cell through LXRs and FXRs, respectively. LXR signalling reduces cholesterol absorption and promotes cholesterol excretion and conversion to bile acids, to prevent cholesterol build-up within the cell (Wójcicka et al. 2007). FXR signalling plays a role in the feed-back regulation of bile acid synthesis to increase conjugation and excretion of bile acids, also to prevent toxicity (Thomas et al. 2008). Cholesterol availability is also a determinant for pregnenolone synthesis which the precursor for natural steroid hormones which are indispensible in the body (Miller 1988).

Cholesterol also plays an important role in the proliferation and survival both normal and cancer cells (Gorin et al. 2012). In addition to being essential for new daughter cell membrane formation, cholesterol is also tightly linked to the cell cycle (P. Singh et al. 2013). Blockade of cholesterol biosynthesis revealed its requirement for G1 to S phase transition (Jakóbisiak et al. 1991). Cancer cells have also reported to have elevated membrane cholesterol content (Hager et al. 2006a; Gorin et al. 2012; Siperstein 1972). This has been shown to elicit a chemo-protective effect in *in vitro*

cancer studies, although the underlying mechanisms of this protective effect are not well understood (Banker et al. 2004; Li et al. 2006). Increased membrane cholesterol levels have been correlated with mediating survival in breast, prostate, liver and colorectal cancer cell lines, and depletion of cholesterol has been shown to enhance cancer cell sensitivity to apoptosis (Li et al. 2006; Hager et al. 2006a; Calleros et al. 2009). Akt survival signalling is dependent on its localisation to lipid rafts (Zhuang et al. 2002). It is proposed that cholesterol depletion disrupts lipid raft organisation and this causes Akt inactivation with a subsequent decrease in anti-apoptotic gene expression and the absence of Akt-mediated inhibitory phosphorylation on pro-apoptotic proteins (Zhuang et al. 2005).

A major source of cholesterol is through dietary uptake. Cholesterol-rich foods include meat, eggs and dairy (O Brien et al. 2000). Intestinal cholesterol absorption is facilitated by cholesterol forming mixed miscelles with bile salts, as cholesterol is a relatively insoluble molecule (Wilson & Rudel 1994). Cholesterol then requires cellular uptake, which is mediated by Niemann–Pick C1-Like 1 (NPC1L1) (Altmann et al. 2004). NPC1L1 is a polytopic transmembrane protein which contains a sterol-sensing domain homologous to that present in HMGCR and SCAP (Yu 2008). It is highly expressed in enterocytes and NPC1L1 null mice have highly impaired intestinal cholesterol absorption (Davis et al. 2004). NPC1L1 primarily resides in the endocytic recycling compartment (ERC) but under cholesterol-deplete conditions, NPC1L1 is relocated from ERC to PM where it binds cholesterol through its sterol sensing domain (Altmann et al. 2004). This cholesterol-bound NPC1L1 protein is then internalised via vesicular endocytosis, for which lipid raft localised flotillins have been shown to be essential (Ge et al. 2011). Internalised cholesterol is then utilised within the cell, distributed throughout the body or excreted in bile. NPC1L1

is closely related to NPC1, which is also involved in cholesterol transport, although it is located in the late endosome/lysosomal membranes and plays a role in transport of low-density lipoprotein (LDL)-derived cholesterol (Wang & Song 2012). Serum cholesterol is transported in esterified form complexed with LDL (Liscum & Munn 1999). LDL-cholesterol is bound by specific LDL-receptors and internalised via endocytosis (Simons & Ikonen 2000). Cholesterol esters are then released from LDL by hydrolysis within the lysosomal compartments and distributed to cellular membranes, facilitated by NPC1 (Liscum 2000). Cholesterol can also be synthesised *de novo* within the cell via a multi-enzymatic process, the expression of the enzymes involved is regulated by the sterol-response element binding protein 2 (SREBP-2) (Sakakura et al. 2001; Horton et al. 1998) (Figure 1.1).

### *The Sterol Response Element Binding Protein (SREBP) Pathway*

Both biosynthesis and uptake of lipid and cholesterol are highly regulated processes, a regulation which is necessary to maintain the balance required for viability and to prevent toxicity. A main point of regulation for the proteins involved is at the transcriptional level. Expression of genes within these pathways are maintained by the actions of ubiquitous transcription factors such as SP-1 and NF-Y, but expression also has the capacity to be enhanced through the action of a family of transcription factors; the Sterol Response Element Binding Proteins (SREBPs) (Amemiya-kudo et al. 2002).

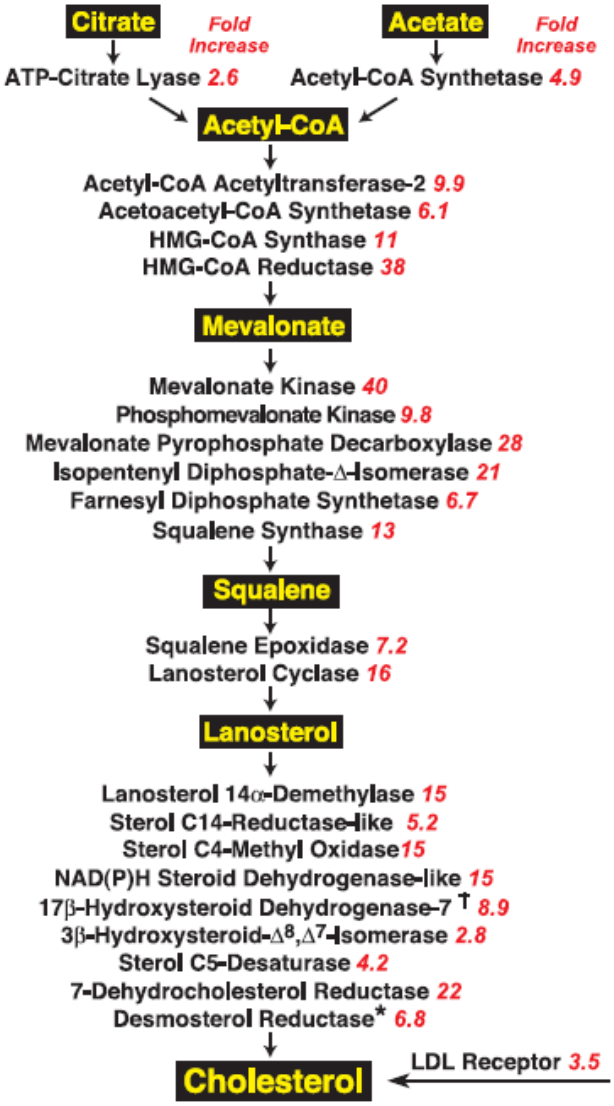


Figure 1.1. SREBP-2 mediated activation of the entire pathway for cholesterol synthesis in mammalian cells. Key biosynthetic intermediates are highlighted in yellow. Red italics denote the fold increase in mRNA levels for each enzyme in TgSREBP-2 liver. Each value is the average of the two microarray hybridizations listed in Tables 1 and 3. *****, Desmosterol reductase was not represented on the microarray. The fold-increase value is from real-time PCR. †, 17_-Hydroxysteroid dehydrogenase-7 has not been confirmed as a cholesterol biosynthetic enzyme (Horton et al. 2003).

The SREBPs were first discovered in 1993 in the laboratory of Michael Brown and Joseph Goldstein and were found to bind to inverted E-box motifs referred to as SRE elements within the promoter regions of such genes (Hua et al. 1993a; Wang et al. 1994). There are three main isoforms of SREBPs which differ in their affinity for variations of this SRE motif, although there are more than 3 SRE elements recognised and there is some cross-over in transcriptional activation capabilities (Edwards et al. 2000). All SREBP transcription factor domains are basic-helix-loop-helix leucine zipper motifs (Figure 1.2). SREBP 1a and SREBP 1c are two proteins produced from the same gene located on chromosome 17p11.2 through use of independent transcriptional start sites (Yokoyama et al. 1993). As a result, SREBP 1a and SREBP 1c are encoded by different first exons and the result is a 1c transcription factor which is a weaker activator than 1a (Shimano, Horton, et al. 1997). This weaker activation capacity is owing to its shorter trans-activation domain. SREBP2 is encoded on chromosome 22q13 (Hua et al. 1995). SREBP1c preferentially regulates genes involved in fatty acid biosynthesis, SREBP2 preferentially regulates genes involved in cholesterol biosynthesis while SREBP1a is believed to have crossover between both areas (Amemiya-kudo et al. 2002). This is highlighted in nSREBP transgenic and knockout animal studies (Table 1.1). Overall, the human SREBPs share 71% identity in their transcription factor domains, and this is reflected in homologous mammalian SREBP proteins. More recent studies are revealing roles for SREBP/SREs outside of the lipogenic pathways. Microarray analyses in a human skeletal muscle cell model over-expressing SREBP1 has revealed roles for the SREBPs in mitochondrial metabolism, the immune response, carbohydrate metabolism and hypoxia, in addition to the lipogenic pathways (Rome et al. 2008).

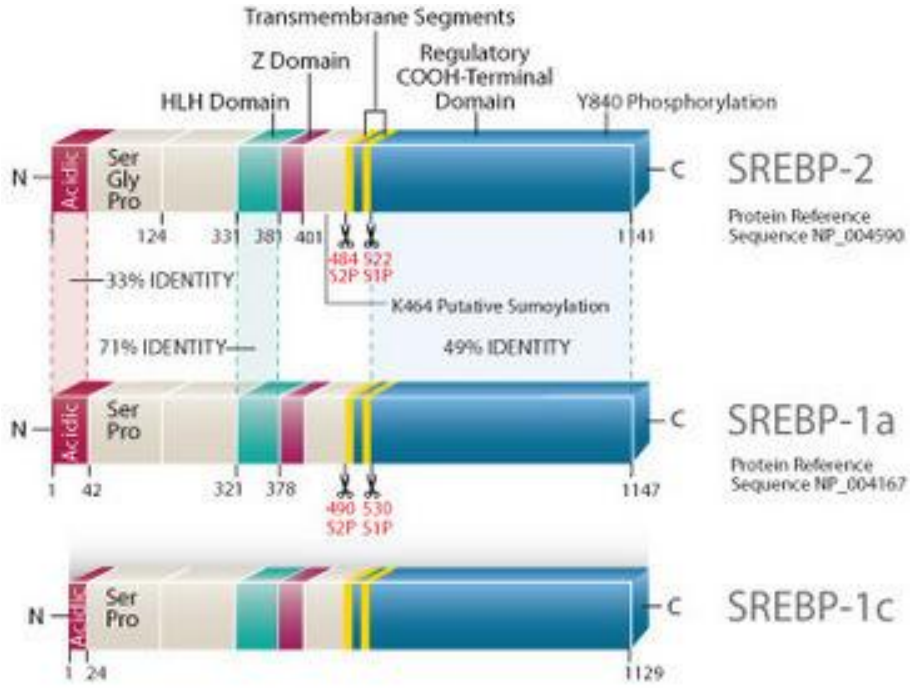


Figure 1.2. Domains and identity of the SREBP isoforms (May 2008), modified from (Hua et al. 1993b); Domain structure of SREBP-2 and -la with numbers corresponding to the amino acid residues (5). The bHLH region is denoted by the green box, the leucine zipper region by the purple box, and the COOH-terminal domain by the blue box. Regions rich in particular amino acids are indicated. The percent identities in the three most homologous regions are indicated.

**Table 1**
Alterations in hepatic lipid metabolism in gene-manipulated mice overexpressing or lacking SREBPs

| Genetic manipulation | Amount of nSREBPs | Expression of target genes | | | Lipid synthesis | | Liver content | | Plasma levels | |
|---|---|---|---|---|---|---|---|---|---|---|
| | | HMGR | FAS | LDLR | Chol | FA | Chol | TG | Chol | TG |
| | | Fold difference relative to values in wild-type mice | | | | | | | | |
| **Transgenic mice** | | | | | | | | | | |
| SREBP-1a (9, 11) | ↑1a | ↑37 | ↑20 | ↑6 | ↑5 | ↑26 | ↑6 | ↑22 | ↓0.7 | ↓0.4 |
| SREBP-1c (10, 11) | ↑1c | n.c. | ↑4 | n.c. | n.c. | ↑4 | n.c. | ↑4 | n.c. | ↓0.6 |
| SREBP-2 (11) | ↑2 | ↑75 | ↑15 | ↑6 | ↑28 | ↑4 | ↑3 | ↑4 | n.c. | ↓0.5 |
| SCAP (D443N) (12) | ↑1a, ↑1c, ↑2 | ↑18 | ↑11 | ↑2 | ↑5 | ↑7 | ↑6 | ↑9 | ↓0.5 | ↓0.5 |
| **Liver-specific knockout mice** | | | | | | | | | | |
| SCAP (14) | ↓1a, ↓1c, ↓2 | ↓0.1 | ↓0.1 | ↓0.3 | ↓0.3 | ↓0.2 | ↓0.8 | ↓0.4 | ↓0.8 | ↓0.4 |
| S1P (15) | ↓1a, ↓1c, ↓2 | ↓0.6 | ↓0.3 | ↓0.5 | ↓0.3 | ↓0.3 | n.c. | ↓0.5 | ↓0.6 | ↓0.6 |
| **Germline knockout mice** | | | | | | | | | | |
| SREBP-1a & 1c (13) | ↓1a, ↓1c, ↑2 | ↑2.2 | ↓0.7 | ↑1.3 | ↑3 | ↓0.6 | ↑1.5 | n.c | ↓0.7 | ↓0.7 |
| SREBP-1c (16) | ↓1a, ↓1c, ↑2 | ↑1.3 | ↓0.3 | n.c | ↑3 | ↓0.5 | ↑1.2 | n.c | ↓0.8 | ↓0.4 |
| SREBP-2 (13) | Embryonic lethal | – | – | – | – | – | – | – | – | – |
| S1P (15, 17) | Embryonic lethal | – | – | – | – | – | – | – | – | – |

HMGR, HMG-CoA reductase; FAS, fatty acid synthase; LDLR, LDL receptor; Chol, cholesterol; TG, triglycerides; n.c., no change.

Table 1.1 (Horton et al. 2002a)

The SREBPs differ from most other transcription factors in that they are synthesised as inactive precursor proteins located in the endoplasmic reticulum (ER) (Hua et al. 1993a; Hoppe et al. 2001). The SREBPs share a common protein structure composed of the transcription factor domain at the amino terminus (NTD), a central transmembrane (TM) loop, and a large regulatory domain at the carboxy terminus (CTD) (Sato et al. 1994). From the moment of their synthesis, SREBPs are bound by the SREBP Cleavage Activating Protein (SCAP), and in the absence of SCAP, SREBP proteins are rapidly degraded (Sakai et al. 1997). The gene encoding SCAP is localised to chromosome 3p21.3 and this encodes a multipass ER-resident transmembrane protein with 8 TM regions and a large CTD (Nakajima et al. 1999a). SCAP contains a multipass transmembrane region which in which TM2-7 has been identified as a sterol-sensing domain (SSD) (Radhakrishnan et al. 2004) (Figure 1.3). The interaction between SCAP and SREBP has been localised to their respective CTDs, which each are sufficient to immunoprecipitate the corresponding full-length interacting protein (Sakai et al. 1997). The CTD of SCAP contains WD40 repeat motifs which are believed to mediate its interaction with SREBP (Hua et al. 1996). WD40 domain proteins are known to facilitate binding of multiple interacting proteins. For example, RACK1 contains 7 WD40 repeats, forms a beta-propeller structure and influences a variety of cellular signalling cascades through interaction with a variety of protein partners (Adams, Ron & P. a Kiely 2011). To date, the SREBPs are the only proteins reported to interact with the WD domain of SCAP. Interestingly, progesterone receptor membrane component 1 (PGRMC1) was identified as interacting with SCAP directly (Suchanek et al. 2005). It would be interesting to see if this interaction is also mediated by the WD domain of SCAP.

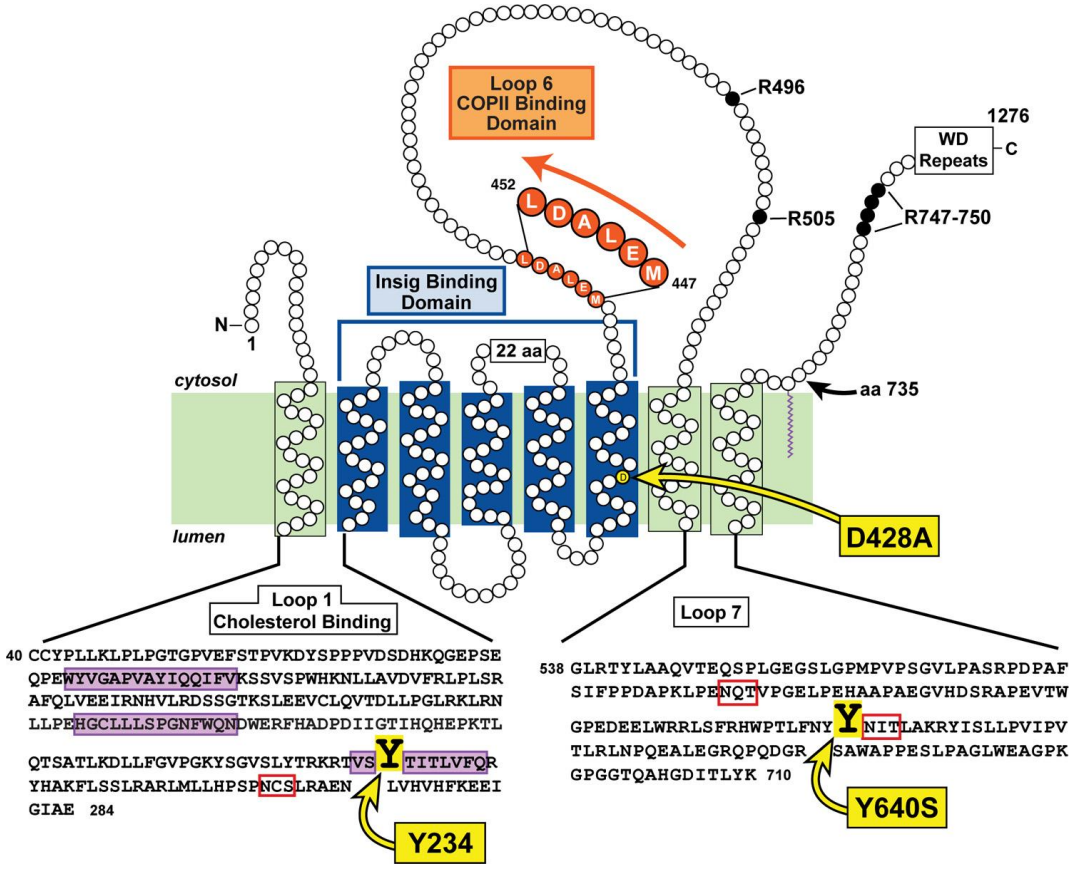


Figure 1.3. **Topology model of the membrane domain of hamster SCAP, showing its three functional domains and the sites of three point mutations (Y234A, D428A, and Y640S) that confer a constitutive cholesterol-bound conformation, even in the absence of sterols.** Amino acids (*aa*) 40–284 correspond to the sequence of luminal Loop 1, the cholesterol-binding domain of Scap. The three hydrophobic patches in the Loop 1 sequence are *shaded in purple*, and the *N*-linked glycosylation site is denoted by the *red box*. The Insig-binding domain is localized to transmembrane helices 2–6, shown by the *blue bracket*. The COPII-binding site is localized to the MELADL sequence in Loop 6, *shaded in orange*. Amino acids 538–710 correspond to the sequence of luminal Loop 7; its two*N*-linked glycosylation sites are denoted by the *red boxes*. In membranes from sterol-deprived cells, trypsin cleaves Scap on itsNH2-terminal side at Arg-496; in sterol-replete membranes, trypsin cleaves at Arg-503/Arg-505. The trypsin-cleavage site on the COOH-terminal side of Scap in both the absence and the presence of sterols occurs within a cluster of arginines (Arg-747–Arg-750). (Y. Zhang et al. 2013)

WD40 motifs follow a loose consensus sequence of $X_{6–94}$-[GH-$X_{23–41}$-WD]$N_{4–8}$ (where N is the number of repeats) (Neer et al. 1994). Each motif folds in a beta-sheet conformation such that the repeats come together to form a propeller-like structure, with each blade of the propeller comprising of strand A-C of one repeat, and strand D of the next repeat (Smith et al. 1999). Strand D is believed to be the most accessible region of each WD40 repeat. This propeller-like structure then acts as a platform in mediating protein-protein interactions. To date, all proteins containing WD40 repeats which have had their crystal structures solved indeed show this to be the case (Renault et al. 1998; Voegtli et al. 2003; Cheng et al. 2004; Adams, Ron & P. a Kiely 2011). However, although the consensus sequence says four to eight repeats can be present, all WD40 proteins that have crystal structures solved have seven to eight repeats forming the propeller, with the optimal beta propeller fold described as a seven bladed structure (Smith 2008).

As well as being essential for stability of the SREBPs, the CTD interaction with SCAP is also required to mediate the transport of the SREBP precursor proteins to the Golgi where a 2-step proteolytic cleavage event results in release of the active transcription factor domain (L.-P. Sun et al. 2007; Duncan et al. 1997a; Duncan et al. 1998). Compartmentalisation of the precursor protein within the ER and the proteases in the Golgi is the only thing preventing unregulated activation of SREBP (DeBose-Boyd et al. 1999). Thus, SCAP-mediated transportation from the ER to the Golgi is the key step for SREBP activation. This transportation event is a highly regulated process. Activation of the SREBP pathway is regulated in a negative feedback manner by biosynthetic products produced by the pathway (Brown & Goldstein 2009). The best characterised is cholesterol-based regulation of the SREBP pathway (Figure 1.4). This is primarily due to the fact that the SREBP

pathway was discovered almost entirely through the works of one group based in Texas, under the direction of Michael S Brown and Joseph L Goldstein. They began pioneering works on identification of regulators of the LDL receptor and their primary area of research was in cholesterol and atherosclerosis (Goldstein & Brown 2009). SCAP is a key regulatory protein in this process, and has been highly studied in this regard.

When cellular sterol levels are low, SCAP is in a conformation which facilitates binding of COPII vesicle packaging proteins, beginning with Sec24 binding to a hexapeptide sequence, Met–Glu–Leu–Ala–Asp–Leu, which is commonly referred to as MELADL (L.-P. Sun et al. 2007). The MELADL sequence is localised to cytosol facing loop 6 of SCAP (Sun et al. 2005). Following vesicle assembly around the SCAP-SREBP complex, it is retrogradedly transported from the ER to the Golgi. The Golgi houses the two proteases required for release of the SREBP transcription factor domain. First, site-1 protease cleaves at Arginine-X-X-Leucine (RXXL) motif site in the luminal loop of the precursor protein, and this is followed by cleavage at a site in the middle of the first transmembrane helix, and this results in a liberated active transcription factor domain (Duncan et al. 1997a; Duncan et al. 1998). These two proteases are not specific to SREBP cleavage and are also known to cleave ATF6 and CREBH ER-stress response proteins (Ye et al. 2000; Zhang et al. 2006). Cleavage by S2P is dependent on S1P cleavage (Sakai et al. 1996). The liberated NTD then requires transport into the nucleus which is facilitated by importin beta (Nagoshi et al. 1999; Nagoshi & Yoneda 2001). Once in the nucleus the NTD transcription factor domain it binds to and activates SREBP target gene expression.

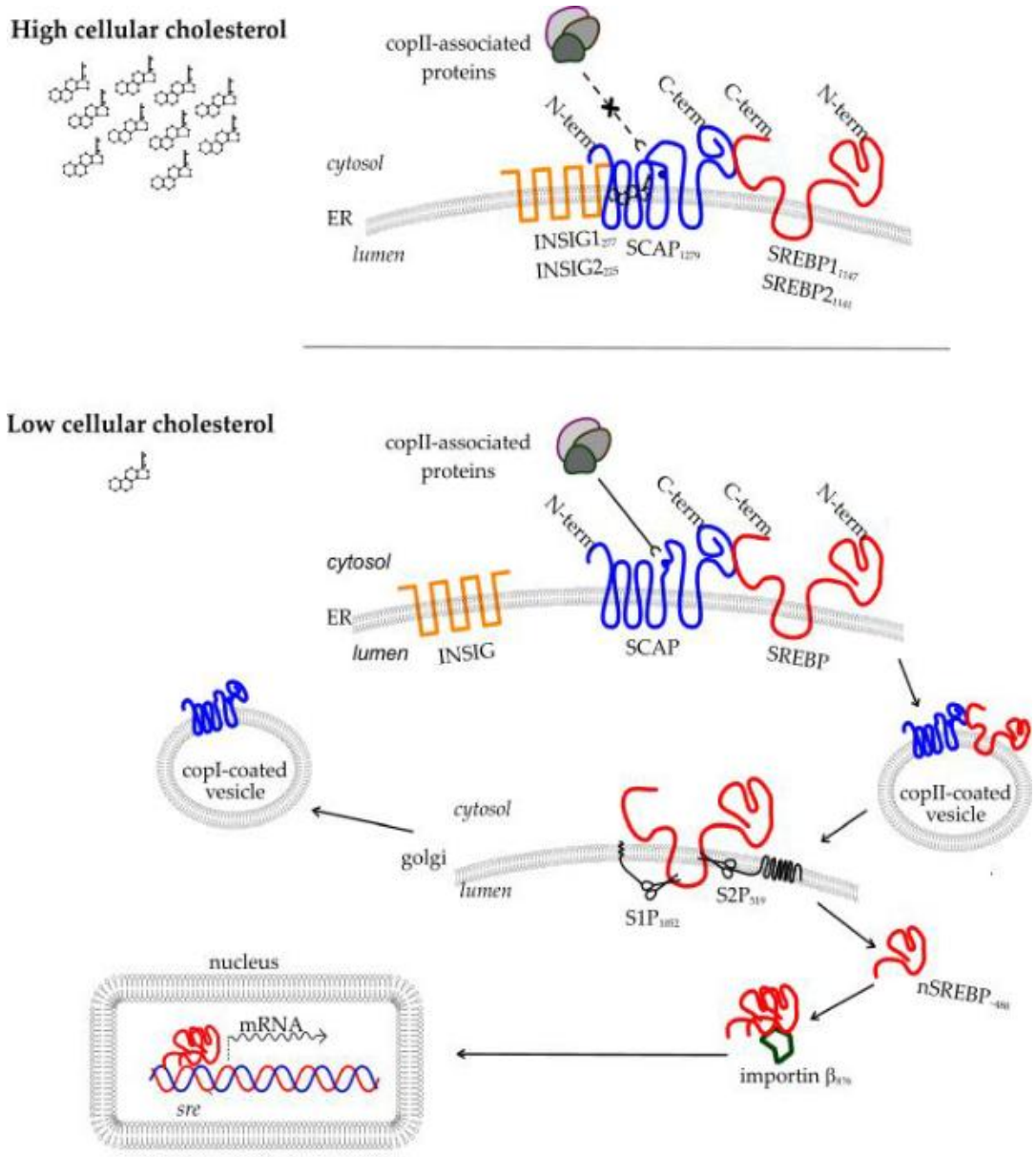


Figure 1.4. Cholesterol-mediated regulation of SREBP processing. High cholesterol conditions are sensed by the SCAP (blue) component of the SCAP-SREBP (blue-red, respectively) complex. This renders SCAP in a confirmation that prevents binding of COPII-associated proteins to the MELADL sequence in SCAP and facilitates binding of INSIG1 (yellow). Thus, the SCAP-SREBP complex is retained in the ER under high cholesterol conditions. Under low cholesterol conditions, SCAP is in a confirmation that allows binding of COPII-associated proteins. The SCAP-SREBP complex is packaged into COPII-coated vesicles and transported to the Golgi where SREBP undergoes a two-step proteolytic cleavage event, mediated by two Golgi-resident proteases. This cleavage releases the active N-terminal transcription factor domain (nSREBP) which is transported into the nucleus by importin-β. nSREBP binds to SRE elements within promoters of target genes, resulting in increased expression.

However, as mentioned, this transport dependent activation is a tightly regulated process and is regulated in a negative feedback manner. When ER membrane cholesterol levels exceed 5%, SCAP undergoes a conformational change in loop 6 that alters the proximity of the MELADL sequence in relation to the ER membrane such that sec24 can no longer bind (Radhakrishnan et al. 2008). This conformational change was demonstrated by a change in pattern of trypsin cleavage bands, where a previously obscured trypsin cleavage site is revealed in low sterol conditions. Cholesterol has been shown to elicit this effect by binding to a region within luminal loop 1 of SCAP (Motamed et al. 2011). A point mutation of Y234A within this loop alters the conformation of loop six, mimicking the effect of bound cholesterol, and SREBP processing does not occur even in sterol deplete conditions (Motamed et al. 2011). This mutant retains the ability to bind SREBPs however and prevent their degradation. A potential mechanism as to how cholesterol binding to loop 1 influences the conformation of loop 6 has recently been proposed. Zhang *et al* identified a critical residue in luminal loop 7 of SCAP which when mutated to serine (Y640S) has the same effect as the Y234A mutation (Y. Zhang et al. 2013). These studies revealed that an interaction between loop 1 and loop 7 of SCAP keeps loop 6 in a conformation with MELADL accessible. Cholesterol binding prevents this interaction from occurring and that this results in the altered conformation of loop6. The mutations in loop 1 or 7 also block this interaction, thus mimicking the effect of cholesterol binding (Y. Zhang et al. 2013).

The conformational change in SCAP also facilitates binding of another ER resident protein called insulin induced gene (INSIG) (Sun et al. 2007). INSIG is also commonly referred to as the ER-retention protein for the SCAP-SREBP complex, and is another key regulatory protein required for modulation of SREBP activity

(Sun et al. 2005). Two paralogs of INSIG exist in the vertebrate genome; INSIG1 and INSIG2. INSIG1 is located at 7q36 and INSIG2 is located at 2q14.1 (Peng et al. 1997; Bressler et al. 2009). These INSIG proteins have six-transmembrane helices with short cytosolic extensions at both the amino and carboxy termini (Feramisco et al. 2004) (Figure 1.5). They share 56% overall sequence identity (Yabe et al. 2002). Both INSIG proteins have demonstrated the capability to mediate the ER-retention of the SCAP-SREBP complex (Yabe et al. 2002). Knockout studies of each have shown that in the absence of INSIG1, INSIG2 compensates, and *vice-versa* (Engelking et al. 2005).

Also, over-expression of each isoform has the same inhibitory effect in the presence of sterols (Yabe et al. 2002). The two INSIG proteins do however differ in their modes of regulation. INSIG2 is constitutively expressed and is not subject to sterol-regulated degradation (Lee, Gong, et al. 2006; Gong, Lee, Lee, et al. 2006a). Conversely, INSIG1 expression is induced by the SREBP transcription factors, which themselves are activated in response to low sterol availability (Lee & Ye 2004). INSIG protein is then stabilised through sterol-mediated binding to SCAP, which displaces the E3 ligase gp78 and prevents degradation of INSIG (Ye & Debose-boyd 2011). INSIG essentially functions to negatively regulate cholesterol biosynthesis through inhibition of cholesterogenic gene expression via ER retention of SREBP-SCAP. Both SCAP and INSIG act to negatively regulate SREBP transport in the presence of sterols. Insig binds within TM 2-6 of SCAP, and three sterol-resistant mutants of SCAP (D443N, Y298C, and L315F) fail to bind INSIG (Yang et al. 2002). INSIG is essential to sterol-regulated retention of SCAP-SREBP processing as in the absence of INSIG, SREBP processing is not regulated by cholesterol, indicating that the conformational change in SCAP alone is not

sufficient to inhibit sec23/24 binding (Sun et al. 2005). INSIG is also essential for oxysterol-mediated regulation of SREBP processing as oxysterols bind to INSIG, not SCAP (Radhakrishnan et al. 2007b).

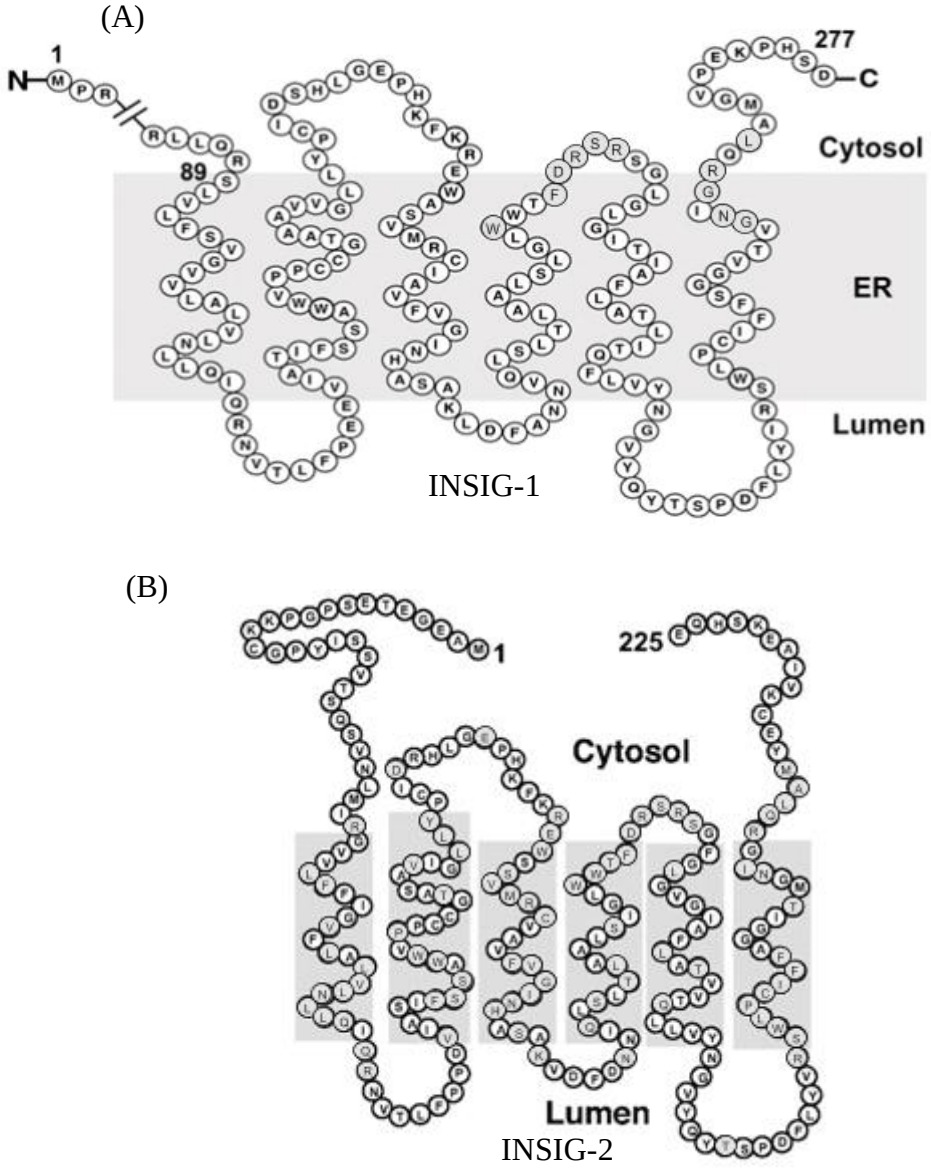


Figure 1.5. Membrane topology of human INSIG proteins. (A) Proposed membrane topology of INSIG-1 (modified from(Gong, Lee, Brown, et al. 2006)). (B) Proposed membrane topology of INSIG-2 (modified from (Radhakrishnan et al. 2007b)).

Cholesterol is not the only regulator of SREBP activation. In 2007, Radhakrishnan et al showed using radio-labelled sterols in competition assays that cholesterol bound the sterol sensing domain of SCAP (Radhakrishnan et al. 2007b). In the same study, other sterols shown to interact with SCAP and prevent SREBP processing included dihydrocholesterol, desmosterol, androstenol and androstanol. They showed using the same methods that other sterols, including 7α-hydroxycholesterol (7α-OHC), 27-hydroxycholesterol (27-OHC), 24*S*-hydroxycholesterol (24*S*-OHC), 25-hydroxycholesterol (25-OHC), 22*R*-hydroxycholesterol (22*R*-OHC), and 24,25-hydroxycholesterol (24,25-OHC) competitively bound INSIG. Oxysterols stabilise INSIG and prevent its ubiquitin-dependent degradation by displacing gp-78. Sterols that were found to bind either of these two proteins demonstrated the ability to prevent SREBP cleavage (Radhakrishnan et al. 2007b). However, not all sterol based molecules displayed these characteristics and were not recognised as regulators of SREBP activity. 25-OHC was identified as the most potent inhibitor of SREBP activation; due to its ease of transport across the membrane, and is commonly used in experiments investigating molecular aspects of SREBP activity and regulation, and as a positive control when identifying novel regulators of the pathway (Figure 1.7).

The mechanisms of fatty acid regulation of the SREBP pathway are less clear, but work in the area is growing. However, it had been shown that poly unsaturated fatty acids (PUFAs) down regulate SREBP1 isoforms at the processing level, and that this inhibitory effect increased with chain length and unsaturation of the FAs (Xu et al. 1999). This was later linked to PUFA binding to and stabilising INSIG, to facilitate ER-retention of SREBP (Lee et al. 2008). Insulin regulation of SREBP1 processing has also been reported (Hegarty et al. 2005; Yellaturu, Deng, Cagen, et al. 2009;

Yellaturu, Deng, Park, et al. 2009). The mechanism by which PUFAs and sterols differentially regulate processing of SREBP1 and SREBP2 isoforms, respectively, has not yet been elucidated.

Non-sterol regulators have also been identified that inhibit SREBP processing. Betulin is a naturally occurring triterpenoid isolated from birch bark (Alakurtti et al. 2006) (Figure 1.7). Betulin has been investigated in relation to cancer cell cytotoxicity but has shown limited beneficial effects (Li et al. 2010; Cichewicz & Kouzi 2004; Rzeski et al. 2009). However, in 2009, treatment of cancer cells with betulin in the presence of cholesterol significantly enhanced cell death beyond that induced by treatment with betulin alone (Mullauer et al. 2009). The authors could not propose a potential mechanism for the enhancing effect of cholesterol on betulin, but suggested it was linked to an effect of cholesterol on membrane integrity enhancing betulin uptake into the cell. In 2010 it was demonstrated that betulin inhibited SREBP processing by promoting the association between SCAP and INSIG (Tang et al. 2011). Thus it is possible that the combined action of betulin and cholesterol on the SREBP pathway resulted in the observed effects.

Recently, a synthetic small molecule inhibitor called Fatostatin was identified as an inhibitor of adipogenesis and also blocked body weight increase and hepatic fat accumulation in obese mice (Kamisuki et al. 2009). Fatostatin was shown to elicit this effect through blocking the ER-Golgi transport of SREBP by binding to SCAP. This effect was shown to be independent of INSIG-mediated ER retention and did not affect SCAP interaction with SREBP, and thus it was proposed to interfere with the binding of COPII associated proteins to SCAP, although this would require further investigation (Kamisuki et al. 2009). Fatostatin was recently demonstrated to

have high anti-cancer activity in prostate cancer (Li et al. 2014). Treatment with Fatostatin induced apoptosis, reduced invasion and migration in prostate cancer cell lines, and inhibited tumour growth and serum PSA levels in mouse models of prostate cancer. Prostate cancer is strongly linked to aberrant lipogenesis and the effects of Fatostatin were attributed to its modulation of the SREBP pathway and androgen receptor signalling (Li et al. 2014).

Mechanisms for activation of SREBP processing have also been reported. Inhibition of the Akt/PI3K pathway has been reported to negatively impact on cholesterol and fatty acid synthesis by disrupting SCAP transport form the ER to the Golgi (Du et al. 2006; Krycer et al. 2010). Insulin has also been shown to enhance processing of SREBP-1c by promoting Akt-mediated phosphorylation of the precursor protein which led to an increased affinity of the SCAP-SREBP complex for COPII packaging proteins (Yellaturu, Deng, Cagen, et al. 2009). However, the same experiment showed insulin to have no effect on SREBP-2 processing. This, taken together with initial reports indicating that Akt inhibition affects both cholesterol and fatty acid synthesis, suggests that the PI3K/Akt pathway has the capability to differentially enhance the processing of SREBPs under different conditions.

Androgen regulation of SREBP processing has also been reported in the prostate cancer cell line, LNCaP, mediated by androgen-induced up-regulation of SCAP (Heemers et al. 2006; Heemers et al. 2001). SCAP was found to contain an androgen response element in intron 8, which allowed androgen receptor mediated regulation of its expression (Heemers et al. 2004).

Surprisingly, SREBP processing has also reported to be activated by cysteine proteases that have a role in apoptosis, although a role for active SREBP in apoptosis is unclear (Pai et al. 1996).

***Oxysterols: Synthesis and Functions***

The SREBP pathway governs cholesterol biosynthesis and is subject to end-product feedback regulation, as described above. However, certain cholesterol-derived molecules have also displayed a regulatory influence over SREBP activation. Oxysterols are derivatives of cholesterol which are produced through enzymatic oxidation and also through non-enzymic oxidation processes (Otaegui-Arrazola et al. 2010). The main enzymes involved in the oxidation of cholesterol are Cytochrome P450 family members (Figure 1.6). (CYP7A1), (CYP27A1), (CYP46A1) catalyse the conversion of cholesterol to 7α-OHC, 27-OHC, 24*S*-OHC, respectively (Otaegui-Arrazola et al. 2010). A small percentage of 25-OHC is reported to be produced through the actions of the aforementioned P450 enzymes, and also through the specific 25-hydroxylase enzyme (Diczfalusy 2013). The distribution and levels of oxysterols vary across tissues, dependent on the expression of a given P450 enzyme. For example, 7α-OHC and 27-OHC levels are high in the liver as they are precursors for bile acids production, while 24*S*-OHC is high in the brain (Garenc et al. 2010). 25-OHC is lowly expressed in comparison.

Non-enzymatic oxidation of cholesterol is also reported. There are two pathways by which this enzyme-independent process can occur, distinguished by the involvement of free-radicals in the process (Iuliano 2011).

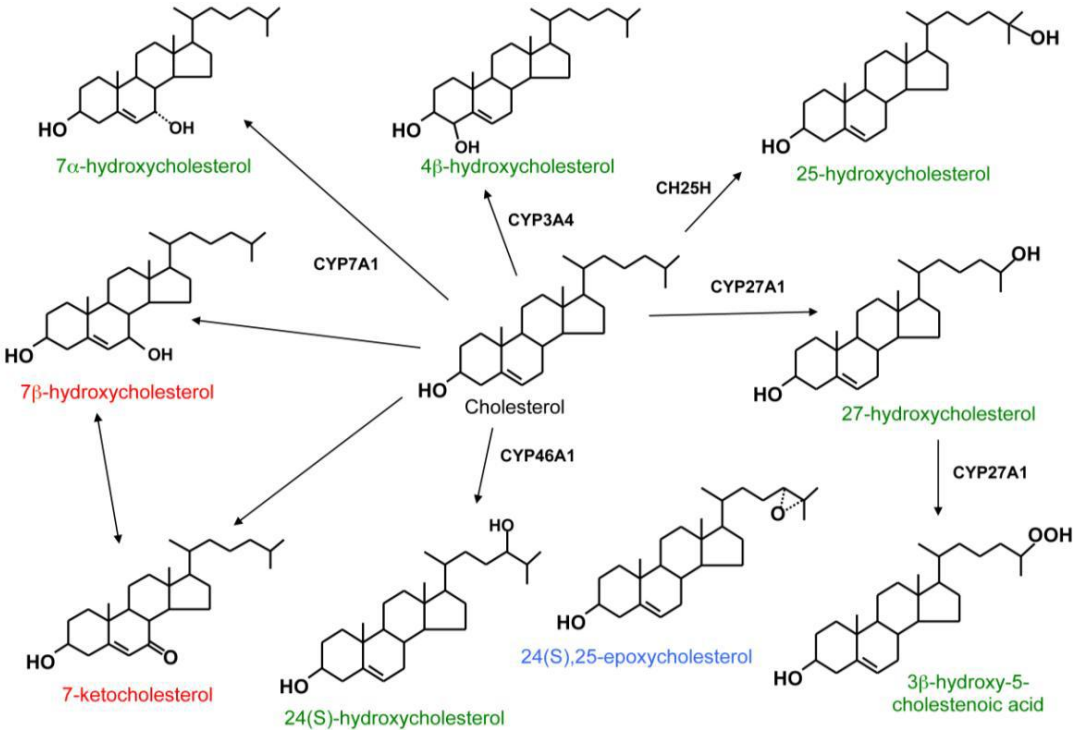


Figure 1.6. Structure and origin of common oxysterols. Most of the oxysterol species displayed are generated by enzymes that belong to the Cytochrome P450 family (CYP). CH25H, cholesterol 25-hydroxylase, is a di-iron enzyme. The enzymatically derived species are indicated with green, products of cholesterol autoxidation with red, and a species derived from a shunt of the cholesterol biosynthetic process with blue print (Olkkonen et al. 2012).

Oxysterols are also available from dietary sources. High cholesterol foods such as meats, eggs and dairy products are also rich in oxysterols, including 7α-OHC, 7β-OHC, 7-ketocholesterol, alpha-epoxycholesterol (α-epox), beta-epoxycholesterol (β-epox), 19-hydroxycholesterol (19-OHC) and 25-OHC (O Brien et al. 2000). Oxysterols modified at the C7 position are usually the highest concentration oxysterol detected in such foods, but limited data exists to determine plasma concentrations achieved following ingestion. Heating cholesterol-rich foods, however, has been shown to significantly increase their oxysterol content (Savage et al. 2002; O Brien et al. 2000).

A number of the oxysterols have been screened for their capacity to regulate SREBP activation. Competitive binding assays revealed that 25-OHC, 22*R*-OHC, 24*S*-OHC, 27-OHC, and 24,25-OHC negatively regulate SREBP processing through binding INSIG (Radhakrishnan et al. 2007b). 7α-OHC, 7β-OHC and 7-ketocholesterol displayed moderate regulatory capacity, although binding to INSIG or SCAP as mechanism was unclear. This study demonstrated that not all oxysterols were capable of regulation, one of which was 19-OHC (Figure 1.7). This group subsequently used 19-OHC as a negative control for many SREBP pathway mechanistic studies, which appeared to confirm that this is the case (Brown et al. 2002a; Sun et al. 2005).

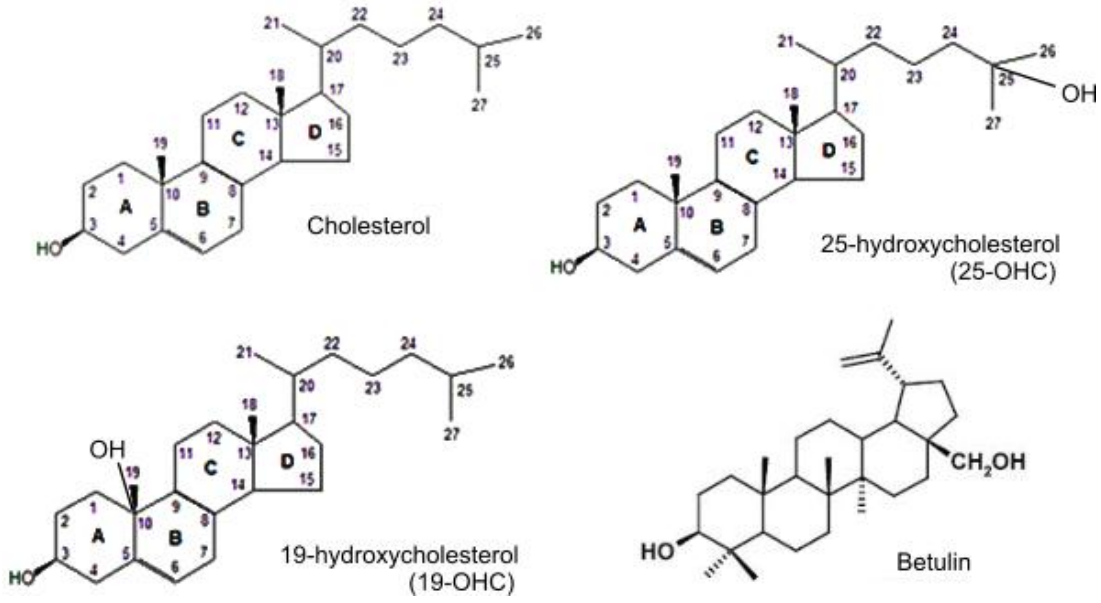


Figure 1.7. Structures of some commonly used regulators (cholesterol, 25-OHC and betulin) and a non-regulator (19-OHC) of SREBP processing.

In addition to regulation of SREBP cleavage and being precursor molecules for bile acid synthesis, oxysterols also function as signalling molecules (Olkkonen et al. 2012). Oxysterol production is proportional to the available cholesterol for modification within the cell. In instances of excess cholesterol, oxysterols signal within the cell to adjust accordingly to the excess of cholesterol present. LXRs are ligand-activated transcription factors which function as heterodimers with RXRs (another ligand-activated TF) (Wójcicka et al. 2007). Oxysterols are the natural ligands for LXR (activation at the micromolar levels (as is in plasma)), and include 4β-OHC, 25- OHC, 22*R*OHC, 24*S*-OHC, 27-OHC, and 24,25-OHC, although 25-OHC and 27-OHC are reported as being relatively weak activators. Activated LXRs stimulate expression of multiple genes involved in removal of excess cholesterol from the cell (Li & Glass 2004; Yoshikawa et al. 2010). LXRs increase expression of Niemann-Pick C1 (NPC1) proteins and ABC transporters which regulate transfer of cholesterols from endosomes to the plasma membrane, followed by their efflux to HDL particles, respectively (Ory 2004; Ma et al. 2009; Repa et al. 2002). Interestingly, cholesterol efflux is actively suppressed through the actions of SREBP2. SREBP2 is transcriptionally regulated by itself, thus in sterol depleted conditions its expression in increased (Sato et al. 1996). An evolutionarily conserved mir-33 was recently identified within intron 16 of the human SREBP2 gene and was found to be co-expressed with SREBP2 mRNA levels. Mir-33 negatively regulates ABC transporters and decreases circulating HDL-cholesterol levels (Marquart et al. 2010; Rayner et al. 2010). Thus SREBP2 acts to co-ordinate increased cholesterol synthesis and decreased cholesterol efflux to raise cellular sterol levels. LXRs also regulate expression of the rate limiting step of bile acid synthesis, CYP7A1, which also functions to increase cellular cholesterol efflux (Peet et al. 1998). Activated

LXRs also limit intestinal cholesterol absorption by increasing ABCG5 and ABCG8 transporter expression in enterocytes, although this is believed to be of minor importance in relation to increasing cholesterol efflux (Repa et al. 2002). Thus, oxysterols function at multiple levels to maintain the tight balance of intra-cellular cholesterol.

Activated LXRs also have roles outside of cholesterol regulation, including in inducing inflammatory mediators, contributing to atherosclerotic plaque formation, and potentiating neurodegenerative diseases (Jamroz-wiśniewska et al. 2007). Oxysterols have also demonstrated apoptotic effects in a variety of non-malignant and cancer cell lines (Lordan et al. 2009). These effects together with their pro-inflammatory links have also linked oxysterols to disease such as irritable bowel syndrome and age-related macular degeneration (Poli et al. 2013). Recently, 27-OHC was identified as a linking factor between hypercholesterolemia and breast cancer (Nelson et al. 2013). 27-OHC was shown to be a ligand for the oestrogen receptor and 27-OHC binding to this receptor increased cell growth. Increased expression of CYP27A1, which converts cholesterol to 27-OHC, was found to be associated with high-grade tumours (Nelson et al. 2013).

***HMGCR***

The rate limiting step of cholesterol biosynthesis is the conversion of HMG CoA to mevalonate in the presence of NADPH, which is catalysed by HMGCR (Brown et al. 1973; Rétey et al. 1970). The HMGCR gene is localised to chromosome 5q13 and encodes an ER-localised protein with an 8 TM region containing an SSD and a cytosolic facing catalytic domain (Lindgren et al. 1985) (Figure 1.8).

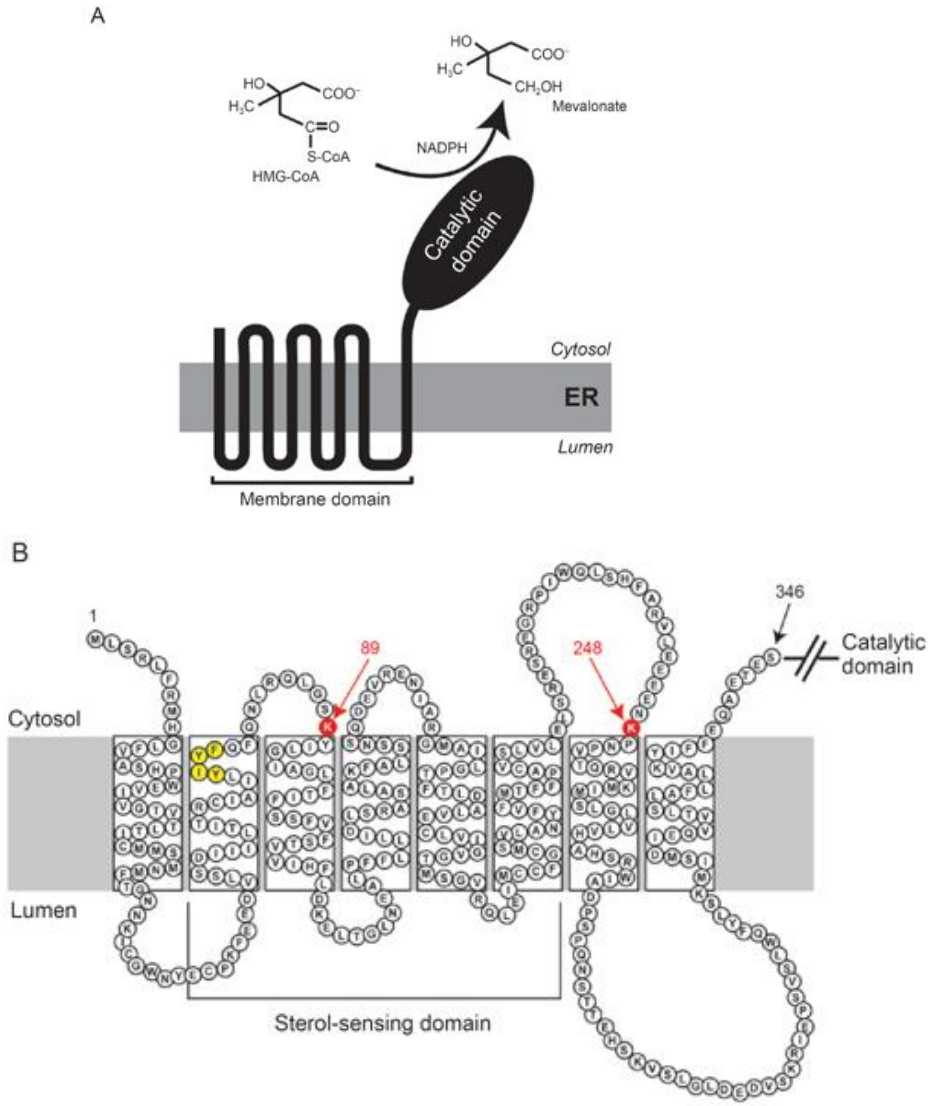


Figure 1.8. Domain structure of hamster HMG CoA reductase. (A) HMG CoA reductase consists of two distinct domains: a hydrophobic N-terminal domain with eight membrane-spanning segments that anchor the protein to ER membranes, and a hydrophilic C-terminal domain that projects into the cytosol and exhibits all of the enzyme's catalytic activity. (B) Amino acid sequence and topology of the membrane domain of hamster HMG CoA reductase. The lysine residues implicated as sites of Insig-dependent, sterol-regulated ubiquitination are highlighted in red and denoted by arrows. The YIYF sequence in the second membrane-spanning helix that mediates Insig binding is highlighted in yellow (DeBose-Boyd 2008)

As well as being required as the precursor for *de novo* cholesterol synthesis; the essential nature of which is highlighted earlier, mevalonate production is also essential to maintain cell viability (Ikonen 2008). Mevalonate itself has an essential role in DNA replication, with an increase in HMGCR expression linked to cell cycle S-phase (Quesney-huneeus et al. 1979; Tatsuno et al. 1997). Mevalonate production is also an absolute requirement for the synthesis of farnesyl pyrophosphate and geranylgeranyl pyrophosphate intermediates of the cholesterol biosynthesis pathway, which are essential for post-translational modification of proteins essential throughout the cell cycle (Sebti & Hamilton 2000; Rilling et al. 1993).

Cellular mevalonate levels are controlled through tight regulation of HMGCR which is centred on the sterol requirements of the cell (Vallett et al. 1996; Horton et al. 2002a). In response to changes in cellular sterol levels, HMGCR is altered at the transcriptional and protein levels (Vallett et al. 1996; Sever et al. 2003a). Low cellular sterol levels activate SREBP transcription factors, as described above, which regulates HMGCR at the transcriptional level (Vallett et al. 1996). Sterols also play a role in regulating HMGCR protein stability, to exert a more immediate stop to mevalonate production under high sterol conditions (Sever et al. 2003a). In the presence of oxysterols, including 25-OHC 24,25-dihydrolanosterol, INSIG binds HMGCR (Lange et al. 2008). This binding event recruits INSIG-associated E3 ubiquitin ligases to HMGCR, resulting in the ubiquitin-dependant degradation of the protein (DeBose-Boyd 2008). Both INSIG isoforms can mediate the degradation of HMGCR, although they do so through distinct E3 ligases. INSIG1 recruits gp78, INSIG2 recruits TRC8 (Jo et al. 2011; Che et al. 2012). It is also reported that HMGCR catalytic activity is regulated at the post-translational modification level, outside of the SREBP pathway regulation. Activated AMPK has been shown to

phosphorylate Ser872 (human) in the HMGCR active site (Clarke & Hardie 1990). This phosphorylation inhibits HMGCR activity and is reversed upon de-phosphorylation by PP2A.

The role of mevalonate in proliferating cells has been established. Unsurprisingly, the mevalonate pathway has also demonstrated links to cancer cell survival and progression (Gorin et al. 2012; Yokomizo et al. 2011; Swanson & Hohl 2006; Wächtershäuser et al. 2001). Constitutively active HMGCR was sufficient to enhance the cancer phenotype of MCF-7 cells, and to induce transformation of their non-malignant counterparts, MCF-10A (Clendening, Aleks Pandyra, et al. 2010). In the same study the authors discuss the correlation between high mRNA levels of HMGCR and other mevalonate pathway genes with poor prognosis for breast cancer patients. Brain and prostate cancers have also been reported as having elevated levels of cholesterol synthesis and cholesterogenic gene expression (Rudling et al. 1990; Hager et al. 2006b). Sterol-feedback regulation of SREBP processing and cholesterogenic gene expression has also been reported for a subset of prostate cancers (Chen & Hughes-Fulford 2001). Studies have also shown an association between statin resistance in a subset of AML cell lines and up-regulation of HMGCR (Clendening, Aleksandra Pandyra, et al. 2010). HMGCR has therefore been proposed as a metabolic oncogene, which would fit within one of the emerging hallmarks of cancer; reprogramming of cellular energy metabolism in order to support continuous cell growth and proliferation (Hanahan & Weinberg 2011). Thus, this further makes HMGCR an attractive target in the treatment of cancer.

The activity of HMGCR is effectively inhibited by a family of drugs known as statins, which are widely used in the treatment of atherosclerosis and other

cholesterol-related disease (Istvan & Deisenhofer 2001; Law et al. 2002; Vaughan et al. 2000). These drugs competitively bind the catalytic site of HMGCR, decrease mevalonate production, and the cell compensates by increasing cholesterol biosynthesis and uptake genes (Istvan & Deisenhofer 2001; Sheng et al. 1995). HMGCR is reported to undergo alternative splicing, with the resultant HMGCR isoform lacking exon 13 (HMGCR-D13) (Medina et al. 2008). Initial reports indicated that this isoform was not catalytically active, but subsequent studies show that this isoform is indeed capable of producing mevalonate (Burkhardt et al. 2008). The key residues for substrate binding are 684 to 692, and are located in exon 16, and thus are not affected by the absence of exon 13, which encodes residues 522 to 574 (Medina et al. 2008). In fact studies have shown both HMGCR and HMGCRD13 transcripts to be up-regulated in response to statin treatment, and that HMGCR-D13 does not display any impaired ability to promote proliferation of HepG2 cells compared to the full length isoform (Clendening, Aleks Pandyra, et al. 2010). It is suggested that the possibility of a heterodimer formation between isoforms may have confounded the first study (Medina & Krauss 2009). However, there are reports that the D13 isoform is less sensitive to statin mediated inhibition of HMGCR enzymatic activity compared to the full length isoform (Medina & Krauss 2009). There has also been reports correlating elevated levels of the HMGCR-D13 isoform in patients with a decreased response to statin-induced plasma LDL-cholesterol lowering, resulting from reduced upregulation of LDLR (Medina et al. 2008; Krauss et al. 2008). Together these data would suggest that the HMGCR-D13 isoform is functional to produce mevalonate but that statins have reduced binding capacity, possible linked to the altered active site conformation, and thus statin-mediated inhibition of HMGCR catalytic activity is impaired. Indeed, it has been

proposed that statins form van der Waals interactions with multiple residues encoded by exon 13 and that loss of these interactions may affect statin action, although this requires further investigation (Istvan & Deisenhofer 2001).

***Statins***

Statins refer to a group of drugs which competitively bind to the catalytic pocket of HMGCR and effectively prevent the enzymatic conversion of HMG-CoA to Mevalonate (Istvan & Deisenhofer 2001). Statins were originally identified as fungal metabolites which effectively and competitively inhibited cholesterol synthesis in mammalian cells. The pioneering statin, compactin, was discovered in the mid-1970s, isolated from *Penicillium citrinium*, followed closely by the identification of another naturally occurring statin from *Aspergillus terreus*, lovastatin (Brown et al. 1978; Alberts et al. 1980; Brown & Goldstein 2004). Natural statins which are currently clinically available are Lovastatin, Pravastatin and Simvastatin (Tobert 2003). Compactin failed to pass clinical trials but is routinely used in the laboratory setting in studies of the SREBP and mevalonate pathways (Kita et al. 1980; Sever et al. 2003a; Goldstein et al. 1979). Synthetic statins are also clinically available; Atorvastatin, Cerivastatin and Fluvastatin, which contain the HMG-like moiety present in all of the naturally occurring statins central to their inhibitory action (Tobert 2003).

Members of the statin family all competitively bind HMGCR and effectively reduce serum cholesterol levels. However they differ in a number of their properties, a comprehensive review by Schachter et al, 2004 gives more detail on this aspect (Schachter 2004). Most notably, differences are seen in statin efficacy and

bioavailability. Statins differ in their potency at achieving plasma cholesterol reduction, with evidence suggesting atorvastatin and simvastatin represent the most effective statins at the recommended daily doses (Solomon & Freeman 2008). These differing effects have been linked to the influence of their chemical structures on solubility and half-lives. Despite their rapid absorption following administration, statins suffer from a high level of first-pass metabolism in the liver (Schachter 2004). However, they differ in the extent to which their bioavailability is affected, ranging from 5-60%. This difference is linked to the P450 enzymes which metabolise each statin differing (Schachter 2004). This issue of bioavailability does not affect statin inhibition of HMGCR in the liver as site of action for serum cholesterol lowering, but requires consideration for possible alternative therapeutic uses of statins.

The primary use of statins is to lower circulating plasma LDL-cholesterol through increasing cell surface LDLR expression, which is triggered upon HMGCR inhibition (Law et al. 2002). The majority of clinical benefits observed with statin use are attributable to cholesterol reduction, however there is emerging evidence to support non-LDL-cholesterol linked or pleiotropic effects of statins (Bonetti et al. 2003; Zhou & Liao 2010). Atherosclerosis is complex disease involving lipid plaque formation combined with chronic inflammation in arterial walls (Fan & Watanabe 2003). In addition to the beneficial impact of cholesterol lowering on this disease, statins are believed to also contribute to a reduction in the associated inflammation (Jain & Ridker 2005). Statins have been shown to modulate the immune system in a number of ways. Statins have been shown to directly decrease the expression of ICAM-1, VCAM-1 and E-selectin endothelial adhesion molecules (Jain & Ridker 2005). Statins have also been shown to indirectly repress major histocompatibility complex class II (MHC-II) mediated T- lymphocyte activation via inhibition of the

expression of a MHC-II transactivator (CIITA) (Kwak et al. 2000). Activated T-lymphocytes play an important role in the pathogenesis of atherosclerosis (Fan & Watanabe 2003). These anti-inflammatory traits of statin use have led to interest in their use for reduced transplant rejection (Lakkis & Billiar 2013). Statins are also currently used for the prevention and treatment of stroke (Prinz & Endres 2011). There is little evidence to connect elevated cholesterol levels with stroke incidence and the anti-inflammatory pleiotropic effect of statins are attributed with the beneficial effects (Prinz & Endres 2011). Such pleiotropic effects are evidence that statins can act systemically, outside of hepatic LDL-cholesterol clearance, despite their high first-pass clearance rate.

Although the clinical tolerance and benefits of statins are apparent, adverse side effects to statin treatment are reported in a portion of patients. The most common reported side effect among statin users is myopathy (Needham & Mastaglia 2014; Joy & Hegele 2009). Patients on high dose statin regimes are more likely to experience myopathic events, although it is also dependant on patient risk factors including age, nutrition, exercise levels and other medications (Escobar et al. 2008; Egan & Colman 2011). A recent clinical trial investigating the effects of statins on skeletal muscle function revealed that high-dose statin treatment over a six month period did produce mild muscle injury in patients, but did not decrease muscle strength or exercise performance (Parker, Capizzi, et al. 2013). The mechanism of statin effect on muscle is not clear. Possible proposed mechanisms include the effect of reduced protein prenylation on the activation capacity of pathways involved in maintaining skeletal muscle homeostasis during exercise (Stark et al. 1998). Reduced isoprenoid synthesis also impacts on ubiquinone production, which may lead to impaired mitochondrial function and reduced energy production (Larsen et al. 2013;

Johnson et al. 2004). Another attractive possibility is the reported effects of statins on cell proliferation, apoptosis, and on the immune system and that these may be linked to skeletal muscle damage (Wong et al. 2002; Jain & Ridker 2005). Statin-associated myopathy is a further indicator of extra-hepatic effects of statin use and may serve as evidence that HMGCR inhibition can occur beyond the liver despite the high level of first-pass clearance. A recent review also discusses genetic susceptibility factors for statin myotoxicity (Needham & Mastaglia 2014). Other less frequent reported statin side effects include hepatotoxicity and diabetes (Wilkinson et al. 2014). It is believed that these effects are likely secondary to the lipid lowering effect of statins.

Statins are one of the most extensively used drugs across the world in the treatment of cholesterol-related disease. Their mechanism of action is well understood and their side-effects are minimal under the recommended dose range (40 mg/day). However, given the pathway that they manipulate to achieve their therapeutic effect and that they influence serum cholesterol levels, there has been significant interest in the effect of statin usage on both cancer risk and prevention (Boudreau et al. 2010; Browning & Martin 2007; Demierre et al. 2005). While early studies on statin users in a clinical trial for coronary heart disease reported an increased cancer incidence among statin users as a secondary finding (Sacks et al. 1996), subsequent meta-analyses of a wide variety of randomised clinical trials taking into account trial size, follow up dates and removal of confounding factors gave a more comprehensive insight (Boudreau et al. 2010; Dale et al. 2006; Browning & Martin 2007; Graaf et al. 2004; Alsheikh-Ali et al. 2008; Liu et al. 2014; X.-L. Zhang et al. 2013; Wang et al. 2013; Chan et al. 2013; X. Zhang et al. 2013). The consensus from a variety of such meta-analyses in recent years is that there is no evidence to support an

increased risk of cancer overall or at specific sites, among statin users. In fact, there is a growing body of evidence to support a chemoprotective effect of statin use (Nielsen et al. 2012). Atorvastatin has been shown to inhibit both pancreatic and intestinal tumourigeneis (Gbelcová et al. 2008; Swamy et al. 2006; Reddy et al. 2006). Simvastatin has been shown to inhibit growth of malignant gliomas (Kikuchi et al. 1997). Lovastatin has been shown to suppress the formation of lung tumours in mice (Feleszko et al. 2000; Hawk et al. 1996). Epidemiological studies on statin use have reported a decreased incidence in a variety of cancer types among statin users (S. Singh et al. 2013; Yi et al. 2014; Mucci & Stampfer 2014). It is important to note, however, that this was not a universal effect observed among patients, and conclusive evidence for an established link between statin use and a reduced incidence of cancer is not yet available. Clinical trials on cancer prevention with statins are underway (Table 1.2).

**Table 1.2. Statins in Cancer Prevention (www.clinicaltrials.gov)**

| **Identifier:** | |
|---|---|
| NCT01349881 | S0820, Adenoma and Second Primary Prevention Trial (PACES) |
| NCT00334542 | Simvastatin in Preventing a New Breast Cancer in Women at High Risk for a New Breast Cancer |
| NCT00285857 | Phase II Trial - Breast Cancer Chemoprevention by Lovastatin |
| NCT00637481 | A Phase I Prevention Study of Atorvastatin in Women at Increased Risk for Breast Cancer |
| NCT01992042 | Novel Window of Opportunity Trial to Evaluate the Impact of Statins to Oppose Prostate Cancer |
| NCT01821404 | Atorvastatin and Prostate Cancer (ESTO1) |
| NCT00335504 | Atorvastatin Calcium, Oligofructose-Enriched Insulin, or Sulindac in Preventing Cancer in Patients at Increased Risk of Developing Colorectal Neoplasia |
| NCT00462280 | Lovastatin in Treating Patients At High Risk of Melanoma |

Based on the cholesterol and isoprenoid requirements of the proliferating cell, statins are attractive adjuvants to reduce cholesterol and mevalonate availability to tumours. *In vitro* studies have demonstrated the effects of statins on current chemotherapeutic strategies. Lovastatin was shown to synergistically act with cytosine arabinoside to induce cytotoxicity in leukemic cell lines (Holstein & Hohl 2001). Mevastatin was shown to enhance the sensitivity of AML cell line to radiochemotherapy (Li et al. 2003). Fluvastatin has been shown to enhance the anti-proliferative effect of the cytosine arabinoside analogue gemcitabine in a cell line model of pancreatic cancer (Bocci et al. 2005). *In vivo* studies also support such findings. Lovastatin was shown to potentiate the anti-tumour activity of doxorubicin in mouse models of colon cancer, sarcoma and lung carcinoma (Feleszko et al. 2000). Lovastatin had a similar effect on the anti-tumour activity of cisplatin in a mouse melanoma model (Feleszko et al. 1998). Atorvastatin was shown to enhance the chemo-preventive efficacy of celecoxib in a mouse model of colorectal cancer (Reddy et al. 2006). A phase 1 study showed pravastatin enhanced the chemotherapeutic effect of a regimen commonly used in the treatment of AML (Kornblau et al. 2007). Statins are also under investigation in a number of clinical trials for use as adjuvants to current chemotherapeutics (Table 1.3)

| Table 1.3. Statins as Adjuvants to Chemotherapeutics (www.clinicaltrials.gov) | |
|---|---|
| **Identifier:** | |
| NCT00816244 | Study of Statin as Neo-Adjuvant Therapy in Postmenopausal Breast Cancer |
| NCT01418729 | Efficacy and Safety Study of Sorafenib Plus Pravastatin to Treat Advanced Hepatocarcinoma (ESTAHEP-2010) |
| NCT02029573 | Efficacy and Safety of Atorvastatin in Combination With Radiotherapy and Temozolomide in Glioblastoma (ART) |
| NCT00583102 | Dose Escalation Phase I/II Study of Lovastatin With High-Dose Cytarabine for Refractory or Relapsed AML |
| NCT01772719 | Overcoming Chemotherapy Resistance In Refractory Multiple Myeloma With Simvastatin and Zoledronic Acid |
| NCT00107523 | Pravastatin, Idarubicin, and Cytarabine in Treating Patients With Acute Myeloid Leukemia |
| NCT00490698 | Zoledronate With Atorvastatin in Renal Cell Carcinoma |
| NCT01831232 | Idarubicin, Cytarabine, and Pravastatin Sodium in Treating Patients With Acute Myeloid Leukemia or Myelodysplastic Syndromes |
| NCT00313859 | Phase II Study of Simvastatin Plus Irinotecan, Fluorouracil, and Leucovorin(FOLFIRI) for Metastatic CRC |
| NCT01238094 | Trial of XELIRI/FOLFIRI + Simvastatin Followed by Simvastatin Maintenance in Metastatic Colorectal Cancer |
| NCT01281761 | Simvastatin + Cetuximab/Irinotecan in K-ras Mutant Colorectal Cancer (CRC) |
| NCT02026583 | Study of Simvastatin Plus XELOX and Bevacizumab as First-line Chemotherapy in Metastatic Colorectal Cancer Patients |
| NCT01441349 | Irinotecan/Cisplatin With or Without Simvastatin in Chemo-naive Patients With Extensive Disease-small Cell Lung Cancer |
| NCT00944463 | Trial of Simvastatin and Gemcitabine in Pancreatic Cancer Patients |
| NCT01478828 | Pre-Prostatectomy Lovastatin on Prostate Cancer |
| NCT00452244 | Gefitinib With or Without Simvastatin in Non-Small Cell Lung Cancer (NSCLC) |
| NCT00433498 | Etoposide and Cisplatin or Carboplatin as First-Line Chemotherapy With or Without Pravastatin in Treating Patients With Small Cell Lung Cancer |
| NCT00354640 | Simvastatin and Anastrozole in Treating Postmenopausal Women With Ductal Carcinoma In Situ or Invasive Breast Cancer |
| NCT00584012 | A Study of the Proper Dosage of Lovastatin and Docetaxel for Patients With Cancer |
| NCT00452634 | Irinotecan/Cisplatin Plus Simvastatin in Extensive Disease-Small Cell Lung Cancer (ED-SCLC) |
| NCT00966472 | Phase I Study of a Statin + Erlotinib for Advanced Solid Malignancies With Focus on Squamous Cell Carcinomas and NSCLC |
| NCT01428869 | Combination Statin, Acetylsalicylic Acid and Dutasteride Use in PC |

Statins have also independently demonstrated anti-cancer effects in a variety of cancer cell line models. Statins, including atorvastatin and simvastatin have been shown to induce apoptosis in myeloma cell lines in a caspase-dependent manner (Cafforio et al. 2005). Mevastatin has been shown to induce apoptosis in colorectal carcinoma cell lines (Wächtershäuser et al. 2001). Lovastatin, mevastatin and simvastatin have all been shown to induce apoptosis in melanoma cell lines, as well as having inhibitory effects on the migration and invasion of these cancer cells (Glynn et al. 2008). Mevastatin and simvastatin have been shown to decrease androgen sensitivity and cell proliferation in androgen receptor (AR)-positive prostate cancer cells, but not in AR-negative cells (Yokomizo et al. 2011). This decrease in proliferation was linked to statin-induced proteolysis of the AR protein, which in turn reduced SREBP pathway activation in these cells.

Tumours of simvastatin treated mice have been shown to have increased levels of apoptosis compared to untreated control mice, as measured by immune-histochemical staining of mammary tumour sections for cleaved caspase-3 (Campbell et al. 2006). Simvastatin also has demonstrated anti-proliferative effects on human glioma cells which was rescuable by mevalonate in a dose dependent manner, and thus attributable to inhibition of HMGCR (Kikuchi et al. 1997). Thus, the anti-cancer potential of statins in cell culture is quite apparent.

However, statin resistant cell lines have also been identified, although the mechanisms underlying this resistance are not clear. Studies of statin-induced apoptosis in a panel of AML cell lines resulted in a group of sensitive and resistant lines, with the discerning feature between the two groups being regulation of the SREBP pathway (Clendening, Aleksandra Pandyra, et al. 2010). In this study the

statin sensitive cell lines were shown to have little or no upregulation of SREBP target genes, while in contrast the resistant cell lines displayed a marked increase in target genes, including HMGCR. In fact over expression of the catalytic domain of HMGCR reduced the statin-sensitivity of the sensitive AML cell lines (Clendening, Aleksandra Pandyra, et al. 2010). This suggests a link between statin sensitivity to cell death and HMGCR levels, and that increased HMGCR may be advantageous to the cancer cell. This finding is consistent with studies from AML patient samples which displayed decreased feedback of LDLR in the presence of 25-OHC, a process which is mediated by SREBPs which co-ordinately increases cholesterogenic target genes, including HMGCR (Tatidis et al. 1997). Interestingly, over-expression of the D13 isoform catalytic domain failed to have a protective effect on the statin sensitive cancer cell lines, suggesting that HMGCR alternative splicing may be linked to statin sensitivity (Clendening, Aleksandra Pandyra, et al. 2010). This possibility has recently been discussed in relation to reduced LDL-cholesterol response to statins among individuals, and siRNA knockdown studies selective for the full length isoform and not the D13 mutant, demonstrated reduced inhibition of HMGCR enzymatic activity (Medina et al. 2008). Heterogeneous nuclear ribonucleoprotein A1 (HNRNPA1) was recently identified as a sterol-regulated splicing factor involved in the regulation of HMGCR alternative splicing (Yu et al. 2014). A CHO-derived cell line selected for statin-resistance revealed impaired degradation of HMGCR protein as the underlying mechanism for resistance (Ravid et al. 1999). Thus existing evidence indicates that statin efficiency is linked to HMGCR levels.

In addition to varying response to statins, there is also debate as to whether the concentrations required to elicit these anti-cancer benefits are achievable *in vivo* (Bonetti et al. 2003; Björkhem-Bergman et al. 2011). The chemotherapeutic

potential of statins cannot be ignored and in recent years there are clinical trials underway specifically investigating statins as a primary form of treatment (Table 1.4). Deregulated inflammation is characteristic of cancer, and has been associated with the progression and in some cases, the initiation of the disease (Candido & Hagemann 2013). The anti-inflammatory effects of statins described earlier also have potential chemotherapeutic benefits.

**Table 1.4. Statins as Primary Chemotherapeutic (www.clinicaltrials.gov)**

| **Identifier:** | |
|---|---|
| NCT00281476 | The Effect of High Dose Simvastatin on Multiple Myeloma |
| NCT00807950 | Phase II Study of Simvastatin in Primary Breast Cancer; Test of Its Potential Selectivity on Basal Subtype Breast Cancer |
| NCT00185731 | Phase II Study of Atorvastatin Safety and Antitumor Effects in Non-Hodgkin's Lymphoma |
| NCT00828282 | High-dose HMG-CoA Inhibitor Simvastatin Relapsed CLL |

### *Thesis Objectives*

The SREBP pathway has a central role in the regulation of *de novo* lipid and cholesterol biosynthesis. Modulation of this pathway activity is of high interest in the context of atherosclerosis, hypercholesterolemia, obesity and cancer (Eberlé et al. 2004). The activity of this pathway is regulated in response to dietary sterols and fatty acids, although novel non-dietary regulators are also emerging (Goldstein et al. 2006; Lee et al. 2008; Kamisuki et al. 2009; Tang et al. 2011). The SCAP-SREBP interaction is essential for SREBP protein stability and for delivery of the SREBP precursor protein to the Golgi for proteolytic processing (Rawson et al. 1999). Thus, small molecule intervention of this interaction would also allow for inhibition of SREBP processing. Also, the SREBPs share approximately 60% identity in their CTD regions and are both bound by SCAP, of which there exists only one isoform. It is not known how SCAP differentially regulates processing of SREBP1 and SREBP2 proteins. Knowing the precise residues involved in the SCAP-SREBP1 and SCAP-SREBP2 interaction would give further insight into this regulation. The aim of this thesis was to map the interaction site between SCAP and SREBP, which would provide valuable information on the mechanisms regulating this pathway.

SREBPs are involved in regulating the expression of genes essential for steroid hormone biosynthesis, including the rate limiting enzyme steroidogenic acute regulatory protein (StAR) and also Steroid 5α-reducate isotype 2 (Srd5a2) which is involved in the conversion of testosterone to dihydrotestosterone (Shea-eaton et al. 2014). Steroid hormone production is also dependent on cholesterol availability, and thus is dependent on SREBP activity (Miller 1988). However, feedback regulation of the SREBP pathway by steroid hormones has not yet been reported. In fact androgen

activation of SREBP processing has been demonstrated (Heemers et al. 2006). In early studies in the lab of Brown and Goldstein, progesterone was shown to have little or no effect on processing of SREBP1 (Wang et al. 1994). However, progesterone membrane receptor component 1 (PGRMC1) has been identified as an interacting partner of SCAP (Suchanek et al. 2005). PGRMC1 is believed to bind progesterone, and also to positively affect its synthesis (Peluso et al. 2006). We hypothesised that PGRMC1 may elicit a regulatory effect on the SREBP pathway, namely on SREBP processing, through its interaction with SCAP. As PGRMC1 is reported to mediate effects of P4, it is possible that progesterone may be required for this regulation. A regulatory effect of P4 on SREBP processing would be in keeping with cholesterol derived molecules regulating SREBP processing. The aim of this thesis was to investigate the regulatory effect of PGRMC1 on SREBP processing, and the requirement of P4 in this potential regulatory role.

INSIG is a key protein involved in the regulation of SREBP processing (L.-P. Sun et al. 2007). It is also central to regulating the degradation of HMGCR (Sever et al. 2003a). There are two isoforms of INSIG1 produced through the use of two alternative in-frame translational start sites (Yang et al. 2002). The significance of having two isoforms produced has not yet been addressed. The aim of this thesis was to investigate the evolutionary conservation of having two INSIG1 isoforms expressed, and to investigate if there was a functional difference between the isoforms with respect to the two known functions of INSIG1.

Statins competitively bind the catalytic site of HMGCR and are widely used in the treatment of cholesterol-related disease (Schachter 2004). Inhibition of HMGCR reduces intracellular cholesterol, mevalonate and isoprenoid levels which triggers a

feed forward response to activate SREBP target genes, including LDLR and HMGCR (Law et al. 2002; Sheng et al. 1995; Vallett et al. 1996). Increased LDLR expression provides the beneficial reduction in plasma LDL-cholesterol levels, while increased HMGCR maintains cell viability in the presence of statins (Law et al. 2002). However, in the presence of excess statin all HMGCR enzymatic activity is inhibited and this has been shown to trigger growth arrest and induce apoptosis in a variety of cell lines. This has led to the investigation of the chemotherapeutic potential of statins (Sleijfer et al. 2005). Central to the mechanism of action of statins is upregulation of SREBP target genes (Sheng et al. 1995). However, this results in statins essentially upregulating their own target. We hypothesised that blocking the HMGCR increase which occurs upon statin treatment would reduce the concentrations required to induce cell death. Statins are subject to high first pass clearance in the liver, resulting in low circulating statin concentrations (Schachter 2004). Extra-hepatic effects of statins are limited by this. Reducing the concentration required to induce statin cell death would be valuable for the potential use of statins as chemotherapeutics, especially outside of hepatocellular carcinomas. The aim of this thesis was to investigate the combined effect of inhibiting SREBP processing in the presence of statins on cancer cell death.

### *Summary of Thesis Aims*

The aims of this thesis were to characterise molecular and cellular aspects of the SREBP pathway, as outlined below.

The SREBP isoforms are differentially activated in response to low cellular fatty acid and cholesterol levels. It is possible that the SREBPs bind to distinct sites within the CTD of SCAP and that this contributes to their differential activation by SCAP. To investigate this possibility we sought to map the interaction site of each SREBP on SCAP. In addition, mapping the precise interaction site of the SREBPs with SCAP is the first step towards small molecule inhibition of SREBP activation.

Proteolytic activaton of the SREBPs is a highly regulated event. Understanding the factors involved in this regulation is key to furthering our understanding of the roles of the SREBPs. The aim was to investigate the role of a potential SREBP regulatory protein PGRMC1, and also to further characterise the role of a known SREBP regulator INSIG1, with respect to regulation of SREBP activation.

The chemotherapeutic potential of statins is limited by failure to achieve serum concentrations of statins sufficient to induce cancer cell death. The final aim of this thesis was to investigate inhibition of the SREBP pathway as a mechanism to lower the concentration of statin required to induce cancer cell death. Expression of the target of statins HMGCR is known to be increased under lipid depleted conditions. This investigation was performed under high and low lipid conditions to investigate potential dietary influences on cancer cells to statin induced cell death.

# Chapter 2
## Materials and Methods

Unless where stated, all products were purchase from Sigma Aldrich, Dublin, Ireland

***Bioinformatic analysis of SCAP CTD***

Sequences homologous to the human SCAP protein sequence were retrieved from the NCBI database using their protein-protein basic local alignment search tool (pBLAST). Sequences were loaded into the alignment explorer function within Molecular Evolutionary Genetics Analysis (MEGA) v4.0 and aligned using ClustalW (Tamura et al. 2007; Higgins et al. 1994). Phylogenetic tree was generated based on the multiple sequence alignment using the Neighbor-Joining method in MEGA, and tree topology confidence scores were calculated using the Bootstrap test of phylogeny. Alignments were saved in FASTA format to allow analysis of conserved regions of interest using GeneDoc multiple sequence alignment editor. Alignments were then transferred to Microsoft Word by saving the alignment blocks in rich text format (.rtf), to facilitate annotation of residues of interest.

***Cloning of GST-SREBPCTD Proteins***

The carboxy-terminal domain (CTD) of human SREBP-2 (amino acid 556 to 1142) was PCR amplified from plasmid template (IMAGE ID 5498684, Geneservices) using Taq DNA Polymerase (New England Biolabs (NEB) ) using the following primer sets;

Forward: 5’ GCAACTAgtcgaCTGCTGGTTCATGGGGAGCCAGTGAT 3’

Reverse: 5’ GTCAAGTgcggccgcTCAGGAGGCGGCAATGGCAGT 3’

The resulting PCR product was digested with SalI and NotI restriction enzymes (NEB) and ligated into pGEX-6p1 vector (GE Lifesciences) using T4 DNA Ligase (Fermentas). Ligations were transformed into chemically competent BL21 *E. coli*

cells (c2525, NEB), as per manufacturer's guidelines. The PCR product was cloned into pEBG mammalian GST expression vector (Addgene) in the same way.

The CTD of human SREBP-1 (amino acid 559 to 1148) was PCR amplified from plasmid template (I.M.A.G.E. ID 5786483, Geneservices) using Taq DNA Polymerase using the following primer sets;

Forward: 5' GCAACTAggatccGTCTCCTTGGTGCTTCTCTTTGTCTA 3'

Reverse: 5' GTCAAGTgcggccgcCGGGGTCTAGCTGGAAGTGACAGT 3'

The resulting PCR product was digested with BamHI and NotI restriction enzymes (NEB) and ligated into pGEX-6p1 vector using T4 DNA Ligase. Ligations were transformed into chemically competent BL21 *E. coli* cells, as per manufacturer's guidelines. The PCR product was cloned into pEBG mammalian GST expression vector (Addgene) in the same way.

Positive transformants were identified by restriction digest screens, followed by sequence verification by Sanger sequencing (Lifesource Bioscience).

***Induction of GST-fusion proteins***

Induced expression of GST alone and GST- $SREBP1_{CTD}$ GST- $SREBP2_{CTD}$ fusion proteins from BL21 *E. coli* was optimised for IPTG concentration, length of induction time, and temperature. Induction of GST-proteins was confirmed by SDS-PAGE and specificity of the band of interest was confirmed by western blot analysis (Anti-GST, 1:1000 dilution, Cell Signalling). Briefly, LB-Ampicillin (50 μg/ml) broth was inoculated 1:100 with an overnight starter culture and grown to an $O.D._{600}$ = 0.5. At this point, IPTG was added to a final concentration of 0mM, 0.5mM, 1mM

and incubated for a further 4 hours, 16hours or 40hours at 37$^{o}$C, as indicated. Bacterial cells were pelleted by centrifugation at 7,700 x g for 10 minutes at 4$^{o}$C. Pellets were stored at -20$^{o}$C.

***Classical Solubilisation of GST-fusion proteins***

Bacterial pellets were resuspended in cold 1X PBS containing lysozyme at 100 µg/ml and sonicated on ice for 8 x 10 second bursts using a probe sonicator at half max intensity (Soniprep 150). Samples were brought to a final concentration of 1% Triton X-100 and incubated for 30 minutes gently rocking at room temperature. Samples were then clarified by centrifugation at 12 000 x g for 10 minutes at 4$^{o}$C. The supernatant was designated the soluble protein fraction, while he pellet was designated the insoluble protein fraction.

***Purification of GST-fusion proteins***

GST proteins were purified according to the batch/column purification using Glutathione Sepharose 4B (GS4B, Amersham Biosciences), as per manufacturer's guidelines. Briefly, equilibrated 50% GS4B slurry was prepared from the stock EtOH solution suspension, then added to soluble protein fractions and incubated for overnight at 4$^{o}$C. The flow through was collected by centrifugation at 500 x g for 5 minutes, the resin was washed 3 times with cold 1X PBS, then incubated for 30 minutes with elution buffer (50 mM reduced-glutathione in 50 mM Tris-HCl, pH8). Eluted protein was collected in fractions, and samples from all fractions were analysed by SDS-PAGE or immunoblot with anti-GST (#2624, Cell Signalling (1:1000 dilution)), as indicated.

***Purifying Inclusion Bodies***

Inclusion bodies were purified from bacteria as previously described (Rodríguez-Carmona et al. 2010). Briefly, bacterial Pellets were resuspended in 1X Sodium chloride-Tris-EDTA (STE) buffer (10 mM Tris pH8, 150 mM NaCl, 1 mM EDTA) and freeze-thawed for 4 cycles in liquid nitrogen. A bacterial protease inhibitor cocktail and lysozyme (1 mg/ml final) were added and lysates were incubated for 2 hours at 37$^{o}$C. Lysates were then brought to 0.5% Triton X-100 and incubated rocking for 1 hour at room temperature (RT). Cell suspensions were then sonicated on ice for 5 x 10 second bursts. NP-40 was then added to a concentration of 0.025% and lysates were incubated at 4$^{o}$C for 1 hour. Samples were then brought to 750 μM $MgSO_4$ and DNAse was added. Samples were incubated at 37$^{o}$C for 45 minutes, followed by centrifugation at 15000 x g for 15 minutes at 4$^{o}$C. The pellet contains inclusion bodies. IBs were washed once in STE buffer containing 0.5% Triton X-100, then centrifuged again. Pellets were resuspended in 1X Laemmli buffer and analysed by SDS-PAGE and immunoblot to confirm presence of the fusion protein. Solubilisation of IBs was optimised, as described below.

***Solubilisation of Inclusion Bodies***

IBs were solubilised based on methods previously described (Frangioni & Neel 1993). Briefly, IB pellets were re-suspended in STE buffer containing lysozyme at 100μg/ml, incubated for 15 minutes on ice, and then adjusted to 5 mM DTT. Cells were lysed by addition of 10% or 1 % sarkosyl, as indicated, then sonicated on ice for 10 x 2 second bursts on Soniprep 150, setting 6. Lysates were clarified by centrifugation at 10 000 x g for 5 minutes at 4$^{o}$C. The soluble fractions were then incubated with various combinations of detergents to enhance affinity purification in

the presence of sarkosyl (Tao et al. 2010). Detergent combinations used ranged from 1-4% Triton X-100 ± 10-40 mM CHAPS, gently rocking for 30 minutes at RT, prior to incubation with GS4B affinity resin.

***Cloning of $His_6$-Fusion Proteins***

The CTD of human SREBP-2 (amino acid 556 to 1142) was PCR amplified from plasmid template (I.M.A.G.E. ID 5498684, Geneservices) using Taq DNA Polymerase (NEB) using the following primer sets;

Forward: *5'* CTGCTGGTTCATGGGGAGCCAGTGAT *3'*

Reverse: *5'* CCAGGAGGCGGCAATGGCAGT *3'*.

The resulting PCR product was ligated into pBADtopo TA expression vector (Invitrogen) as per manufacturer's guidelines. Ligations were transformed into Top10 chemically competent cells, supplied with the vector, as per manufacturer's guidelines.

The CTD of human SREBP-1 (amino acid 559 to 1148) was PCR amplified from plasmid template (I.M.A.G.E. ID 5786483, Geneservices) using Taq DNA Polymerase (NEB) using the following primer sets;

Forward: *5'* GTCTCCTTGGTGCTTCTCTTTGTCTA *3'*

Reverse: *5'* CGGGGTGTAGCTGGAAGTGACAGT *3'*

The resulting PCR product was ligated into pBADtopo TA expression vector as per manufacturer's guidelines. Ligations were transformed into Top10 chemically competent cells, as per manufacturer's guidelines.

Positive transformants were identified by restriction digest screens, followed by sequence verification by Sanger sequencing (Lifesource Bioscience).

***Induction and Lysis of His-Fusion Proteins***

Overnight cultures containing *E.coli* expressing His-fusion proteins were inoculated 1:100 in pre-warmed LB media containing ampicillin at 75 μg/ml (either 500 ml or 5L (5 x 1L) of LB, as indicated). Cultures were grown to an $OD_{600}$=0.5 (37$^{o}$C, 200 rpm), at which point L-arabinose was added to a final concentration of 0.02%. Cultures were induced for a period of 4 hours. Bacteria were pelleted by centrifugation at 7700 x g for 15 minutes at 10$^{o}$C. Pellets were stored at -20$^{o}$C until ready for affinity purification.

For lysis prior to purification, bacterial pellets were thawed on ice and re-suspended in 1X His-Native Loading Buffer (50 mM $NaH_2PO_4$ pH 8, 500 mM NaCl, solution adjusted to pH 8) (50 ml per 5L pellet). Lysozyme was added to a concentration of 1 mg/ml and samples were incubated on ice for 30 minutes. Samples were then sonicated on ice for 10 x 40 second bursts on 75% intensity, with minimum of 1 minute rests on ice in between (Soniprep 150). Cell debris was removed by centrifugation at 3000 x g for 15 minutes at 4$^{o}$C. Supernatants contained the soluble protein fraction and could be stored at -20$^{o}$C prior to nickel-affinity purification.

***Purification of His-Fusion Proteins***

Probond nickel affinity resin (Invitrogen) was equilibrated in 1X His-Native Loading Buffer from the EtOH storage solution, as per manufacturer's guidelines. 5 ml resin was added per 50 ml soluble protein fraction and incubated for 1.5 hours, gently rocking at 4$^{o}$C. Resin was sedimented by centrifugation at 800 x g for 1 minute and the supernatant was designated the flow through fraction. The resin was washed by gentle re-suspension in 1X His-Native Wash Buffer (50 mM $NaH_2PO_4$ pH 8, 500 mM NaCl, 20mM Imidazole pH 6, solution adjusted to pH 8) (25 ml per 5 ml resin),

followed by centrifugation at 800 x g for 1 minute. The resin was washed a total of 3 times. 1X His Elution Buffer (50 mM $NaH_2PO_4$ pH 8, 500 mM NaCl, 250 mM Imidazole, solution adjusted to pH 8) was then incubated with the resin for 1 hour, gently rocking at 4°C. This suspension was then loaded onto a disposable column (PD-10), the resin was allowed to settle by gravity for 20 minutes at 4°C, and then elution fractions were collected, also at 4°C. Fractions were analysed by SDS-PAGE, immunoblot with anti-His (A00186-100, Genescript (1:2500 dilution)), or subject to fast protein liquid chromatography (FPLC), as indicated.

***SDS-PAGE and Immunoblot Analysis of Bacterial Proteins***

Bacterial cell pellets were resuspended in 1X Laemmli buffer for analysis (4% SDS, 10% 2-mercaptoehtanol, 20% glycerol, 0.004% bromophenol blue, 0.125 M Tris-HCl, pH to 6.8), while soluble fractions was mixed in a 1:1 ratio with the 2X Laemmli buffer. All samples were boiled for 5 minutes in a water bath. Sample volumes of 15 µl were loaded onto a 0.75 mm SDS-PAGE gel in all cases. Samples were run through the stacking gel (5% acrylamide) at 75V and through the resolving gel (10% acrylamide) at 150V. The 1X SDS-PAGE running buffer (25 mM Tris, 250 mM Glycine (pH 8.3), 0.1% SDS) was ice-cold prior to use. Separated protein samples were transferred to Whatman Protran nitrocellulose membranes nitrocellulose membrane using wet transfer conditions (1X Transfer Buffer: 25 mM Tris, 192 mM Glycine, 20% methanol, 0.1% SDS) and running at 100V for 1 hour. Sponges, filter paper and membranes were all equilibrated in transfer buffer for 10 minutes prior to cassette assembly and transfer. An ice pack was included during transfer and the buffer was ice-cold prior to use. Successful transfer was confirmed by Ponceau S staining of the nitrocellulose membrane prior to antibody detection.

Membranes were then gently washed in 1X TBS-T (50 mM Tris-Cl, pH 7.6; 150 mM NaCl, 0.1% Tween) to remove the Ponceau S stain, followed by incubation with blocking buffer (5% dry skimmed milk (Marvel) dissolved in 1X TBS-T) for 1 hour gently rocking at RT. Blocking buffer was removed and membranes were probed with the indicated primary antibodies overnight (16 hours) gently rocking at 4$^{o}$C. Primary antibodies were removed and stored at -20$^{o}$C for reuse. Membranes were washed 3 x 10 minutes with 1X TBS-T, gently rocking at RT. This was followed by incubation with the appropriate infrared (IR)-conjugated secondary antibody for 1 hour, gently rocking at RT (mouse IRDye680LT (1:20 000), rabbit 1RDye800CW (1:15 000), Li-cor). Membranes were washed 3 x 10 minutes with 1X TBS-T, gently rocking at RT, followed by detection on the Odyssey IR imaging system (Li-cor).

***Gel Filtration Fast protein liquid chromatography (FPLC)***

Analysis was performed on an AKTA purification system (GE Life Sciences), as per the recommended guidelines. All buffers were de-gased prior to use. Samples were sterile-filtered prior to use using 0.45 micron syringe filter. BSA was used as an elution profile control protein.

The sample was first run through a Hi-Trap desalting column (GE Life Sciences) to exchange the eluted proteins from the imidazole containing His Elution Buffer to 1X His-Native Loading Buffer. Samples were taken up 0.7 ml at a time into a 1 ml needle-syringe, all bubbles were removed and the sample was injected. The flow rate was maintained at 0.5 ml per minute and protein concentration was assessed by absorbance peaks at a wavelength of 280 nm ($A_{280}$). All fractions containing high $A_{280}$ readings were saved to apply to the FPLC column.

The Superdex gel filtration column (GE Life Sciences) was equilibrated with 1X His-Native Loading Buffer, as per manufacturer's guidelines. Samples were taken up 0.7 ml at a time into a 1 ml needle-syringe, all bubbles were removed and the sample was injected. Fractions were collected at a rate of 0.5 ml per minute. This was injection/collection process was repeated until the total sample volume had been applied to the column. Fractions were analysed by SDS-PAGE or immunoblot, as indicated.

***Peptide Array Analysis***

Peptide arrays were provided by Dr Emilie Tresse from the lab of Prof. Rosemary O' Connor, School of Biochemistry and Cell Biology, UCC. Arrays consisted of the amino acid sequence of $SCAP_{CTD}$ immobilised on a cellulose membrane in a series of 18-mer peptides with each peptide overlapping with the next by a five amino acids. The array was received dried in a sealed plastic bag.

The array was bathed in 100% ethanol for 5 minutes at RT, and then equilibrated in 1X TBS-T for 10 minutes. The array was then blocked with a solution of 5% milk/1X TBS-T, gently rocking for 1 hour at RT. The membrane was then incubated with 6 mLs of the eluted fractions of the indicated fusion protein containing 1% milk gently rocking overnight at $4^{o}C$ (16 hours). The array was then washed 3x5 minutes in 1X TBS-T, followed by incubation with anti-His primary antibody (A00186-100, Genescript (1:2500 dilution in 5% milk/TBS-T)) gently rocking for 2 hours at RT. The array was washed 3x5 minutes in 1X-TBS-T, followed by incubation with HRP-conjugated anti-mouse secondary antibody (NXA931, GE Healthcare (1:1000 dilution in 5% milk/TBS-T)) gently rocking for 1 hour at RT. Fusion protein binding

was visualised by ECL. Peptides with fusion protein positively bound were indicated by dark spots, while unbound peptides remained blank.

Alanine scanning arrays were treated in the same way as peptide arrays, as described above.

***Cell Culture***

A-498, DU-145, HeLa, HeLa-PHGL, HT-29, KYSE-70 and MeWo cell lines were maintained in RPMI-1640 medium containing 10% foetal bovine serum (FBS), 1% Penicillin/Streptomycin (P/S) at 37$^{o}$C, 5%$CO_2$. HepG2 and MCF-7 cell lines were maintained in DMEM containing 10% FBS, 1% (P/S) at 37$^{o}$C, 5%$CO_2$. For all cell lines, FS culture conditions refer to cells cultured in the aforementioned full-serum formulations. For some experimental conditions, cells were incubated with media containing 10% lipid-depleted serum (LDS) in place of 10% FBS, and this is referred to as LDS culture conditions.

For all experiments, cells were seeded on day 1 at 40% confluency. In a 24-well tissues culture plate (Sarstedt) with a growth surface area of 2 $cm^2$, this corresponds to the following cell number seeded in 500 µl FS media per well: A-498 (4 x $10^4$), DU-145 (7 x $10^4$), HeLa (4 x $10^4$), HepG2 (1.2 x $10^5$), HT-29 (1 x $10^5$), KYSE-70 (1 x $10^5$), MCF-7 (1 x $10^5$), MeWo (5 x $10^4$).

***Preparation of LDS***

LDS was prepared by incubating 100 ml of FBS with 2 g fumed silica (Sigma) gently swirling overnight at room temperature. The LDS was clarified by centrifugation at 2000 x g for 10 minutes at 10$^{o}$C. The supernatant was sterile filtered using 0.45 micron filter, aliquoted and stored at -20$^{o}$C. Cholesterol content

was assayed using a cholesterol assay kit (Audit Diagnostics, Ireland) and was >99% depleted of cholesterol compared to FBS.

***Cloning of luciferase gene reporters***

The HMGCR promoter (-270 to +77) was amplified from human DNA by PCR and cloned into both the *Firefly* luciferase reporter plasmid pGL3-Basic (Promega) and the *Guassia* luciferase plasmid pGLuc-Basic (New England Biolabs) using EcoRI and HindIII restriction sites. The LDLR promoter (-590 to +93) was also amplified from human DNA by PCR and cloned into pGL3-Basic vector using BglII and HindIII restriction sites and into pGLuc-Basic vector using EcoRI and HindIII restriction sites. Cloned promoter sequences were verified by DNA sequencing.

***DLR Assay***

HeLa cells were seeded at 4 x $10^4$ cells in 500 µL FS media per well in a 24-well plate ($37^oC$, 5% $CO_2$). After 18-24 hr incubation, cells were transfected for 6-9 hours with 450 ng of reporter plasmid and 50 ng of control reporter plasmid (pRL-TK, Promega) using 1 µL TurboFect (Thermoscientific) in 100 µL serum-free media, according to manufacturer's instructions. Following transfection, media was replaced with 500 µL LDS media and incubated for a further 6 hours. 25-OHC was then added to a final concentration of 1.25 µM and incubation was continued for a further 16 hours. Cells were harvested by aspirating media, washing once in ice-cold phosphate buffered saline (PBS), and incubated shaking for 30 minutes in 100 µL Passive Lysis Buffer (Promega) at room temperature. 10 µL of each sample was removed and assayed for *Firefly* and *Renilla* luciferase activity using a microplate luminometer. The substrates used (luciferin and coelenterazine for *Firefly* and

*Renilla* luciferases respectively) were purchased from Nanolight Technology and the DLR assay buffers were prepared from individual components essentially as described previously (16).

*Firefly* luciferase assay buffer contained 25 mM glycylglycine, 15 mM $K_2PO_4$ pH8, 4 mM EGTA, 15mM $MgSO_4$, 0.1 mM coenzyme-A, 1 mM DTT, 2 mM ATP, 75 µM luciferin. *Renilla* luciferase assay buffer contained 1.1 M NaCl, 2.2 mM EDTA, 220 mM $K_2PO_4$ pH5.1, 0.44 mg/mL BSA, 1.3 mM $NaN_3$, 1.43 µM coelenterazine. Stock solutions for all of the above were prepared in water, except for coelenterazine which was prepared in methanol and kept protected from light.

***SSLR Assay***

Transfection was as described for the DLR assay. Total amount of plasmid DNA transfected was maintained at 500ng and comprised of reporter plasmid or a combination of reporter plasmid and empty vector plasmid. Following transfection, media was replaced with 500 µL LDS media. Small aliquots of media were removed at intervals and stored at -20$^{o}$C until assayed for luciferase activity. 25-OHC treatment was as described for the DLR assay. 10 µL samples were assayed for *Guassia* luciferase activity using a microplate luminometer in the *Renilla* luciferase assay buffer. A simple *Guassia* luciferase assay buffer (PBS with 1.43 µM coelenterazine) was also tested and yielded similar results.

***HeLa Cell Line Stably Expressing pGLuc-promHMGCR***

HeLa cells were seeded at 40% confluency in under FS conditions in 10 cm dishes. Cells were transfected at 80-90% confluency with 15 µg of pGLuc-promHMGCR using 30 µl TurboFect reagent (Thermo Fisher Scientific) added in 3 ml of serum-

free media. The transfection mixture was removed and replaced with fresh FS medium after 6 hours incubation. Cells were trypsinized 48 hours post-transfection and re-seeded at different dilutions in FS media supplemented with 400 µg/ml G-418. Every 3-4 days G-418/FS media was renewed until individual clones were identified. These individual clones were then isolated using cloning discs and grown up in 24 well plates. Stable integrants were identified by trypsinizing and re-seeding cells and assaying for the highest consistent luciferase activity levels and responsiveness to 25-OHC treatment under LDS conditions.

***Effect of PGRMC1 and progesterone on SREBP luciferase reporter activity***

On day 1, HeLa-PHGL cells were seeded at 4 x $10^4$ cells in 500 µL FS medium per well in a 24-well plate (37$^o$C, 5% $CO_2$). On day 2, cells were transfected with 0.5 µg of each of the indicated plasmids for a total of 1 µg of plasmid DNA to 2µL of TurboFect transfection reagent (Thermoscientific) in 100 µL of serum-free medium, per well, according to manufacturer's instructions. Following transfection, media was replaced with either FS or LDS media, containing progesterone or EtOH only control, as indicated in the figure legend. Aliquots of media (25µl) were taken at 24 and 48 hour timepoints and stored at -20$^o$C until ready to be assayed for *Gaussia* luciferase enzyme activity. MTT assay was then performed immediately after the 48 hour timepoint was taken to determine cell viability in response to the treatments.

***Bioinformatic analysis of INSIG1***

Sequences homologous to the human INSIG1 protein sequence were retrieved from the NCBI database using their protein-protein basic local alignment search tool (pBLAST). mRNA sequences corresponding to each of the INSIG1 homologs were retrieved via the desource accession number associated with each protein sequence.

All sequences were loaded into the alignment explorer function within Molecular Evolutionary Genetics Analysis (MEGA) v4.0 and aligned using ClustalW (Tamura et al. 2007; Higgins et al. 1994). Phylogenetic tree was generated based on the INSIG1 protein sequence alignment using the Neighbor-Joining method in MEGA, and tree topology confidence scores were calculated using the Bootstrap test of phylogeny (Nei & Kumar 2000; Saitou & Nei 1987). Alignments were saved in FASTA format to allow analysis of conserved regions of interest using GeneDoc multiple sequence alignment editor. Alignments were then transferred to Microsoft Word by saving the alignment blocks in rich text format (.rtf), to facilitate annotation of residues of interest.

***Generation of INSIG1 isoform mutants by site directed mutagenesis***

INSIG1 mutants were generated using Stratagene Quikchange II kit (Agilent Technologies), as per manufacturer's guidelines. pCMV6-AC-HA -INSIG1 was used as the template plasmid for mutagenesis. This plasmid was generated by sub-cloning the INSIG1 cDNA sequence from pCMV6-AC-Myc/DDK-INSIG1 (RC200312, Origene) into the precision shuttle pCMV6-AC-HA destination vector (PS100004, Origene). The primer sets used for mutagenesis were designed using the Stratagene custom primer design software programme (http://labtools.stratagene.com/QC).

$INSIG1_{WT}$:
Forward: 5' GATCTGCCGCCGCGATCCCGATGCCCAGATTGCACG 3'
Reverse: 5' CGTGCAATCTGGGCATCGGGATCGCGGCGGCAGATC 3'

$INSIG1_{2ND\text{-}AAA}$ :
Forward: 5' CGGCCAAGGTTGGGGAGAAAATCAACGTTTCCGTGTCCG 3'
Reverse: 5' CGGACACGGAAACGTTGATTTTCTCCCCAACCTTGGCCG 3'

$INSIG1_{1ST\text{-}AAA}$:
Forward: 5' GCCGCCGCGATCGCCAAACCCAGATTGCACGACC 3'
Reverse: 5' GGTCGTGCAATCTGGGTTTGGCGATCGCGGCGGC 3'

Positive transformants were confirmed by Sanger Sequencing (GATC).

***Comparing the effect of INSIG1 isoform mutants on SREBP luciferase reporter activity***

On day 1, HeLa-PHGL cells were seeded at 40% confluency in 500µl in 24-well plates. On day 2, cells were transfected with either pCMV6-AC-HA empty vector, or the indicated INSIG isoform plasmid. A ratio of 0.5µg of DNA to 1µl TurboFect transfection reagent was used, as per manufacturer's guidelines, in 100µl of serum-free media. The total 600µl transfection mixture was removed from cells following a six hour incubation and replaced with LDS media with or without 25-OHC (1µg/ml), as indicated. Cells were cultured for a further 20 hours, after which a 50µl media aliquot was removed and stored at -20$^{o}$C, until ready to be assayed for luciferase activity. MTT assay was performed to ensure an equal level of cell viability.

***Comparing the effect of INSIG1 isoform mutants on HMGCR protein stability***

On day 1, HeLa-PHGL cells were seeded at 40% confluency in 10 ml FS media in 10 cm dishes. On day 2, cells were transfected with either pCMV6-AC-HA empty vector (Origene), or the indicated INSIG isoform plasmid. A ratio of 8µg of DNA to 16µl TurboFect transfection reagent was used, as per manufacturer's guidelines, in 1 ml of serum-free media. The total 11ml transfection mixture was removed from cells following a six hour incubation and replaced with LDS media with or without 25-OHC; (concentration of 300 ng/ml, 600 ng/ml or 900 ng/ml, as indicated). Cells were cultured for a further 20 hours. Prior to harvesting the cells the media was aspirated and the cell monolayer was washed once with ice-cold PBS. Cells were scraped into 500 µl of ice-cold PBS and centrifuged at 1500 rpm for 5 minutes in a tabletop centrifuge at 4$^{o}$C. The PBS was aspirated and the cell pellets were stored at -20$^{o}$C until ready for immunoblot analysis.

***Preparation of Sterol Compounds***

Cholesterol, 25-hydroxycholesterol (25-OHC (Avanti Polar Lipids) ) and 19-hydroxycholesterol (19-OHC (Santa Cruz) ) were all prepared as 1 mg/ml stocks in EtOH, and stored at -20$^{o}$C. Betulin was prepared as a 1 mg/ml stock in cell culture grade dimethyl-sulfoxide (DMSO).

Methyl-β-cyclodextrin (MβCD)-sterol complexes were prepared as described previously (Brown et al. 2002a; Radhakrishnan et al. 2007a). Briefly, cholesterol and 25-OHC were prepared as 10 mg/ml (25 mM) stocks in EtOH. An aliquot of 100 µl of sterol stock solution was added drop-wise to a stirred 1 ml solution of 5% w/v MβCD at 80$^{o}$C, until the solution became clear. This solution then contained sterols at a final concentration of 2.5 mM. The MβCD-sterol complexes were then lyophilised using a vacuum-centrifuge at 45$^{o}$C on high pressure (Thermo Scientific) to remove the ethanol from the solution, then resuspended in 1 ml millipore water (sterol stock concentration remains at 2.5 mM). A no-sterol MβCD solution was also prepared in the same manner to be used as vehicle only control.

***Transient transfection of cell lines with pGLuc-promHMGCR***

Cell transfection was optimised for each cell line using pCMV-GLuc (NEB), for cells seeded at 40% confluency in a 24-well plate. For all cell lines a ratio of 0.5 µg plasmid DNA to 1 µl transfection reagent was determined to be optimal per well. Maximal transfection efficiency was achieved for A-498, KYSE-70 and MeWo using Lipofectamine 2000 (Invitrogen), for DU-145, HT-29, and MCF-7 using Xtremegene (Roche), and for HepG2 and HeLa using TurboFect (Thermo

Scientific). All transfections were performed according to manufacturer's guidelines, with cells at approximately 80% confluency at the time of transfection. Transfection mixtures were added to 500 µl per well (Optimem or existing FS media) and were removed following 6 hour incubation in all cases. Media replaced was either FS or LDS media, as per the indicated experiment.

***Dose-Response Curves***

On day 1 cells were seeded at 40% confluency in 24-well plate in 500 µl under FS conditions. On day 2, cells (except HeLa-PHGL) were transfected with pGLuc-promHMGCR, as described above. Following six hours incubation, the transfection mixture was removed replaced with either 500 µl FS or LDS media only. Cells were incubated for a further six hours, at which point a 50 µl aliquot of media was removed for normalisation purposes (T6). The treatments of statin and/or oxysterols were made up in concentrated amounts in either FS or LDS media, such that 50µl volumes could be added back to the remaining 450µL per well, to return the total culture volume per well to 500µl that then contained the indicated final concentrations of statin and/or oxysterols for each cell line (as described in the associated figure legends). Cells were incubated with treatments for a period of 48 hours, after which a 50µl aliquot of media was removed for end point luciferase analysis (T48). Media samples were stored at -20$^{o}$C until ready for luciferase analysis. MTT assay was then performed immediately to determine cell viability. An Excel add-in ED50V10-2 was used for calculating half maximal effective concentration of statin ($ED_{50}$), calculated from the MTT dose-response curves.

***Luciferase Assay of SREBP Reporter Activity***

Media samples were thawed and 10µl was transferred to a polystyrene, solid white 96-well microplate, which is suitable for luciferase analysis (Nunc, Thermo Fisher Scientific). Samples were assayed for *Guassia* luciferase activity using a microplate luminometer (Veritas) which auto-injects 50µl of 1X PBS containing coelenterazine (Nanolight Technologies) at a concentration of 1.43 µM. Coelenterazine was added fresh to the 1X PBS prior to use from a 1.43 mM stock in methanol which was stored protected from light at -20$^{o}$C.

***MTT Assay of Cell Viability***

The 3-(4, 5-dimethylthiazol-2-yl)-2, 5-diphenyltetrazolium bromide (MTT) assay was optimised for use as an end-point analysis for experiments described above. Stocks were prepared by dissolving MTT powder in phenol-red-free RPMI-1640 media at a concentration of 5mg/ml, and stored at -20$^{o}$C (protected from over-exposure to light). MTT was added to cells at a final concentration of 0.5mg/ml and incubated for 90minutes at 37 $^{o}$C, 5% $CO_2$ (ie. 50µl of MTT stock solution was added to 450µl remaining media, per well). All media was the aspirated carefully and purple formazan crystals were dissolved instantly upon addition of 150µl DMSO per well. Aliquots of MTT samples were transferred to a 96-well microtest plate (Sarstedt) and absorbance read at 570nm on an Infinite 2000 spectrophotmetric plate reader (Tecan).

***Immunoblot Analysis of SREBP and HMGCR in response to statin and oxysterols***

For immunoblot analysis, experiments were performed in 10 cm tissue culture dishes. Cells were seeded at 40% confluency on day 1 in FS conditions. On day 2, media was aspirated and replaced with either FS or LDS media, containing the indicated concentrations of statin and/or oxysterols for each cell line (as described in the associated figure legends). All treatments contained mevalonate at 100 μM to maintain cell viability. Cells were incubated with treatments for a period of 48 hours. Prior to harvesting the cells, media was aspirated and the cell monolayer was washed once with ice-cold PBS. Cells were transferred to eppendorf tubes in 500 μl of ice-cold PBS using sterile cell scrapers (Sarstedt) and centrifuged at 1500 rpm for 5 minutes in a tabletop centrifuge at 4$^{o}$C. The PBS was aspirated and the cell pellets were stored at -20$^{o}$C until ready for analysis.

***Immunoblot Analysis (mammalian samples)***

For regular cell lysis, cell pellets were resuspended in ice-cold Radio Immuno Precipitation Assay (RIPA) buffer (150 mM sodium chloride, 1.0% NP-40, 0.5% sodium deoxycholate, 0.1% SDS, 50 mM Tris, pH 8.0) containing 1X Halt protease inhibitor cocktail (Thermo Fisher Scientific) and 1mM PMSF. For regular cell lysis, cells were incubated for 1 hour with end-over-end rotation at 4$^{o}$C. Cell debris was removed by centrifugation for 10 minutes at max on tabletop centrifuge at 4$^{o}$C. The soluble fraction was mixed in a 1:1 ratio with the 2X Laemmli buffer for analysis (4% SDS, 10% 2-mercaptoehtanol, 20% glycerol, 0.004% bromophenol blue, 0.125 M Tris-HCl, pH to 6.8) and boiled for 5 minutes in a waterbath. For detection of membrane proteins a homemade whole cell lysis buffer was used (1X Buffer: 10% SDS, 4 M Urea, 40 mM Tris-HCl pH 6.8, 9% Glycerol, 50 mM DTT 2.5 mM β-

mercaptoethanol, 0.02% Bromophenol blue) which is based on a combination of buffers used by the Brown and Goldstein lab (ref). Samples were not boiled. Instead, resuspended whole cell pellets (300 µl per 10 cm dish) were vortexed briefly, incubated in a water bath at 37$^{o}$C for 30 minutes, sonicated at 20% power for 6 x 10 second bursts until the DNA has been sheared. This was followed by another incubation at 37$^{o}$C for 30 minutes. Sample volumes of 15 µl were loaded onto a 0.75 mm SDS-PAGE gel in all cases. Samples were run through the stacking gel (5% acrylamide) at 75V and through the resolving gel (10% acrylamide) at 120V. The 1X SDS-PAGE running buffer (25 mM Tris, 250 mM Glycine (pH 8.3), 0.1% SDS) was ice-cold prior to use. Separated protein samples were transferred to Whatman Protran nitrocellulose membrane using wet transfer conditions (1X Transfer Buffer: 25 mM Tris, 192 mM Glycine, 20% methanol, 0.1% SDS) and running at 100V for 1 hour. Sponges, filter paper and membranes were all equilibrated in transfer buffer for 10 minutes prior to cassette assembly and transfer. An ice pack was included during transfer and the buffer was ice-cold prior to use. Successful transfer was confirmed by Ponceau S staining of the nitrocellulose membrane prior to antibody detection. Membranes were then gently washed in 1X TBS-T (50 mM Tris-Cl, pH 7.6; 150 mM NaCl, 0.1% Tween) to remove the Ponceau S stain, followed by incubation with blocking buffer (5% dry skimmed milk (Marvel) dissolved in 1X TBS-T) for 1 hour gently rocking at RT. Blocking buffer was removed and membranes were probed with the indicated primary antibodies overnight (16 hours) gently rocking at 4$^{o}$C. Primary antibodies were removed and not saved for reuse (except actin). Membranes were washed 3 x 10 minutes with 1X TBS-T, gently rocking at RT. This was followed by incubation with the appropriate horseradish peroxidise (HRP)-conjugated secondary antibody for 1 hour, gently rocking at RT. Membranes were

washed 3 x 10 minutes with 1X TBS-T, gently rocking at RT, followed by enhanced chemiluminescent (ECL) detection. Primary antibodies used were anti-SREBP2 1C6 (sc-13552, Santa Cruz (1:200 dilution)), Santa Cruz), anti-HMGCR (sc-271595, Santa Cruz (1:500 dilution)), anti-FLAG (F1804, Sigma (1:1000 dilution)), anti-HA (MMS-1001R, Covance (1:1000 dilution)), anti-β-Actin (A5441, Sigma (1:1000 dilution)). (HRP)-conjugated secondary antibodies used were Anti-mouse IgG (NXA931, GE Healthcare (1:1000 dilution)), Anti-rabbit IgG (NA934V, GE Healthcare (1:1000 dilution)).

***ECL Detection***

Excess moisture was removed from the membrane by touching a corner (ie. not a region with transferred protein) against tissue. ECL substrate (Pico, Thermo Scientific) was mixed fresh prior to use, the membrane was covered with a thin layer and incubated for 5 minutes at RT. Excess substrate was removed from the membrane, again by touching a corner against tissue and the membrane was placed between plastic. Membranes were brought to the dark room where several exposures to CL-XPosure film (Medical Supply Company) using a x-ray film cassette were taken and developed using a laboratory scale-developer (Kodak).

***Measurement of Apoptosis/Cell Cycle Analysis by DNA Content***

On Day1, HeLa-PHGL cells were seeded at 40% confluency (1.66 x $10^6$ cells) in 10cm dishes (Sarstedt) in 10ml FS media. On Day2, media was replaced to contain simvastatin, with or without 25-OHC at the concentrations indicated in the figure legends. Cells were incubated with treatments for a period of 24 hours. Cells were then harvested in trypsin, centrifuged at 1500 rpm and the pelleted cells were washed

once in ice-cold 1X PBS. Cells were centrifuged at 1500 rpm and the pelleted cells were resuspended by adding 1ml of ice-cold 70% EtOH drop-wise, while vortexing the sample. Samples were incubated for 30 minutes at RT. Cells were then stored at -20$^{o}$C for at least 24-hours. Cells were then removed from the EtOH solution by centrifugation at 200xg for 10 minutes at 4$^{o}$C. The cell pellet was resuspended in 1 ml 1X PBS/0.2%Triton X-100 and incubated at RT for 10 minutes. Cells were removed from suspension by centrifugation at 200 x g for 10 minutes at 4$^{o}$C, and then washed once with 1X PBS. Cells were centrifuged at 200 x g for 10 minutes at 4$^{o}$C, then resuspended in 250 µl of DNA staining solution (100µg/ml propidium iodide (PI), 0.2mg/ml RNAse A (DNAse-free) in PBS). An untreated, no PI control was also included. Samples were transferred to FACS analysis tubes, the open tops covered with parafilm to prevent evaporation, and incubated in a water bath for 30 minutes at 37$^{o}$C. Sample were then analysed on flow cytometer (Accuri) using the recommended parameters for PI fluorescence detection. (excitation-488nm, red fluorescence emission-600 nm). 40,000 events were collected.

***Statistical Analysis***

Statistical analysis was performed using Student's *t*-test, two-way ANOVA or mixed model ANOVA (as indicated) to evaluate the difference between experimental and control groups. Significance was defined as *$p<0.05$, **$p<0.005$ or $p<0.000\%$, as indicated.

# Chapter 3
## Mapping the SCAP:SREBP Interaction Site

**Abstract**

The sterol response element binding proteins (SREBPs) are a family of transcription factors which are central to regulating *de novo* lipid biosynthesis. The activity of the SREBPs is regulated by the requirement to cleave the amino-terminal transcription factor domain from the inactive precursor protein. This cleavage event occurs in response to the sterol requirements of the cell and requires interaction of the SREBPs with the SREBP cleavage activating protein (SCAP). SCAP acts as a sensor for cellular sterol levels and has an essential role in chaperoning the SREBPs from their location in the ER to the Golgi where the cleavage takes place.

The interaction between SCAP and the SREBPs is mediated by their respective carboxy-terminal regulatory domains (CTDs). These CTDs each consist of over 500 amino acids. Mapping the exact SREBP binding site on SCAP would contribute to the knowledge base surrounding SREBP transcription factor regulation. In addition, mapping the precise site on SCAP which binds SREBP would be the first step in allowing for development of a small molecule inhibitor of the SCAP-SREBP interaction which could have potential use for treatment of a number of conditions including atherosclerosis, obesity and cancer. This chapter describes the steps taken towards identifying the residues within SCAP which bind each SREBP isoform using a peptide array approach. Numerous obstacles were encountered in the purification of the SREBP proteins required to probe the peptide array of SCAP. In this chapter the measures taken to overcome these obstacles to obtain purified SREBP protein are described. The results of the peptide array analysis have highlighted peptide regions within SCAP which may be key to mediating its interaction with SREBP1. These results require further investigation.

## Introduction

The Sterol Response Element Binding Proteins (SREBPs) are a family of transcription factors involved in the regulation of lipogenic gene expression. The SREBPs are distinct from most other transcription factors in that they are translated as inactive precursor proteins where the amino terminus transcription factor domain (NTD) is tethered to the endoplasmic reticulum (ER) via two transmembrane helices followed by a large regulatory domain at the carboxy terminus (CTD) (Hua et al. 1993b; Hoppe et al. 2001). Immediately following their translation and insertion into the ER membrane, the SREBPS are bound by the SREBP cleavage activating protein (SCAP) (Sakai et al. 1997). SCAP is essential for facilitating the proteolytic release of the active SREBP NTD. All three isoforms of SREBP (1a, 1c, 2) appear to bind the one isoform of SCAP, as evidenced by the amounts of the active form of all three SREBP isoforms increasing in transgenic mice expressing a constitutively active form of SCAP (Korn et al. 1998). This interaction with SCAP is essential for SREBP protein stability and in the absence of SCAP, SREBP proteins are rapidly degraded (Rawson et al. 1999). Liver-specific knockout of SCAP results in a decrease in the amount of all SREBP proteins and a decrease in expression of SREBP target genes (Matsuda et al. 2001). Germline deletion of SREBP2 in a mouse model is embryonically lethal, thus a germline deletion model of SCAP has not been attempted (Shimano, Shimomura, et al. 1997).

Activation of SREBPs is a tightly regulated process and is regulated in response to fluctuations in cellular sterol levels in a negative feed-back manner (Brown & Goldstein 2009). This feedback regulation is necessary as excessive levels of cholesterol and its oxidation products have been shown to be toxic to the cell

(Simons & Ikonen 2000; Aye et al. 2010). Aberrant SREBP activation also leads to high circulating cholesterol and fatty acid levels which can lead to disease such as atherosclerosis and obesity, respectively (Eberlé et al. 2004). Radhakrishnan et al previously showed that ER membrane cholesterol levels are maintained at 5% through a combination of cholesterol biosynthesis and uptake mediated by SREBP activity, and that an increase of just 0.5% above this threshold is sufficient to trigger feedback inhibition of SREBP (Radhakrishnan et al. 2008). ER membrane cholesterol levels are communicated to SREBP through the sterol-sensing domain of SCAP(Motamed et al. 2011). Competitive binding studies using unlabelled and [$^{3}$H]-labelled cholesterol revealed that cholesterol binds SCAP within this sterol sensing domain (Radhakrishnan et al. 2007b). SREBP activation is also regulated by other sterol-based compounds such as oxysterols, although threshold levels for these are less clear (Radhakrishnan et al. 2007b). It is clear, however, that certain oxysterols are more potent inhibitors of cholesterol biosynthesis and uptake *in vitro* than cholesterol itself.

Briefly, when cellular sterol levels are low, the SCAP-SREBP complex is transported from the ER to the Golgi where Golgi-resident proteases cleave SREBP at two sites to release the soluble transcription factor domain into the cytosol (Duncan et al. 1997a; Duncan et al. 1998; Sakai et al. 1996). This is then bound by the nuclear import protein, importin-β, which transports the transcription factor into the nucleus where is serves as an activator for a large number of target genes (Nagoshi et al. 1999; Nagoshi & Yoneda 2001). SCAP serves as the chaperone in this process as the COPII vesicle required for ER to Golgi transport assembles around Sec24 binding to a hexapeptide 'MALADL' sequence located near the membrane at the cytosol-facing loop 6 of SCAP (L.-P. Sun et al. 2007). Conversely,

when sterols reach sufficient levels, the SCAP-SREBP complex is retained in the ER through the combined action of SCAP undergoing a conformational change which prevents Sec 24binding, and SCAP interacting with the ER-retention protein INSIG (Adams et al. 2003; Brown et al. 2002a). Transport of the SCAP-SREBP complex to the Golgi is a central event for regulation of SREBP activation. Experiments in which the protease responsible for release of the NTD was relocated to the ER removed the requirement of ER to Golgi transport for SREBP target gene upregulation (DeBose-Boyd et al. 1999). SCAP is a key limiting factor in SREBP activation. SCAP expression is under the control of SREBP so levels of both increases in parallel (Nakajima et al. 1999b). Over expression of the membrane domain of SCAP alone has been shown to remove the sterol mediated feedback inhibition of SREBP activity through saturation of INSIG proteins and facilitate free delivery of the SCAP-SREBP complex to the Golgi for processing (Yang et al. 2000).

In 1997, Sakai et al demonstrated that the CTD of SCAP was sufficient to pull down the full length SREBP precursor protein (Sakai et al. 1997). Similarly the CTD of SREBP was found to be sufficient to pull down the full length SCAP protein. Thus the SCAP-SREBP interaction site has been localised to these two approximately 550 amino acid CTD regions. Although it plays a key role SCAP-SREBP interaction the CTD of SCAP is much less studied than its transmembrane region. Analysis of the SCAP amino acid sequence in 1996/8 showed that the $SCAP_{CTD}$ contained four/five Trp-Asp 40 (WD40) motifs (Hua et al. 1996; Nohturfft et al. 1998).

WD40 motifs are found in repeats of four to eight, and were originally defined as following a loose consensus sequence of $X^{6–94}$-[GH-$X^{23–41}$-WD]$^{N4–8}$ (where *N* is the

number of repeats) (Neer et al. 1994). The motifs also have defined strand regions A-D, which refer to folds formed by the motif (Figure 3.1A). Each motif folds in a β-sheet conformation such that the repeats come together to form a propeller-like structure, with each blade of the propeller comprising of strand A-C of one repeat, and strand D of the next repeat (Smith et al. 1999; Garcia-Higuera et al. 1996). Strand D is believed to be the most accessible region of each WD40 repeat. This propeller-like structure then acts as a platform in mediating protein-protein interactions. To date, all proteins containing WD40 repeats which have had their crystal structures solved indeed show this to be the case. However, although the consensus sequence indicates that four to eight repeats can be present in the SCAP CTD, all WD40 proteins that have crystal structures solved have seven to eight repeats forming the propeller, with the optimal beta propeller fold described as a seven bladed structure (Adams, Ron & P. a Kiely 2011; Cheng et al. 2004; Renault et al. 1998; Garcia-Higuera et al. 1996; Voegtli et al. 2003). Despite knowledge of the tertiary structure that these repeats tend to form, the loose nature of the consensus sequence which defines a WD40 repeat limits molecular homology modelling for proteins whose crystal structure is not yet formed. WD40 domain proteins are known to facilitate binding of multiple interacting proteins. For example, RACK1 contains 7 WD40 repeats, forms a beta-propeller structure and acts as a scaffold for multiple interacting protein partners (Chen et al. 2004; Adams, Ron & P. a Kiely 2011).

Since the discovery that the CTD region of SCAP binds SREBP, these WD40 domains have been predicted to mediate the interaction. Based on the literature available on other WD40 domain proteins, it is plausible that these domains are involved however WD40 repeats comprise just less than half of the entire CTD, and no work has been published to confirm their involvement. It has also been shown

that in other instances where the entire protein does not form the β-propeller structure that proteins may also interact with this non-WD40 region. Also, as mentioned, most other WD40 domain proteins interact with multiple other proteins. The only protein currently known to interact with the CTD of SCAP is SREBP. Thus the presence of WD repeats in this region offers the possibility of SCAP interacting with more proteins, and this may add additional layers of complexity to the already tightly regulated SREBP feedback process. It could also potentially reveal new roles for SCAP outside of SREBP regulation.

Our hypothesis is that SREBP1 and SREBP2 may bind to distinct regions within $SCAP_{CTD}$, possibly within different WD40 repeats. In this chapter the steps taken towards identifying the residues within SCAP which bind each SREBP isoform are described. Mapping the SREBP binding site on SCAP would provide valuable information on how SCAP differentially regulates activation of the different SREBP isoforms and would further contribute to the knowledge base surrounding SREBP transcription factor regulation. In addition, mapping the precise site on SCAP which binds SREBP would be the first step in allowing for development of a small molecule inhibitor of the SCAP-SREBP interaction which could have potential use for treatment of a number of conditions including atherosclerosis, obesity and cancer. The experimental design to investigate this hypothesis involved the cloning, over-expression and purification of both SREBP1 and SREBP2 CTDs. Purified protein was then used to probe a peptide array of $SCAP_{CTD}$ to identify residues of importance. However, numerous obstacles were encountered in the purification of the SREBP proteins. In this chapter the measures taken to overcome these obstacles to obtain purified SREBP protein are described. A bioinformatic approach was also taken to investigate the conservation of WD40 domains and to complement the

peptide array approach to possibly rule out false positives, since the crystal structure of SCAP has not yet been solved.

## Results

### *Bioinformatic Analysis of SCAP Carboxy Terminal Domain*

The human SCAP protein sequence contains two main domains, a sterol-sensing transmembrane domain and a large cytosolic CTD tethered to the ER membrane by the transmembrane region of the protein. The CTD of SCAP is known to contain 5 WD repeat motifs. Further analysis of human $SCAP_{CTD}$ protein sequence using Simple Modular Architecture Research Tool (SMART) identified the presence of a sixth WD repeat, now designated WD2 (Figure 3.1B). To investigate the conservation of these WD40 repeats, a multiple sequence alignment of SCAP protein sequences ranging from human to zebrafish was performed. This analysis revealed 46% sequence identity over the entire CTD region and an average of 70% identity within each WD40 repeat outside of WD2 (Figure 3.2). While this level of sequence conservation within the WD40 repeats is indicative of their importance, this makes it difficult to identify any critical residues of importance within the WD repeats which could be essential to the interaction. Also, since the crystal structure of SCAP is not solved, this makes it difficult to focus in on residues that may be available on the protein surface. However, while the crystal structure is not known, the folding of a WD repeat is quite well characterised. Based on the consensus sequence for a WD40 repeat, the region of each repeat predicted to be at the protein surface, strand d, is highlighted in Figure 3.1A. However, the distance of WD1 from WD2-6 suggests that it is too far to be a part of a beta propeller structure, and unless there is another unidentified WD40 repeat located between WD1 and WD2, then predicting the surface residues is not reliable.

SMART analysis of SCAP homolog sequences from *Drosophila (dSCAP)* and *Caenorrhabditis* species (*scp-1*) reveal conservation of the presence of WD40 repeats within the CTD, although the number of repeats are five and four, respectively (Figure 3.1B). The reduced number of repeats in these less complex organisms may be related to the fact that they have only one SREBP isoform. The conservation of WD40 repeats in such divergent species highlights their importance and suggests that they have a role in mediating the only known function of $SCAP_{CTD}$, which is interacting with SREBP.

A phylogenetic tree was constructed based on the multiple sequence alignment of SCAP from vertebrate species (Figure 3.1C). The reliability of this tree was assessed using the bootstrap test of phylogeny. The high bootstrap values illustrate the overall sequence conservation in SCAP vertebrate homologs.

Knowing the crystal structure of a protein assists in confirming true positive residues of importance identified by peptide array by informing as to which residues are accessible for binding. However the crystal structure of SCAP has not been solved. Thus, homology modelling was performed using SWISS-MODEL to generate a hypothetical 3D protein structure of the CTD of SCAP based on sequence similarity with other WD domain proteins which have crystal structures available. The best fit homology model for SCAP CTD was modelled based on RACK1 (Figure 3.3A). RACK1 is also a WD domain protein whose crystal structure is a seven-bladed propeller, which is characteristic of WD domain proteins. However half of the SCAP CTD is excluded from this model, which includes WD1. In the structure shown, WD2-WD6 are forced into the seven-bladed structure of RACK1 (Figure 3.3B). Thus, homology modelling was not deemed useful for SCAP.

**A)**

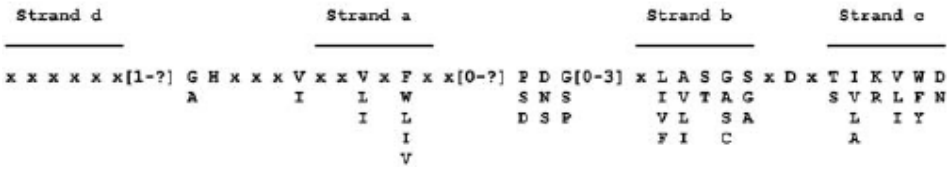
Strand d
Strand a
Strand b
Strand c
x x x x x x[1-?] G H x x x V x x V x F x x[0-?] P D G[0-3] x L A S G S x D x T I K V W D
A I L W S N S I V T A G S V R L F N
I L S D S P V L S A L I Y
I A
F I C
V

**B)**

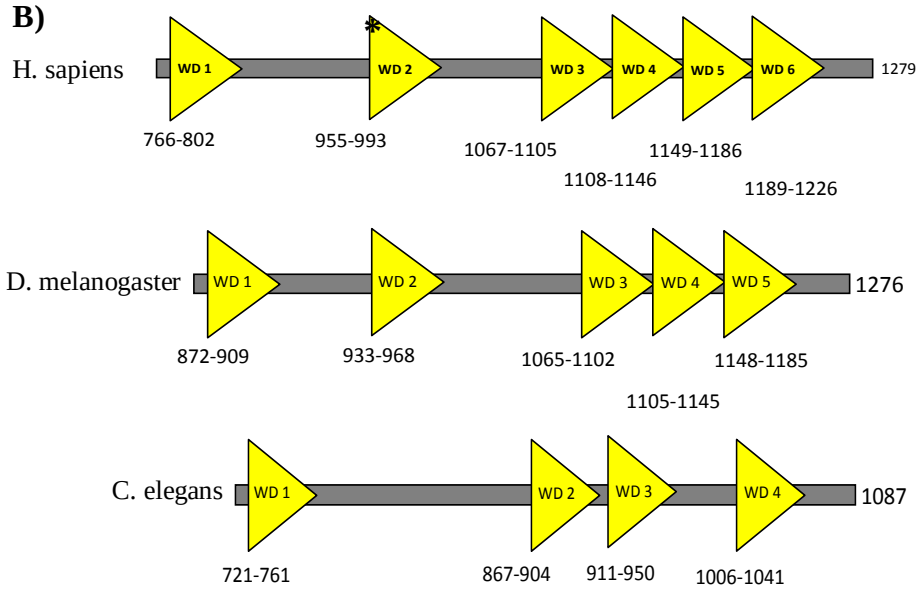
H. sapiens
WD 1
WD 2
WD 3
WD 4
WD 5
WD 6
1279
766-802
955-993
1067-1105
1108-1146
1149-1186
1189-1226
D. melanogaster
WD 1
WD 2
WD 3
WD 4
WD 5
1276
872-909
933-968
1065-1102
1105-1145
1148-1185
C. elegans
WD 1
WD 2
WD 3
WD 4
1087
721-761
867-904
911-950
1006-1041

**C)**

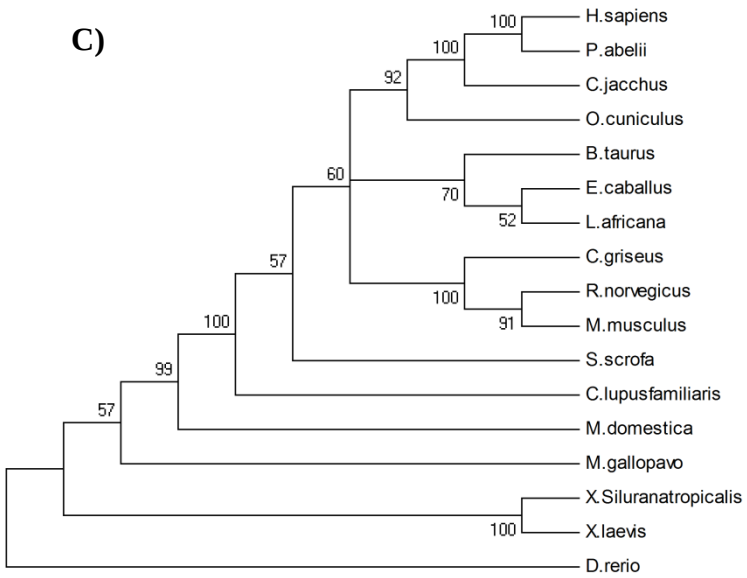
H.sapiens
P.abelii
C.jacchus
O.cuniculus
B.taurus
E.caballus
L.africana
C.griseus
R.norvegicus
M.musculus
S.scrofa
C.lupusfamiliaris
M.domestica
M.gallopavo
X.Siluranatropicalis
X.laevis
D.rerio
100
100
92
60
70
52
57
100
91
100
99
57
100

Figure 3.1. Conservation of WD40 repeat motifs within the carboxy terminal domain of SCAP. A) Consensus sequence for a WD40 repeat (taken from Neer *et al*, 1994). B) Schematic representation of WD40 repeat distribution within the carboxy-terminal domains of SCAP homologs from human, fruitfly and worm (* indicates the novel WD repeat identified using SMART motif analysis tool). C) Phylogenetic tree based on multiple sequence alignment of SCAP from vertebrates. Alignments were performed using Clustal W. The tree was constructed using the neighbourhood-joining method, and reliability was assessed using Bootstrap test of phylogeny. Analysis was performed in MEGA version 4.0.

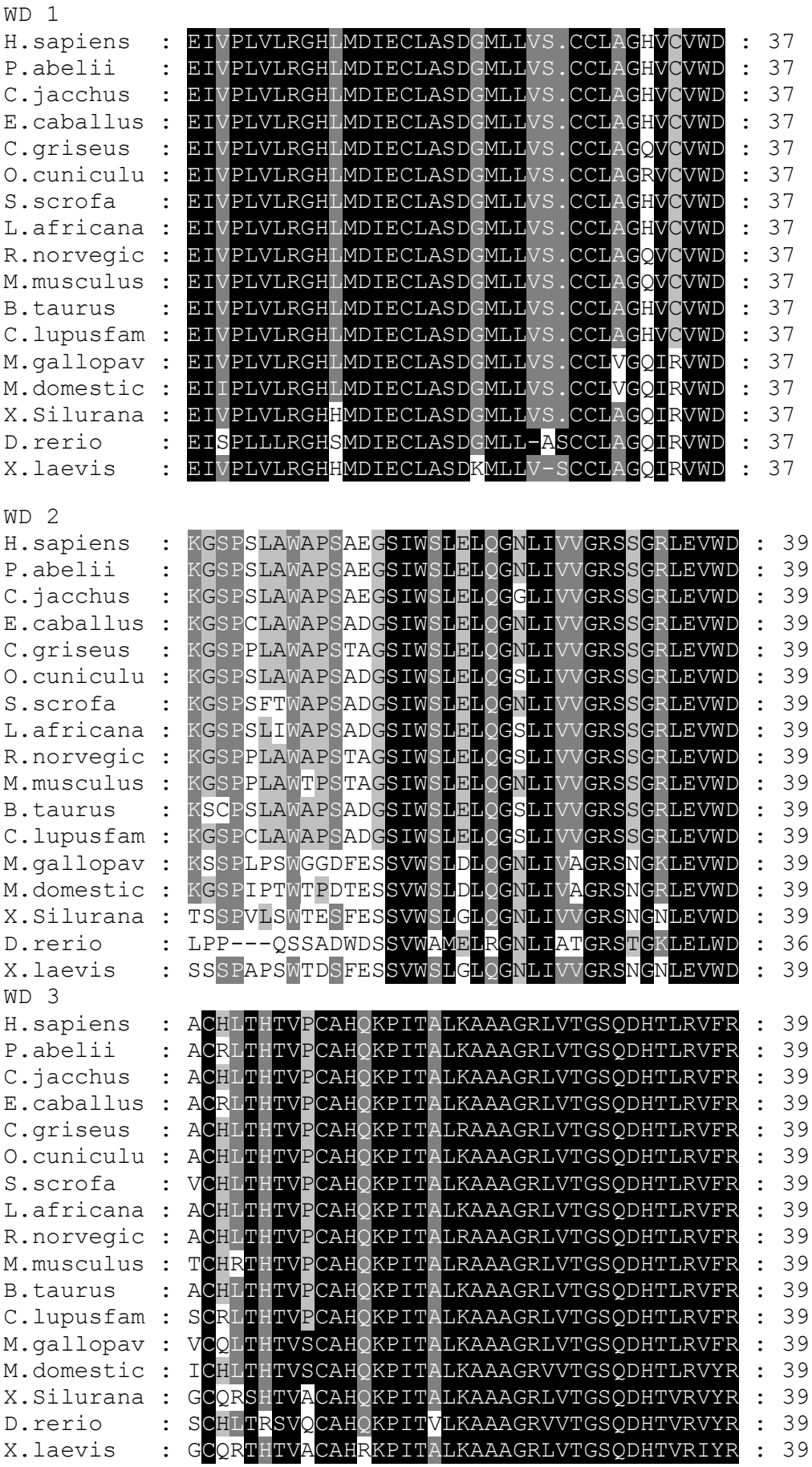
WD 1
H.sapiens : EIVPLVLRGHLMDIECLASDGMLLVS.CCLAGHVCVWD : 37
P.abelii : EIVPLVLRGHLMDIECLASDGMLLVS.CCLAGHVCVWD : 37
C.jacchus : EIVPLVLRGHLMDIECLASDGMLLVS.CCLAGHVCVWD : 37
E.caballus : EIVPLVLRGHLMDIECLASDGMLLVS.CCLAGHVCVWD : 37
C.griseus : EIVPLVLRGHLMDIECLASDGMLLVS.CCLAGQVCVWD : 37
O.cuniculu : EIVPLVLRGHLMDIECLASDGMLLVS.CCLAGRVCVWD : 37
S.scrofa : EIVPLVLRGHLMDIECLASDGMLLVS.CCLAGHVCVWD : 37
L.africana : EIVPLVLRGHLMDIECLASDGMLLVS.CCLAGHVCVWD : 37
R.norvegic : EIVPLVLRGHLMDIECLASDGMLLVS.CCLAGQVCVWD : 37
M.musculus : EIVPLVLRGHLMDIECLASDGMLLVS.CCLAGQVCVWD : 37
B.taurus : EIVPLVLRGHLMDIECLASDGMLLVS.CCLAGHVCVWD : 37
C.lupusfam : EIVPLVLRGHLMDIECLASDGMLLVS.CCLAGHVCVWD : 37
M.gallopav : EIVPLVLRGHLMDIECLASDGMLLVS.CCLVGQIRVWD : 37
M.domestic : EIIPLVLRGHLMDIECLASDGMLLVS.CCLVGQIRVWD : 37
X.Silurana : EIVPLVLRGHHMDIECLASDGMLLVS.CCLAGQIRVWD : 37
D.rerio : EISPLLLRGHSMDIECLASDGMLL-ASCCLAGQIRVWD : 37
X.laevis : EIVPLVLRGHHMDIECLASDKMLLV-SCCLAGQIRVWD : 37
WD 2
H.sapiens : KGSPSLAWAPSAEGSIWSLELQGNLIVVGRSSGRLEVWD : 39
P.abelii : KGSPSLAWAPSAEGSIWSLELQGNLIVVGRSSGRLEVWD : 39
C.jacchus : KGSPSLAWAPSAEGSIWSLELQGGLIVVGRSSGRLEVWD : 39
E.caballus : KGSPCLAWAPSADGSIWSLELQGNLIVVGRSSGRLEVWD : 39
C.griseus : KGSPPLAWAPSTAGSIWSLELQGNLIVVGRSSGRLEVWD : 39
O.cuniculu : KGSPSLAWAPSADGSIWSLELQGSLIVVGRSSGRLEVWD : 39
S.scrofa : KGSPSFTWAPSADGSIWSLELQGNLIVVGRSSGRLEVWD : 39
L.africana : KGSPSLIWAPSADGSIWSLELQGSLIVVGRSSGRLEVWD : 39
R.norvegic : KGSPPLAWAPSTAGSIWSLELQGSLIVVGRSSGRLEVWD : 39
M.musculus : KGSPPLAWTPSTAGSIWSLELQGNLIVVGRSSGRLEVWD : 39
B.taurus : KSCPSLAWAPSADGSIWSLELQGSLIVVGRSSGRLEVWD : 39
C.lupusfam : KGSPCLAWAPSADGSIWSLELQGSLIVVGRSSGRLEVWD : 39
M.gallopav : KSSPLPSWGGDFESSVWSLDLQGNLIVAGRSNGKLEVWD : 39
M.domestic : KGSPIPTWTPDTESSVWSLDLQGNLIVAGRSNGRLEVWD : 39
X.Silurana : TSSPVLSWTESFESSVWSLGLQGNLIVVGRSNGNLEVWD : 39
D.rerio : LPP---QSSADWDSSVWAMELRGNLIATGRSTGKLELWD : 36
X.laevis : SSSPAPSWTDSFESSVWSLGLQGNLIVVGRSNGNLEVWD : 39
WD 3
H.sapiens : ACHLTHTVPCAHQKPITALKAAAGRLVTGSQDHTLRVFR : 39
P.abelii : ACRLTHTVPCAHQKPITALKAAAGRLVTGSQDHTLRVFR : 39
C.jacchus : ACHLTHTVPCAHQKPITALKAAAGRLVTGSQDHTLRVFR : 39
E.caballus : ACRLTHTVPCAHQKPITALKAAAGRLVTGSQDHTLRVFR : 39
C.griseus : ACHLTHTVPCAHQKPITALRAAAGRLVTGSQDHTLRVFR : 39
O.cuniculu : ACHLTHTVPCAHQKPITALKAAAGRLVTGSQDHTLRVFR : 39
S.scrofa : VCHLTHTVPCAHQKPITALKAAAGRLVTGSQDHTLRVFR : 39
L.africana : ACHLTHTVPCAHQKPITALKAAAGRLVTGSQDHTLRVFR : 39
R.norvegic : ACHLTHTVPCAHQKPITALRAAAGRLVTGSQDHTLRVFR : 39
M.musculus : TCHRTHTVPCAHQKPITALRAAAGRLVTGSQDHTLRVFR : 39
B.taurus : ACHLTHTVPCAHQKPITALKAAAGRLVTGSQDHTLRVFR : 39
C.lupusfam : SCRLTHTVPCAHQKPITALKAAAGRLVTGSQDHTLRVFR : 39
M.gallopav : VCQLTHTVSCAHQKPITALKAAAGRLVTGSQDHTLRVFR : 39
M.domestic : ICHLTHTVSCAHQKPITALKAAAGRVVTGSQDHTLRVYR : 39
X.Silurana : GCQRSHTVACAHQKPITALKAAAGRLVTGSQDHTVRVYR : 39
D.rerio : SCHLTRSVQCAHQKPITVLKAAAGRVVTGSQDHTVRVYR : 39
X.laevis : GCQRTHTVACAHRKPITALKAAAGRLVTGSQDHTVRIYR : 39

```
WD 4
H.sapiens  : DSCCLFTLQGHSGAITTVYIDQTMVLASGGQDGAICLWD : 39
P.abelii   : DSCCLFTLQGHSGAITTVYIDQTMVLASGGQDGAICLWD : 39
C.jacchus  : DSCCLFTLQGHSGAITTVYIDQTMVLASGGQDGAICLWD : 39
E.caballus : DSCCLFTLQGHSGAITTVYIDQTMVLASGGQDGAICLWD : 39
C.griseus  : DSCCLFTLQGHSGAITTVYIDQTMVLASGGQDGAICLWD : 39
O.cuniculu : DSCCLFTLQGHSGAITTVYIDQTMVLASGGQDGAICLWD : 39
S.scrofa   : DSCCLFTLQGHSGAITTVYIDQTMVLASGGQDGAICLWD : 39
L.africana : DSCCLFTLQGHSGAITTVYIDQTMVLASGGQDGAICLWD : 39
R.norvegic : DSCCLFTLQGHSGAITTVYIDQTMVLASGGQDGAICLWD : 39
M.musculus : DSCCLFTLKGHSGAITAVYIDQTMVLASGGQDGAICLWD : 39
B.taurus   : DSCCLFTLQGHSGAITTVYIDQTMVLASGGQDGAICLWD : 39
C.lupusfam : DSCCLFTLQGHSGAITTVYIDQTMVLASGGQDGAICLWD : 39
M.gallopav : DSCCLFTLQGHSGAITAVYIDQTMVLASGGQDGAICLWD : 39
M.domestic : DSCCLFTLQGHSGAITAVYIDQTMVLASGGQDGAICLWD : 39
X.Silurana : DACCLFTLQGHSGGITAIYIDETMVLASGGQDGAICLWD : 39
D.rerio    : DSCCLFTLQGHSGGITAIYIDQTMVLASGGQDGAICVWD : 39
X.laevis   : DACCLFTLQGHSGGITAIYIDETMVLASGGQDGAICLWD : 39
WD 5
H.sapiens  : TGSRVS.HVFAHRGDVTSLTCTTSCVISSGLDDLISIWD : 38
P.abelii   : TGSRVS.HVFAHRGDVTSLTCTTSCVISSGLDDLISIWD : 38
C.jacchus  : TGSRVS.HMFAHRGDVTSLTCTTSCVISSGLDDLISIWD : 38
E.caballus : TGSRVS.HMFAHRGDVTSLTCTTSCVISSGLDDLISIWD : 38
C.griseus  : TGSRVS.HTFAHRGDVTSLTCTTSCVISSGLDDLINIWD : 38
O.cuniculu : TGSRVS.HMFAHRGDVTSLTCTASCVISSGLDDLISIWD : 38
S.scrofa   : TGSRVS.HMFAHRGDVTSLTCTTSCVISSGLDDLISIWD : 38
L.africana : TGSRVS.HMFAHRGDVTSLTCTTSCVISSGLDDLISIWD : 38
R.norvegic : TGSRVS.HTFAHRGDVTSLTCTTSCVISSGLDDFINIWD : 38
M.musculus : TGSRVS.QTFAHRGDVTSLTCTASCVISSGLDDFISIWD : 38
B.taurus   : TGSRVS.HMFAHRGDVTSLTCTTSCVISSGLDDLISIWD : 38
C.lupusfam : TGSRVS.HMFAHRGDVTSLTCTTSCVISSGLDDLISIWD : 38
M.gallopav : TGSKVS.HMYAHRGDVTSLTCTTSCVISSGLDDVISIWD : 38
M.domestic : TGSRVS.HMFAHRGDVTSLTCTTSCIISSGLDDLISIWD : 38
X.Silurana : TGSRVS.HMFGHRGDVTSLLCTTSCVISSGLDDVICIWD : 38
D.rerio    : TGSRVS.HVYGHRGDVTSLVCTTSCIISSGLDDLICIWD : 38
X.laevis   : TGSRVS.HMFGHRGDVTSLLCTASCVISSGLDDVISIWD : 38

WD 6
H.sapiens  : TGIKFYSIQQDLGCGASLGVISDNLLVTGGQGCVS.FWD : 38
P.abelii   : TGIKFYSIQQDLGCGASLGVISDNLLVTGGQGCVS.FWD : 38
C.jacchus  : TGIKFYSIQQDLGCGASLGVISDNLLVTGGQGCVS.FWD : 38
E.caballus : TGIKLYSIQQDLGCGASLGVISDNLLVTGGQGCVS.FWD : 38
C.griseus  : TGIKLYSIQQDLGCGASLGVISDNLLVTGGQGCVS.FWD : 38
O.cuniculu : TGIKLYSIQQDLGCGASLGVISDNLLVTGGQGCVS.FWD : 38
S.scrofa   : TGIKLYSIQQDLGCGASLGVISDNLLVTGGQGCVS.FWD : 38
L.africana : TGIKLYSIQQDLGCGASLGVISDNLLVTGGQGCVS.FWD : 38
R.norvegic : TGIKLYSIQQDLGCGASLGVISDNLLVTGGQGCVS.FWD : 38
M.musculus : TGIKLYSIQQDLGCGASLGVISDNLLVTGGQGCVS.FWD : 38
B.taurus   : TGIKLYSIQQDLGCGASLGVISDNLLVTGGQGCVS.FWD : 38
C.lupusfam : TGIKLYSIQQDLGCGASLGVISDNLLVTGGQGCVS.FWD : 38
M.gallopav : SGIKLYSIQQEMGCGSSLGVISDNLLVTGGQGCVS.FWD : 38
M.domestic : TNIKLYSIQQDMGCGSSLGVISDNLLVTGGQGCVS.FWD : 38
X.Silurana : TAIRLYSIQQDLGCGSSLGLISDNLLVTGGQGCVS.FWD : 38
D.rerio    : TGIKLYSIQQEVGCGASLGVISENLLVTGGQGCVS.FWD : 38
X.laevis   : TAIKLYSIQQDLGCGSSLGLISDNLLVTGGLGCVS.FWD : 38
```

Figure 3.2. Multiple sequence alignments of vertebrate SCAP WD40 repeats. Full length protein sequences of SCAP from vertebrates were aligned using ClustalW algorithm in MEGA 4.0 software. Shown here are WD repeats only, labelled WD1-WD6, in accordance with their distribution with $SCAP_{CTD}$ as outlined in Figure 1B. Alignments visualised using the multiple sequence alignment analysing tool GeneDoc. Black indicates 100% identity between residues (including synonymous substitutions), grey indicates a high level of residue identity between sequences, and white are non-identical residues between sequences.

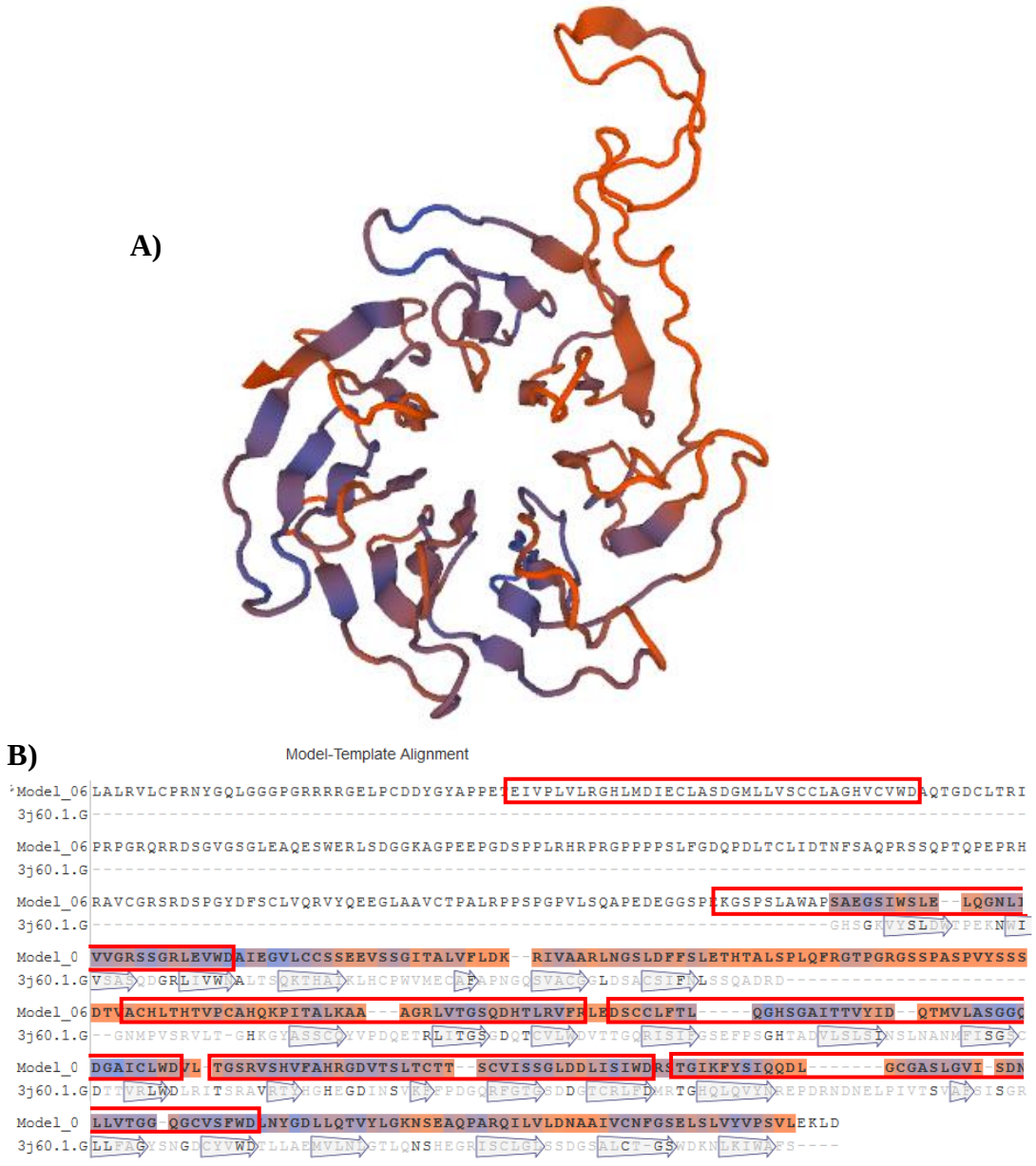


Figure 3.3. Homology model of $SCAP_{CTD}$. SWISS-MODEL was used to predict the 3D protein structure of SCAP CTD using proteins containing similar structural domains which have their crystal structures solved. (A) SCAP CTD structure modelled on the crystal structure of RACK1 (B) SCAP CTD amino acid sequence aligned with the template RACK1 sequence. SCAP CTD WD1-WD6 repeats are highlighted by red boxes. Red/blue shaded regions are present in the homology model.

***Optimising Expression, Solubility and Purification of GST-SREBP1 and GST-SREBP2 CTDs***

Based on the knowledge that the $SCAP_{CTD}$ is sufficient to pull down full length SREBP protein and *vice versa*, the aim of this work was to further characterise this interaction to the amino acid level by mapping the SREBP interaction site on the $SCAP_{CTD}$. The central approach to achieve this aim was to purify the $SREBP_{CTD}$ to probe a peptide array of the $SCAP_{CTD}$.

In order to over-express and purify the CTD domains of SREBP1 and SREBP2, 1776bp of the SREBP1 gene and 1761bp of the SREBP2 gene encoding the CTD domains were cloned into an inducible bacterial expression vector (pGEX-6p1). The CTD domains in this vector are tagged with an amino terminal GST to facilitate affinity purification (Figure 3.4). The GST gene in the vector encodes a 26kDa protein while the SREBP1 CTD and the SREBP2 CTD both encode approximately 65kDa proteins. The expression of the GST-$SREBP1_{CTD}$ fusion protein (~91 kDa) and GST-$SREBP2_{CTD}$ fusion protein (~91 kDa) in E. coli was analysed under different induction times and IPTG concentrations. Both CTD domains were strongly induced at 4, 16 and 30 hrs using 0.5 mM or 1 mM IPTG and the 16 hr timepoint was chosen for convenience (Figure 3.5A and 3.5B). Induction of GST alone was used as a positive control throughout (data not shown).

Bacterial cell cultures over-expressing the SREBP proteins were grown and the cells were harvested by centrifugation for affinity purification of the tagged proteins. Soluble cell extracts were prepared from harvested cell pellets using the standard approach which employs lysozyme and sonication and removal of cell debris by centrifugation.

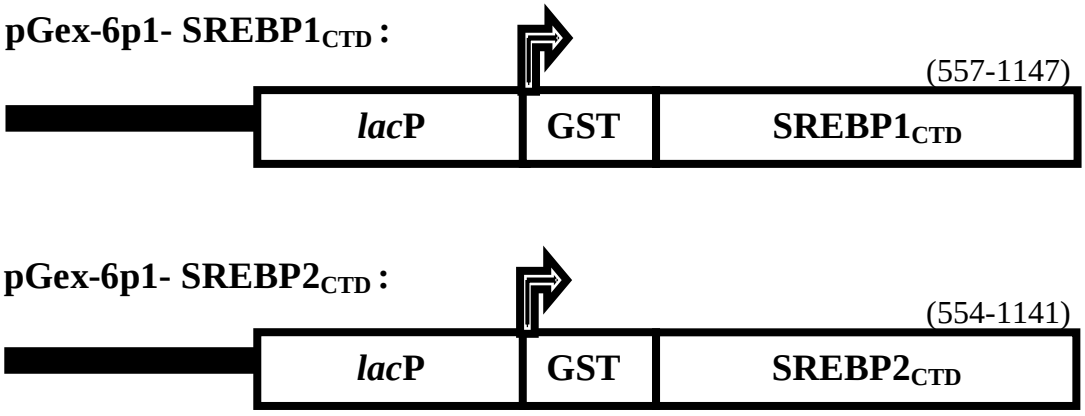


Figure 3.4. Schematic representation of pGEX-6p1-SREBP1$_{CTD}$ and pGEX-6p1-SREBP2$_{CTD}$. The lac promoter (*lac*P) allows regulated induction of gene expression by IPTG. Numbers in brackets refer to the amino acid section of the SREBPs inserted into the vector.

SREBP fusion proteins were clearly present in whole cells lysed in SDS loading dye (Figure 3.5C and 3.5D, Ind lane), they were not visible in the soluble cell extracts (Figure 3.5C and 3.5D Sup lanes) and no SREBP protein was recovered following glutathione affinity chromatography (Figure 3.5C and 3.5D, E1-E4 lanes). By comparison, a control sample over-expressing GST alone had protein in both the whole cell lysate and in the soluble fractions (data not shown). The simplest explanation for this result is that the SREBP proteins are sequestered into inclusion bodies (IBs) within the bacteria. Inclusion bodies are aggregates of protein that occur in bacteria due to mis-folding of endogenous proteins, but also often as a result of recombinant protein over-expression.

A common approach to producing soluble over-expressed protein in bacteria is to grow the bacteria at lower temperatures and for longer times. These conditions slow down protein production and can often lead to increased chances of producing correctly folded proteins with improved solubility. To investigate if this was the case for the SREBP$_{CTD}$, cultures were grown to an $OD_{600}$ of 0.5, at temperatures of 30$^{o}$C

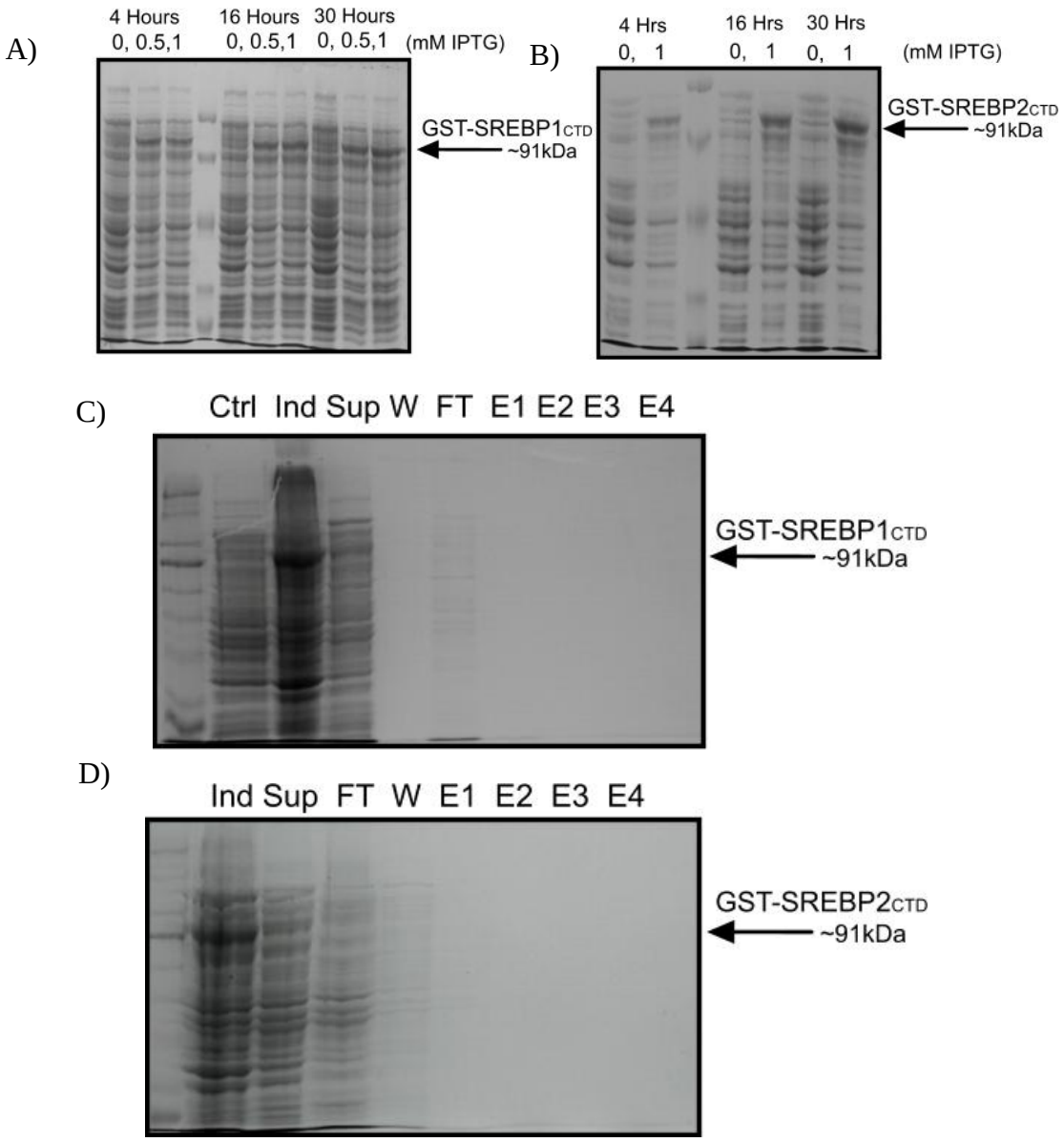


Figure 3.5. Analysis of GST- $SREBP_{CTD}$ fusion protein expression. SDS-PAGE analysis of E. coli bearing (A) pGEX-6p1-$SREBP1_{CTD}$ or (B) pGEX-6p1-$SREBP2_{CTD}$ .Following induction with the indicated concentrations of IPTG for different lengths of time samples of the E. coli were removed from the culture and pelleted by centrifugation. Whole cell lysis was carried out by boiling the pellets in SDS loading dye and samples were then clarified by centrifugation and analysed by SDS-PAGE on 10% polyacrylamide gels and visualised by staining with coomassie blue. Analysis of affinity purification of GST- $SREBP1_{CTD}$ (C) and GST-$SREBP2_{CTD}$ (D). E. coli bearing pGEX-6p1- $SREBP1_{CTD}$ or pGEX-6p1- $SREBP1_{CTD}$ were induced for 16 hrs in the presence of 0.5 mM IPTG. Following induction whole cell lysis was carried out by boiling the pellets in SDS loading dye (Ind samples) or cell extracts were prepared and incubated with GST beads. Beads were then collected by centrifugation and the supernatant was removed. Beads were then washed in PBS and protein was eluted from the beads with PBS containing reduced glutathione. Samples analysed: Ctrl, no IPTG added; Ind, induced for 16 hrs with 0.5 mM IPTG; Sup, soluble supernatant; W, wash; FT, flow through; E1-4, elutions with reduced glutathione. Samples were analysed by SDS-PAGE on 10% acrylamide gel and staining with coomassie blue.

and 27$^{o}$C, which took approx 7 and 16 hours, respectively, as opposed to the 2.5-3hours when grown at 37$^{o}$C. They were then induced with IPTG for the indicated lengths of time, using GST alone again as positive control. However, these changes to growth conditions failed to induce expression of any fusion protein detectable by SDS-PAGE (data not shown) and this approach was not pursued any further.

It was originally believed that all IBs comprised of misfolded proteins and that their formation was an undesired effect. However, more recent studies have demonstrated sequestration of functional protein within IBs and some purification approaches now use IB formation to separate their target protein from all the soluble protein and then proceed to solubilise their target protein from the inclusion body and refold it. This approach was attempt here.

Bacteria were cultured at 37$^{o}$C, brought to an $OD_{600}$ of 0.5, and then induced with IPTG for 16 hours. Based on the methods described by Rodríguez-Carmona et al., IBs were purified from bacterial whole cell pellets. Briefly, bacterial pellets were resuspended in buffer and freeze-thawed for 4 cycles in liquid nitrogen. Cell suspensions were then incubated for 2 hours at 37$^{o}$C in the presence of lysozyme, followed by addition of Triton X-100 and incubation for a further hour at RT. Cell suspensions were then sonicated on ice for 5 x 10 second bursts, NP-40 was added and lysates were incubated at 4$^{o}$C for 1 hour. $MgSO_4$ and DNAse were then added and samples were incubated at 37$^{o}$C for 45 minutes, followed by centrifugation at 15000 x g for 15 minutes at 4$^{o}$C. The pellet contains inclusion bodies. SDS-PAGE analysis of the prepared IBs showed that the GST-SREBP2$_{CTD}$ fusion protein was present (Figure 3.6A).

Frangioni and Neel reported increased solubilisation of functional aggregated over-expressed proteins in the presence of sarkosyl detergent and sarkosyl was used here

in an attempt to solubilise the over-expressed $SREBP_{CTD}$ proteins (Frangioni & Neel 1993). In this approach IBs were first harvested by centrifugation and sarkosyl was then added to these IBs. High concentrations of sarkosyl (10%) increased solubility of the $SREBP_{CTD}$ proteins to 90% as assessed by the levels of the 91 KDa proteins remaining in the soluble fraction following centrifugation. However, at this concentration of sarkosyl the GST alone positive control protein did not bind the affinity resin (data not shown) and consequently it was necessary to reduce the sarkosyl concentration.

Purification of the proteins was then attempted in the presence of 1% sarkosyl as outlined in materials and methods. GST alone did bind the affinity resin and could be purified to a high level in the presence of 1% sarkosyl. However, little GST-$SREBP2_{CTD}$ fusion protein was recovered in the purification process and the 91 kDa protein was barely detectable by coomassie staining (Figure 3.6B).

Tao et al previously showed that sarkosyl solubilisation of aggregated protein in the presence of other non-ionic detergents can improve fusion protein binding to affinity resin (Tao et al. 2010). Triton X-100 and CHAPS have both been reported to increase binding of sarkosyl-solubilised proteins to affinity resin. Various combinations of these detergents were investigated with respect to improving fusion protein binding to affinity resin. Combinations ranged from 1-4% Triton X-100 with or without 10-40 mM CHAPS, all in the presence of 1% sarkosyl. The combination which yielded the best results was inclusion of 2% Triton X-100 with 1% sarkosyl prior to incubation of the soluble fraction with the affinity resin, although this was only a marginal improvement in yield over sarkosyl alone purified protein (Figure 3.6C vs. 3.6B, 3.6D and 3.6E). Considering that the overall yield of $SREBP_{CTD}$

proteins recovered by the IB solubilisation approach was low, that the purification was only partial and that a considerable amount of protein was likely to be lost during the removal of the detergents prior to using the proteins for interaction studies it was decided to switch to a different expression system/fusion tag/purification method to try and improve the yield of and purification quality of the $SREBP2_{CTD}$ proteins.

A)

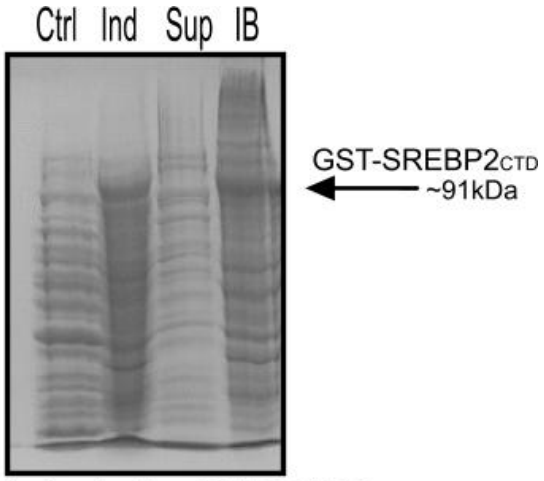


Inclusion bodies GST-SREBP2CTD

B)

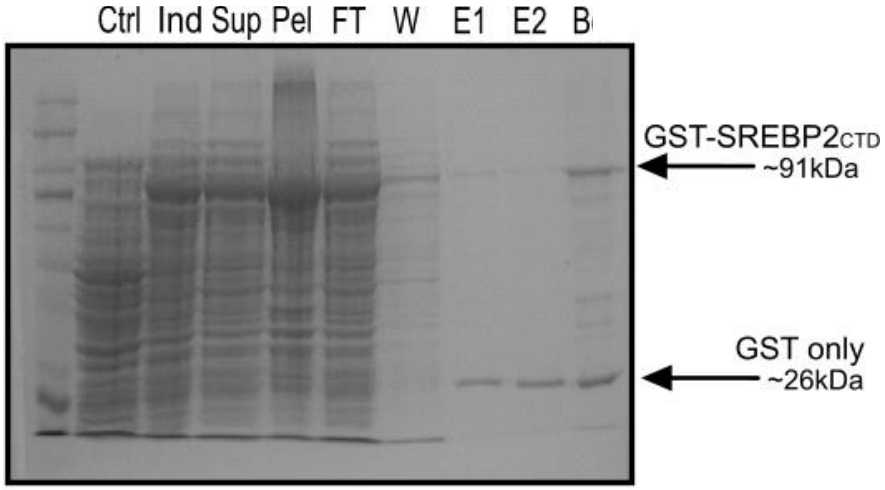


GST-SREBP2CTD Purification with 1%Sarkosyl

C)

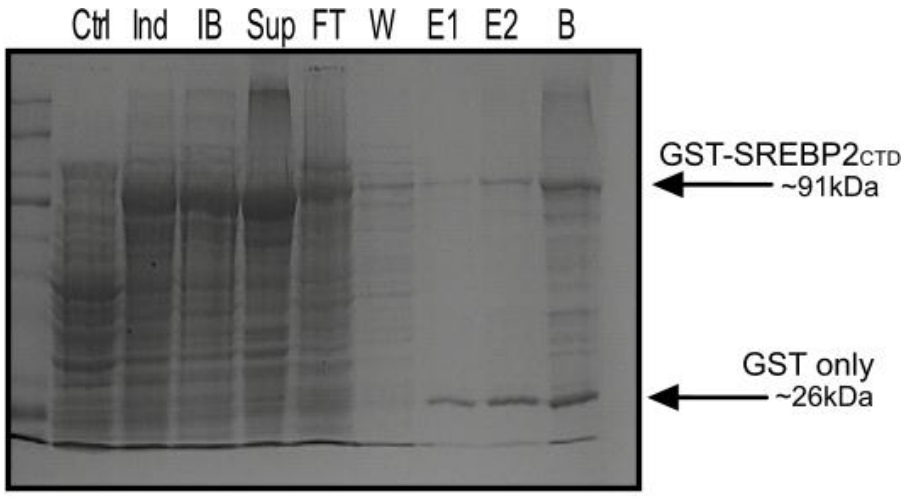


GST-SREBP2CTD Purification with 1%Sarkosyl
+2%Triton X-100

D)

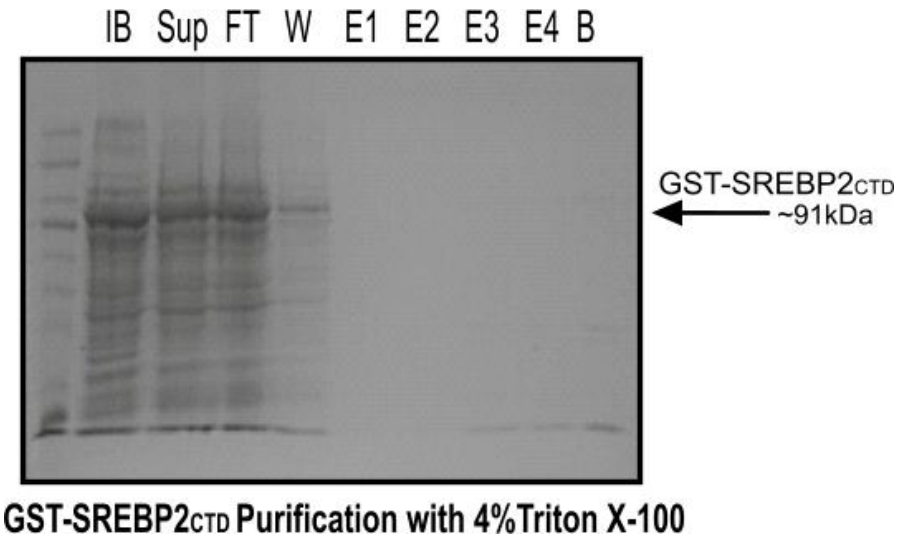


GST-SREBP2CTD Purification with 4%Triton X-100

E)

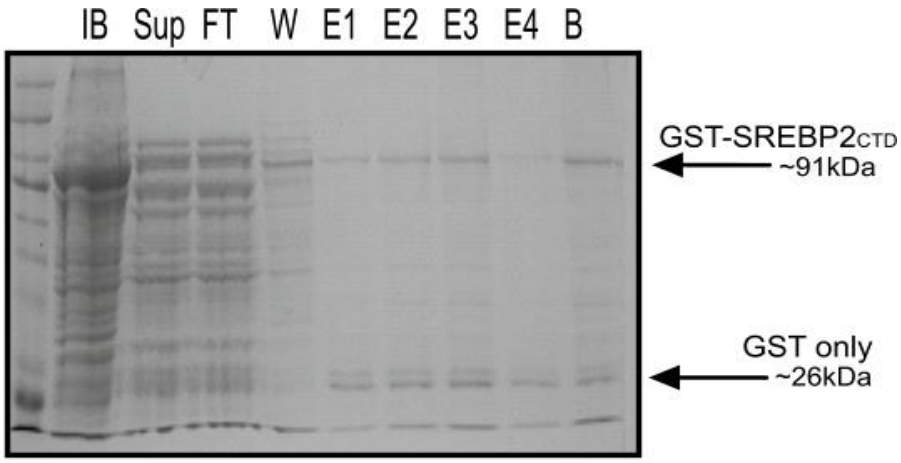


GST-SREBP2CTD Purification with 1% Sarkosyl,
+4%Triton X-100
+40mM CHAPS

Figure 3.6. SDS-PAGE analysis of GST- SREBP2$_{CTD}$ fusion protein in IBs before and after solubilisation in detergent. E. coli bearing pGEX-6p1- SREBP2$_{CTD}$ were induced for 16 hrs in the presence of 0.5 mM IPTG. Following induction IBs were prepared in the presence of the indicated detergents followed by incubated with GST beads. Beads were then collected by centrifugation and the supernatant was removed. Beads were then washed in PBS and protein was eluted from the beads with PBS containing reduced glutathione. Samples analysed: Ctrl, no IPTG added; Ind, induced for 16 hrs with 0.5 mM IPTG; IB, Inclusion bodies; Sup, soluble supernatant; W, wash; FT, flow through; E1-4, elutions with reduced glutathione; B, beads. Samples were analysed by SDS-PAGE on a 10% polyacrylamide gel and staining with coomassie blue.

### *Optimising Expression and Purification of SREBP1$_{CTD}$-His$_6$ and SREBP2$_{CTD}$-His$_6$*

Given that the GST-SREBP$_{CTD}$ over-expressed proteins were problematic with respect to solubility an alternative over-expression system was attempted. The alternative system is based on tagging of the proteins with six histidines residues at the carboxy terminus whereas the tag was at the amino terminus in the GST system already described. It was hoped that placing a smaller tag at a different location might improve solubility. The same protein sequences of SREBP1 and SREBP2 CTDs as for the GST expression system outlined above were cloned into a pBADtopo TA expression vector, such that each SREBP is tagged with six histidines (His$_6$) at the carboxy terminus. The molecular weight of the His6 tagged proteins is approximately 65 kDa and is close to the native size of the SREBP$_{CTD}$ proteins as the tag is small (Figure 3.7). GST-GFP-His$_6$ (~53 kDa) was used as a positive control for expression and purification throughout.

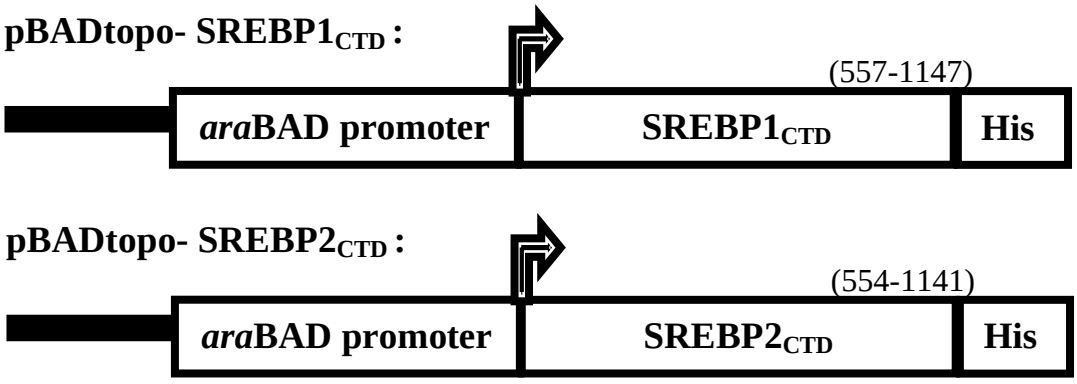


Figure 3.7. Schematic representation of pBADtopo- SREBP1$_{CTD}$ and pBADtopo-SREBP2$_{CTD}$. The *ara*BAD promoter provides tight, dose-dependent regulation of gene expression by L-arabinose. Numbers in brackets refer to the amino acid section of the SREBPs inserted into the vector.

In order to over-express the $His_6$ tagged SREBPs, bacterial cultures containing these constructs were grown to an $OD_{600}$ of 0.5 and induced with 0.02% of L-arabinose for four hours. Unlike the GST fusion proteins, induction of the His fusion proteins could not be detected by coomassie staining and were checked instead by immunoblot analysis using an anti His tag antibody which confirmed the presence of the fusion proteins. Scale up to 500 mL using these induction conditions followed by cell lysis and preparation of cell extracts indicated that the majority of the protein expressed was in the soluble fraction (Figure 3.8A, Sol vs. Ind lane). Purification of the tagged proteins was attempted using nickel affinity chromatography. Initially, affinity purification of the fusion protein from this soluble fraction, as described under materials and methods, yielded very small amounts of purified SREBP2 fusion protein detectable by immunoblot (Figure 3.8A, E1-E5 lanes) while the positive control fusion protein (GST-GFP-$His_6$) was present at higher levels (Figure 3.8B, E1-E5 lanes).

To achieve a higher yield of purified $SREBP_{CTD}$-$His_6$, the culture volume was scaled up to 5L of bacteria over-expressing pBADtopo-$SREBP2_{CTD}$ or pBADtopo-$SREBP1_{CTD}$ (or pBADtopo-GFP-GST control), induced as outlined above and lysed in a 50-fold more concentrated volume of buffer than the recommended volume of buffer required for lysis of a 5L culture. Again, following lysis by sonication, the majority of the SREBP protein was present in the soluble fraction (Figure 3.8C and 3.8D, Sol lane). Nickel affinity purification of the fusion protein yielded quantities detectable by immunoblot, however compared to the signal obtained for control protein, both the expressed and purified fractions for $SREBP2_{CTD}$-$His_6$ and $SREBP1_{CTD}$-$His_6$ were much lower (Figure 3.8C and 3.8D vs. 3.8E, E1-E5 lanes).

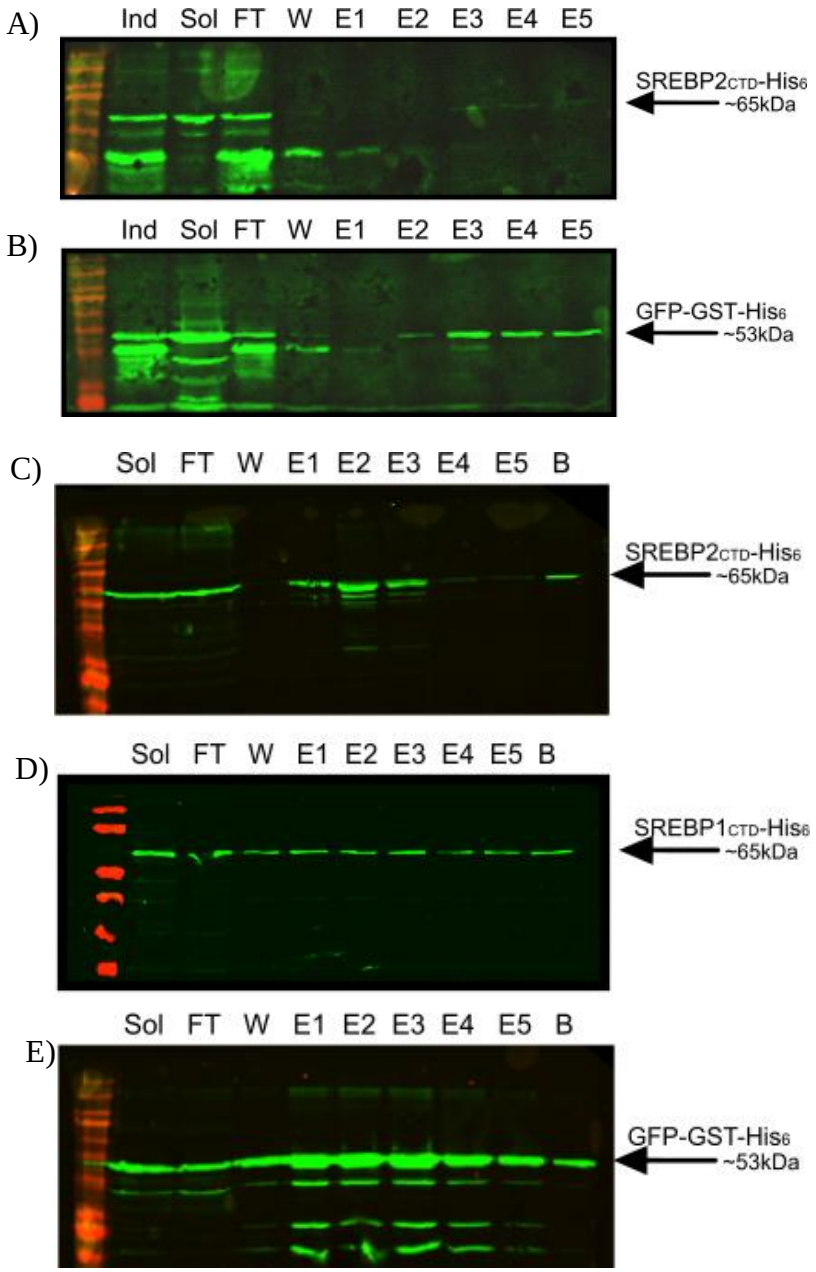


Figure 3.8. Immunoblot analysis of $SREBP_{CTD}$ and GFP-GST $His_6$-fusion proteins. E. coli bearing pBADtopo-$SREBP2_{CTD}$ (A,C), pBADtopo-$SREBP1_{CTD}$ (D) or pBADtopo-GFP-GST (B,E) were induced for 4 hrs in the presence of 0.02% L-arabinose, in either 500mL LB (A,B) or 5L LB(C,D). Following induction, bacterial cells were pelleted by centrifugation, lysed by sonication in the presence of lysozyme in hypotonic buffer, followed by incubation with nickel affinity resin. The resin was then collected by centrifugation and the supernatant was removed. The resin was then washed in buffer containing 20mM of imidazole and protein was eluted from the resin with buffer containing a 250mM of imidazole. Samples analysed: Ind, induced for 4 hrs with 0.02% L-arabinose; Sol, soluble cell extract fraction; W, wash; FT, flow through; E1-4, elutions with reduced glutathione; B, beads (resin). Samples were analysed by SDS-PAGE on a 10% acrylamide gel. Protein was transferred to nitrocellulose membrane by wet transfer and immunoblot analysis was performed using mouse anti-His primary antibody incubated overnight at 4$^{o}$C (Genescript, 1:2500) and goat anti-mouse IRDye680LT incubated for 1hour at RT (Li-cor, 1:20 000). Blots were visualised on Odyssey Infrared Imaging System (Li-cor).

In addition, the majority of the fusion protein did not bind to the resin and was present in the flow through (Figure 3.8C and 3.8D, Sol vs. FT lanes). Attempts to purify more fusion protein from the flow through fraction by re-incubation with fresh resin, did not result in any extra yield (data not shown) indicating that the bound protein has different properties to the protein that did not bind. The basis of this difference is unclear.

The eluted fractions which were positive for $SREBP2_{CTD}$-$His_6$ protein by immunoblot from the 5L preparation were run on an SDS-PAGE gel to assess the purity of the eluted fusion protein. The results showed the presence of a large amount of contaminating protein in the fractions (Figure 3.9A). Attempts to increase purity by re-incubation of the eluted fractions with fresh affinity resin did not increase purity (Figure 3.9B). Gel filtration FPLC was then attempted as to increase fusion protein purity. BSA was run separately on the column as a protein standard of similar molecular weight and apparent size. The $SREBP2_{CTD}$-$His_6$ tagged fusion protein, like BSA, eluted from the column in fraction B1 (Figure 3.10A and 3.10B). There was a significant amount of protein in the other peaks on the chromatogram but these were negative for the $SREBP2_{CTD}$-$His_6$ fusion protein by immunoblot analysis (Figure 3.10B). The fractions flanking fraction B1 also contained fusion protein but at lower levels (Figure 3.10C). However, as indicated by the chromatogram, the fractions containing the fusion protein appeared to contain quite a small amount of the total protein applied. The low concentration of the $SREBP2_{CTD}$-$His_6$ fusion protein was confirmed when the FPLC fusion protein fractions were run on an SDS-PAGE gel along with serial dilutions of a BSA protein standard (Figure 3.10D). The concentration of the $SREBP2_{CTD}$-$His_6$ fusion protein was maximally (but could be significantly below this) 0.1 µg/ml as the BSA standard was not

detectable by coomassie blue staining at this concentration, and neither was the $SREBP2_{CTD}$-His6 tagged fusion protein. In addition, following the FPLC cleanup, the fusion protein was still not the primary protein in the fraction, as detected by coomassie staining. There was a lower molecular weight band detectable at approximately 1 µg/ml concentration, which is likely either a contaminating protein or a degradation product of $SREBP2_{CTD}$-His6. While this method did decrease contaminating protein from the $SREBP_{CTD}$-His6 tagged fusion protein, it failed to increase yield sufficiently for peptide array studies. The required amount of fusion protein to probe the peptide array is 6 mLs at 100 µg/mL, and this method yielded only 1.5 mL of protein at a concentration of less than 1 µg/mL, from a total starting culture volume of 5 L.

The anti-His antibody used was highly sensitive and gave a strong clean signal for the $SREBP_{CTD}$-$His_6$ fusion proteins in the pre FPLC crudely purified fractions. Therefore the crudely purified fusion protein was used for probing of $SCAP_{CTD}$ peptide array.

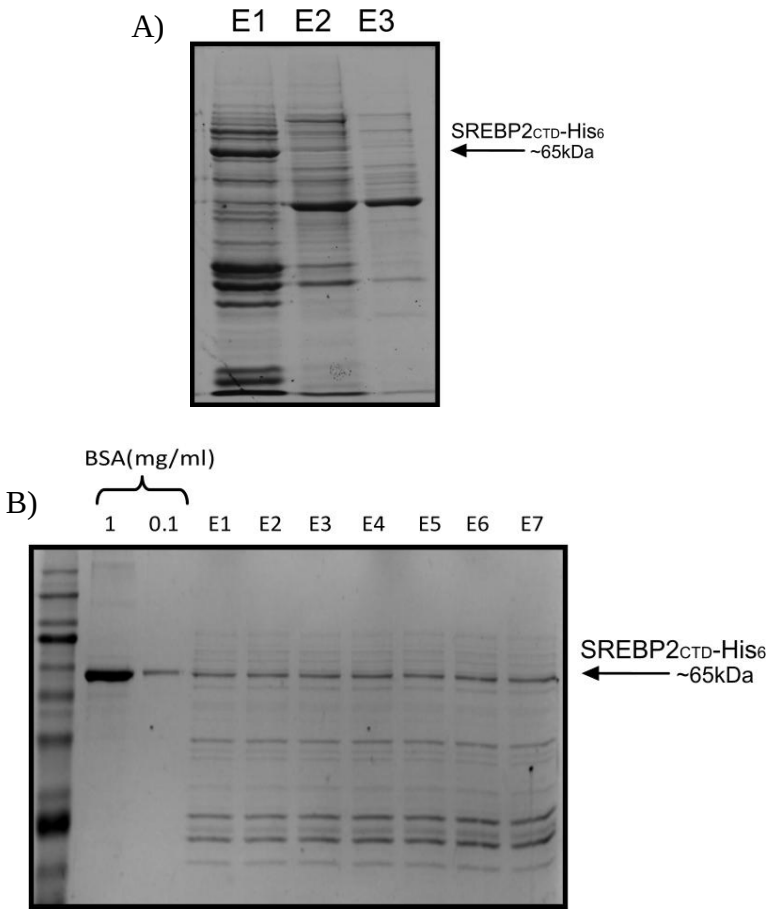


Figure 3.9. SDS-PAGE analysis of $SREBP2_{CTD}$-$His_6$ eluted protein fractions. (A)Eluted fractions E1, E2 and E3 containing purified $SREBP2_{CTD}$-His6 fusion protein were analysed by SDS-PAGE on a 10% polyacrylamide gel and staining with coomassie blue. (B) Fractions E1, E2 and E3 from (A) were pooled and re-incubated with Nickel affinity resin. The resin was then collected by centrifugation and the supernatant was removed. The resin was then washed in buffer containing 20mM of imidazole and protein was eluted from the resin with buffer containing a 250mM of imidazole. Samples analysed: BSA, 1 and 0.1 mg/ml; E1-E7, eluted fractions. Samples were analysed by SDS-PAGE on a 10% polyacrylamide gel and stained with coomassie blue.

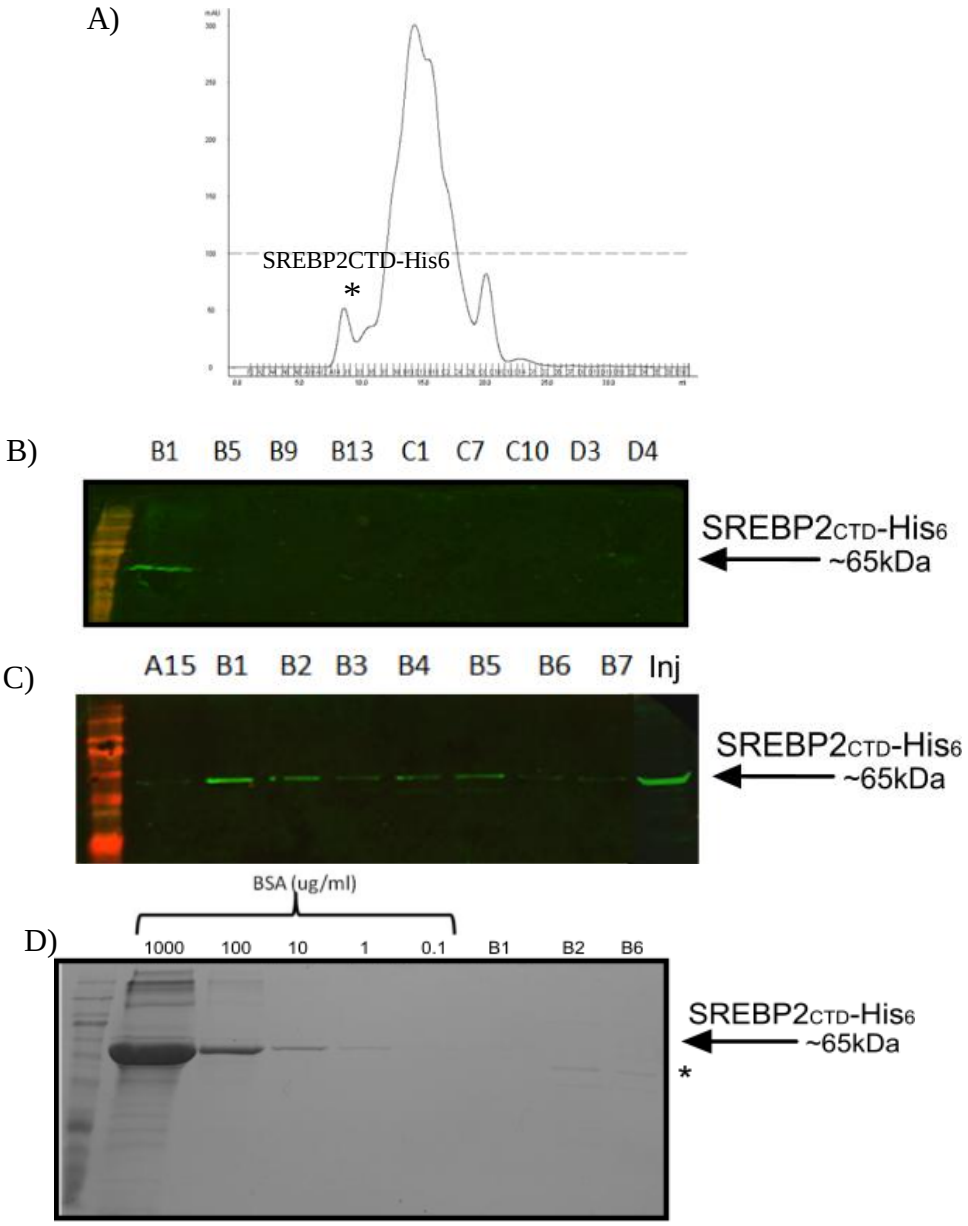


Figure 3.10. Analysis of purity of FPLC Nickel-affinity purified $SREBP2_{CTD}$-$His_6$. (A) Absorbance spectra of protein fractions following separation by gel filtration FPLC. E. coli bearing pBADtopo-$SREBP2_{CTD}$ were induced for 4 hrs in the presence of 0.02% L-arabinose, in 5L LB. Following induction, bacterial cells were pelleted and lysed, and $SREBP2_{CTD}$-$His_6$ fusion protein was applied to a nickel affinity chromatography column. The eluted fractions were pooled and separated by gel filtration FPLC. (*, peak containing $SREBP2_{CTD}$-$His_6$ fusion protein), (B and C) Analysis of eluted fractions following FPLC for presence of $SREBP2_{CTD}$-$His_6$ fusion protein. Eluted fractions were analysed by SDS-PAGE on a 10% polyacrylamide gel. Protein was transferred to nitrocellulose membrane by wet transfer and immunoblot analysis was performed using mouse anti-His primary antibody incubated overnight at 4$^{o}$C (Genescript, 1:2500) and goat anti-mouse IRDye680LT incubated for 1hour at RT (Li-cor, 1:20 000). Blots were visualised on Odyssey Infrared Imaging System (Li-cor). D) Estimation of the concentration of $SREBP2_{CTD}$-$His_6$ fusion protein yield following FPLC clean-up using a BSA standard. Samples analysed: BSA, 1000, 100, 10, 1 and 0.1µg/ml; B1, B2 and B6, FPLC eluted fractions. Samples were analysed by SDS-PAGE on a 10% polyacrylamide gel and staining with coomassie blue.* is a non-specific band.

### *Peptide array analysis of $SCAP_{CTD}$ probed with $SREBP2_{CTD}$-$His_6$ fusion protein*

In order to identify residues within $SCAP_{CTD}$ involved in the SCAP-SREBP2 interaction, the CTD of SCAP was immobilised in a peptide array. The peptide array was synthesised by Dr. Emilie Tresse in the laboratory of Prof. Rosemary O' Connor, Biosciences, UCC and consisted of a series (107 peptides in total) of 18-mer peptides attached to a cellulose membrane, with each peptide overlapping by a 5 amino acid window. The array was incubated with $SREBP2_{CTD}$-$His_6$ fusion protein for 16 hours at 4 $^{o}$C. Following washing, mouse anti-His primary antibody was used to detect $SREBP2_{CTD}$-$His_6$ bound to the array. Two spots (spots 3 and 4) gave positive signal (Figure 3.11A) and there was no binding of a non-specific control $His_6$ fusion protein (EndoIV-$His_6$) to these spots in a duplicate $SCAP_{CTD}$ peptide array (Figure 3.11B). The latter was stripped and reprobed with $SREBP2_{CTD}$-$His_6$ fusion protein and also resulted in fusion protein binding to spots 3, 4 and also to spot 5 (Figure 3.11C).

Binding of the $SREBP2_{CTD}$-$His_6$ fusion protein to spot 3 gave the strongest signal. This corresponds to the peptide GGPGRRRRGELPCDDYGY. An alanine scanning array based on the parent peptide of spot 3 was generated in which each amino acid was sequentially and individually substituted with alanine. Alanine scanning arrays are used to identify which residues within a given 18-mer peptide are essential to the fusion protein binding to a given spot. This array was probed with $SREBP2_{CTD}$-$His_6$ fusion protein and surprisingly there was no fusion protein bound to spot 1 of the alanine scanning array (Figure 3.11D). Spot 1 is based on the unmodified parent peptide and is the sequence to which the $SREBP2_{CTD}$-$His_6$ fusion protein originally bound strongly. Thus, in the absence of this control spot being positive for

interacting with SREBP2$_{CTD}$-His$_6$ fusion protein, the presence and absence of other spots in the alanine scanning array cannot be interpreted with confidence.

The batch of SREBP2$_{CTD}$-His$_6$ fusion protein used to probe the original SCAP$_{CTD}$ peptide arrays was different to the batch of SREBP2$_{CTD}$-His$_6$ fusion protein used to probe the alanine scanning array. Both of these batches were purified in the same way and both were confirmed as having fusion protein present. In the repeat array, the peptide spots which previously came up as positive for binding SREBP2$_{CTD}$-His$_6$ fusion protein were now absent, and different peptide spots were positive (Figure 3.11E). The reasons for this discrepancy are unclear but are likely to be linked to the problematic purification of the SREBP-His$_6$ fusion proteins. The initial binding to peptide spots 3 and 4 shown in Figure 3.11A and 3.11C was achieved using the same batch of purified SREBP2$_{CTD}$-His$_6$ fusion protein.

A)

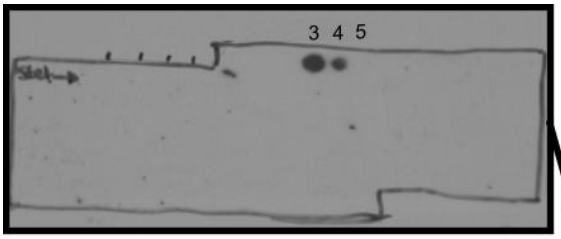


Peptide array of SCAP$_{CTD}$
probed with SREBP2$_{CTD}$-His$_6$ fusion protein

B)

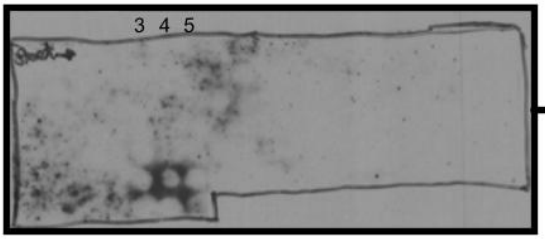


Peptide array of SCAP$_{CTD}$
probed with control His$_6$ fusion protein

Spot3:GGPGRRRRGELPCDDYGY
Spot4:RRRGELPCDDYGYAPPET
Spot5:LPCDDYGYAPPETEIVPL

C)

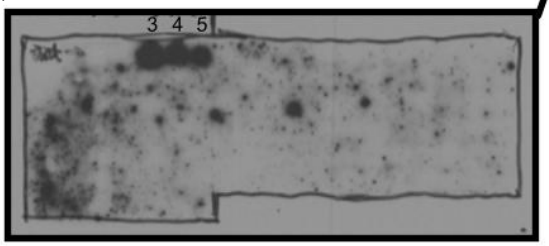


Peptide array of SCAP$_{CTD}$
probed with SREBP2$_{CTD}$-His$_6$ fusion protein

D)

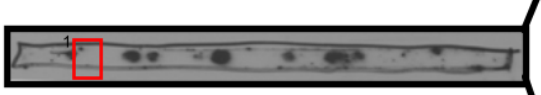


Alanine scan of spot 3 from SCAP$_{CTD}$ peptide array
probed with SREBP2$_{CTD}$-His$_6$ fusion protein

1GGPGRRRRGELPCDDYGY
AGPGRRRRGELPCDDYGY
GAPGRRRRGELPCDDYGY
GGAGRRRRGELPCDDYGY
GGPARRRRGELPCDDYGY
GGPGARRRGELPCDDYGY
GGPGRARRGELPCDDYGY
GGPGRRRARGELPCDDYGY
GGPGRRRRAGELPCDDYGY
GGPGRRRRRAELPCDDYGY
GGPGRRRRGALPCDDYGY
GGPGRRRRGEAPCDDYGY
GGPGRRRRGELACDDYGY
GGPGRRRRGELPADDYGY
GGPGRRRRGELPCADYGY
GGPGRRRRGELPCDAYDY
GGPGRRRRGELPCDDAGY
GGPGRRRRGELPCDDYAY
GGPGRRRRGELPCDDYGA

E)

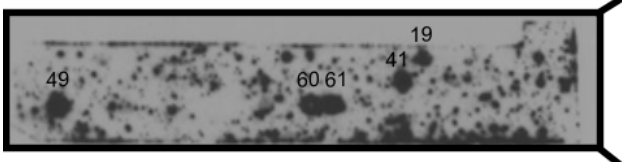


New SCAP$_{CTD}$ peptide array probed with
new batch SREBP2$_{CTD}$-His$_6$ fusion protein

Spot19: GKAGPEEPGDSPPLRHRP
Spot41: LELQGNLIVVGRSSGRLE
Spot49: VAARLNGSLDFFSLETHT
Spot60: AAAGRLVTGSQDHTLRVF
Spot61: VTGSQDHTLRVFRLEDSC

Figure 3.11. Probing of peptide array analysis of $SCAP_{CTD}$ with $SREBP2_{CTD}$-$His_6$ . Independent peptide arrays of immobilized peptide 'spots' of overlapping 18-mer peptides each shifted along by a five amino acid window in the CTD sequence of human SCAP were probed with either purified $SREBP2_{CTD}$-$His_6$ fusion protein (A) or purified non-specific control $His_6$ fusion protein (EndoIV-$His_6$) (B). The control protein array from (B) was then stripped and re-probed with purified $SREBP2_{CTD}$-$His_6$ fusion protein (C). A peptide array based on 18 amino acids of the parent peptide corresponding to spot 3 in which each amino acid was sequentially and individually substituted for alanine was probed with purified $SREBP2_{CTD}$-$His_6$ fusion protein (D). A newly synthesised peptide array of the CTD sequence of human SCAP was incubated with a new batch of purified $SREBP2_{CTD}$-$His_6$ fusion protein (E). Spot numbers relate to peptides in the scanned array. Interactions were detected by immunoblotting with mouse anti-$His_6$ antibody and visualised by ECL. Positively interacting peptides generate dark spots and non interacting peptides remain blank.

### *Peptide array analysis of $SCAP_{CTD}$ probed with $SREBP1_{CTD}$-$His_6$ fusion protein*

In order to identify residues within $SCAP_{CTD}$ involved in the SCAP-SREBP1 interaction a peptide array of $SCAP_{CTD}$ was probed with the SREBP1-$His_6$ fusion protein. The peptide array again consisted of a series of 18-mer peptides attached to a cellulose membrane, with each peptide overlapping with the next by 5 amino acids. Protein-peptide interactions were detected by immunoblot using the anti-His antibody. Probing of this peptide array with $SREBP1_{CTD}$-$His_6$ fusion protein resulted in the fusion protein binding to spots 3, 17, 25, 49, and 57-60 (Figure 3.12A). Spot 59 gave the strongest signal spot in a run of four spots and therefore was chosen for further investigation.

Spot 59 corresponds to the peptide ARLNGSLDFFSLETHTAL. An alanine scanning array based on the parent peptide of spot 59 was generated in which each amino acid was sequentially and individually substituted for alanine. This array was probed with $SREBP1_{CTD}$-$His_6$ fusion protein and surprisingly there was no fusion protein bound to spot 1 of the alanine scan array (Figure 3.12B). Spot1 is based on the unmodified parent peptide and is the sequence to which the fusion protein originally bound strongly. Thus, similar to the situation for the alanine scan using $SREBP2_{CTD}$-$His_6$ described earlier the alanine scanning array cannot be interpreted with confidence.

Also similar to the scenario seen with $SREBP2_{CTD}$-$His_6$ fusion protein different batch of $SREBP1_{CTD}$-$His_6$ fusion protein was used for probing the original full array than was used to probe the alanine scanning array. To investigate the reproducibility of specific binding a new batch of $SREBP1_{CTD}$-$His_6$ fusion protein was used to probe a new peptide array of $SCAP_{CTD}$. In this repeat array almost all of the peptide

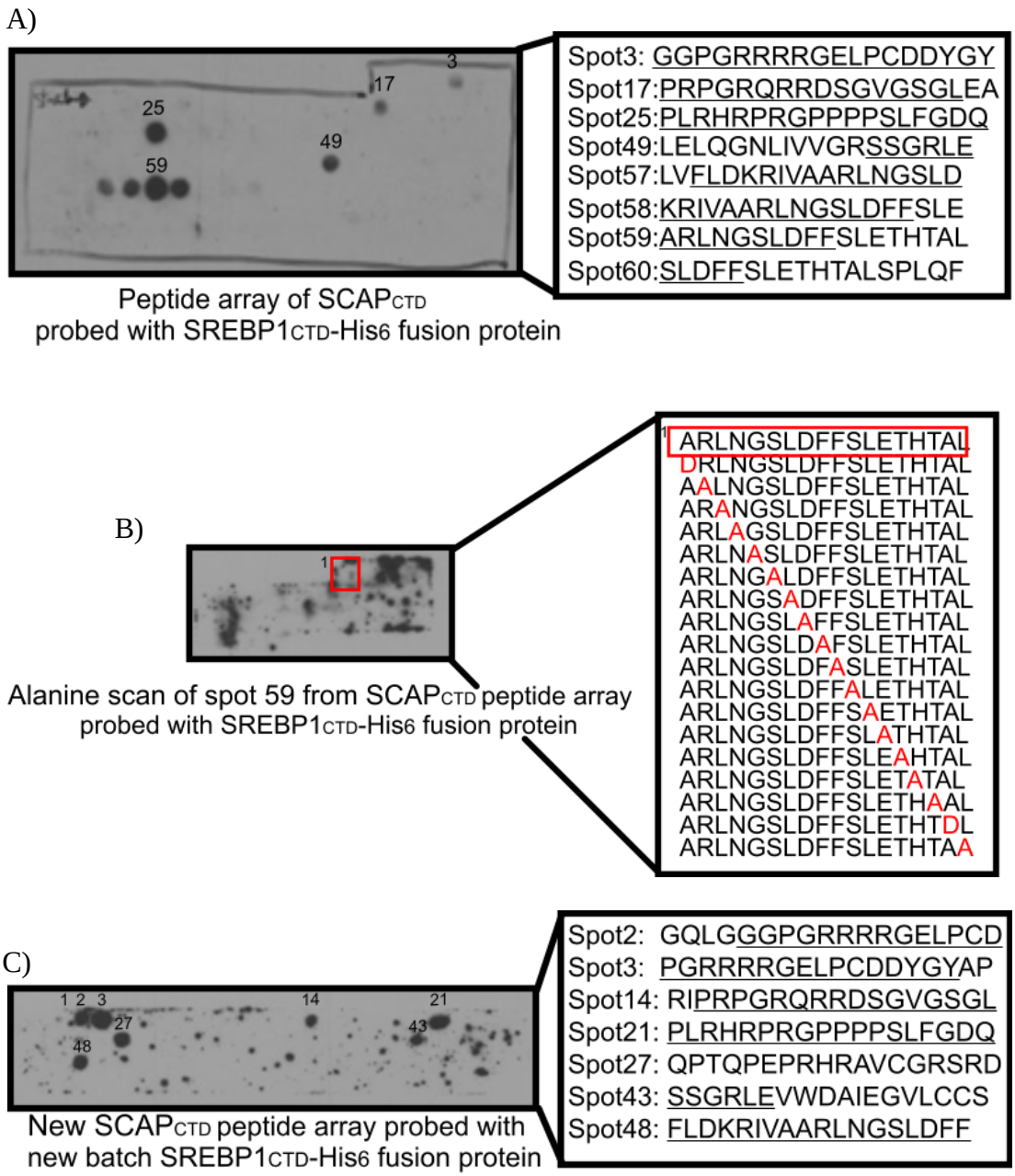


Figure 3.12. Peptide array analysis of $SCAP_{CTD}$. Peptide array of immobilized peptide 'spots' of overlapping 18-mer peptides each shifted along by five amino acids in the CTD sequence of human SCAP were probed with purified $SREBP1_{CTD}$-$His_6$ fusion protein (A). A peptide array based on 18 amino acids of the parent peptide corresponding to spot 3 in which each amino acid was sequentially and individually substituted for alanine was probed with purified $SREBP1_{CTD}$-$His_6$ fusion protein (B). A new peptide array of the CTD sequence of human SCAP was incubated with a new batch of purified $SREBP2_{CTD}$-$His_6$ fusion protein (C). Spot numbers relate to peptides in the scanned array. Interactions were detected by immunoblotting. Positively interacting peptides generate dark spots and non interacting peptides remain blank.

sequences which were positive for SREBP1$_{CTD}$-His$_6$ fusion protein binding in the first array were positive in the repeat array also (Figure 3.12C)including the peptide sequence which was used for the alanine scanning array and to which the SREBP1$_{CTD}$-His$_6$ fusion protein failed to bind. The reasons for SREBP1$_{CTD}$-His$_6$ fusion protein not binding the control peptide in the alanine scanning array are unclear.

The distribution of the SCAP$_{CTD}$ peptide sequences which bound SREBP1$_{CTD}$-His$_6$ fusion protein are shown in Figure 13. Within these peptide sequences, only some of the residues are conserved among vertebrate SCAP homologs. The conserved residues are initial candidate residues for mutating by site directed mutagenesis (SDM) and investigating the impact of their absence on SCAPs interaction with SREBP1. Interestingly, there is overlap between the peptide sequences bound by SREBP1$_{CTD}$-His$_6$ and the peptide sequences bound by SREBP2$_{CTD}$-His$_6$ (Figure 3.13, blue vs. underlined). The significance of this overlap with respect to the sites at which SREBP1 and SREBP2 interact with SCAP remains to be determined and requires clarification of the peptide array analysis with SREBP2$_{CTD}$-His$_6$ fusion protein, in addition to follow up SDM investigations for both SREBP1 and SREBP2.

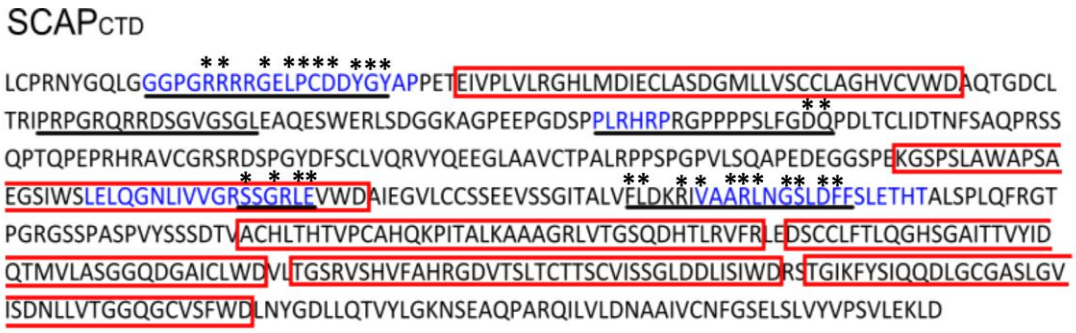


Figure 3.13. $SCAP_{CTD}$ amino acid sequence. WD40 repeats are highlighted in red boxes. Peptides of SCAP bound by preparations of $SREBP1_{CTD}$-$His_6$ are underlined. Amino acids present in peptides bound by preparations of $SREBP1_{CTD}$-$His_6$ and $SREBP2_{CTD}$-$His_6$ are in blue. Residues conserved in $SCAP_{CTD}$ among vertebrates are indicated with asterisks.

## Discussion

The SREBP family of transcription factors are central in regulating the expression of genes involved in sterol and fatty acid biosynthesis. The interaction of SCAP with the SREBPs is essential for maintaining SREBP protein stability (Rawson et al. 1999). The interaction of SCAP with the SREBPs is also essential for regulating the proteolytic processing of the SREBP precursor proteins which yields the active transcription factor domain (Korn et al. 1998). The interaction between the SREBP and SCAP has been localised to the respective CTDs of these two proteins (Sakai et al. 1997). The CTD of SCAP is a large cytosolic portion of the protein which was initially reported to contain five WD40 repeat motifs (Nohturfft et al. 1998). Analysis of human $SCAP_{CTD}$ protein sequence using EMBL's SMART tool indicated the presence of a sixth WD40 motif, designated WD2. The loose nature of the WD40 consensus sequence may be a reason for this extra motif not being recognised when initial sequence analysis was performed by others.

The WD40 repeats within $SCAP_{CTD}$ are attributed with mediating SCAPs interaction with SREBP. Conservation of these repeats in SCAP protein homologs from other vertebrate species was investigated at the protein level to gain insight into identifying residues of importance within these WD repeat regions. Multiple sequence alignment of SCAP amino acid sequences from a wide variety of vertebrates ranging from humans to zebrafish revealed 46% sequence identity within the CTD. It also showed conservation of the presence of all six WD repeats. Within the WD40 repeats only there is an average of 70% identity, with the exception of WD2 which had 44%. This high level of identity within the WD repeats relative to the rest of the CTD is a strong indication of their functional importance. However this high level of identity

makes identification of residues critical to the SCAP-SREBP interaction more difficult. While analysis of SCAP homologs from invertebrates showed that they also contain a number of WD repeats, their overall SCAP protein sequences are quite divergent from vertebrate SCAP. Similarly their SREBP homolog with also has a sequence highly divergent from vertebrate SREBP. Thus for the purpose of identifying residues important for vertebrate SCAP-SREBP interaction, comparison with invertebrate SCAP was not deemed appropriate. However, the evolutionary conservation of WD repeats is a strong indicator of their importance in mediating the interaction with SREBPs, which is the only known function of $SCAP_{CTD}$.

Identifying a protein interaction site by peptide array analysis involves one protein being immobilised as 18-25mer overlapping peptides and being probed with the interacting protein in its native state. Although the protein on the array is not in its natively folded state, this approach has been successfully used in many other cases to identify key interacting sites. SCAP CTD is a WD domain protein but its crystal structure is not known. Other WD domain proteins that have crystal structures available appear to form a consensus β-propeller structure. Attempts to generate a predicted 3D structure of SCAP CTD by homology modelling based on other WD domain proteins proved unsuccessful. This is likely limited by the WD domain proteins with crystal structures solved as they contain seven or eight WD repeats, and no protein structures with six WD repeats are available.

The above bioinformatic analysis was performed to compliment experimental determination of the binding site for each SREBP1 and SREBP2 on SCAP by peptide array analysis.

Determining the site on SCAP which interacts with SREBP1 and SREBP2 by peptide array analysis required cloning, over-expression and purification of human SREBP1 and SREBP2 CTDs fused to an epitope tag to facilitate purification by affinity chromatography. However, several issues were encountered in attempts to purify this protein. Firstly, GST-SREBP$_{CTD}$ was found to be insoluble by conventional bacterial cell lysis using a combination of lysozyme and sonication. The fusion protein aggregated in insoluble IBs. IBs are a common occurrence when forcing exogenous protein over-expression but are believed to contain correctly folded proteins (Frangioni & Neel 1993). Attempts to solubilise these IBs with detergents under conditions that would facilitate purification of the GST-SREBP$_{CTD}$ fusion proteins were somewhat successful but were not pursued as the downstream removal of the detergents combined with the low yield of protein was considered problematic. Thus an alternate approach to clone and over-express SREBP$_{CTD}$ fused to a carboxy terminal$His_6$ tag was pursued.

SREBP$_{CTD}$-$His_6$ fusion proteins were expressed at much lower concentrations than the GST-SREBP$_{CTD}$ fusion proteins. The reason for this difference is unclear but is likely to be due to the context of translation in GST being higher than the context for translation in SREBP$_{CTD.}$ Fortuitously, the lower expression of SREBP$_{CTD}$-$His_6$ resulted in a higher yield of soluble fusion protein. Attempts to purify the SREBP$_{CTD}$-$His_6$ fusion proteins resulted in only a small fraction of the fusion protein binding the nickel affinity column and the rest remained in the flow through fraction. Re-purification of the flow through fraction did not result in any further SREBP$_{CTD}$-$His_6$ fusion protein binding. A likely explanation for this occurring is that there are two conformations of fusion protein present in the soluble fraction; one with $His_6$ tag available for binding the affinity resin (<10%), and the other (>90%) in a

conformation which has the tag occluded. We chose to proceed with the fraction that was binding the resin, as detection with the His antibody at the peptide array stage would only be possible for this fraction.

Analysis of the fractions containing purified $SREBP_{CTD}$-$His_6$ by coomassie staining indicated there was substantial contaminating protein present. Increasing the amount and stringencies of the wash steps prior to elution did not remove this contamination. Gel filtration FPLC of the eluted fractions did reduce contaminating protein present with the $SREBP_{CTD}$-$His_6$ fusion protein, but also resulted in lowering the fusion protein concentration to less than 0.1µg/ml. This is 100-fold less than the minimum concentration of fusion protein required for probing the peptide array. However, the anti-His antibody used was highly sensitive and gave a strong clean signal for the $SREBP_{CTD}$-$His_6$ fusion proteins in the pre FPLC crudely purified fractions. Therefore the crudely purified fusion protein was used for peptide array experiments.

A peptide array of $SCAP_{CTD}$ probed with $SREBP2_{CTD}$-$His_6$ identified one peptide region of interest with respect to SREBP2 binding. However $SREBP2_{CTD}$-$His_6$ failed to bind the positive control peptide of an alanine scanning array of this peptide. The batch of $SREBP2_{CTD}$-$His_6$ used to probe the alanine scanning array was different to that used in the initial array, and it was suspected that the issues surrounding fusion protein purification were causing the differences between the two results. However, not only did a new batch of $SREBP2_{CTD}$-$His_6$ fusion protein fail to bind the initially identified peptides but bound to new peptides not recognised by the original batch. This variability between batches of purified $SREBP2_{CTD}$-$His_6$ offers an explanation for the results of the alanine scanning array, but how to limit this variability is

unclear. This issue requires clarification before results from the $SCAP_{CTD}$ peptide array probed with $SREBP2_{CTD}$-$His_6$ can be interpreted correctly.

A peptide array of $SCAP_{CTD}$ probed with $SREBP1_{CTD}$-$His_6$ indicated multiple peptide spots of interest. The strongest spot in a run of four spots in a row was deemed the strongest candidate to follow up first. However similar to what occurred with $SREBP2_{CTD}$-$His_6$, $SREBP1_{CTD}$-$His_6$ failed to bind the positive control peptide of an alanine scanning array of this peptide. The batch of $SREBP1_{CTD}$-$His_6$ used to probe the alanine scanning array was also different to that used in the initial array. However, unlike what occurred with $SREBP2_{CTD}$-$His_6$, probing of the repeat $SCAP_{CTD}$ array with the new batch of $SREBP1_{CTD}$-$His_6$ fusion protein confirmed the original peptides of interest. Thus in this instance, the reason for $SREBP1_{CTD}$-$His_6$ not binding alanine scanning array is not likely due to differences between the batches of purified fusion protein and remains unclear.

In the absence of a crystal structure to narrow the amino acids of interest down, all of the residues in the $SCAP_{CTD}$ peptides detected as binding $SREBP1_{CTD}$-$His_6$ require follow up with SDM and co-immunoprecipitation and/or SREBP bioassay screening experiments before any inferences on residues mediating the binding of SCAP to SREBP1can be made. However, the residues which are conserved among vertebrate SCAP homologs are ideal candidates to investigate first.

Interestingly, there are several motifs present within the $SCAP_{CTD}$ peptides detected as binding $SREBP1_{CTD}$-$His_6$ when analysed using ‘Motif Scan’, which is available on the ExPASy bioinformatics resource portal. The ‘PGRR’ motif in the first peptide was identified as candidate amidation site. The ‘RRDS’, ‘GVGSGL’ and ‘SGLE’ motifs in the second peptide were identified as candidate sites for cAMP-dependent

protein kinase phosphorylation, N-myristoylation and casein kinase II phosphorylation, respectively. The third peptide 'PLRHRPRGPPPP', together with the eight amino acids upstream of this peptide sequence within $SCAP_{CTD}$ (PEEPGDSP) was identified as a proline rich region. Finally the 'GVLCCS' motif in the fourth peptide was identified as another candidate N-myristoylation site. However it is important to note that the match score given for the above post-translational modification sites (based on their similarity to template motifs in the Prosite database) was 'questionable' and would require biological evidence to confirm post-translational modification on SCAP within these sites. It would be interesting to see if SDM of the residues of these motifs would influence the interaction of SCAP with SREBP1. The presence of a proline rich region within the $SCAP_{CTD}$ is interesting as other proteins contain domains which are known to bind proline rich motifs. Domains which bind proline rich motifs include SH3, WW, EVH1, GYF, UEV and profilin domains (Ball et al. 2005). It would be interesting to see if the proline region within SCAP is a binding site for a protein containing one of the already characterised proline motif binding domains. $SREBP_{CTD}$ does not appear to contain any of the characterised proline motif binding domains when the $SREBP_{CTD}$ amino acid sequence was analysed in Motif Scan, although this does not rule out $SREBP_{CTD}$ containing a novel proline rich motif binding domain, if this proline rich region was found to mediate the interaction of SCAP with SREBP.

# Chapter 4

## Development of a Single Secreted Luciferase Gene Reporter Assay

## Abstract

Promoter analysis typically employs a reporter gene fused to a test promoter combined with a second reporter fused to a control promoter which is used for normalisation purposes. However, this approach is not valid when experimental conditions affect the control promoter. We have developed and validated a single secreted luciferase reporter assay (SSLR) for promoter analysis that avoids the use of a control reporter. The approach uses an early level of expression of a secreted luciferase linked to a test promoter as an internal normalisation control for subsequent analysis of the same promoter. Comparison of the SSLR assay with the dual luciferase reporter (DLR) assay using HMGCR and LDLR promoter constructs, which are down regulated by 25-hydroxycholesterol, show that both assays yield similar results. Comparison of the response of the HMGCR promoter in SSLR transient assays compared very favourably with the response of the same promoter in the stable cell line. Overall the SSLR assay proved to be a valid alternative to the DLR assay for certain applications and had significant advantages in that only measurement of one luciferase is required and monitoring can be continuous as cell lysis is not necessary.

## Introduction

Gene reporter assays are widely used to study the composition and activity of promoters under different experimental conditions. In such assays, the reporter gene is placed under the control of a promoter of interest and serves as a quantitative readout of promoter activity. These assays have a very high utility and are commonly used for mapping promoters and investigating the response of promoters to transcription factor activity or upstream signalling pathway activity. Several reporter genes encode enzymes whose activity can be readily and easily monitored in a quantifiable fashion. Luminescent reporter gene assays utilising luciferases are arguably the most prominent for promoter analysis in cell culture models and in biomolecular cell screening. The high signal to noise ratio and the wide dynamic range of luminescent reporter gene assays make them particularly suited for high throughput screening applications and the development of modified, or use of novel luciferases has greatly extended the utility of these assays (Miraglia et al. 2001), (Fan & Wood 2007). The recent development of secreted luciferases (Nakajima et al. 2004; Verhaegen & Christopoulos 2002) has removed the requirement for cell lysis and has extended the utility of these assays even further enabling continuous monitoring of promoter activity in a single sample.

The employment of luminescent reporter gene assays for investigation of promoters is typically performed by transient transfection of a promoter-luciferase construct into a host cell and measuring luciferase activity in control and test samples under different conditions. As transient transfection efficiencies can vary across samples, this approach requires an internal transfection control in each sample for normalisation purposes. In addition to normalising for transfection efficiencies, the internal transfection control also normalises for other variables including variations

in cell plating and cell lysis efficiencies, toxicity and pipetting inconsistencies (Schagat et al. 2007).

A DLR assay system has been developed for the use of promoter-luciferase constructs in transient transfections (Dyer et al. 2000) and is widely used. In this dual system one luciferase, whose activity can be determined using a specific substrate, is used for reporting on the test promoter while a second luciferase, whose activity can be determined using a different substrate, and which is linked to a constitutively active promoter (such as that of thymidine kinase (TK), cytomegalovirus (CMV) or simian virus 40 (SV 40)) functions as the control. This DLR assay system typically employs *Firefly* (*P. Pyralis)* luciferase as the reporter for the promoter being tested and *Renilla* (*R. Reniformis*) luciferase as the reporter for the control promoter. *Firefly* and *Renilla* luciferases both generate light but utilise distinct substrates (D-luciferin and coelenterazine, respectively) which enables the activity of each enzyme in a single sample to be measured (Dyer et al. 2000). More recently, a DLR assay has been developed which utilises secreted luciferases from *Cypridina* and *Gaussia* species (Wu, Suzuki-ogoh, et al. 2007). The sensitivity and ease of measurement of this dual secreted luciferase assay is comparable to the original DLR assay, but it has advantages in that cell lysis is not required and readings can be taken across multiple time points from the same cell population. Like the original DLR assay, this method also requires normalisation to a control reporter plasmid (Wu, Suzuki-ogoh, et al. 2007). However, the secreted dual assay has not been widely adopted largely due to the instability of the *Cypridina* substrate (Wu, Kawasaki, et al. 2007). One concern with the DLR assay system is that an assumption is made that the transfection efficiency of the test plasmid is tightly correlated with the transfection efficiency of the control plasmid. In addition,

the utility of the DLR assay is limited in some situations where the promoter driving the control reporter is affected by experimental conditions (Ibrahim et al. 2000)(Chatterjee et al. 2009). Thus the use of the control reporter in the DLR assay system requires preliminary investigation to ensure that the control promoter is not affected by the test conditions. If the control promoter is affected by the test conditions, this obstacle may be overcome in some cases through the use of alternative control promoters, however, in many cases factors that affect one control promoter also affect other control promoters (Ho & Strauss III 2004). During the course of this thesis it was realised that progesterone negatively affected readout of both CMV and TK promoters of the Renilla control reporter plasmid. This meant that the DLR assay system was not suitable for investigation of progesterone. This prompted the development of a luciferase reporter system that was independent of a control reporter and better suited our needs.

Here we report and validate a single secreted luciferase (SSLR) assay approach for promoter analysis that avoids the use of a control reporter. This assay provides a valid alternative to the DLR assay particularly for situations where experimental factors affect control promoters. In addition, the assay offers a simpler approach than the DLR assay and can be used to replace it in appropriate situations.

The promoters used in the development of the SSLR are regulated by the transcription factor (TF) SREBP2. SREBPs are synthesised as inactive precursor proteins and SREBP target gene expression is induced upon proteolytic processing and release of the TF domain. A HeLa stable cell line was also generated which contained the secreted luciferase reporter used in the development of the SSLR to facilitate convenient and routine monitoring of SREBP processing.

## Results

### *Development and Validation of SSLR Assay*

We have employed a secreted luciferase from *Gaussia* (GLuc) species for use in this assay system. The advantage of a secreted luciferase is that lysing of cells is not necessary and production of the luciferase from the cells can be monitored continuously. In addition, GLuc is stable and easy to assay and like *Renilla* luciferase oxidises coelenterazine (Wurdinger et al. 2008). The basis of the approach reported here is that an early level of expression of luciferase from a promoter-GLuc reporter plasmid can be used as an internal normalisation control for experimental variables that occur in analysis of the promoter using the same plasmid.

To validate and demonstrate the use of the SSLR assay we applied it to the sterol response element binding protein (SREBP) pathway. Briefly, SREBPs are a family of transcription factors that regulate expression of genes involved in lipid and cholesterol synthesis, including HMGCR (3-hydroxy-3-methylglutaryl-Coenzyme A reductase receptor) and LDLR (low density lipoprotein receptor) (Horton et al. 2002a). These SREBP proteins are synthesised as endoplasmic reticulum (ER)-membrane bound inactive transcription factors and following release from the ER, they undergo proteolytic processing in the Golgi to yield a large N-terminal product which serves as an active transcription factor (nSREBP) (Goldstein and Brown, 1999). nSREBP activates target gene expression through binding to sterol response elements (SREs) within a large number of target promoters including the HMGCR and the LDLR promoter. 25-hydroxycholesterol (25-OHC) is a potent inhibitor of SREBP activation and functions by preventing SREBP release from the ER. It is well established that incubation of cells with this oxysterol results in a decrease in SREBP target gene expression including HMGCR and LDLR (Adams et al. 2004).

HMGCR and LDLR promoter reporter plasmids were constructed by inserting the core promoter region of either the HMGCR (-270 to +77) gene or the LDLR gene (-590 to +93) directly upstream of the GLuc in the plasmid pGLuc-basic and were designated pGLuc-promHMGCR and pGLuc-promLDLR, respectively (Figure 4.1).

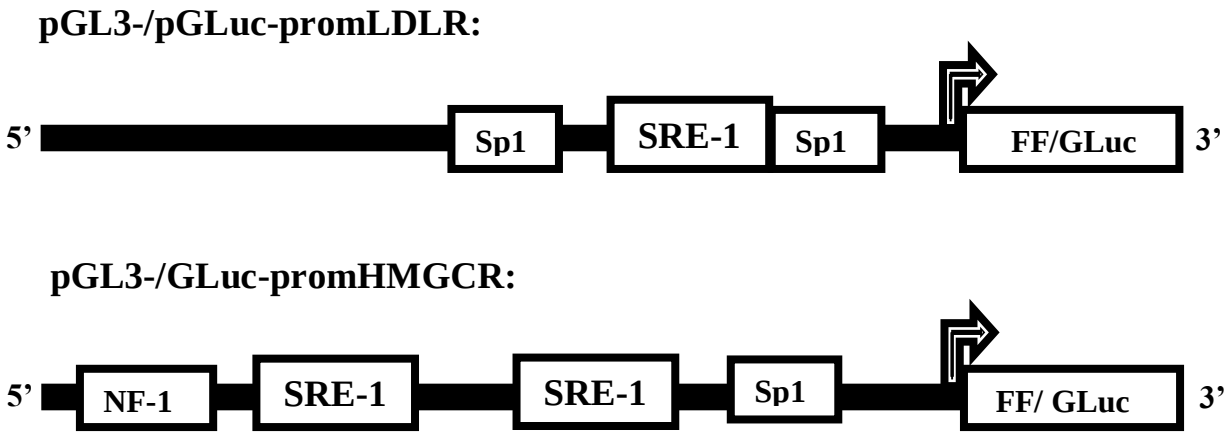


Figure 4.1. Sterol regulatory elements (SRE) within the human LDLR and HMGCR promoters cloned into pGL3-basic and pGLuc-basic luciferase reporter plasmids.

To simulate a large difference in transfection efficiency, HeLa cells were transfected with two different amounts (250ng or 500ng) of pGLuc-promHMGCR or pGLuc-promLDLR plasmid DNA. Fresh media was added to the cells following removal of the transfection agent and secreted luciferase activity was measured at hourly intervals over a 15 hr period (Fig. 4.2A and 4.2C). As expected, the level of luciferase secreted was greater in the cells transfected with 500ng vs. 250ng of the construct. The fold difference in secreted luciferase activity was calculated across all of the time points for the 500ng vs. 250ng of plasmid transfected (data not shown). A

two-fold difference was expected for a scenario whereby transfection efficiencies were identical and experimental variables were absent. The fold differences observed varied substantially from two fold and ranged from 2.76 to 3.60 for pGluc-promHMGCR and 1.34 to 1.84 for pGluc-promLDLR. The variation observed presumably reflects experimental variables including transfection and cell plating efficiencies. Normalisation of output to input should correct for the experimental variables as long as the output and input are from the same transfected cells. Normalisation is possible using secreted luciferase since secreted luciferase from the same transfected cells can be measured at an early point (input) and measured again at a later point (output). The normalised secreted luciferase activity should be the same for a given reporter construct and should be independent of reporter plasmid concentration since there should be a direct correlation between input and output. Normalisation was examined statistically using two different approaches. In the first approach, data from each timepoint for the 250ng and 500ng pGLuc-promHMGCR or pGLuc-promLDLR transfections was normalised to the data from each time point from one to eight hours and statistical analysis using a mixed-model ANOVA was performed. P values for normalisation of the pGLuc-promHMGCR readout using time points from 1 to 8 hours were 0.0001, 0.233, 0.01, 0.429, 0.081, 0.052, 0.052, and 0.796 respectively while P values for normalisation of the pGLuc-promLDLR readout using time points from 1 to 8 hours were 0.961, 0.116, 0.070, 0.116, 0.175, 0.717, 0.781 and 0.359 respectively. Thus significant differences were only observed using 1 or 3hr time points for normalisation. Normalisation of the pGLuc-promHMGCR data using the 5, 6 and 7hr time points were close to being significantly different (P= 0.081, 0.052 and 0.052 respectively). However, close inspection of the data shows that a dip at a single time point, namely the 9hr time

point for the 250ng pGLuc-promHMGCR transfection is contributing substantially to this. In the second normalisation approach the 15 hour time point was normalised to each time point from 1 to 8 hours and statistical analysis was performed using the Student t test. P values for normalisation of the data using time points from 1 to 8 hours were 0.04, 0.385, 0.003, 0.955, 0.367, 0.332, 0.593 and 0.491 respectively for pGLuc-promHMGCR and 0.956, 0.099, 0.067, 0.163, 0.260 and 0.671, 0.764 and 0.399 respectively for pGLuc-promLDLR. Thus, both statistical approaches are in agreement with statistically significant differences only observed using 1 hour and 3 hour points for normalisation for the pGLuc-promHMGCR data across all the data sets. We assume that the differences observed using early time points for normalisation reflect a) variation in cell recovery time following removal of the transfection agent and b) variation in time required to achieve full establishment of expression of luciferase post transfection. Informed by this analysis, we chose the six hour time point for normalisation in further experiments as we deemed three additional recovery hours after the latest point where statistical differences were observed (3 hours) a sufficient margin to ensure for full recovery post transfection and achievement of steady state expression in the protocol outlined here. Plotting of the data normalised to the 6hr timepoint shows that the approach did indeed correct for transfection efficiencies and experimental variables as little appreciable difference was observed between the 500ng and 250ng samples at each timepoint (Fig. 4.2B, 4.2D) and fold variation only ranged from 0.85 to 1 for pGLuc-promHMGCR and 0.92 to 1.09 for pGLuc-promLDLR. In the DLR assay, data points are typically generated for a single time point and compared using the Student's t test. In essence, comparison of the final 15hr time point normalised to the 6hr time point simulates a typical single point DLR assay.

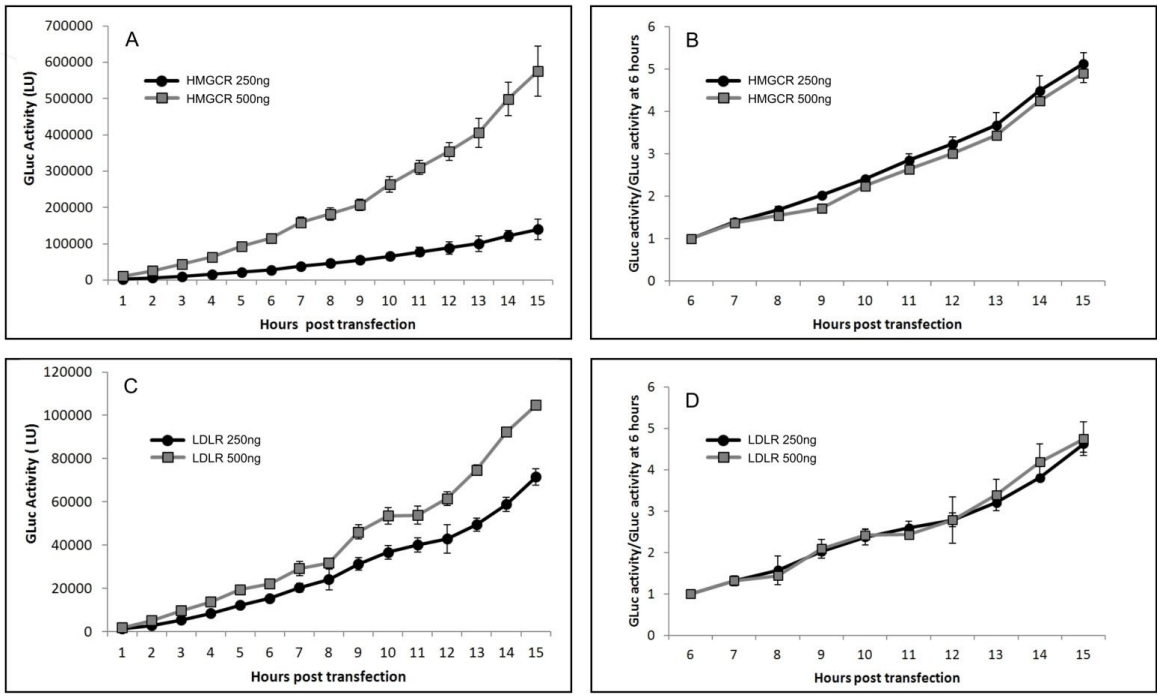


Figure 4.2. Normalising secreted GLuc data to an initial secretion time point corrects for differences in plasmid transfection efficiencies. HeLa cells were transfected for 6- 9 hours with 250ng or 500ng of luciferase reporter construct. Following removal of the transfection agent, secreted luciferase activity was measured at hourly intervals. A) Luciferase activity after transfection with 250 ng or 500 ng pGluc-promHMGCR, B) pGluc-promHMGCR luciferase activtity normalised to the 6 hour time point, C) Luciferase activity after transfection with 250 ng or 500 ng pGluc-promLDLR, D) pGluc-promLDLR luciferase activtity normalised to the 6 hour time point. The values shown represent the average from three independent transfection experiments (±S.D.).

As outlined above no significant difference was observed between the HMGCR samples (P=0.332) or between the LDLR samples (P=0.671) normalised in this manner. These data show that normalisation using this SSLR assay approach essentially corrects for experimental variables and this method should be a viable alternative for the DLR assay.

As 25-OHC is a potent inhibitor of SREBP activation and down regulates both the HMGCR and LDLR promoters we compared the results of the effect of 25-OHC on the activity of these two promoters using the SSLR and the DLR assay. The concentration of 25-OHC chosen was checked to determine if it had any inhibitory or stimulatory effect on HeLa cell proliferation using a MTT assay. No significant change in cell proliferation was observed with the addition of the 25-OHC to the media over the treatment period (data not shown). For the DLR assay, the core promoter regions of HMGCR and LDLR in pGLuc-promHMGCR and pGLuc-promLDLR were cloned directly upstream of *Firefly* luciferase in the plasmid pGL3-basic, and designated pGL3-promHMGCR and pGL3-promLDLR, respectively. HeLa cells were transfected with a) pGLuc-promHMGCR or pGLuc-promLDLR, or b) pGL3-promHMGCR or pGL3-promLDLR with a reporter control plasmid (pRL-TK) comprising the *Renilla* luciferase fused to the TK promoter. Fresh media was added following removal of the transfection mixture and cells were allowed to recover for 6 hours, at which point a small aliquot of media was removed from the SSLR samples for normalisation purposes and 25-OHC was added at a final concentration of 1.25 µM. After a 16 hour incubation period in the presence of the oxysterol, samples were collected and analysed (Fig. 4.3A). Analysis of the raw data showed that the 25-OHC down regulated luciferase readout from all the constructs. Without normalisation, 25-OHC treatment registered a 3.83 fold decrease in pGLuc-

promHMGCR and a 2.92 fold decrease in pGL3-promHMGCR (Fig. 4.2A and Table 4.1). Normalisation of the data showed that both assays had generated similar results with a 2.03 fold and a 2.8 fold decrease recorded using the SSLR and DLR assays respectively (Fig. 4.3B and Table 4.1). For the LDLR promoter without normalisation, 25-OHC treatment registered a 3.71 fold decrease in pGLuc-promLDLR and a 1.87 fold decrease in pGL3-promLDLR, while normalisation of the data showed a 4.28 fold and 1.95 fold decrease using the SSLR and DLR assays respectively (Table 4.1). For comparison purposes, we removed the experimental variables associated with the transfection by generating stable HeLa cell lines (A6, B2 and B3) using the pGLuc-promHMGCR construct. Treatment of the A6, B2 and B3 stable cell lines with 25-OHC in a similar manner to the transfected cells resulted in a 2.23, 2.81 and 2.20 fold decrease in HMGCR promoter activity respectively. The decrease recorded was similar to that observed in the transfected HeLa cells using the SSLR assay and the DLR assay.

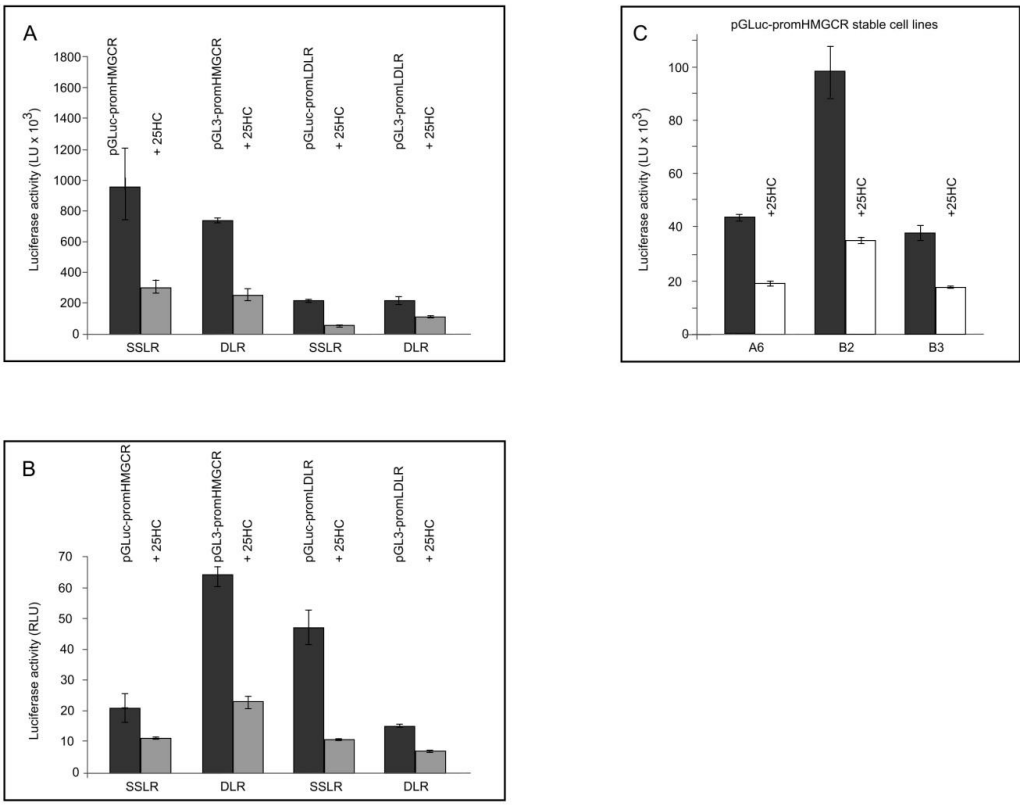


Figure 4.3. Comparison of the SSLR Assay and DLR Assay. HeLa cells, transfected with pGLuc-promHMGCR, pGLuc-promLDLR, pGL3-promHMGCR/ pRL-TK or pGL3-promLDLR/ pRL-TK or stable pGLuc-promHMGCR Hela cell lines were incubated in the absence or presence of 25-OHC. For SSLR assay samples, luciferase activity was measured 6 hours after transfection agent removal prior to 25-OHC treatment and after 16 hours incubation with 25-OHC. (A) HMGCR and LDLR promoter activity ±25-OHC, not normalised. (B) HMGCR and LDLR promoter activity ± 25-OHC, normalised to secreted luciferase at 6hours for the SSLR Assay and normalised to Renilla for the DLR Assay The values shown represent the average from three independent transfection experiments (±S.D.). (C) HMGCR promoter activity ± 25-OHC in the stable pGLuc-promHMGCR Hela cell lines A6, B2 and B3.

Table 4.1: Comparison of the levels of repression of the HMGCR promoter and the LDLR promoter by 25-OHC in HeLa cells as measured by the SSLR and the DLR assay.

| | ***Fold repression of HMGCR promoter by 25-hydroxycholesterol**** | ***Fold repression of LDLR promoter by 25-hydroxycholesterol**** |
|---|---|---|
| SSLR assay<br>- not normalised | 3.83 (± 0.356) | 3.71 (± 0.122) |
| SSLR assay<br>- normalised | 2.03 (± 0.536) | 4.28 (± 0.657) |
| DLR assay<br>- not normalised | 2.92 (± 0.428) | 1.87 (± 0.141) |
| DLR assay<br>- normalised | 2.80 (± 0.210) | 1.95 (± 0.138) |
| Control pGLuc-promHMGCR stable cell lines (A6, B2, B3) | (A6) 2.23 (± 0.266)<br>(B2) 2.81 (± 0.523)<br>(B3) 2.20 (± 0.186) | |

The values shown represent the average from three independent transfection experiments.

### *Generation of HeLa-PHGL Stable Cell Line*

In order to conveniently and routinely monitor SREBP activity in response to various treatments or culture conditions, a HeLa cell line was generated which stably expresses the pGLuc-promHMGCR secreted luciferase reporter plasmid. Activation of SREBP target genes, including HMGCR, serves as an accurate readout for SREBP processing. Briefly, HeLa cells were transfected at 80-90% confluency with pGLuc-promHMGCR using TurboFect transfection reagent (as described under methods). Following six hour incubation, the transfection mixture was removed and replaced with FS media. Cells were cultured for a further 48 hours, at which point they were trypsinized and re-seeded in selection media (FS media containing 400 µg/ml G-418). The selection media was replenished every 3-4 days to identify individual clones expressing the luciferase reporter construct, which were then isolated using cloning discs. Eight single stable integrants were grown up and assayed for SREBP feedback response in the presence of 25-OHC under LDS conditions (Figure 4.4A). The three best responding colonies; A6, B2 and B3, were grown up and again assayed assayed for SREBP feedback response in the presence of 25-OHC under LDS conditions (Figure 4.4B). Colony B2 displayed the maximum fold repression of the HMGCR reporter plasmid (4.03-fold, $p=0.0189$) and thus was the stable cell line selected for experimental use. This stable cell line was designated HeLa-PHGL.

A)

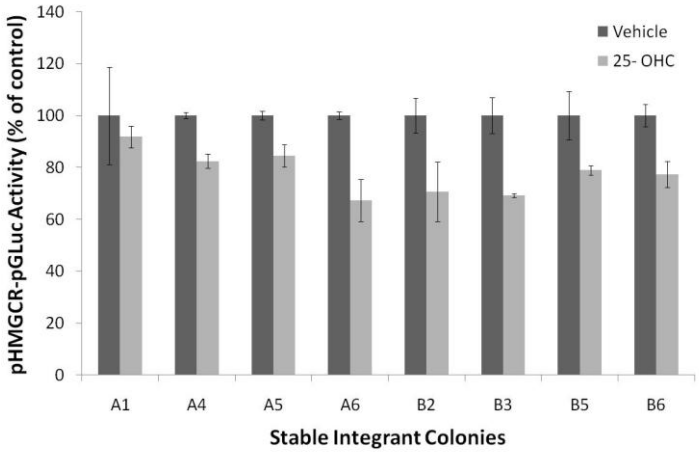


B)

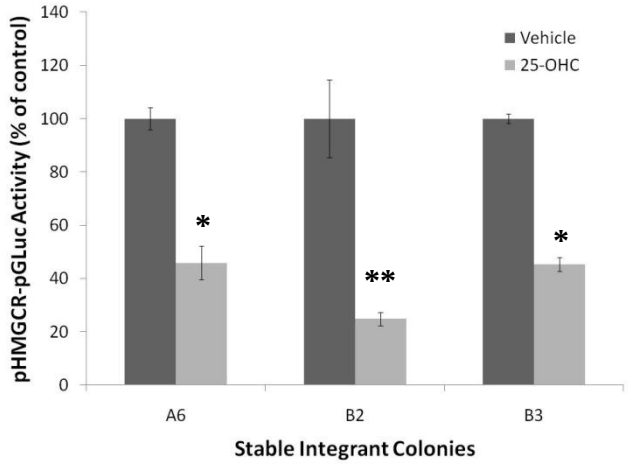


Figure 4.4. Assessment of HeLa pGLuc-promHMGCR stable cell lines for secreted luciferase activity and cholesterol feedback response. (A) Eight HeLa cell lines selected for stable pGLuc-promHMGCR integration were grown to 80% confluency and assayed for SREBP feedback response in the presence of 1µg/ml 25-OHC in LDS conditions. (B) The three best responding colonies (A6, B2, B3) were sub-cultured, grown to 80% confluency and assayed for SREBP feedback response in the presence of 25-OHC in LDS conditions. Experiments were performed in triplicate and error bars represent ± SD. Significance of maximum reporter repression was measured using Student's t-Test (*$p<0.05$).

## Discussion

These results show that the SSLR assay is a valid substitute for the DLR assay and offers an alternative approach to overcome circumstances where the control reporter is affected in the DLR assay. In addition, we find this assay to have a number of advantages over the widely used DLR assay. Firstly, the assay has a lower number of experimental variables as a co-transfection of a control reporter plasmid is not required. Secondly, unlike the DLR assay, normalisation does not assume correlation of transfection efficiency between the test and control reporters. Finally, the DLR assay requires two different substrates whereas the SSLR assay system only requires a single substrate and consequently requires less time and is more cost-effective. In addition, it has been reported that GLuc works efficiently in simple buffers (Verhaegen & Christopoulos 2002), and worked well in phosphate buffered saline (PBS) in our hands. The secreted aspect of the luciferase provides an additional significant advantage over the standard DLR as measurements can be made continuously from a single transfection and cell lysis is not required. The results suggest that the SSLR assay has a similar accuracy level to the DLR assay since the down regulation of the HMGCR promoter by 25-OHC recorded using the SSLR and DLR assays were in the same range as the down regulation observed in the cell lines. The robust nature of the GLuc, the simplicity of the SSLR assay and the lack of a requirement for cell lysis makes the SSLR an attractive platform for promoter analysis particularly in the area of analysing of the effect of small molecules on promoter activity in transient assay systems.

This SSLR assay and the HeLa-PHGL stable cell line proved to be valuable tools in monitoring SREBP processing and were subsequently used throughout the course of this thesis.

# Chapter 5
## Characterisation of SCAP Interacting Proteins

# Chapter 5A

## Investigation of the Regulation of SREBP Processing by PGRMC1

## Abstract

The activity of the sterol response element binding protein (SREBP) family of transcription factors is regulated by a proteolytic processing event which requires translocation of inactive SREBP precursor proteins from the endoplasmic reticulum (ER) to the Golgi. The SREBP cleavage activating protein (SCAP) is essential for regulating this translocation in response to cellular sterol levels. A direct interaction between SCAP and progesterone receptor membrane component 1 (PGRMC1) was recently identified. In this chapter, PGRMC1 was investigated with respect to regulation of SREBP processing. The results indicate that over-expression of PGRMC1 does not affect SREBP processing, as measured by SREBP/HMGCR luciferase reporter readout. Co-expression of SCAP with PGRMC1 caused a minor, yet significant, increase in SREBP processing under lipid depleted conditions only. PGRMC1 is a putative progesterone (P4) binding protein. The presence of P4 did not change the lack of effect of PGRMC1 on regulating SREBP processing. Interestingly, P4 decreased cell viability under FS conditions but not under LDS conditions. Over-expression of PGRMC1 was found to abolish the protective effect against P4 observed in LDS and decreased cell viability. Over-expression of SCAP was found to have the same effect, but to a lesser extent. While PGRMC1 appears to not regulate SREBP processing, the significance of PGRMC1 interacting with SCAP is unclear, but may be linked to mediating the cytotoxic effects of P4 in lipid depleted conditions.

## Introduction

The human progesterone receptor membrane component-1 (PGRMC1) gene maps to chromosome Xq22-24 (Mansouri et al. 2008). This gene encodes a protein comprising an amino-terminal membrane spanning domain which anchors a larger cytoplasmic domain (Mifsud & Bateman 2002). Literature surrounding PGRMC1 is documented under a number of names owing to its discovery in distinct scientific areas. The history surrounding this and distant PGRMC1 homologs is found in a comprehensive review by Cahill (Cahill 2007). Expression of human PGRMC1 was first reported in 2002, although this was not the original work on this protein. Vertebrate non-genomic progesterone receptors were identified in 1996 and this was closely followed by cloning of the human gene in 1998 under the name heme progesterone receptor 6.6 (Hpr 6.6).

The PGRMC1 protein is localised to the ER membrane, however evidence also exists for its translocation to both the plasma membrane surface and the nucleus, although regulation surrounding such translocation is unclear (Nölte et al. 2000; Peluso et al. 2010; Peluso et al. 2005). Homology sequence analysis revealed that the cytosolic domain of PGRMC1 is highly similar to the heme-binding domain of Cytochrome b5 (Song et al. 2004). PGRMC1 is broadly expressed and has elevated levels in the liver and adrenal glands, which are sites of high P450 activity (Meyer et al. 1996; Raza et al. 2001). Subsequently, evidence emerged that PGRMC1 was in fact a heme-binding protein, and elicits similar effects to Cytochrome b5 in regulating the activity of Cytochrome P450 proteins (Min et al. 2005). Cytochrome P450 proteins are a large family of proteins that are involved in the oxidation of a wide variety of substrates. P450 proteins have a variety of roles within the cell, including in the metabolism of drugs, toxins and hormones, as well as sterol and bile

acid synthesis (Bistolas et al. 2005). PGRMC1 is reported to interact with multiple P450 enzymes in humans, one of which is CYP51A (Hughes et al. 2007). CYP51A is also known as lanosterol 14-α demethylase, which is the only P450 enzyme involved in cholesterol biosynthesis, and regulates the conversion of lanosterol to 4,4-dimethyl-5α-cholest-8,14,24-triene-3β-ol, which is an essential step in the cholesterol biosynthetic/mevalonate pathway (Strömstedt et al. 1996). PGRMC1 binding to Cyp51A has a similar effect to that of Cytochrome *b5*, and it acts as the electron donor to facilitate P450 oxidation of substrates. Loss of PGRMC1 has also been shown to reduce the activity of CYP51A and negatively impact on cholesterol biosynthesis (Hughes et al. 2007). PGRMC1 also has been shown to alter proteins involved in cell proliferation and cell survival (Peluso, Liu, et al. 2008; Peluso 2011; Ahmed et al. 2010). PGRMC1 has also been shown to be up-regulated in a variety of cancers (Craven 2008; Mir et al. 2012; Difilippantonio et al. 2003; Nie et al. 2006).

In addition to its regulatory effect on CYP51A activity, PGRMC1 also has other links to the cholesterol biosynthesis pathway. CYP51A is an SREBP regulated gene whose expression is induced under sterol limited conditions (Rozman et al. 1996). SREBP regulation of PGRMC1 expression has not yet been conclusively shown, although the promoter region does contain an SRE-element (Lösel et al. 2008). The yeast homolog of PGRMC1 (Dap1), however, is under regulation by SREBP homolog (SRE-1) (Hughes et al. 2007). Further to this, PGRMC1 was recently identified as interacting directly with both SCAP and INSIG1 (Suchanek et al. 2005). A novel method for photo-cross-linking proteins in living cells to identify protein-protein interactions was used to investigate if PGRMC1 interacted with members of the INSIG1-SCAP-SREBP complex, as all of these proteins reside in the ER membrane (Sakai et al. 1997). A direct interaction between PGRMC1 and

INSIG1 and between PGRMC1 and SCAP was identified, while an unrelated ER membrane protein failed to bind PGRMC1 (Suchanek et al. 2005). Both SCAP and INSIG1 are key proteins involved in regulating the localisation, and thus activation, of the SREBP family of transcriptions factors in response to cellular fluctuations in sterols (Goldstein et al. 2006; Radhakrishnan et al. 2007b). SCAP contains a WD domain within its carboxy-terminal regulatory region (Hua et al. 1996). This region mediates its binding to SREBP, but no other function/interaction is reported for this CTD region of SCAP (Sakai et al. 1997). Other WD domain proteins have been shown to have multiple interaction partners (Adams, Ron & P. A. Kiely 2011; Chen et al. 2004). Thus identification of PGRMC1 as a SCAP interacting is consistent with the presence of WD domains on SCAP. This interaction, together with its regulatory effect on CYP51A, suggested a possible role for PGRMC1 in the regulation of SREBP processing.

A role for PGRMC1 in regulating SREBP processing may be linked to progesterone (P4). SREBP processing is regulated by end product feedback inhibition. Outside of cholesterol, other known regulators include oxysterols (24,25-, 25, 27 and 7beta hydroxycholesterol)(Radhakrishnan et al. 2007b). Regulation by these compounds has been demonstrated through their binding to either SCAP or INSIG1 (Radhakrishnan et al. 2007b). P4 is a steroid hormone involved in the regulation of the female menstrual cycle, embryogenesis and maintaining pregnancy (Stormshak & Bishop 2008). It also has roles in the body outside of reproduction, including a positive effect on axonal myelin sheath formation in the brain (Baulieu & Schumacher 2000). P4 is synthesised from cholesterol in a 5-step enzymatic process, the rate limiting step of which is delivery of cholesterol to the inner mitochondrial membrane (Stocco 2001). This action is regulated by StAR protein, which is an

SREBP regulated gene (Christenson et al. 1998; Shea-eaton et al. 2014). Given that SREBPs are involved in the regulated availability of cholesterol both by *de novo* synthesis and uptake, and in the expression of the rate limiting step of P4 biosynthesis, it seems possible that P4 levels may elicit a regulatory effect on SREBP cleavage (Horton et al. 2002b; Shea-eaton et al. 2014). This is consistent with the current regulatory model of sterol based products' feedback inhibition of SREBP cleavage (Brown & Goldstein 2009). Also, despite the lack of a link to the SREBP pathway, P4 has demonstrated an inhibitory effect on cholesterol biosynthesis in a variety of human cell lines, although this regulation was at higher P4 concentrations than physiological levels (Metherall et al. 1996).

Whether or not PGRMC1 binds P4 appears to be a bone of contention in the literature. PGRMC1 shares no sequence homology and has a completely different protein structure to the classical P4-binding receptor (PR) (Mifsud & Bateman 2002). There exists evidence both for and against this issue. Most notably, recombinant PGRMC1 purified from a bacterial expression system was shown not to bind [$^3$H]-P4 (Min et al. 2005). It appears that the most accepted view to date is that PGRMC1 is part of a multi-protein complex, which requires another protein; plasminogen activator inhibitor 1 RNA binding protein (PAIR-BP), to mediate its P4 action, but that PGRMC1 itself is not capable of binding P4 (Cahill 2007; Peluso et al. 2013). However, Peluso et al demonstrated in partially purified preparations from rat SIGCs that recombinant PGMRC1 bound [$^3$H]-P4, although the exact P4-binding site has not yet been elucidated, and that this binding enhances PGRMC1 association with another protein; PAIR-BP1 (Peluso et al. 2013). Peluso et al. acknowledge the requirement of PAIR-BP to mediate P4 actions in SICGs, but maintain the direct binding capacity of PGRMC1 itself, and have demonstrated that depletion of PAIR-

BP does not limit the ability of PGRMC1 to bind P4 (Peluso et al. 2013). This group also suggest P4-mediated regulation of gene expression. This is evidenced by their detection of PGRMC1 dimers exclusively in the nucleus, and they have demonstrated that P4 decreases Tcf/Lef transcription factor activity in a PGRMC1 dependent manner (Peluso et al. 2010; Peluso et al. 2012). PGRMC1 is also up-regulated in a number of cancer cell lines and in tumours (Craven 2008; Mir et al. 2012; Difilippantonio et al. 2003). PGRMC1 was also reported to be one of six genes consistently up-regulated in response to carcinogens in rats (Nie et al. 2006). PGRMC1-depleted tumours are reportedly more sensitive to DNA damage (Crudden et al. 2006). PGRMC1 has also been shown to be essential for mediating the anti-apoptotic action of P4 in spontaneously immortalised granulosa cells (SIGCs), which lack classic nuclear P4 receptors (Peluso, Romak, et al. 2008).

Activation of the SREBPs is primarily regulated by end product feedback inhibition (Goldstein et al. 2006). The evidence that exists for the idea that PGRMC1 binds P4, together with this receptor being ER membrane localised and its association with cholesterol biosynthesis supports the merit of further investigation of the SREBP-regulatory potential of PGRMC1. While P4 has previously been characterised as not regulating SREBP cleavage levels, it has some links to the cholesterol biosynthesis/SREBP pathways (Wang et al. 1994). Our hypothesis is based on its regulatory capacity potentially being dependant on PGRMC1 availability.

For the purpose of the experiments reported here, a luciferase-based gene reporter system responsive to SREBP activation was used. By cloning the promoter region of an SREBP target gene upstream of a gene encoding a luciferase enzyme, this serves as an accurate, rapid method of detecting SREBP activation. A well characterised

SREBP target gene promoter; HMGCR, was utilised for this gene reporter assay. Initial experiments indicated that the commonly used dual luciferase reporter assay system (DLR) was not suitable for our investigation. This assay system requires co-transfection of a constitutively active control luciferase reporter plasmid along with the test reporter plasmid for internal normalisation purposes (Sherf et al. 1996). Expression of this control reporter plasmid is regulated by a constitutive TK, CMV or SV-40 promoter. The results indicate that progesterone (P4) down regulated expression of luciferase from TK and CMV Renilla reporters which is problematic for analysis. Regulation of control luciferase reporter plasmids by compounds and cDNAs has been reported previously (Ho & Strauss III 2004; Ibrahim et al. 2000). Normalisation in this case would mask test reporter results and thus is not suitable. This prompted us to develop the novel luciferase-based SSLR assay (Chapter 4). In the process of developing this assay, a HeLa cell line stably expressing the secreted *Gaussia* luciferase driven by the HMGCR promoter was also generated and designated HeLa-PHGL (Chapter 4). This SREBP/HMGCR luciferase reporter system is an accurate means of assessing processing of the active nSREBP transcription factor domain from the full length precursor protein. SCAP and INSIG1 are central proteins involved in the regulation of SREBP processing in response to cellular sterol levels (Radhakrishnan et al. 2007b). In this chapter, the effect of PGRMC1 binding to SCAP and/or INSIG was investigated with respect to regulation of SREBP processing. The requirement of P4 in this potential regulatory role of PGRMC1 was also investigated.

## Results

### *P4 decreases Renilla luciferase expression from constitutive promoters*

The DLR assay system was initially investigated for use as a gene reporter system to measure SREBP activity in response to PGRMC1 over-expression in the absence and presence of P4. Transient transfection of luciferase gene reporter plasmids requires co-transfection of a constitutively active luciferase control reporter which serves as an internal control to which the test reporter is normalised. Based on previously published literature, certain compounds and some cDNA over-expression clones have been known to affect expression of constitutive control reporter plasmids. Therefore, the control reporter assay requires initial characterisation in the context of your experimental parameters. HeLa cells were transfected with the control reporter, pRL-TK. This construct has *Renilla* luciferase under the control of the constitutive promoter thymidine kinase (TK). A decrease in control reporter readout was observed in response to increasing concentrations of P4 (Figure 5.1A). Analysis of cell viability revealed that the decrease in promoter activity was greater than the decrease in cell viability induced by P4 (Figure 5.1C). At 100 nM P4, there was a 2.48-fold decrease in luciferase reporter readout while there was only 1.13-fold decrease in cell viability at the same concentration. The same effect in response to P4 was observed with another commonly used constitutively active luciferase control reporter where is the *Renilla* luciferase is under the control of the constitutive promoter cytomegalovirus (CMV) promoter (Figure 5.1B). At 100 nM P4, there was a 1.38-fold decrease in luciferase reporter readout. Thus, the use of control promoter proved problematic for P4 treatments and this prompted development of the alternative SSLR system, described in Chapter 4. Following development of the SSLR method, a further appropriate advancement was made by making a stable

HeLa cell line (HeLa-PHGL) with a SREBP target promoter (the HMGCR promoter which has three SRE elements) linked to a secreted luciferase insert.

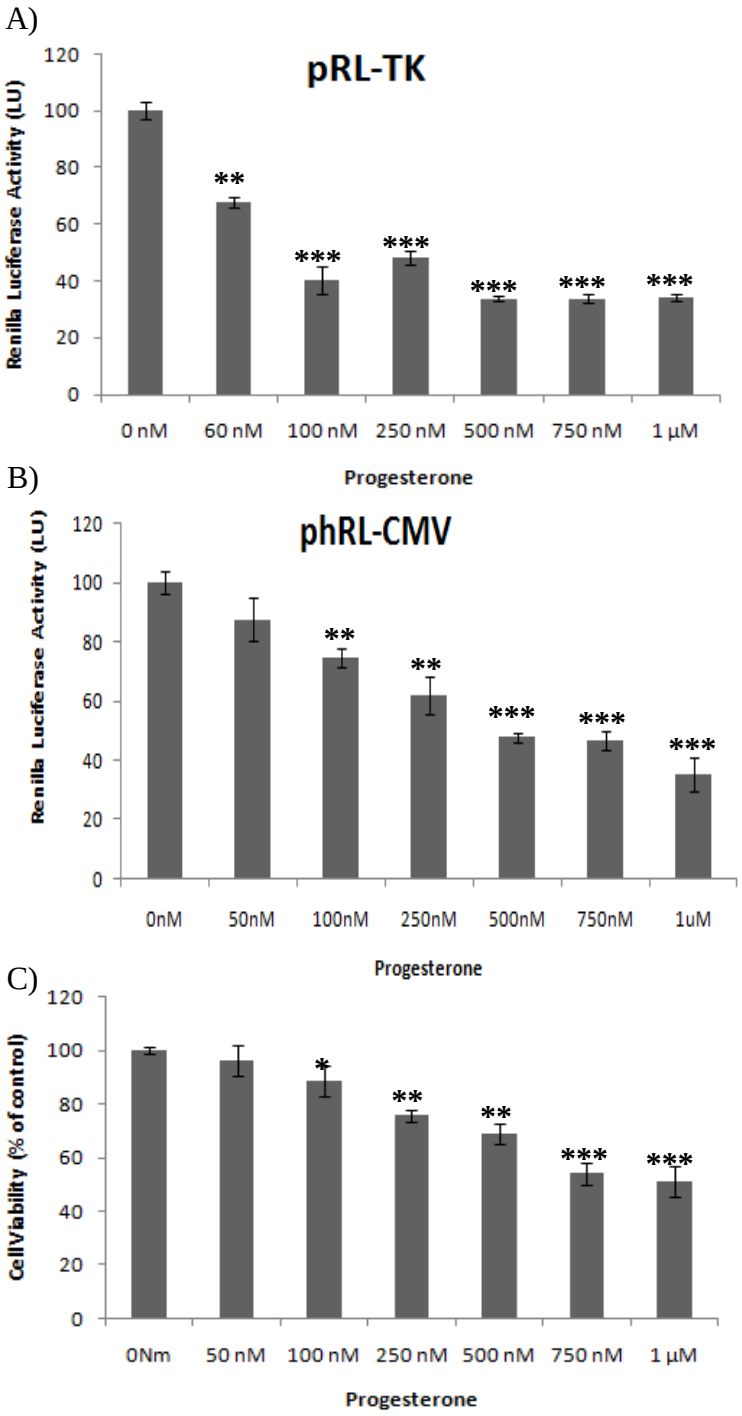


Figure 5.1. Analysis of P4 effect on *Renilla* luciferase control reporter plasmid expression. (A and B) HeLa cells were transfected at approximately 80% confluency with the either pRL-TK or pRL-CMV Renilla luciferase plasmid. Following a 6 hour transfection period, cells were treated with increasing concentrations of P4 in EtOH for 24 hours. Cells were then harvested and luciferase analysis performed. (C) HeLa cell viability in response to increasing concentrations of P4, as measured by the MTT assay. All experiments were performed in triplicate. Error bars represent ±SD. Statistical significance was measured using Student's t-test (*$p<0.05$, **$p<0.005$, ***$p<0.0005$).

***PGRMC1 regulation of SREBP processing***

To investigate if PGRMC1 has an effect on SREBP processing, HeLa-PHGL cells were transfected with plasmid DNA over-expressing human PGRMC1. Over-expression of PGRMC1 failed to change SREBP luciferase reporter readout significantly compared to the empty vector control, under FS ($p=0.96$) or LDS ($p=0.26$) culture conditions (Figure 5.2A; Control vs. PGRMC1). PGRMC1 was recently identified as interacting with SCAP. To investigate if SCAP was required for a regulatory effect of PGRMC1 on SREBP processing, HeLa-PHGL cells were transfected with SCAP in the absence and presence of PGRMC1. Over-expression of SCAP alone caused a significant increase in luciferase reporter readout in both FS and LDS ($p=0.02$ and $p=4.3E-03$, respectively) compared to empty vector control (Figure 5.2A; Control *vs.* SCAP). This is as expected as SCAP is a limiting factor in SREBP processing and its over-expression has been shown to increase SREBP processing. Co-expression of PGRMC1 with SCAP did not significantly alter this SCAP-mediated increase in luciferase reporter readout in FS ($p=0.88$) (Figure 5.2A; SCAP *vs.* PGRMC1+SCAP). However, co-expression of PGRMC1 with SCAP in LDS significantly increased luciferase reporter readout beyond that achieved with over-expression of SCAP alone ($p=0.03$) (Figure 5.2A; SCAP *vs.* PGRMC1+SCAP). Over-expression of PGRMC1 or SCAP, individually or together had no significant effect on HeLa-PHGL cell viability compared to cells transfected with empty vector only ($p>0.05$ for all) (Figure 5.2B).

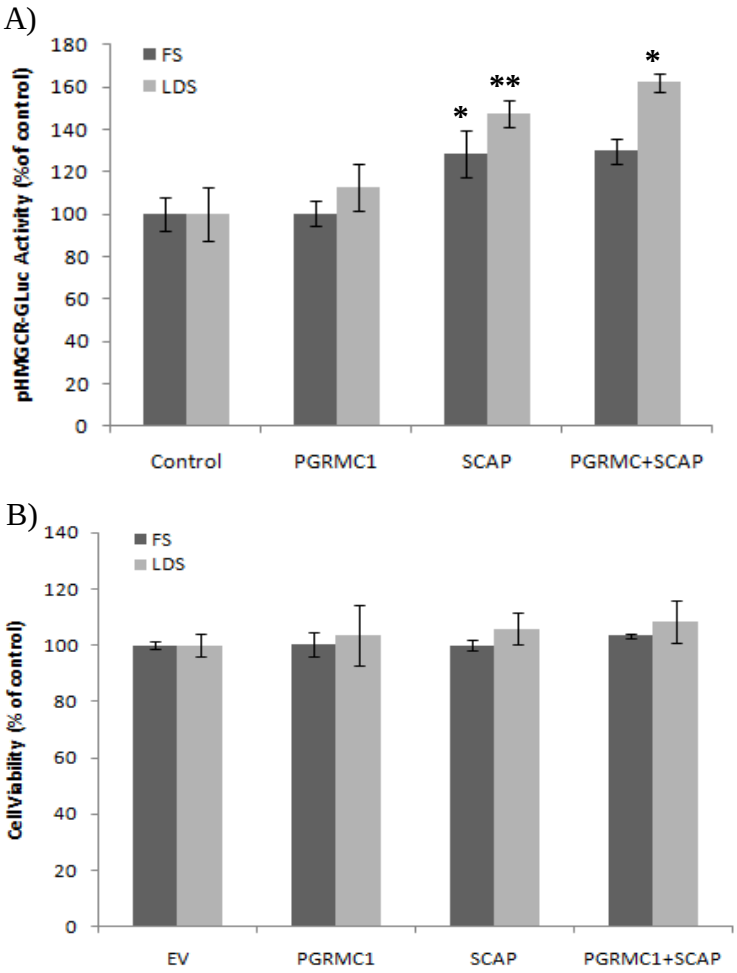


Figure 5.2. Effect of PGRMC1 expression on SREBP luciferase reporter activity. (A) HeLa-PHGL cells were transfected at approximately 80% confluency with the indicated over-expression plasmids, or empty vector control, under FS culture conditions. Following a six hour transfection period, cells media was replaced with either FS or LDS media, as indicated. Cells were incubated for a further 24 hours, followed by analysis of luciferase levels. (B) HeLa cell viability in response to protein over-expression, as measured by the MTT assay. All experiments were performed in triplicate. Error bars represent ±SD. Statistical significance was measured using Student's t-Test (*$p<0.05$, **$p<0.005$).

***PGRMC1 effects on SREBP in the presence of P4***

PGRMC1 is a potential P4 binding protein. To investigate if P4 is required for PGRMC1 regulation of SREBP processing, HeLa-PHGL cells transfected with PGRMC1 in the absence or presence of SCAP were treated with increasing concentrations of P4. Under FS conditions, treatment of cells with 10 nM and 100 nM concentrations of P4 alone did not result in any significant decrease in SREBP luciferase reporter readout ($p=0.27$ and $p=0.06$, respectively) (Figure 5.3A; Control). Treatment with 500 nM P4 reduced reporter readout 4.1 fold compared to vehicle treated control ($p=1.23E-04$) (Figure 5.3A; Control). However analysis of cell viability for the same experiment indicates that this reduction is linked to the 2.6-fold decrease in cell viability induced with 500 nM P4 ($p=9.85E-06$) (Figure 5.3B; Control). P4 at 10 nM and 100 nM also significantly affected cell viability ($p=0.02$ and $p=5.32E-04$, respectively) (Figure 5.3B; Control). Over-expression of PGRMC1 under FS conditions did not significantly alter the luciferase readout or cell viability in response to increasing P4 compared to empty vector control, as measured by student's t-test ($p>0.05$ for all) (Figure 5.3A and 5.3B, Control vs. PGRMC1). Over-expression of SCAP increased luciferase reporter readout 1.44-fold in the presence of 10 nM ($p=0.006$) and 1.43-fold in the presence of 100 nM P4 ($p=0.003$) compared to empty vector transfected cells, but failed to impact on the P4-induced decrease in cell viability (Figure 5.3A and 5.3B, Control *vs.* SCAP). Co-expression of PGRMC1 with SCAP had no significant effect on the SCAP induced increase on luciferase reporter readout for 10 nM and 100 nM P4 ($p=0.67$ and $p=0.17$, respectively), and also did not impact on the P4 induced decrease in cell viability (Figure 5.3A and 5.3B, SCAP vs. PGRMC1+SCAP).

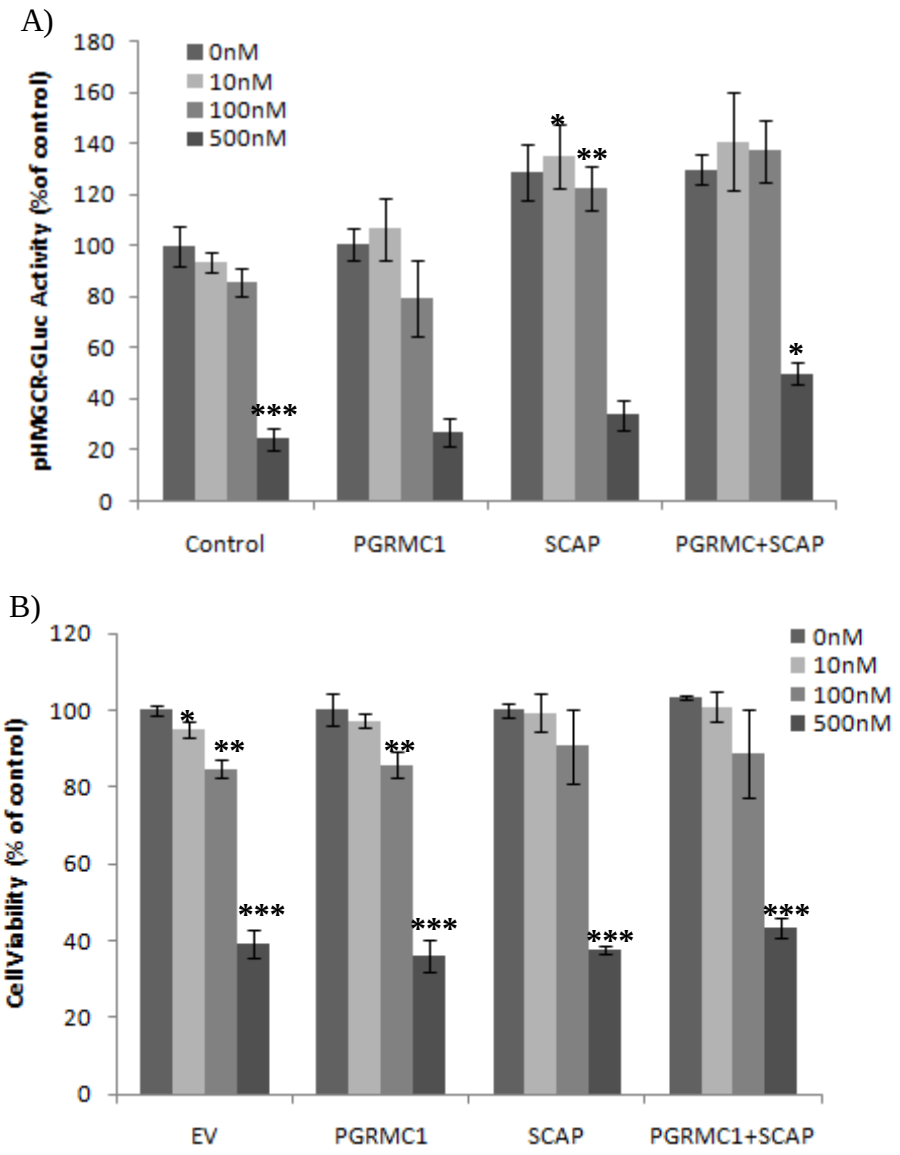


Figure 5.3. Effect of P4 on SREBP luciferase reporter activity in the presence and absence of PGRMC1 under FS conditions. (A) HeLa-PHGL cells were transfected at approximately 80% confluency with the indicated over-expression plasmids, or empty vector control, under FS culture conditions. Following a six hour transfection period, media was replaced with FS media, containing P4 at the indicated concentrations. Cells were incubated for a further 24 hours, followed by analysis of luciferase levels. (B) HeLa cell viability in response to protein over-expression in the presence of P4, as measured by the MTT assay. All experiments were performed in triplicate. Error bars represent ±SD. Statistical significance was measured using Student's t-test (*$p<0.05$, **$p<0.005$).

At 500 nM P4, co-expression of PGRMC1 with SCAP did significantly increase luciferase reporter readout 1.16-fold beyond that achieved with SCAP alone (p=0.02) (Figure 5.3A; PGRMC1+SCAP vs. SCAP). Cell viability was also significantly increased in the presence of 500 nM P4 by co-expression of PGRMC1 with SCAP (p=0.02) (Figure 5.3B; PGRMC1+SCAP vs. SCAP). Changes in luciferase reporter expression levels are linked to changes in cell viability. Whether this small increase observed here in SREBP luciferase reporter readout for 500 nM P4 with PGRMC1+SCAP is a consequence of an impact on cell viability, or specifically linked to SREBP pathway remains to be determined.

When the same experiment was performed under LDS culture conditions, similar results were obtained. Treatment with 10 nM and 100 nM P4 alone did not significantly affect luciferase reporter readout (p=0.15 and p=0.61) or cell viability (p=0.34 and p=0.16) (Figure 5.4A and 5.4B; control). However, treatment with 500 nM P4 under LDS conditions only resulted in a 1.17-fold decrease in luciferase reporter readout (p=0.18) and a 1.15-fold decrease in cell viability (p=0.007). While the decrease in cell viability is statistically significant, it differs from the effects of 500 nM P4 on cell viability under FS conditions which caused a decrease of 2.56-fold compared to vehicle treated cells (p=9.85E-06). Over-expression of PGRMC1 did not significantly alter luciferase reporter readout at 10 nM and 100 nM P4 (p=0.08 and p=0.17, respectively) (Figure 5.4A; control vs. PGRMC1). Cell viability in the presence of 10 nM and 100 nM P4 was also unaffected by over-expression of PGRMC1 compared to empty vector transfected cells (p=0.72 and p=0.17, respectively) (Figure 5.4B; control vs. PGRMC1). However, over-expression of PGRMC1 in the presence of 500 nM P4 caused a 1.76-fold decrease in luciferase reporter readout (p=0.02) with a corresponding 1.66-fold decrease in cell viability

(p=0.007) compared to the corresponding 500nM P4 control (Figure 5.4A and 5.4B; PGRMC1). Thus the presence of PGRMC1 counteracts the anti-cytotoxic effect that LDS has on 500 nM P4 and returns it to the cytotoxic effect that 500 nM P4 alone has under FS conditions. Under LDS conditions, over-expression of SCAP alone causes a 1.48-fold increase in luciferase reporter readout (p=0.004), and this increase is not affected by 10 nM or 100 nM P4 (p=0.76 and p=0.43, respectively) (Figure 5.4A; SCAP). Over-expression of SCAP does not affect cell viability for 10 nM or 100 nM P4 compared to that seen for empty vector treated cells (p=0.72 and p=0.60, respectively) (Figure 5.4B; control vs. SCAP). However, over-expression of SCAP alone decreases cell viability 1.31-fold (p=0.03) in the presence of 500 nM P4 under LDS conditions (Figure 5.4B; SCAP vs. Control), although this is not to the same extent as the 1.66-fold decrease seen with PGRMC1 alone in the presence of 500 nM P4 (Figure 5.4B; PGRMC1 vs. Control). Over-expression of SCAP in the presence of 500 nM P4 results in a decrease of 1.09-fold in luciferase reporter readout compared to empty vector transfected cells (p=0.42) (Figure 5.4A; SCAP vs. Control). While the effects on luciferase reporter readout are not statistically significant, this data suggests that over-expression of SCAP contributes to the cytotoxic effects of 500 nM P4 under LDS conditions, but to a lesser extent than PGRMC1. Co-expression of PGRMC1 with SCAP did not affect the SCAP-mediated increase in luciferase reporter activity in the presence of 10 nM or 100 nM P4 (p=0.45 and p=0.45, respectively) (Figure 5.4A; PGRMC1+SCAP vs. SCAP). PGRMC1 with SCAP also had no significant effect on cell viability in the presence of 10 nM or 100 nM P4 compared to cells transfected with SCAP alone (p=0.35 and p=0.28, respectively) (Figure 5.4B; PGRMC1+SCAP vs. SCAP). In the presence of 500 nM P4 in LDS, co-expression of SCAP with PGRMC1 causes a 2.42-fold

decrease in cell viability compared to cells transfected with empty vector only (p=2.41E-05) (Figure 5.4B; PGRMC1+SCAP vs. Control). This is compared to the 1.66-fold and 1.31-fold decrease seen with PGRMC1 and SCAP alone, respectively. The 1.6-fold decrease luciferase reporter readout (p=0.01) for PGRMC1 with SCAP in the presence of 500 nM P4 compared to empty vector transfected cells treated with 500 nM P4 reflects this decrease in cell viability (Figure 5.4A; PGRMC1+SCAP vs. Control). This data would indicate an additive effect of PGRMC1 and SCAP in mediating the cytotoxic effect of 500 nM P4 under LDS conditions.

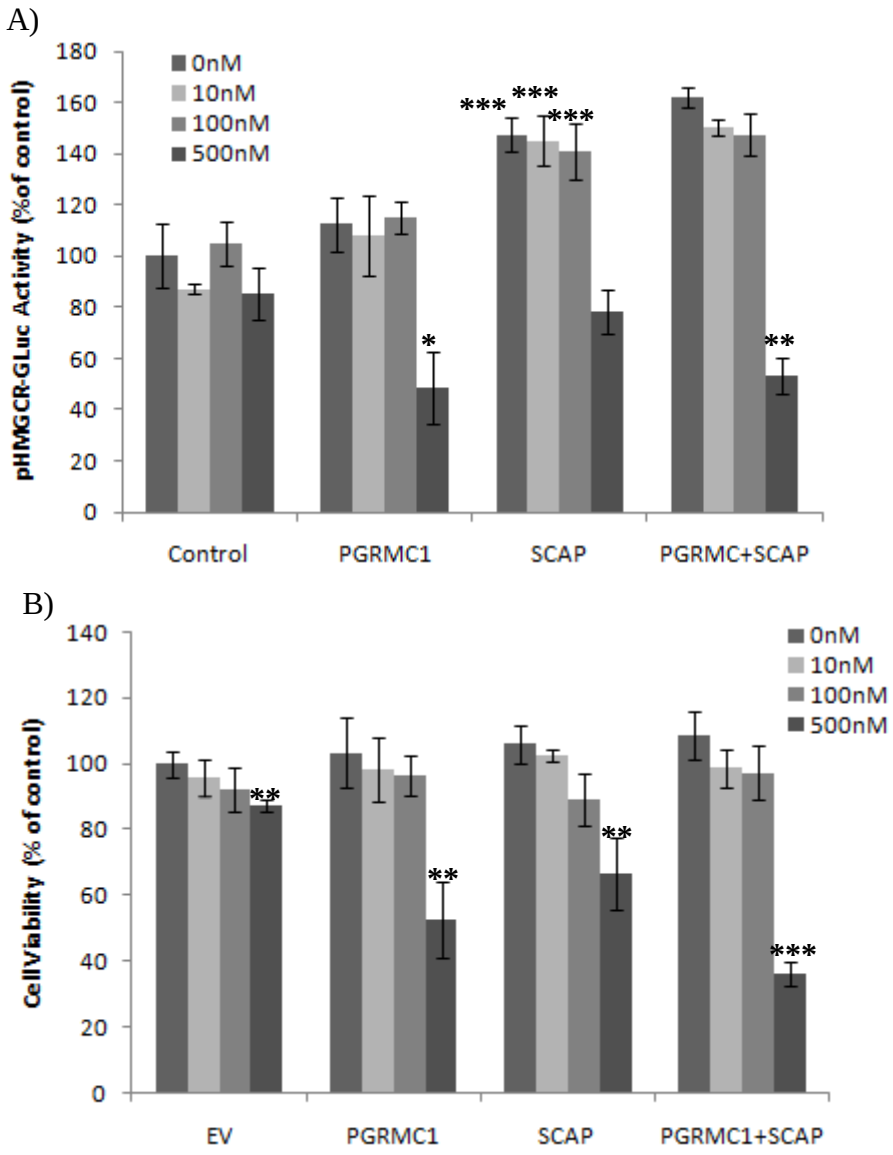


Figure 5.4. Effect of P4 on SREBP luciferase reporter activity in the presence and absence of PGRMC1 under LDS conditions. (A) HeLa-PHGL cells were transfected at approximately 80% confluency with the indicated over-expression plasmids, or empty vector control, under FS culture conditions. Following a six hour transfection period, media was replaced with LDS media, containing P4 at the indicated concentrations. Cells were incubated for a further 24 hours, followed by analysis of luciferase levels. (B) HeLa cell viability in response to protein over-expression in the presence of P4, as measured by the MTT assay. All experiments were performed in triplicate. Error bars represent ±SD. Statistical significance was measured using Student's t-test (*$p<0.05$, **$p<0.005$, ***$p<0.0005$).

## Discussion

PGRMC1 was identified as interacting with the SREBP regulatory proteins SCAP and INSIG1 (Suchanek et al. 2005). SCAP is an ER-localised sensor protein for cellular sterol levels and in sterol depleted conditions it chaperones the SREBP precursor protein to the Golgi for proteolytic processing and release of the active SREBP transcription factor domain (Radhakrishnan et al. 2008; Nohturfft et al. 1999). In sterol rich conditions, SCAP is bound by the ER-retention protein INSIG1, and SREBP processing does not occur (L. Sun et al. 2007). The reported interaction of PGRMC1 with SCAP and INSIG1 suggests that it may have a functional role in the regulation of SREBP processing.

The HeLa-PHGL cell line was used for the purpose of investigating the effect of PGRMC1 on SREBP processing. If PGRMC1 were exerting either a positive or negative effect on SREBP processing, this would be reflected by an increase or decrease on the SREBP/HMGCR luciferase reporter readout respectively. Thus, PGRMC1 over-expression was performed in both FS and LDS conditions, to simulate low and high levels of both SCAP and INSIG1. The results indicate that over-expression of PGRMC1 alone does not significantly affect SREBP processing in FS or LDS conditions. SCAP is a limiting factor in SREBP processing and over-expression of SCAP increases SREBP/HMGCR luciferase reporter readout. PGRMC1 failed to impact on the increase in SREBP processing achieved when SCAP is over-expressed in HeLa-PHGL cells in FS conditions. However it did marginally but significantly increase SREBP processing a further 9% in LDS. These results suggest that PGRMC1 may have a role in increasing the regulation of SREBP processing, and that the presence of lipids in FS prevents this regulation.

PGRMC1 has been reported to mediate the anti-apoptotic effects of P4 (Peluso, Romak, et al. 2008). The effects of P4 on amplifying PGRMC1s effect on SREBP processing were investigated to explore if PGRMC1 was involved in mediating regulatory effects of P4 on SREBP processing. In FS conditions, the results indicate that P4 alone had no effect on SREBP processing, which is consistent with the previous report that P4 failed to influence SREBP1 processing. The observed decreases in luciferase reporter readout (Figure 5.3A) were due to the effects of P4 on cell viability and were deemed not to be specific to SREBP processing. Over-expressed PGRMC1 failed to rescue the decrease in cell viability induced by P4. This is surprising since previous studies have shown that PGRMC1 was required to mediate the anti-apoptotic effects of P4 in spontaneously immortalised granulose cells (SIGCs) (Peluso, Romak, et al. 2008). Co-expression of PGRMC1 with SCAP in the presence of 500 nM P4 did display a slight increase in luciferase readout compared to the levels achieved with SCAP alone. However, 500nM P4 caused a 50% reduction in cell viability, thus the significance of an increase in SREBP luciferase reporter readout under these conditions is difficult to interpret. Also, both of the lower concentrations (10nM and 100nM) of P4 failed to elicit a significant increase in reporter readout under the same conditions. Taken together, these results indicate that PGRMC1 does not have any significant effect on SREBP processing in FS, and that this is not altered by P4.

However, somewhat different results were obtained when the same set of experiments were performed in LDS. The first interesting finding is that under LDS conditions, there was no significant decrease in cell viability induced upon incubation with low or high concentrations of P4 alone. However, a role for PGRMC1 in this protective response of HeLa-PHGL cells to P4-induced

cytotoxicity under LDS conditions was ruled out as over-expression of PGRMC1 decreased the cell viability in the presence of 500 nM P4 back to the levels seen with 500 nM P4 alone under FS conditions. Again, this is surprising based on reports that PGRMC1 mediates the anti-apoptotic action of P4 (Peluso, Romak, et al. 2008). Current literature on the roles of PGRMC1 indicates a proliferative effect and also a role in cell survival. However, one group did report in 2003 that PGRMC1 sensitised MCF-7 breast cancer cells to death following oxidative stress suggesting that there may be a link between this finding and the results presented here (Hand & Craven 2003). A role for SCAP in the protective response to P4-induced cell death under LDS conditions was also ruled out as over-expression of SCAP also caused a decreased the cell viability in the presence of 500 nM P4, although not to the same extent as PGRMC1. Over-expression of PGRMC1 and SCAP together did not enhance the decrease in cell viability in the presence of 500nM P4 beyond that achieved with PGRMC1 alone. There was no change in the SREBP/HMGCR luciferase reporter readout in the presence of 500nM P4 in response to over-expression of PGRMC1 that was not caused by the decrease in cell viability.

The aim of the work in this chapter was to investigate a role for PGRMC1 in the regulation of SREBP processing based on its reported interaction with the SREBP regulatory proteins, SCAP and INSIG1. The results presented here suggest that PGRMC1 neither promotes nor inhibits SREBP processing, and that P4 is not a limiting factor required for regulation of SREBP processing by PGRMC1. However, further investigations would be required to conclusively determine that this is the case.

An interesting finding was that culturing HeLa-PHGL cells in LDS induced a cellular response which resulted in protection from P4-induced cytotoxicity that is seemingly absent in FS conditions. Although PGRMC1 has previously been implicated in mediating the anti-apoptotic action of P4, the results presented here indicate that it may be involved in mediating a cytotoxic or pro-apoptotic action of P4. These findings also suggest a novel role for SCAP in mediating an inhibitory or cytotoxic action of P4, which is likely independent of its role in regulating SREBP processing. The roles of PGRMC1 and SCAP in mediating the inhibitory or cytotoxic action of P4 were not pursued in the course of this work, but merit further investigation.

# Chapter 5B

## Investigating the Functional Differences between Two INSIG1 Isoforms

## Abstract

INSIG1 has a central role in regulating cellular lipid homeostasis. In the presence of excess lipids, INSIG1 functions as an ER-retention protein for the SREBP family of transcription factors which prevents their proteolytic processing. INSIG1 also facilitates the degradation of HMGCR, the rate limiting enzyme in cholesterol biosynthesis. There are two protein isoforms of human INSIG1 produced through the use of two in-frame alternative start sites. However, the functional significance of having two INSIG1 proteins produced has not been investigated. Bioinformatic analysis indicates that the presence of two in-frame start sites within the 5-prime region of INSIG1 mRNA is highly conserved among vertebrate species and that production of two isoforms of INSIG1is likely a conserved event. Investigation of the functional differences between the two INSIG1 isoforms indicated no observed difference in a) negative regulation of SREBP processing and c) facilitation of HMGCR degradation. While bioinformatic analysis suggests there is likely a regulatory mechanism surrounding translation initiation occurring at one start site over the other, the functional significance of having two isoforms of INSIG1 is as yet unclear.

## Introduction

Under high cellular sterol conditions, the SCAP-SREBP complex is retained in the ER through SCAP undergoing a conformational change which a) prevents COPII vesicle formation and b) facilitates binding of the SCAP ER-retention protein INSIG1 (L.-P. Sun et al. 2007). While it has been identified that the transmembrane region (TM1-6) of SCAP is sufficient to bind INSIG and that a mutant SCAP Y298C fails to bind INSIG (Yang et al. 2002). The region within INSIG which binds to SCAP has not yet been identified. INSIG1 has two known functions. In addition to binding and retaining the SCAP-SREBP complex in the ER, INSIG1 also mediates the degradation of HMGCR which is the rate limiting enzyme in cholesterol biosynthesis. In this case, INSIG1 recruits the ER-resident E3 ubiquitin ligase gp78 to HMGCR and this initiates the proteasomal degradation of HMGCR, although the specific involvement of gp78 is not always clear (Che et al. 2012) (Sever et al. 2003b). It is believed that INSIG1 mediates its different effects on SCAP and HMGCR through whether binding affects its association with gp78. Upon binding to SCAP, gp78 is displaced from INSIG1 and thus INSIG1 does not promote the degradation of SCAP (Lee, Song, et al. 2006). Upon binding to HMGCR, gp78 remains associated to INSIG1 and thus promotes the degradation of HMGCR (Song et al. 2005).

Two isoforms of INSIG exist in the vertebrate genome; INSIG1 and INSIG2. INSIG1 is located at 7q36 and INSIG2 is located at 2q14.1 (Peng et al. 1997) (Bressler et al. 2009). These INSIG proteins have six-transmembrane helices with short cytosolic extensions at both the amino and carboxy termini (Feramisco et al. 2004) (Yabe et al. 2002). They share 59% overall sequence identity (Yabe et al. 2002). Both INSIG proteins have demonstrated the capability to mediate both

inhibition of SREBP processing and facilitating degradation of HMGCR (Yang et al. 2002)(Yabe et al. 2002)(Sever et al. 2003b). INSIG2 is believed to mediate degradation of HMGCR through recruitment of a different E3 ligase, TRC8 (Jo et al. 2011). Knockout studies of each have shown that in the absence of INSIG1, INSIG2 compensates, and *vice-versa* (Engelking et al. 2005). The two INSIG proteins do however differ in their modes of regulation. INSIG2 is constitutively expressed and is not subject to sterol-regulated degradation (Lee & Ye 2004). Conversely, INSIG1 expression is induced by the SREBP transcription factors, which themselves are activated in response to low sterol availability, and the INSIG protein is then stabilised by sterols when the cellular levels are sufficiently high (Horton et al. 2003) (Gong, Lee, Lee, et al. 2006b). INSIG essentially functions to negatively regulate cholesterol biosynthesis through a) inhibition of cholesterogenic gene expression via ER retention of SREBP-SCAP complex and b) via a more immediate inhibition through degradation of HMGCR.

INSIG1 was originally identified as an insulin-induced gene (Mohn et al. 1991). However, it was later discovered that induction of INSIG1 by insulin was indirect. INSIG1 expression is induced by the SREBP transcription factors as it contains an SRE element in its promoter (Horton et al. 2003). It was discovered that insulin stimulates transcription of SREBP-1c and this was responsible for the insulin associated increase in INSIG1 (Kim et al. 1998). More recently, insulin has also been shown to promote SREBP-1c processing through down regulation of INSIG2 (Yellaturu, Deng, Cagen, et al. 2009). INSIG1 expression is also regulated by members of the peroxisome proliferator-activated receptor (PPAR) family (Kast-woelbern et al. 2004). PPARs are nuclear hormone receptors which have regulatory roles in lipid metabolism and insulin sensitisation. PPARγ has been implicated in

inducing expression of INSIG1, through interplay with SREBP (Yoshikawa et al. 2010). The link of INSIG1 with PPARs provides a more direct link between insulin signalling and INSIG1.

INSIG1 is reported to have two proteins produced from the same mRNA through translation initiating from two alternative start sites (Yang et al. 2002). Both start sites are in-frame and are located 105 nucleotides apart. This gives rise to two proteins that are identical over the transmembrane region of INSIG1 but differ in their amino terminal cytosolic extensions by a region of thirty-six amino acids (~4 kDa). The presence of both isoforms has been confirmed by immunoblot analysis (Yang et al. 2002). The majority of experiments carried out in the literature involving INSIG1 utilise the over-expressed gene in a plasmid from which two proteins isoforms are produced. Both isoforms have been confirmed by protein sequencing analysis and correspond to translation initiation occurring at both translation start sites. There are few reports in the literature pertaining to endogenous INSIG1 protein expression. Only a single INSIG1 isoform is reported in the human liver carcinoma cell line HepG2 (Qin et al. 2008). Mouse is also reported to have a single INSIG1 protein expressed with an approximately molecular weight of 28 kDa (Engelking et al. 2004). However expression of two endogenous INSIG1 isoforms in hamster cells has been reported (Gong, Lee, Lee, et al. 2006b). Expression of two INSIG1 isoforms for other vertebrate species, however, has not been reported. Invertebrate species lack a cholesterol biosynthetic pathway since they are cholesterol auxotrophic, and therefore lack an INSIG1 homolog for comparison (Karlson, P 1986). However, there is a homologous sterol biosynthetic pathway in yeast which is primarily responsive to changes in oxygen availability (Bien & Espenshade 2010). The *S. pombe* INSIG1 homolog, Ins-1, has very low sequence

identity to the human protein, but is believed to have the same basic structure of six membrane-spanning helices with amino- and carboxy-terminal cytosolic extensions (Hughes et al. 2005). Interestingly, there are also two Ins-1 isoforms produced as a result of translation initiating from two in frame start sites located within the region encoding the amino-terminal cytosolic extension (Burg et al. 2009). The resultant proteins again differ in molecular weight by approximately 4 kDa, and are identical after this second start site position. For human INSIG1 over-expression constructs, the ratio of expression is in favour of the longer isoform of the protein. However, the ratios of expression for the endogenous isoforms appear to vary. In fission yeast, over-expression of Ins-1 yields two protein isoforms which appear to be expressed strongly and at equal levels. Endogenous Ins-1, however, appears to only have a single isoform expressed, but it is not clarified which Ins-1 protein isoform this band corresponds to (Burg et al. 2009).

The first aim of this work was to further explore the likelihood of two INSIG1 protein isoforms being produced in other vertebrate species through bioinformatic investigation of conservation of the two start sites. The second aim of the work was to investigate whether the alternate translation start points impart any additional function to one isoform over the other.

A major factor influencing translation initiation occurring at a given AUG sequence are its surrounding nucleotides which together comprise the Kozak sequence. The importance of the flanking nucleotides in AUG recognition was first recognised by Marilyn Kozak (Kozak 1987). Subsequently, a Kozak consensus sequence emerged for eukaryotic translation initiation (Table 5.1).

Nucleotides at certain positions relative to the AUG start have more influence over translation initiation than others. The most important nucleotides are located at positions -3 and +1 of the AUG start (Kozak 1999). In constitutive over-expression constructs, the cDNA start site is often placed in an optimal Kozak sequence setting. However, expression patterns of endogenous INSIG1 protein isoform ratios suggest that this may not be the case.

Table 5.1. Vertebrate Kozak consensus sequences. Purine bases are represented by '**r**', while '*n*' represents any of the four nucleotide bases. 'AUG's are taken together as being position 0. Residues at positions -3 and +1 have the most influence on translation initiation (Kozak 1987).

| | |
|---|---|
| Optimal | gcc**r**ccAUG**r** |
| Strong | **r***nn*AUG**r** |
| Weak | *nnn*AUG*n* |

The aim of the work described here was to further examine the Kozak sequence surrounding each AUG start site in the human INSIG1 mRNA sequence. This analysis was then extended to INSIG1 transcripts from other vertebrates. Conservation of a second in-frame start site within the region encoding the amino-terminal cytosolic extension of INSIG1 in other species would highlight an importance for having two INSIG-1 isoforms produced. As shown in Table 1, nucleotides at the -3 and +1 positions relative to the AUG start site influence the strength of translation initiation occurring at a particular start site. Thus conservation of nucleotides at the -3 and +1 positions would further highlight the importance of

two translational start sites for INSIG1 and possibly lean towards some sort of translational regulatory control over INSIG1 isoform expression.

While the presence of two human INSIG1 isoforms is accepted, there has been no investigation into their individual function. Analysis of each INSIG1 isoform function is necessary since the first translational start site is placed within an optimal Kozak context in over-expression plasmids used in the majority of INSIG1 functional studies. This results in translation initiation at the first start site being favoured over translation initiation from the second start site, resulting in more of the full length INSIG1protein being produced than the shorter isoform. Such expression ratios may not reflect *in vivo* INSIG1 isoform expression. In this chapter, each isoform of the human INSIG1 protein has been examined to determine if they exhibit the same functional characteristics in response to a) high cellular sterol levels b) negative regulation of SREBP processing and c) facilitation of HMGCR degradation.

## Results

### *Bioinformatic Analysis*

There are two proteins produced from the INSIG1 mRNA through the use of in-frame alternative translational start sites within the amino terminal region of the protein. Multiple sequence alignment of INSIG1 protein sequences from a wide variety of vertebrates was performed and the alignment indicates a strong level of sequence conservation over the transmembrane region of INSIG1 (data not shown). However there is much less sequence identity within the short cytosolic amino terminal region of the protein and it is within this region that the two alternative start sites are located (Figure 5.5). Interestingly, despite the lack of sequence identity among vertebrate INSIG1 within the translation initiation region, the presence of a second starter methionine thirty-five amino acids downstream from the first starter methionine, is highly conserved (Figure 5.5). In rodent species, however, a second starter methionine thirty-five amino acids is not present downstream from the first starter methionine. There is however a conserved second starter methionine present but it is located closer at 25 residues downstream from the first methionine (Figure 5.5). Two human INSIG1 isoforms are expressed from over-expression constructs from two start sites within the amino-terminal of the transcript. The conservation of two methionines within the amino-terminal region of the protein sequence among vertebrates shown here suggests that production of two INSIG1 isoforms may also occur in other vertebrate species. Conservation of two in-frame start sites within this poorly conserved region of INSIG1 among vertebrates suggests a potential function to having to INSIG1 isoforms produced.

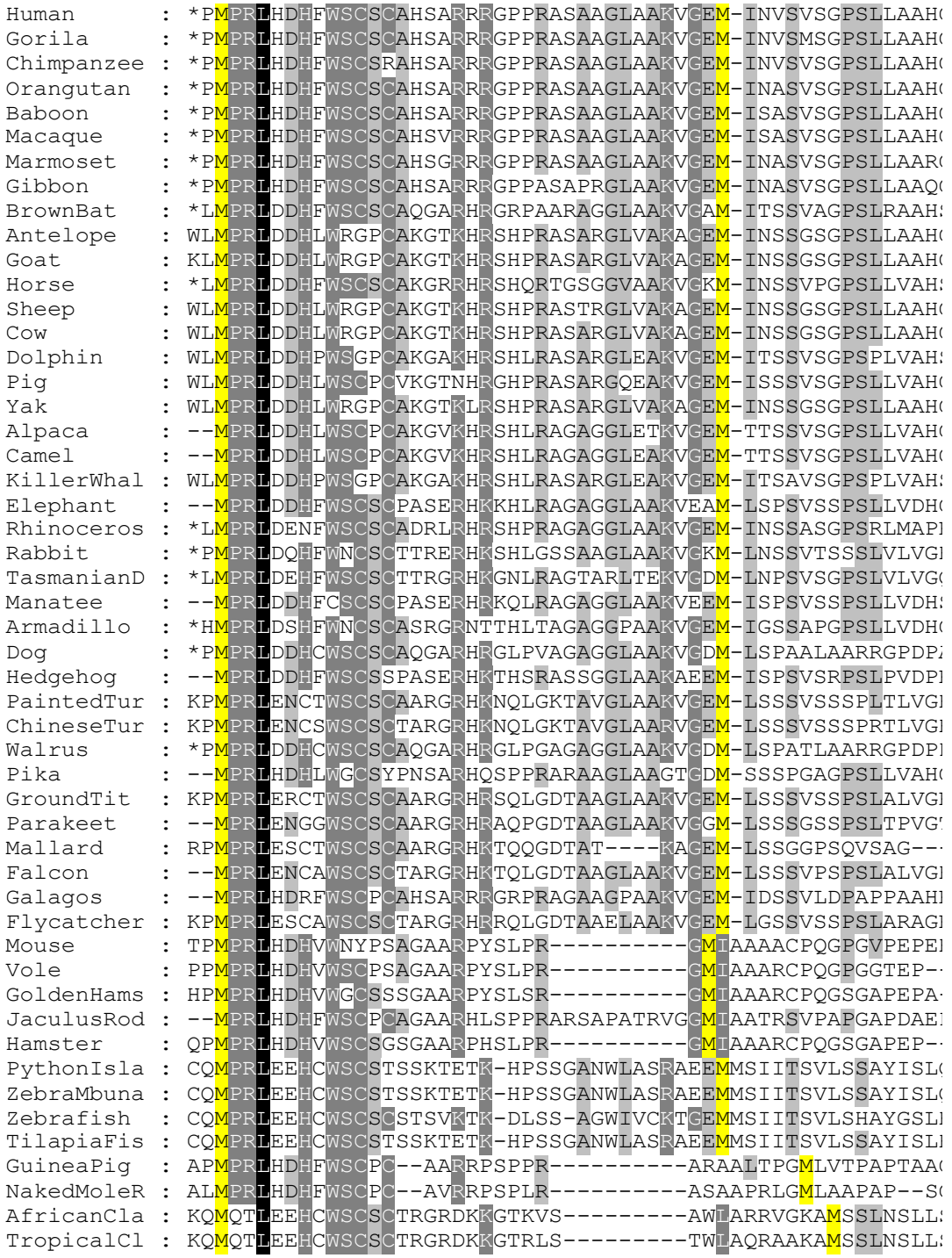

Figure 5.5. Conservation of a second in-frame start site within the region encoding the amino-terminal cytosolic extension of vertebrate INSIG1. Human INSIG1 homologs were retrieved from the NCBI database using their protein-protein basic local alignment search tool (blastp). Sequences were downloaded to and aligned in MEGA alignment explorer, which uses the Clustal W multiple alignment programme. Multiple sequence alignment was then edited in GeneDoc. Black=100% residue identity, grey=high level of residue identity, white= non-identical residues, yellow=methionine start.

Translational start sites have different stringencies of activation depending on their context. The context of a translational start site refers to its Kozak sequence for start site recognition. Studies have identified that the key nucleotides involved in determining the efficiency of initiation at a given ATG start site are the -3 and +1 nucleotides. Purine bases at these positions indicate a strong initiation site, while pyrimidine bases are less favourable. Analysis of the context surrounding the two translational start sites found in INSIG1 will inform on which isoform is likely expressed *in vivo*.

Analysis of the context of the first INSIG1 translational start site at the mRNA level in humans shows a cytosine at both the -3 and +1 positions. Having pyrimidine nucleotides at both of these positions is considered a very poor context start site. Surprisingly, this poor start site context is highly conserved across INSIG1 mRNA sequences (Figure 5.6A), with a wide range of vertebrate species retaining the cytosine nucleotides at -3 and +1 positions relative to the ATG start.

Analysis of the Kozak sequence associated with the second ATG start site indicated a lot more variability compared to the highly conserved nature of the first start site. In the human INSIG1 sequence, the second ATG has a guanine nucleotide at the -3 position and an adenine nucleotide at the +1 position (Figure 5.6A). Having purine nucleotides at both of these positions is considered to be a strong context start site for translation initiation. This Kozak motif at the second start site appears to be highly conserved among vertebrates, with the guanine at the -3 position being 100% conserved. The adenine at the +1 position is also conserved among a large number of the INSIG1 mRNA sequences, but in certain sequences a substitution does occur. The most common substitution is for a pyrimidine, which is the least favourable nucleotide at the +1 position and contributes to a start site being in poor context.

This substitution is not localised to any one clade of species in particular, as highlighted by the phylogenetic tree (Figure 5.7). The relevance of this limited conservation of a strong context second translation initiation start site for INSIG1 among vertebrates will be discussed below.

Translation initiation occurring from the poor context first start site in human and mouse is unexpected based on the strong context of the second start site. However, translation from the first start site is known to occur in human, mouse and hamster. RNA secondary structures are known to be involved in the regulation of translation initiation (Kozak 1986; Kozak 1989). It is a possibility that an RNA secondary structure may be causing ribosome stalling at the second start site which could cause an increase in translation initiation from the first start site, despite its poor context. Therefore, the mRNA sequence surrounding the second start site was analysed for the presence of potential secondary structure formation. Preliminary sequence analysis suggested two strong stem-loop structures forming in the region of the second start site in the human INSIG1 mRNA sequence, with the ATG being involved in the base pairing of the second stem (Figure 5.8A, red arrow). This structure was conserved in other mammalian INSIG1 mRNA sequences (data not shown). If RNA secondary structure formation was a mechanism by which translation initiation was occurring at the first start site, then it would be expected that secondary structure formation, in which the second ATG start site was involved in base-pairing, would be conserved among other vertebrate species. Analysis of the nucleotide sequence surrounding the second start site in INSIG1 mRNA sequences from frog, fish and rodent species indicate the possibility of stem-loop structure formation in which the second ATG start site is involved in base pairing (Figure 5.8B, 5.8C and 5.8D, respectively). The presence and relevance of these predicted

secondary structures with respect to influencing translation initiation at the first poor context start site remains to be investigated.

The overall conservation of two start sites and their initiation contexts among vertebrates presented here suggests a functional significance to having two INSIG1 protein isoforms produced. In this chapter, the function of each INSIG1 isoform was investigated with respect to the two known cellular functions of the INSIG1 protein; a) inhibition of SREBP processing and b) mediating the degradation of HMGCR.

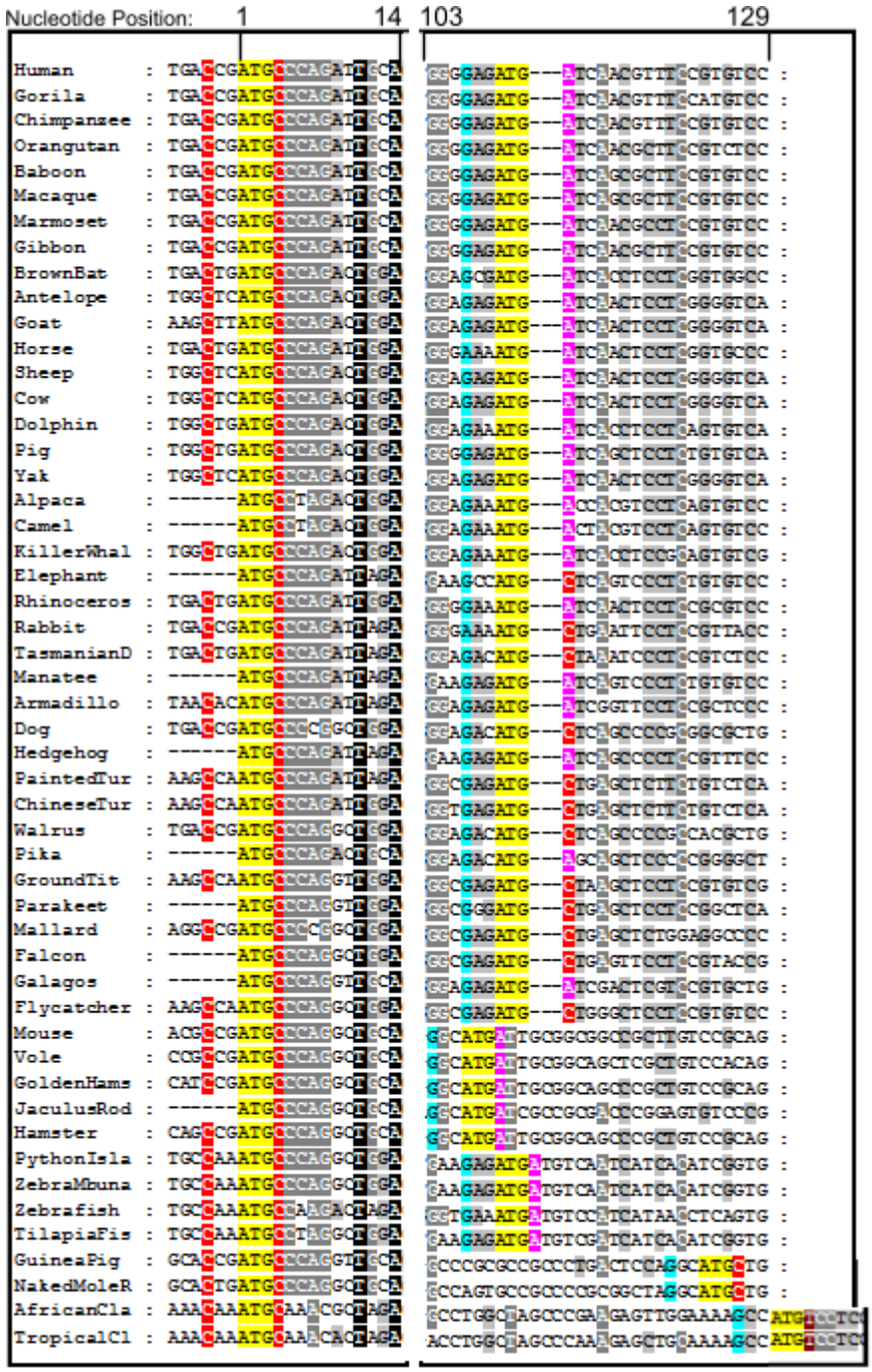
Nucleotide Position: 1 14 103 129
Human
Gorila
Chimpanzee
Orangutan
Baboon
Macaque
Marmoset
Gibbon
BrownBat
Antelope
Goat
Horse
Sheep
Cow
Dolphin
Pig
Yak
Alpaca
Camel
KillerWhal
Elephant
Rhinoceros
Rabbit
TasmanianD
Manatee
Armadillo
Dog
Hedgehog
PaintedTur
ChineseTur
Walrus
Pika
GroundTit
Parakeet
Mallard
Falcon
Galagos
Flycatcher
Mouse
Vole
GoldenHams
JaculusRod
Hamster
PythonIsla
ZebraMbuna
Zebrafish
TilapiaFis
GuineaPig
NakedMoleR
AfricanCla
TropicalCl

A)

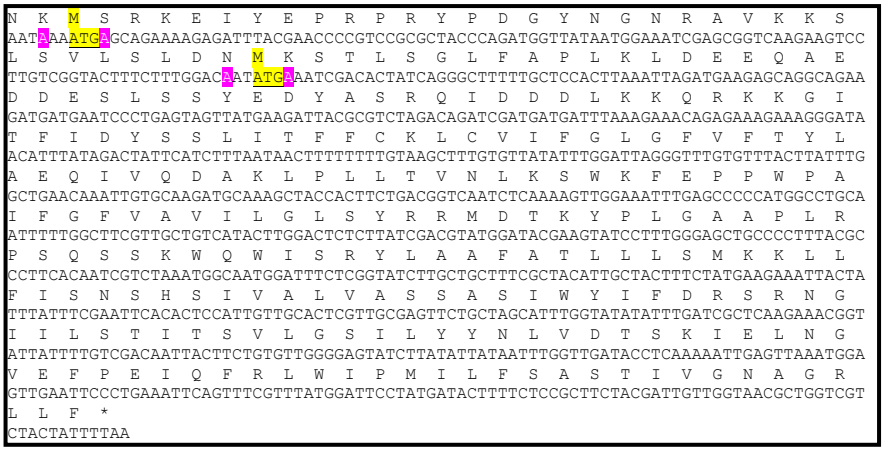


B)

Figure 5.6. Analysis of Kozak sequence surrounding INSIG1 translation initiation start sites A) Vertebrate mRNA sequences were retrieved from the NCBI database using the desource accessions associated with the INSIG1 protein sequences. Sequences were downloaded to and aligned in MEGA alignment explorer, which uses the ClustalW multiple alignment programme. Nucleotide positions shown refer to positions in the human INSIG1 mRNA sequence. Highlighted in yellow are the ATG start sites, red are cytosines, blue are guanines, pink are adenines and brown are thymines B) mRNA and protein sequence of *S. pombe* Ins-1 shown both initiator ATGs (yellow), and adenines at both -3 and +1 positions (pink).

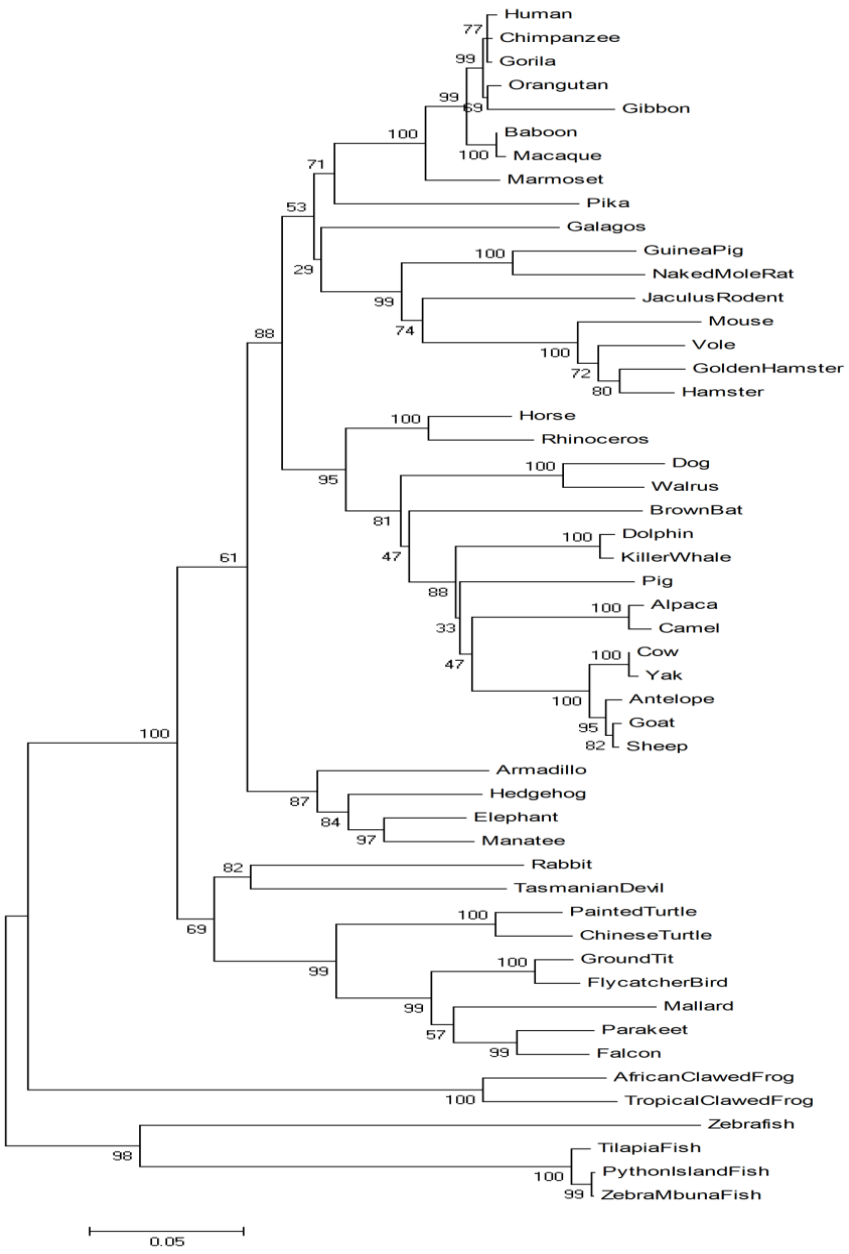


Figure 5.7. Phylogenetic tree illustrating the relationship between INSIG1 protein homologs. A phylogenetic tree was constructed based on the multiple sequence alignment of vertebrate INSIG1 protein sequences using the Neighbour-Joining method in MEGA 4.0. Branch values are and indicator of confidence in tree branch topology, as measured using the Bootstrap test of phylogeny.

A)

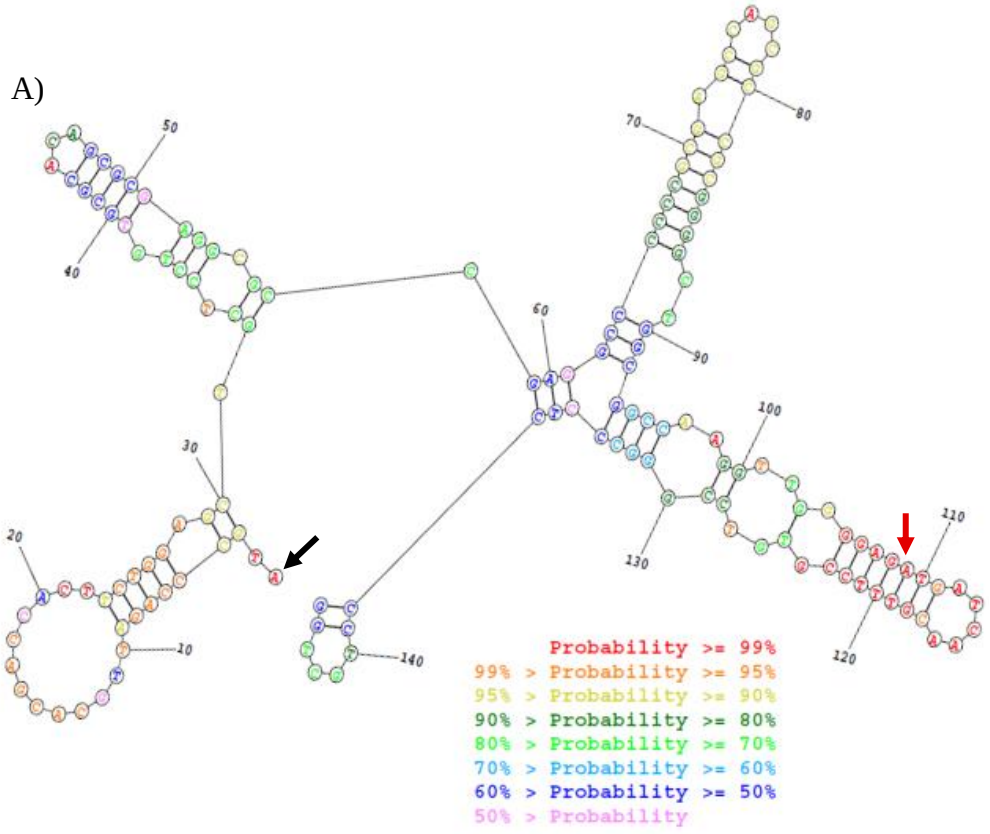


**Human**

B)

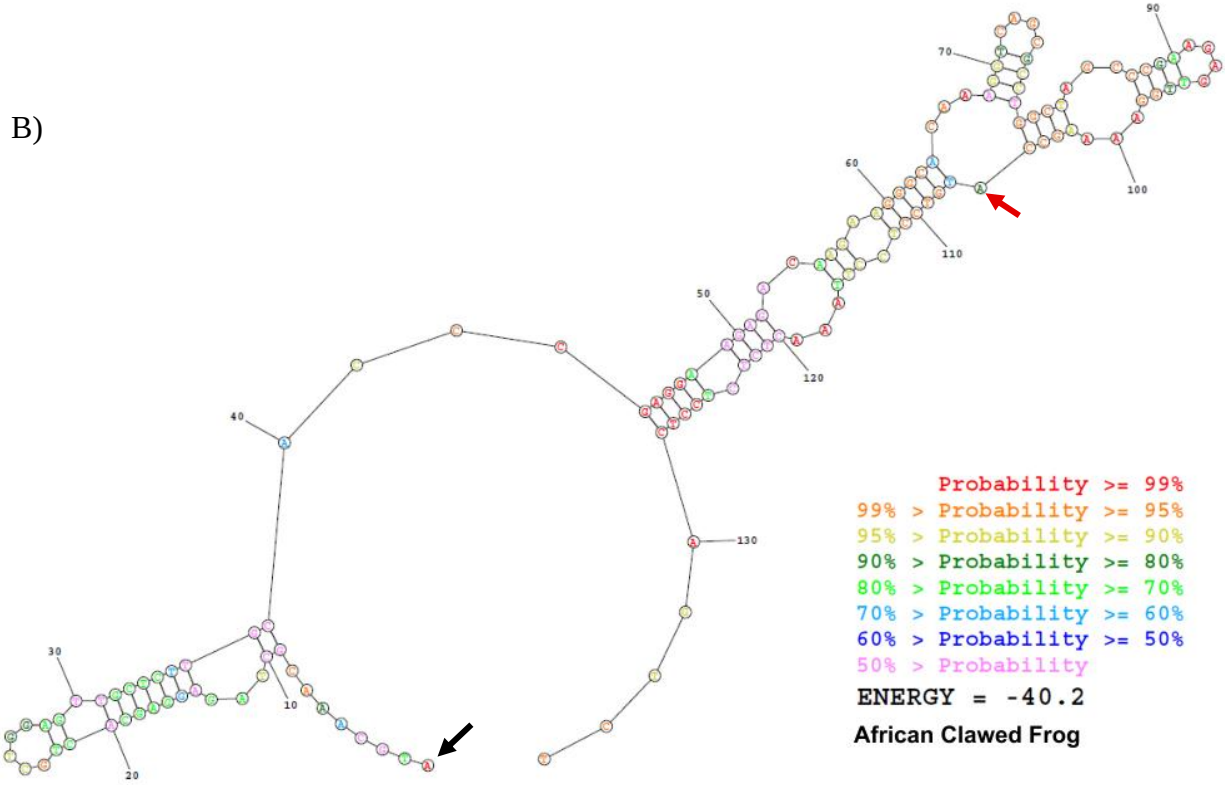


**African Clawed Frog**

C)

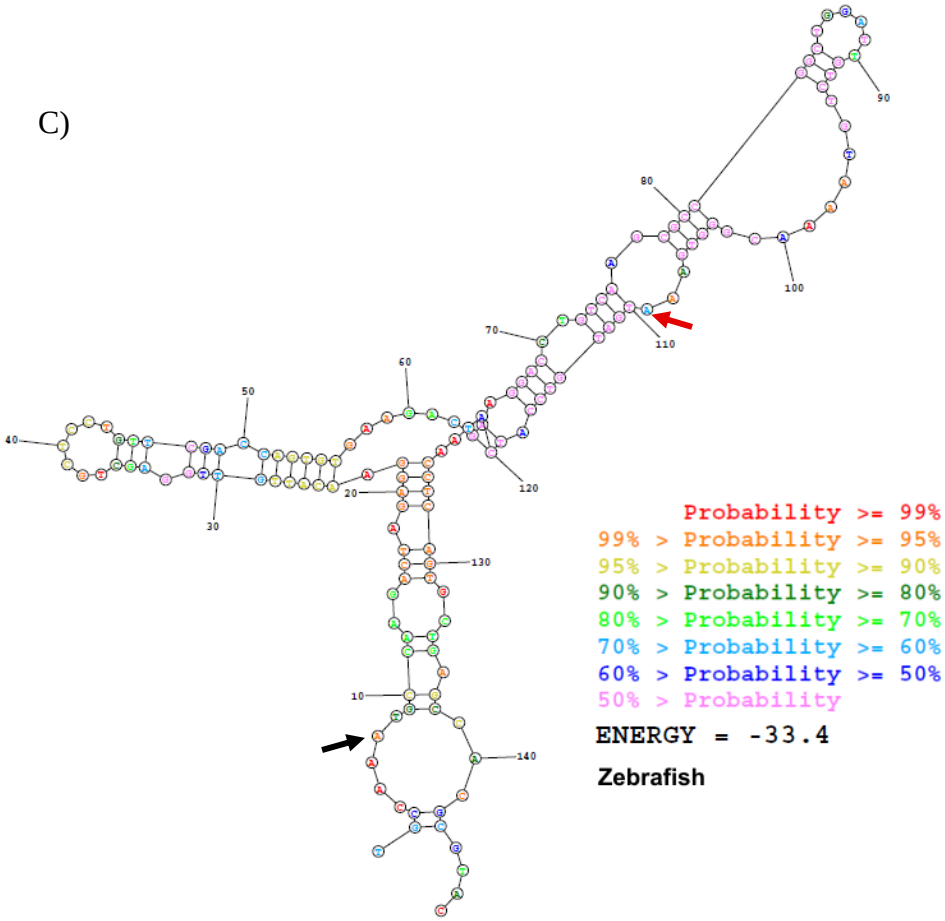
Probability >= 99%
99% > Probability >= 95%
95% > Probability >= 90%
90% > Probability >= 80%
80% > Probability >= 70%
70% > Probability >= 60%
60% > Probability >= 50%
50% > Probability
ENERGY = -33.4
Zebrafish

D)

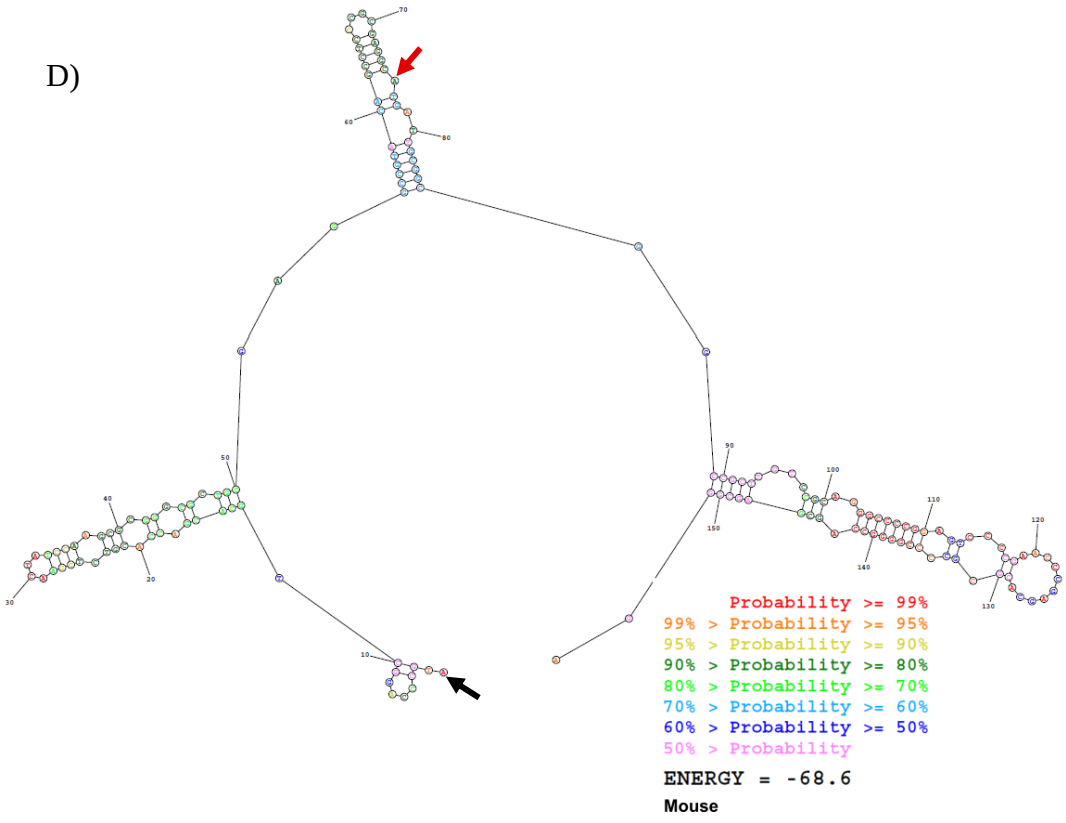
Probability >= 99%
99% > Probability >= 95%
95% > Probability >= 90%
90% > Probability >= 80%
80% > Probability >= 70%
70% > Probability >= 60%
60% > Probability >= 50%
50% > Probability
ENERGY = -68.6
Mouse

Figure 5.8. Predicted RNA secondary structures within the 5-prime region of vertebrate INSIG1 mRNA sequences. A) Human, B) African clawed frog, C) Zebrafish and D) Mouse. Structures represent the lowest free energy structures generated using 'Fold' of the RNAstructure Web Server (Reuter and Mathews,2010). The first ATG start site is indicated with the black arrow, the second ATG start site is indicated with the red arrow.

### *Investigation of effects of individual INSIG1 isoforms on SREBP retention in the ER*

INSIG1 is involved in mediating the inhibitory effects of oxysterols on SREBP activation. This inhibitory effect is achieved by INSIG1 binding to the transmembrane region of SCAP and anchoring SCAP in the ER which in turn retains SREBP in the ER preventing its transport to the Golgi and subsequent activation by the site-1 and site-2 proteases. To investigate if either isoform of INSIG1 displayed a difference in its ability to inhibit SREBP activity three mutants of INSIG1 were generated (Figure 5.9). The first mutant generated was a modification of an INSIG1 expression plasmid to restore its initiator ATG codons to the same context as the native human INSIG1 mRNA. Thus, this mutant INSIG1 construct mimics the native mRNA and allows an accurate reflection of the expression ratios from the first and second INSIG1 start sites *in vivo*. This mutant was designated $INSIG1_{WT}$. The second mutant ($INSIG1_{2ND\text{-}AAA}$) had the second start site mutated from ATG to AAA so that transcription only occurred from the first ATG start site. The size of the INSIG1 protein produced from this mutant form should be approximately 30 kDa. The third mutant ($INSIG1_{1ST\text{-}AAA}$) had the first start site mutated to AAA so that transcription only occurred from the second ATG start site and encodes a shorter INSIG1 isoform of 26 kDa.

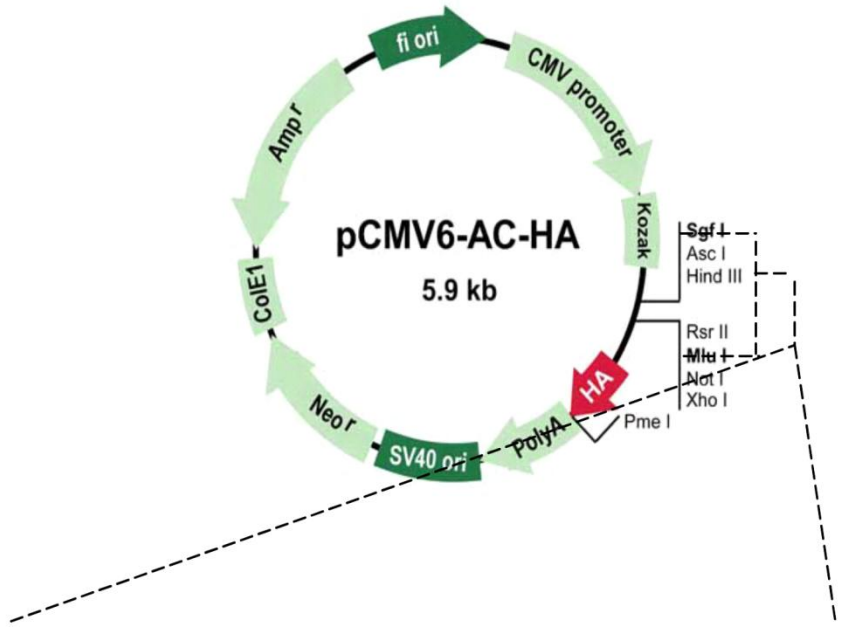


**Original Construct:**

GCGATCGCCATGCCCAGATTGCACGACCACTTCTGGAGCTGCTCCTGTGCGCACAGCGCGAG
GCGCCGAGGCCCCCCGC GAGCCAGCGCCGCGGGGCTGGCGGCCAAGGTTGGG GAGATGATC
AACGTTT.....

**INSIG1$_{WT}$:**

GCGATCCCCATGCCCAGATTGCACGACCACTTCTGGAGCTGCTCCTGTGCGCACAGCGCGAGG
CGCCGAGGCCCCCCGCGAGCCAGCGCCGCGGGGCTGGCGGCCAAGGTTGGG GAGATGATCA
ACGTTT.....

**INSIG1$_{2ND-AAA}$:**

GCGATCGCCATGCCCAGATTGCACGACCACTTCTGGAGCTGCTCCTGTGCGCACAGCGCGAG
GCGCCGAGGCCCCCCGCGAGCCAGCGCCGCGGGGCTGGCGGCCAAGGTTGGG GAGAAAAT
CAACGTTT.....

**INSIG1$_{1ST-AAA}$:**

GCGATCGCCAAACCCAGATTGCACGACCACTTCTGGAGCTGCTCCTGTGCGCACAGCGCGAG
GCGCCGAGGCCCCCCGCGAGCCAGCGCCGCGGGGCTGGCGGCCAAGGTTG GGGAGATGATC
AACGTTT.....

Figure 5.9. Schematic representation of INSIG1 mutants generated. The original construct used was purchased from Origene and had the INSIG1 ORF inserted into the vector pCMV6-AC-HA Mutant constructs were generated by site directed mutagenesis of the indicated sites above (highlighted in green) using QuikChange II Site-Directed Mutagenesis Kit.

The effects of $INSIG1_{WT}$, $INSIG1_{2ND\text{-}AAA}$ and $INSIG1_{1ST\text{-}AAA}$ on25-OHC prevention of SREBP processing as measured by SREBP/HMGCR luciferase reporter readout were analysed using the HeLa-PHGL cell line which has the SREBP responsive promoter HMGCR fused to *Gaussia* luciferase. Cells were transfected with either empty vector (EV) or each of the INSIG1 mutant constructs respectively. Following transfection, cells were incubated in the presence or absence of 25-OHC for sixteen hours and assayed for secreted luciferase activity (Figure 5.10). Incubation with 25-OHC alone yielded a 2.38-fold reduction in luciferase readout. As expected, over-expression of $INSIG1_{WT}$ further increased the fold repression to 4.50. The $INSIG1_{2ND\text{-}AAA}$ mutant increased it further to 5.56 while the increase observed for $INSIG1_{1ST\text{-}AAA}$ increased was 4.55 (Table 5.2). Thus, each mutant INSIG1 protein was capable of significantly enhancing the oxysterol inhibitory effect on SREBP readout compared to 25-OHC alone (25-OHC vs. $INSIG1_{WT}$, P=0.0012; 25-OHC vs. $INSIG1_{2ND\text{-}AAA,}$ P=0.0007; 25-OHC vs. $INSIG1_{1ST\text{-}AAA}$ P=0.0013). However, no significant difference was observed when the inhibitory effect between the INSIG1 mutants was assessed (p-values > 0.05; Table 5.3).

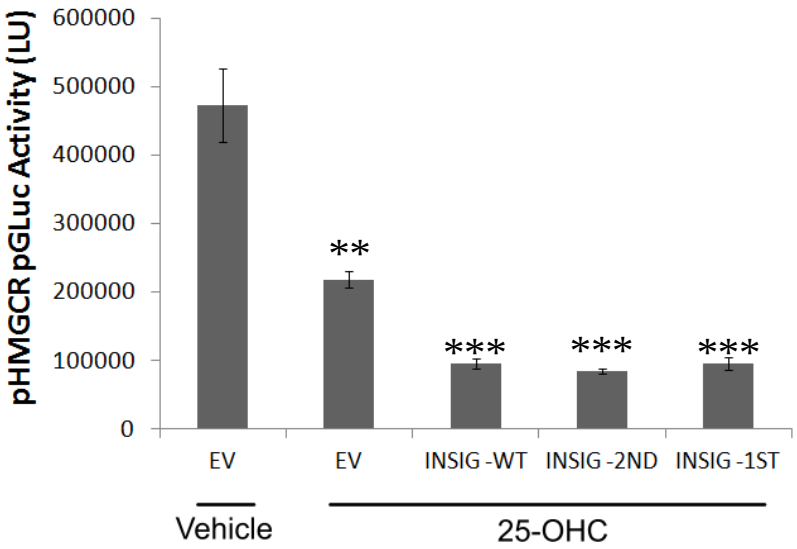


Figure 5.10. Comparison of the effects of each INSIG1 isoform on SREBP/HMGCR luciferase reporter readout. HeLa-PHGL Cells were transfected with either empty vector (EV) or one of the three INSIG1 mutant constructs; $INSIG1_{WT}$, $INSIG1_{2ND\text{-}AAA}$ or $INSIG1_{1ST\text{-}AAA}$, using TurboFect transfection reagent. Following transfection, cells were cultured in media containing 10% LDS, in the presence of 25-OHC for 16 hours, after which aliquots of media were assayed for luciferase activity. (** $p<0.005$, *** $p<0.0005$, as compared using Student's t-Test).

Table 5.2. Repression of the SREBP/HMGCR luciferase reporter readout in HeLa-PHGL cells transfected with the different INSIG1 mutants in the presence of 25-OHC.

| ***Fold repression of HMGCR promoter**** | |
|---|---|
| EV | 2.38 (± 0.190) |
| $INSIG1_{WT}$ | 4.50 (± 0.629) |
| $INSIG1_{2ND\text{-}AAA}$ | 5.56 (± 0.290) |
| $INSIG1_{1ST\text{-}AAA}$ | 4.55 (± 0.608) |

* The values shown represent the average from three independent transfection experiments, ± standard deviation.

Table 5.3. Significance of repression of SREBP/HMGCR luciferase reporter readout in HeLa-PHGL cells between each INSIG1 mutant in the presence of 25-OHC.

| ***Difference between INSIG mutants in fold repression of HMGCR promoter**** | | | |
|---|---|---|---|
| | $INSIG1_{WT}$ | $INSIG1_{2ND\text{-}AAA}$ | $INSIG1_{1ST\text{-}AAA}$ |
| $INSIG1_{WT}$ | 1.0000 | 0.0918 | 0.9977 |
| $INSIG1_{2ND\text{-}AAA}$ | 0.0918 | 1.0000 | 0.1404 |
| $INSIG1_{1ST\text{-}AAA}$ | 0.9977 | 0.1404 | 1.0000 |

* The values shown represent the average from three independent transfection experiments, ± standard deviation.

***Effects of individual INSIG1 translation isoforms on HMGCR degradation***

INSIG1 is known to be essential for sterol-induced degradation of HMGCR. A population of INSIG1 proteins are known to be constitutively bound by the ER-resident E3 ligase gp78. Upon sterol-regulated binding of HMGCR by INSIG1, gp78 is recruited to HMGCR and this triggers the ubiquitin-mediated degradation of HMGCR. It has not yet been identified which region of INSIG1 interacts with gp78. There are believed to be two portions of INSIG1 within the ER membrane, distinguished by whether or not they are bound by gp78. If the two isoforms of INSIG1 make up the two populations which are either gp78 bound or not, then they would display differences in their ability to mediate the degradation of HMGCR. To investigate if there is a difference between the longer and shorter translation isoforms of INSIG1 in promoting the sterol-mediated HMGCR degradation, HeLa-PHGL cells were transfected with $INSIG1_{WT}$, $INSIG1_{2ND\text{-}AAA}$ or $INSIG1_{1ST\text{-}AAA}$. Following transfection, cells were incubated in the absence or presence of increasing concentrations of 25-OHC, which is known to promote the degradation of HMGCR.

In cells transfected with empty vector, incubation with 25-OHC alone was sufficient to induce a rapid decrease in HMGCR at the protein level at the lowest concentration used (Figure 5.11). This is mediated by endogenous INSIG1. Over-expression of $INSIG1_{WT}$ enhanced the degradation of HMGCR to below detectable levels. Both $INSIG1_{2ND\text{-}AAA}$ and $INSIG1_{1ST\text{-}AAA}$ displayed the capacity to enhance the sterol-mediated degradation of HMGCR to below detectable levels, similar to the effects of $INSIG1_{WT}$. These results demonstrate indirectly that both isoforms of INSIG1 must be capable of binding gp78 as over-expression of each isoform individually displayed the same enhancing effect on sterol-mediated degradation as wild-type INSIG1.

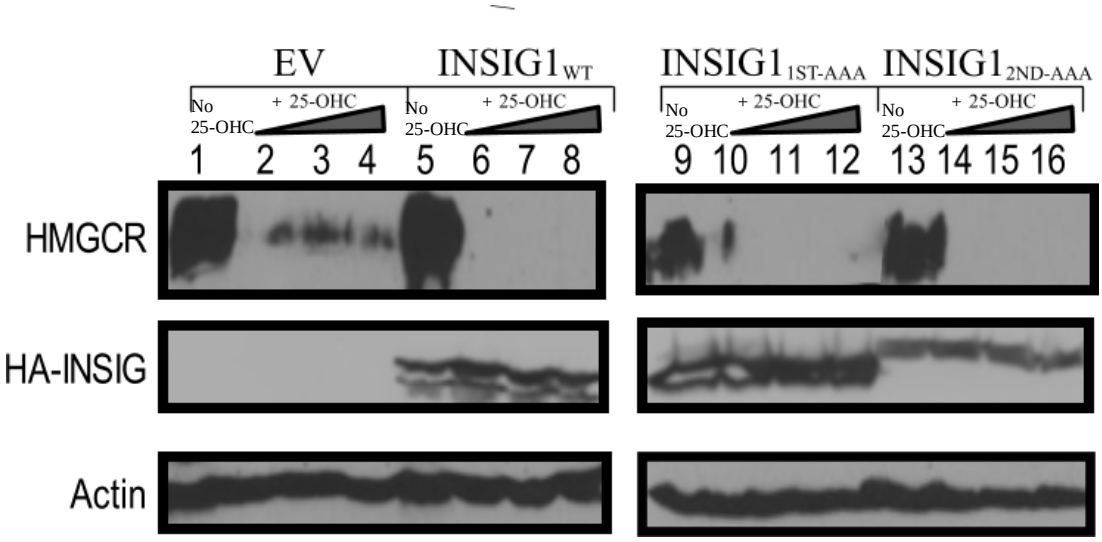


Figure 5.11. Comparison of the effects of each mutant isoform of INSIG1 on oxysterol-mediated degradation of HMGCR. HeLa-PHGL cells were transfected with either empty vector (EV) or one of the three INSIG1 mutant constructs; $INSIG1_{WT}$, $INSIG1_{2ND\text{-}AAA}$ or $INSIG1_{1ST\text{-}AAA}$, using TurboFect transfection reagent. Following transfection, cells were cultured in media containing 10% LDS, in the absence or presence of increasing concentrations of 25-OHC (0.3 µg/ml, 0.6 µg/ml and 0.9 µg/ml) for 20 hours. Whole cell extracts were prepared using homemade high SDS lysis buffer, as described in methods. Note: The grey in the centre of the $INSIG1_{1ST\text{-}AAA}$ bands are as result of becoming over-exposed in attempts to get a signal for $INSIG1_{2ND\text{-}AAA}$ alongside it for comparison. Please note that the edges of the bands are intact and that two bands are not being produced from $INSIG1_{1ST\text{-}AAA}$.

## Discussion

Human INSIG1 has two protein isoforms produced through translation initiation occurring from two alternative in-frame start sites (Yang et al. 2002). The work in this chapter sought to examine the phylogenetic conservation of these two start sites. The work also sought to elucidate if each INSIG1 isoform functioned differently with respect to the two known cellular functions of INSIG1; a) repressing SREBP processing and b) promoting degradation of HMGCR.

Multiple sequence alignment of INSIG1 protein sequences from a wide variety of vertebrate species indicated a high level of sequence conservation over the entire transmembrane domain of the protein. However, there was much less conservation within the amino terminus of the protein. Despite the low level of sequence identity within this region, the presence of the second initiator methionine is shown to be conserved among vertebrates. The production of two proteins from the one INSIG1 mRNA is only reported for human and hamster INSIG1, but not in other vertebrates (Gong, Lee, Lee, et al. 2006b). Mouse is reported as having one INSIG1 isoform, corresponding to translation initiation occurring from the first translational start site (Engelking et al. 2004). The fission yeast homolog Ins-1 also contains a second initiation methionine, located thirty four residues upstream of the first (Burg et al. 2009). Ins-1 does have two Ins-1 protein isoforms produced corresponding to translation initiation occurring from the two in-frame start sites, which is consistent with human INSIG1 scenario.

Analysis of the Kozak sequence surrounding the two methionine residues at the nucleotide level was performed in vertebrates to provide insight into whether translation from this second start site may also occur in other species. The positions

within the Kozak sequence found to influence translation initiation the most are the -3 and the +1 position relative to the ATG initiation codon (Kozak 1999). Pyrimidines are the least favourable nucleotides to have at these positions with respect to translation initiation efficiency. Surprisingly, the first start site in human INSIG1 has cytosines located at both the -3 and +1 positions, and this context was found to be highly conserved among vertebrates. Translation from a start site in this context would be expected to be very low but this work and the work of others have shown that both the long and short translation isoform are translated in INSIG1 over-expression constructs. Endogenous INSIG1 expression has shown the longer protein isoform to be the main isoform detected, suggesting that initiation is occurring at a higher rate from the first start site. There is no immunoblot evidence to indicate protein molecular weight for INSIG1 from most of the species present in the alignments. However, for mouse and hamster immunoblot analysis indicates that the molecular weight of INSIG1 lies between that of each human INSIG1 isoform at 28 kDa, which corresponds to translation initiation from the first start site. Our analysis indicates that this first start site in rodents is also in poor context.

Translation initiation from the first start site appears even less likely when you consider the Kozak sequence surrounding the second start site. The second start site has purine nucleotides at the -3 and the +1 positions which is considered a good context start site. The good context of the second start site is also conserved for the most part among vertebrates, including in rodents. However, it is important to consider that a purine-pyrimidine substitution occurs in some instances at the +1 position, which is the least favourable substitution with respect to translation initiation and previous findings suggest that this could reduce translation initiation efficiency from this second start site. In the case of start site contexts of human

INSIG1, the scanning ribosome would be expected to read through the first start site and initiate translation at the second (Dr. Ivaylo Ivanov, personal communication). However, it is clear that read through of the first translational start site is not occurring. Our analysis indicates that translation from the first start site in rodents occurs despite the second start site being in better context, which is consistent with the human INSIG1 scenario. Thus, it would be reasonable to predict that translation occurs from this poor context first start site in INSIG1 from all species shown.

A possible explanation for translation occurring from a poor context first start site is through ribosome stalling at the second site. Ribosome stalling is a possibility when you consider the distance between the two start sites is 105 nucleotides and the average length covered by a ribosome is 32 nucleotides (Dr. Ivaylo Ivanov, personal communication). While this distance is the same for most other vertebrates, in rodent species the distance between the two start sites is less and would correspond to just over twice the length of a stalled ribosome. A brief analysis of the region surrounding the second ATG start sites in human INSIG1 mRNA for potential RNA secondary structures which may influence ribosome stalling revealed the possibility that the second start site may be occluded within a hairpin structure. Analysis of the same region in other species suggested that the second ATG being in stem-loop structure appeared to be a conserved event. However, a more detailed investigation of conservation of an RNA secondary structure contributing to reduced initiation of translation at the second start site would be necessary. It would also be necessary to mutate the nucleotides involved this structure formation to confirm its involvement in promoting initiation at the first poor context start site. Whether ribosome stalling is involved in translation initiation occurring from the first poor context start site was not pursued in these works but merits further investigation.

Another possibility is that the different translational contexts of the two start sites allow recognition by different eukaryotic translation initiation factors (eIFs). In the scanning ribosome complex, eIFs are central to selecting translational start sites within the 5' region of an mRNA transcript. It is has been demonstrated that different eIFs have varied affinities for translation start sites depending on their Kozak sequence (Ivanov et al. 2010; Loughran et al. 2012). For example, eIF5 has been shown to reduce the stringency of start codon selection and induce translation from poor context start sites. In contrast, eIF1 has been shown to increase stringency of start codon selection and translation initiation from optimal context start sites. The cellular signals which regulate which eIFs are present in the scanning ribosome are as yet unclear, but are under investigation. INSIG1 having both a poor context and an optimal context start site may ensure that if transcription of INSIG1 is induced that translation will be initiated regardless of which eIF is present in the scanning ribosome. It is also possible that under conditions which induce a change in eIF proteins, that this would allow increased expression of one isoform over the other. Whether eIFs can alter the ratio of INSIG1 isoform expression merits further investigation, but functional significance of such a regulation is unclear and is currently under investigation in the lab.

The production of two INSIG1 isoforms in human from translation occurring from two in-frame start sites, and the conservation of two in-frame start sites among vertebrates and yeast prompted up to investigate if there was a functional difference between the two human INSIG1 isoforms. The effect of over-expression of each INSIG1 isoform on mediating sterol-induced inhibition of SREBP activation was assessed using the HeLa-PHGL cell line. In this model, HMGCR promoter activity serves as an accurate measure of SREBP activation and is quantifiable through

assaying for luciferase enzyme levels. The effects of the INSIG1 isoforms were compared in the presence of 25-OHC, as certain oxysterols are required to mediate INSIG1 effects (Sun et al. 2005). The presence of 25-OHC alone caused a significant decrease in SREBP reporter readout, mediated by endogenous INSIG proteins. Over-expression of all three INSIG1 proteins; $INSIG1_{WT}$, $INSIG1_{2ND\text{-}AAA}$ and $INSIG1_{1ST\text{-}AAA}$, significantly enhanced the oxysterol inhibitory effect. However, there was no significant difference observed between the level of repression achieved between the INSIG1 isoforms or compared to wild-type. Thus, both isoforms appear to possess the ability to suppress SREBP activation in the presence of sterols to the same degree. While these results give a strong indication towards there being no difference between INSIG1 isoforms in this context, the window available to study this effect is quite small owing to the large inhibitory effect of oxysterol alone. It would be appropriate to conduct these experiments in an $INSIG1^{-/-}/INSIG2^{-/-}$ background to remove the effect of the endogenous INSIG. It was not possible to do this here as such mutants were not available.

$INSIG1_{WT}$, $INSIG1_{2ND\text{-}AAA}$ and $INSIG1_{1ST\text{-}AAA}$ were also investigated with respect to their ability to mediate the degradation of HMGCR. Due to the presence of endogenous INSIG proteins, the presence of 25-OHC alone caused a significant decrease in HMGCR at the protein level. Over-expression of all three INSIG1 proteins; $INSIG1_{WT}$, $INSIG1_{2ND\text{-}AAA}$ and $INSIG1_{1ST\text{-}AAA}$, all enhanced the oxysterol degradation effect on HMGCR, decreasing protein levels to amounts below the range of detection by immunoblot. Thus, both isoforms appear to possess the ability to mediate the degradation of HMGCR in the presence of sterols. However, due to the large effect that the oxysterol has on inducing HMGCR degradation mediated by endogenous INSIG1, it would also be appropriate to conduct these experiment in an

INSIG1$^{-/-}$/INSIG2$^{-/-}$ background to remove the effect of the endogenous INSIG proteins. The results presented here indicate that the function of having two INSIG1 isoforms produced is not likely to differentially mediate either of the two known functions of INSIG1.

# Chapter 6

# Inhibition of SREBP Processing Enhances the Cytotoxic Action of Statins

## Abstract

Statins are a family of drugs which efficiently and specifically inhibit the catalytic activity of the rate limiting enzyme in cholesterol biosynthesis, 3-hydroxy-3-methylglutaryl coenzyme A reductase (HMGCR). Inhibition of HMGCR results in a decrease in intracellular cholesterol, as well as essential sterol intermediates. The cell compensates by increasing cholesterol biosynthesis and uptake through increasing processing of the SREBP2 transcription factor. By this mechanism, statins increase LDLR which results in the decrease of serum LDL-cholesterol characteristic of statin treatment, but they also increase their own target HMGCR. There is increased interest in the potential use of statins as anti-cancer agents based on their ability to induce apoptosis. One of the limitations of their potential use in this area is that the concentrations required to induce cancer cell death *in vitro* are much higher than the serum concentrations currently achieved with the recommended dosage of 40-80 mg/day. Higher serum concentrations can be achieved with higher daily doses, but this causes adverse effects, including myopathy. Thus lowering the concentrations of statin required to induce cancer cell death is of high value.

The aim of this chapter was to investigate the effect of targeted inhibition of SREBP processing on the cytotoxicity induced by statins in cancer cell lines. The results indicate that inhibition of SREBP processing using oxysterols significantly enhances statin cytotoxicity in HeLa cells, and that this inhibition is related to protein levels of active nSREBP2 and HMGCR. The results indicate that this approach is also valid to enhance statin cytotoxicity in cancer cells, but may be limited by deregulation of SREBP processing and off target effects of statins, which were observed for some of the cancer cell lines screened.

## Introduction

Maintenance of cholesterol homeostasis is central to cell viability (Mclean et al. 2012). Homeostasis is achieved through regulated cholesterol uptake and *de novo* biosynthesis (Davis et al. 2004; Brown & Goldstein 1986). The cholesterol biosynthesis pathway comprises multiple enzymes whose expression is regulated by the transcription factor (TF) SREBP2 (Horton et al. 2002a). SREBP2 is part of a family of transcriptions factors involved in regulating lipid synthesis (Eberlé et al. 2004; Hua et al. 1995). The other family members are SREBP1a and SREBP1c which are both expressed from the *SREBF1* gene through the use of alternative first exons (Shimomura et al. 1997). SREBP1c primarily regulates genes involved in fatty acid biosynthesis, while SREBP1a has been shown to regulate expression of both cholesterol and fatty acid biosynthetic enzymes (Horton et al. 2003; Amemiya-kudo et al. 2002; Shimano, Horton, et al. 1997). SREBP2 binds to SRE elements within the promoter region of key cholesterogenic genes including 3-hydroxy-3-methylglutaryl coenzyme A synthase (HMGCS), 3-hydroxy-3-methylglutaryl coenzyme A reductase (HMGCR), mevalonate kinase and lanosterol synthase (Figure 1) (Horton et al. 1998; Horton et al. 2002). The promoters also contain transcription factor element binding sites for common TFs such as for SP-1 and NF-Y (Amemiya-kudo et al. 2002). The availability of active SREBP2 is highly regulated. The SREBP proteins are synthesised as inactive precursor proteins where the transcription factor domain is tethered to the ER (Hua et al. 1993b; Sakai 1995) . When cellular sterols deplete below threshold levels, SREBP2 is transported to the Golgi facilitated by the chaperone action of its interacting partner SCAP (Brown et al. 2002a). In the Golgi, two endogenous proteases cleave the SREBP2 precursor protein to liberate the soluble N-terminal transcription factor domain (nSREBP2)

(Duncan et al. 1997a; Duncan et al. 1997b). This sterol regulated release of SREBP2 allows for rapid induction of the entire cholesterol biosynthetic pathway upon sterol depletion within the cell. When cellular sterols return above threshold concentrations, transport of the SCAP-SREBP complex does not occur due to retention of the complex in the ER, thus preventing excess build-up of cholesterol which is toxic to the cell (Radhakrishnan et al. 2008; Adams et al. 2003).

The cholesterol biosynthesis pathway is also commonly referred to as the mevalonate pathway. Mevalonate production is the rate limiting step in cholesterol biosynthesis (Brown et al. 1973). Mevalonate is produced by the enzymatic reduction of HMG-CoA in the presence of NADPH, by the enzyme HMGCR (Retey et al. 1970). As well as cholesterogenesis being essential for new cell membrane synthesis, mevalonate has been shown to be essential in many cellular processes (Ikonen 2008). As early as 1979, mevalonate was recognised as having an essential role in DNA replication (Quesney-huneeus et al. 1979). An increase in HMGCR expression co-ordinates with the cell cycle S-phase, and statin-mediated inhibition of HMGCR activity prevents S-phase associated DNA synthesis (Tatsuno et al. 1997). This statin effect is reversed upon addition of mevalonate but not cholesterol to the cells (Tatsuno et al. 1997). It was identified subsequently that the sterol intermediates farnesyl pyrophosphate and geranylgeranyl pyrophosphate, which cannot be produced in the absence of mevalonate, are essential for post-translational modification of proteins essential throughout the cell cycle (Sebti & Hamilton 2000; Rilling et al. 1993). Such proteins include nuclear lamins, Ras and other G-proteins (Luckman et al. 1998; Lutz et al. 1991). Since mevalonate is upstream of these pathway intermediates, their synthesis is dependent on its availability (Rilling et al. 1993). Thus a reduction in cellular mevalonate levels is in itself an issue for cell

viability, but also prevents production of other essential pathway intermediates (Kita et al. 1980).

The catalytic activity of HMGCR is specifically and efficiently inhibited by a group of drugs called statins (Istvan & Deisenhofer 2001). Statins are the one of the highest selling group of drugs in the world today and are widely used in the treatment of cholesterol-related diseases including atherosclerosis and hypercholesterolemia (Vaughan et al. 2000; Law et al. 2002; Aronow 2013). Statins are a family of drugs that differ in their chemical structure and potency, but all competitively bind to the catalytic site of HMGCR via their HMG-like moiety, thus preventing binding of the HMG-CoA substrate (Istvan & Deisenhofer 2001). The pioneering statin, compactin, was discovered in the mid-1970s, isolated from *Penicillium citrinium*, followed closely by the identification of another naturally occurring statin from *Aspergillus terreus*, Lovastatin (Brown et al. 1978; Alberts et al. 1980; Brown & Goldstein 2004). Natural statins which are currently clinically available are Lovastatin, Pravastatin and Simvastatin (compactin failed to pass clinical trials), while synthetic statins are also available; Atorvastatin, Cerivastatin and Fluvastatin (Tobert 2003). Despite their differences, statins are all metabolised in the liver by Cytochrome P450 enzymes. Metabolism by P450 enzymes results in statins suffering from low bioavailability, as evidenced by low plasma levels detectable following a 40 mg/day oral dose ranging from 10ng/ml to 50 ng/ml, depending on the statin (Schachter 2004). However, the desired site of action for the cholesterol lowering properties of statin is in the liver. Thus the low serum levels of statins that result from P450 metabolism are beneficial in limiting off-target effects in the rest of the body.

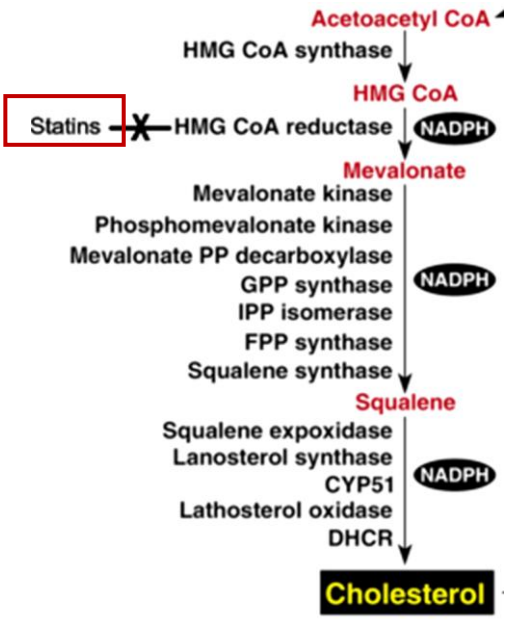


Diagram 6.1. SREBP2 target genes (in black) in the cholesterol biosynthesis pathway (modified from (Horton et al. 2002b)).

The mechanism of action of statins exploits the tight regulation that governs mevalonate pathway activity (Stancu & Sima 2001; Vaughan et al. 2000; Yang et al. 1994). Expression of HMGCR is regulated by the SREBP family of transcription factors, primarily SREBP2 (Vallett et al. 1996; Horton et al. 2002b). When HMGCR catalytic activity is inhibited through the use of statins, cellular mevalonate levels fall, and thus sterol intermediates and cholesterol decrease (Kita et al. 1980). The cell acts to compensate for this decrease by raising the levels of active SREBP2 transcription factor (Sheng et al. 1995). Depletion of sterols within the cell is sensed by the SCAP component of the SREBP pathway via its sterol sensing domain and this leads to dissociation of the SCAP-SREBP2 complex from the ER-retention protein INSIG (Adams et al. 2003; Brown et al. 2002b). The two proteases required for the release of the active SREBP2 transcription factor domain from the inactive precursor protein reside in the Golgi (Duncan et al. 1997a; Duncan et al. 1998). The

SCAP-SREBP complex is transported from the ER to the Golgi via COPII vesicles facilitated by the interaction of scaffolding proteins with SCAP (Espenshade et al. 2002). The result is a global increase in SREBP2 target gene expression (primarily, but not limited to, genes of cholesterol pathways) to restore the cholesterol balance within the cell (Horton et al. 2002b; Amemiya-kudo et al. 2002; Sakakura et al. 2001). The therapeutic benefit of statins takes advantage of this induction of the SREBP pathway as the LDLR is one of these target genes. Increased levels of LDLRs on the cell surface increases LDL-cholesterol uptake and clearance from the circulation (Law et al. 2002; Goldstein et al. 1979). Once taken into hepatocytes, excess cellular cholesterol is converted into bile acids or excreted as free cholesterol. The rate limiting step of bile acid synthesis, cholesterol 7-alpha-hydroxylase (CYP7A1), is induced under high levels of cholesterol and this enzyme oxidises cholesterol for the production of primary bile acids (Li et al. 1990; Russell 2003). The latter are then secreted into the intestinal lumen, conjugated to form bile salts, which cannot be re-adsorbed from the intestine, and they function to emulsify fats to facilitate their excretion (Solaas et al. 2000). Together bile acid formation and function act to eliminate cholesterol and fats from the body. Excess cholesterol can also be excreted by its conversion to a less absorbed form in the intestine, coprostanol, prior to hepatocellular uptake (Kruit et al. 2005; Gérard et al. 2004). Gut microbial populations produce a cholesterol reductase enzyme which converts cholesterol to coprostanol (Ren et al. 1996; Wilson 1961).

HMGCR itself is also induced in response to statin treatment (Kita et al. 1980) . The doses of statins given to patients in the treatment of hypercholesterolemia (average 40 mg/day) is sufficient to inhibit HMGCR sufficiently to limit mevalonate availability and trigger the cholesterol depletion feed-forward response to increase

cell surface LDLR expression (Law et al. 2002). However, the statin-mediated inhibition of HMGCR does not outweigh the new HMGCR being produced, thus allowing cell viability to be maintained. In fact this property that statins increase all SREBP2 target genes is widely used in biochemical and molecular biological studies of the HMGCR protein and its regulation (Sever et al. 2003b). Cells cultured in the absence of cholesterol in the presence of a high concentration of statin (most often compactin) significantly increases expression of all SREBP target genes above basal levels. This greatly improves the detection and study capacity of both the SREBP and mevalonate pathways. However to achieve this amplification with high concentrations of statin cell viability is only maintained with the inclusion of exogenous mevalonate in the medium (Sever et al. 2003b).

In recent years, there have been a growing number of investigations regarding the chemotherapeutic potential of statins (Sleijfer et al. 2005). Treatment with statins has been shown to induce growth arrest and apoptosis in a variety of cancer cell lines. Statins, including atorvastatin and simvastatin have been shown to induce apoptosis in myeloma cell lines in a caspase-dependent manner (Caffario et al. 2005). Recently it was shown that sensitivity of acute myeloid leukaemia (AML) cell lines to lovastatin induced apoptosis was linked to a deregulated SREBP feed-forward response to the statin treatment (Clendening, Aleksandra Pandyra, et al. 2010). AML cell lines which were insensitive to statin induced apoptosis retained the ability to increase SREBP target genes, including HMGCR. This study also showed that primary cells from patients with multiple myeloma expressing a lower level of HMGCR were more sensitive to lovastatin and atorvastatin induced apoptosis than cells with higher HMGCR expression (Clendening, Aleksandra Pandyra, et al. 2010). Mevastatin has been shown to induce apoptosis in colorectal carcinoma cell

lines (Wächtershäuser et al. 2001). Lovastatin, mevastatin and simvastatin have all been shown to induce apoptosis in melanoma cell lines, as well as having inhibitory effects on the migration and invasion of these cancer cells (Glynn et al. 2008).

Prostate cancers have been shown to have high cholesterol content, and a loss of cholesterol feedback inhibition of the SREBP pathway has been shown for prostate tumours (Pelton et al. 2012; Hager et al. 2006b; Ettinger et al. 2004a; Chen & Hughes-Fulford 2001). SREBP-2 has also been implicated as a key transcription factor required for elevated cholesterol in prostate cancer tissues (Ettinger et al. 2004a). An androgen-mediated increase in key lipogenic genes, including fatty acid synthase (FASN) and HMGCR, has also been reported (Huang et al. 2012). SCAP has also been shown to contain an androgen response element within intron 8 and is increased in response to androgen treatments (Heemers et al. 2004). Mevastatin and simvastatin have been shown to decrease androgen sensitivity and cell proliferation in androgen receptor (AR)-positive prostate cancer cells, but not in AR-negative cells (Yokomizo et al. 2011). This decrease in proliferation was linked to statin-induced proteolysis of the AR protein, which in turn reduced SREBP pathway activation in these cells.

Tumours of simvastatin treated mice have been shown to have increased levels of apoptosis compared to untreated control mice, as measured by immune-histochemical staining of mammary tumour sections for cleaved caspase-3 (Campbell et al. 2006). Simvastatin also has demonstrated anti-proliferative effects on human glioma cells which was rescuable by mevalonate in a dose dependent manner, and thus attributable to inhibition of HMGCR (Kikuchi et al. 1997). Interestingly, in this study they also took advantage of statin induced up-regulation

of LDLR. They found an additive cytotoxic effect between simvastatin and a peroxidised LDL molecule when they were directly injected into a mouse model of glioma.

However, it has also been reported that lovastatin induced G1 arrest in an epithelial cell line, independent of HMGCR inhibition, through inhibition of the proteasome and accumulation of cyclin-dependent kinase inhibitors (CKIs) p27 and p21 (Rao et al. 1999). They attributed this proteasome inhibition effect to the β-lactone ring of the lovastatin pro-drug, although they did show that mevalonate reversed this action.

The SREBP and mevalonate pathways have also demonstrated links to cancer cell survival and progression. Studies have demonstrated the over-expression of the HMGCR catalytic domain of was sufficient to enhance the cancer phenotype of MCF-7 cells, and to induce transformation of their non-malignant counterparts, MCF-10A (Clendening, Aleks Pandyra, et al. 2010). There is also a correlation between high mRNA levels of HMGCR and other cholesterol biosynthetic genes with poor prognosis for breast cancer patients (Clendening, Aleks Pandyra, et al. 2010). Elevated levels of cholesterol synthesis and mevalonate pathway gene expression have also been detected in brain and prostate cancers (Rudling et al. 1990; Hager et al. 2006b). A deregulation of SREBP-mediated feedback regulation of mevalonate pathway gene expression has also been reported for a subset of prostate cancers (Chen & Hughes-Fulford 2001). HMGCR has therefore been proposed as a metabolic oncogene, which would fit within one of the emerging hallmarks of cancer, namely reprogramming of cellular energy metabolism in order to support continuous cell growth and proliferation (Hanahan & Weinberg 2011). Taken together, these findings make HMGCR an attractive chemotherapeutic target.

However, the statin concentrations required to achieve statin induced cell death *in vitro* are in the mid to high micro-molar range. The highest serum concentration of statin recorded from the recommended 40 mg/day dosage is in the nano-molar range (Chan et al. 2003; Solomon & Freeman 2008; Wong et al. 2002). When it comes to translating *in vitro* experiments to a clinical setting, many are sceptical as to whether the doses required to achieve cancer cell death may not be achievable *in vivo* (Bonetti et al. 2003). Achieving high serum concentrations of statins would be necessary for use of statins as chemotherapeutic agents, as low concentrations may simply act to increase SREBP pathway activity, and this would only prove advantageous to the disease. Also, high dose-regimes of statins in the treatment of hypercholesterolemia have been documented to have adverse effects on the body, including liver damage and myopathy (Needham & Mastaglia 2014; Wilkinson et al. 2014). While the mechanism surrounding myopathy phenotype remains unclear, it is believed to be linked to apoptosis induced by statin treatment in the muscle (Needham & Mastaglia 2014). Another proposed mechanism for statin associated myopathy is that inhibition of farnesylpyrophosphate synthesis reduces ubiquinone (Coenzyme $Q_{10}$) production which is required for mitochondrial function and energy production. The role of mitochondrial dysfunction in statin associated myopathy has not been conclusively shown, but clinical trials are underway investigating the effects of ubiquinone supplementation on statin associated myopathy (Parker, Gregory, et al. 2013). These distal effects from statin treatment suggest that effects beyond the liver can be realised. If the primary aim of the statin treatment was not to target increase LDL-cholesterol clearance, then perhaps the drug could be modified in a way that allowed direct injection to the region of the cancer, circumventing liver clearance or to be specifically targeted to the tumour in some way. A possibility may

be to exploit the property that certain anaerobic bacteria migrate specifically to hypoxic tumour sites following oral administration (Cronin et al. 2010). Thus, lowering the effective chemotherapeutic concentrations of statins would be highly desirable.

In spite of these reservations, there are ongoing clinical trials in which statins are being investigated in the treatment of a variety of cancers. Trials underway where statins are being investigated as the primary chemotherapeutic agent include in the treatment of multiple myeloma, breast cancer, non-Hodgkin's lymphoma and chronic lymphocytic leukaemia respectively (Chapter 1; Table 1.4). There are also multiple trials, both underway and completed, investigating the effects of statins on cancer incidence and effects on other approved cancer therapies (Chapter 1; Tables 1.2 and 1.3). The advantage of developing statins as an anti-cancer agent is that the pharmacokinetic and pharmacodynamic properties of the drug are already known, and they have already passed FDA approval for use as a human therapeutic, which means the approved doses are safe and give minimal side effects overall. If the effective chemotherapeutic concentration of statin could be lowered to ranges currently used clinically, then this would be considered a safe effective dose with no global adverse effects.

The hypothesis relating to the statin based research in this chapter is that preventing the SREBP-mediated activation of cholesterogenic genes that occurs upon statin treatment would reduce the level of the HMGCR gene and protein expression and thus reduce the effective statin concentration required to induce cancer cell apoptosis via mevalonate starvation and consequently improve the chemotherapeutic potential of the statins.

As described earlier, SREBPs are synthesised as inactive precursor proteins and release of the active transcription factor domain is regulated by sterols (Hua et al. 1993b; Wang et al. 1994). Apart from cholesterol, there are many other known regulators of SREBP activation, many of which are dietary in origin. These include oxysterols and poly unsaturated fatty acids (PUFAs) (Radhakrishnan et al. 2007b; Lee et al. 2008; Xu et al. 1999). Modulation of the SREBP pathway is of critical importance to several disease areas including hypercholesterolemia, atherosclerosis and liver disease (Tang et al. 2011; Miserez et al. 2002; Horton et al. 2002b). Thus, the mechanisms of how these dietary oxysterols and PUFAs regulate SREBP activation is quite well characterised. Oxysterols, such as 25-OHC, have been shown to bind the ER-retention protein, INSIG, and stabilise it through blocking its ubiquitination (Gong, Lee, Lee, et al. 2006b; Radhakrishnan et al. 2007b). This results in INSIG binding to SCAP and inhibiting the delivery of the SCAP-SREBP complex to the Golgi for proteolytic processing (Espenshade et al. 2002). Oxysterols also have a direct effect on stimulating degradation of HMGCR. This is also achieved through their binding of INSIG1 (Jo et al. 2011). It is believed that PUFAs inhibit SREBP cleavage in a similar manner, except that they act following the ubiquitination stage of INSIG. Following ubiquitination, INSIG requires removal from the ER membrane in order to be degraded by the proteasome, and PUFAs are reported to block this extraction (Lee et al. 2008). Due to the dietary nature of oxysterols and PUFAs they are known to be tolerated well at low doses and do not exhibit adverse effects on the body (Otaegui-Arrazola et al. 2010). Statin-mediated inhibition of HMGCR triggers the cholesterol depletion feed-forward response via SREBP (Sheng et al. 1995). The negative regulation of SREBP activation by

oxysterols and PUFAs, combined with them being present in the everyday diet, make them ideal candidates to investigate to enhance statin induced cell killing.

This chapter describes: a) The response of the cell line HeLa-PHGL to statin induced cytotoxicity under FS and LDS culture conditions with respect to SREBP2 and HMGCR, b) How the inhibition of SREBP processing enhances the cytotoxic effects of statin in HeLa-PHGL through limiting HMGCR expression, and c) The statin induced cytotoxic response in a panel of cancer cell lines under FS and LDS conditions. The enhancing effects of SREBP inhibition on statin-associated cytotoxicity are also presented for a subset of the cell line panel. The data presented in this chapter indicate that prevention of SREBP processing is a viable method for enhancing the cytotoxic effects of statins in a sub-set of cancer cell lines.

The data also highlight a number of key points for consideration for the potential use of statins in the treatment of cancer, including: a) the effects of lipid-depletion on the cytotoxic effects of statins, b) that deregulation of the sterol-SREBP negative feedback loop was observed in half of the cancer cell lines screened, and c) that high concentrations of statins are likely to induce cell death outside of inhibiting HMGCR catalytic activity.

## Results

### *Lipid depletion increases HeLa-PHGL cell resistance to statin-mediated cell killing*

Inhibition of HMGCR catalytic activity by statins depletes the cellular pool of mevalonate, thus limiting essential isoprenoid and cholesterol availability. To maintain cell viability the cell compensates by increasing SREBP2 target gene expression including HMGCR. Culturing cells in the presence of LDS is a well documented method to amplify mevalonate pathway activity through promoting SREBP processing in response to low lipid availability. A main question addressed in this work was to determine if altering the lipid availability to HeLa cells in culture would influence their response to statin-mediated cell death. HeLa-PHGL is a cell line which stably expresses the HMGCR promoter fused to a secreted *Gaussia* luciferase gene (Chapter 4) was used here, and is used for all subsequent investigations in HeLa within this chapter. This luciferase gene reporter assay serves as an accurate readout for SREBP activation. HeLa-PHGL cells were seeded in medium containing 10% FBS on day 1. The following day, cells were switched to fresh medium containing either 10% FBS (FS) or 10% LDS (LDS) supplemented with increasing concentrations of Simvastatin. HeLa-PHGL cells cultured in FS have a simvastatin $ED_{50}$ of 2µM (Figure 6.1A). HeLa-PHGL cells cultured in LDS have a much higher simvastatin $ED_{50}$ of 25µM (Figure 6.1C). The results indicate that HeLa-PHGL cells display an increased resistance to simvastatin induced cytotoxicity under LDS culture conditions. Two-way ANOVA analysis of the simvastatin dose response curves under FS and LDS conditions indicated that there was a statistically significant difference between FS and LDS conditions (Figure 6.1A; p=1.45E-42). Simvastatin is a naturally occurring statin. Statins differ in their molecular structure

and effectiveness, and thus comparison was carried out with a synthetic statin, Atorvastatin. HeLa-PHGL cells cultured under LDS conditions and in the presence of increasing atorvastatin concentrations displayed a similar resistance to statin mediated cytotoxicity. HeLa-PHGL cells cultured in FS have an atorvastatin $ED_{50}$ of 7µM (Figure 6.1B). HeLa-PHGL cells cultured in LDS have a much higher atorvastatin $ED_{50}$ of 30µM (Figure 6.1C). Two-way ANOVA analysis indicated that the difference in atorvastatin dose-response curves were statistically significant in FS and LDS conditions (Figure 6.1B; p=1E-18). Overall, the concentrations of statin required to kill half of the cells were higher for both simvastatin and atorvastatin in cells cultured in LDS compared to those cultured in FS. The ED50 for simvastatin was 12.5-fold higher in LDS compared to FS. Similarly, the ED50 for atorvastatin was 4.3-fold higher in LDS compared to FS.

To investigate if the resistance seen under LDS was due to a SREBP-mediated increase in HMGCR expression, secreted luciferase enzyme activity was assayed in HeLa-PHGL cells cultured in both FS and LDS conditions. Cells cultured in FS displayed a significant increase in HMGCR reporter readout in response to low doses of statin over control cells with zero statin added with a maximal and significant increase of 2 and 1.7 fold being observed with 1.5µM simvastatin (p=0.009) and 4 µM atorvastatin (p =0.014), respectively (Figure 6.2A and 6.2B). Cells cultured in LDS exhibited a greater response than cells cultured in FS with a maximum 2.6-fold increase in HMGCR reporter readout at 2µM simvastatin (p=1.8E-04) and 2.3-fold increase at 4µM atorvastatin (p-value=1.50E-04) (Figure 6.2A and 6.2B). The statin-resistant phenotype of HeLa-PHGL cells in LDS conditions is linked to the larger fold-increase in HMGCR promoter activity compared to FS conditions.

Cell death induced by statins is likely to result from limiting the availability of the HMGCR product, mevalonate. If this is the case then addition of exogenous mevalonate to the cells grown in FS culture should confer resistance to cells under these conditions to the same extent (or higher) than when the cells are grown in LDS. Figure 6.3A shows that this indeed is the case, with mevalonate conferring statin resistance on the cells grown in FS (Figure 6.3A). Mevalonate also has the capacity to rescue statin-mediated cell death for cells cultured under LDS conditions (Figure 6.3B). However, unlike in FS conditions, 50µM mevalonate fails to completely rescue cytotoxicity at simvastatin concentrations higher than 40 µM. A concentration of 70 µM simvastatin is required to achieve a 100% decrease in cell viability in LDS, and the presence of 50 µM mevalonate increases cell viability to 50% ($p=1.46E-04$). Increasing mevalonate to 100µM slightly improved on the rescue observed at 50 µM and 60 µM simvastatin, but again failed to completely rescue the cytotoxic effects of simvastatin. In the presence of 70 µM simvastatin, 100 µM mevalonate fails to increase cell viability above 60% ($p=7.37E-05$). Concentrations of mevalonate higher than 100 µM were not used in these studies as it has previously been shown that high concentrations of mevalonate negatively affect the activity of HMGCR through increasing degradation of the HMGCR protein and decreasing translation of HMGCR mRNA. This lack of complete rescue of simvastatin induced cytotoxicity suggests that the cytotoxicity occurring at high statin concentrations is likely to be due to additional mechanism(s) outside of HMGCR inhibition.

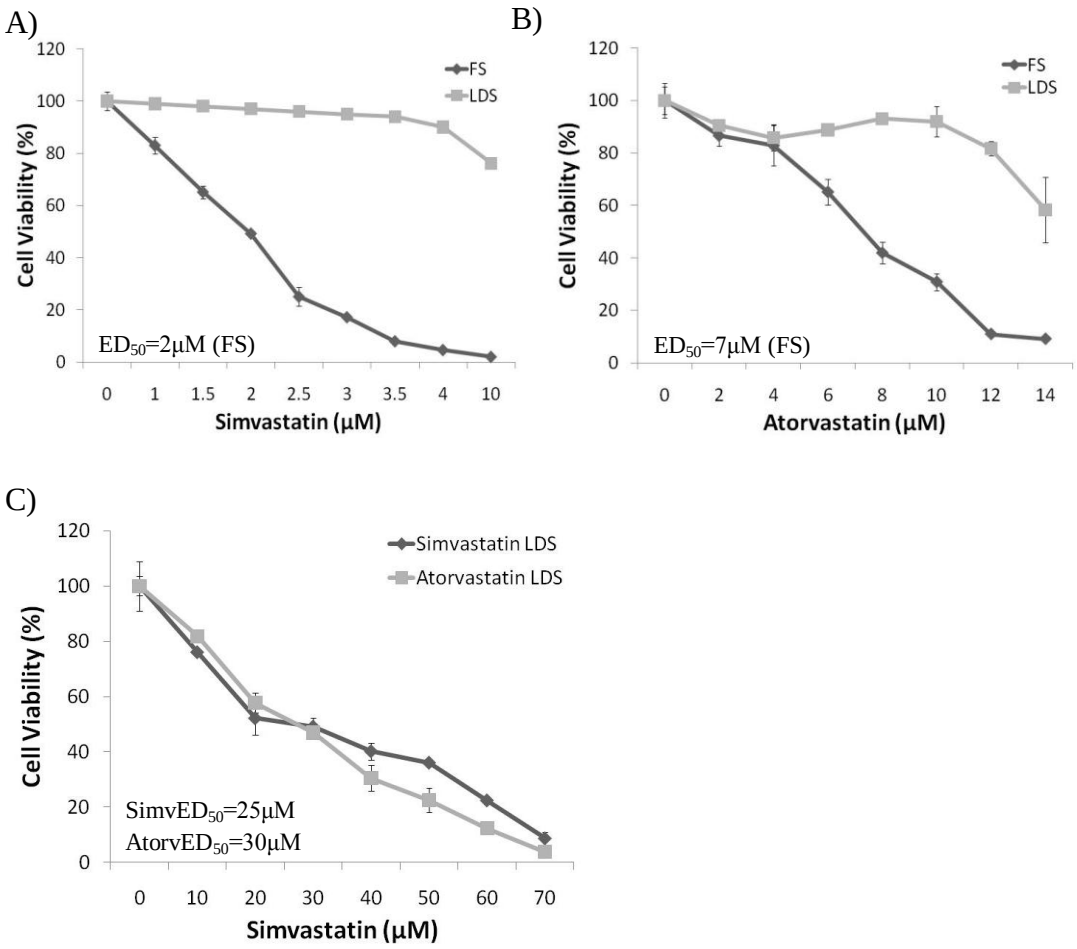


Figure 6.1. HeLa-PHGL cells display an increased resistance to statin-mediated cell death in LDS versus FS culture conditions. HeLa-PHGL cells were treated with increasing concentrations of either (A) Simvastatin or (B) Atorvastatin under FS or (C) LDS conditions. . (D) The $ED_{50}$ values for Simvastatin and Atorvastatin were calculated using the Excel plug-in ED50 plus v1.0. Experiments were performed in triplicate and error bars represent ± SD. Significance of statin resistance in FS versus LDS was compared for simvastatin ($p<0.05$) and atorvastatin ($p<0.05$ ) using two-way ANOVA.

A)

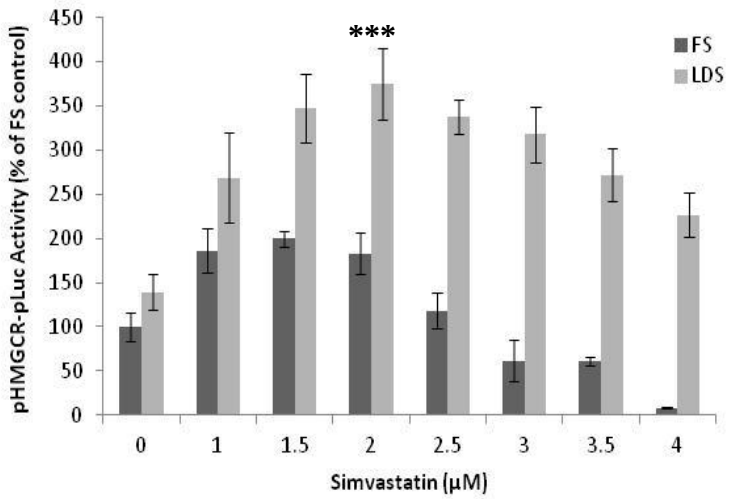


B)

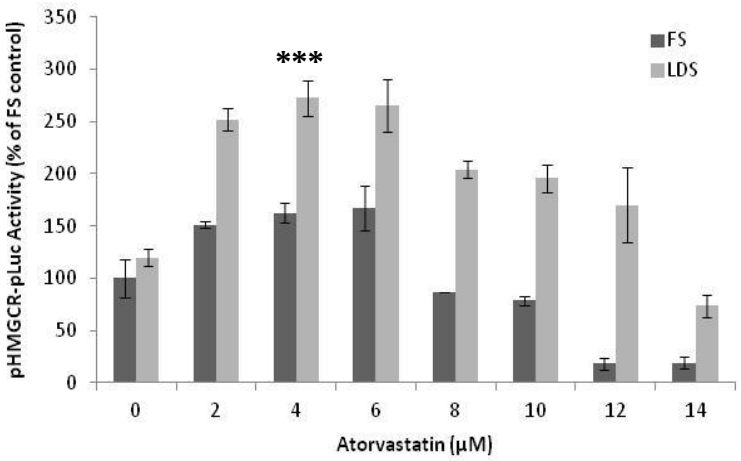


Figure 6.2. SREBP luciferase reporter expression in response to statin treatment. HeLa-PHGL cells were cultured in the presence of increasing concentrations of either (A) Simvastatin or (B) Atorvastatin in both FS and LDS conditions. Following a 48 hour incubation period, media samples were assayed for luciferase activity. Experiments were performed in triplicate and error bars represent ± SD. Significance of the maximum point reporter increase was measured using Student's t-Test ($p<0.05$).

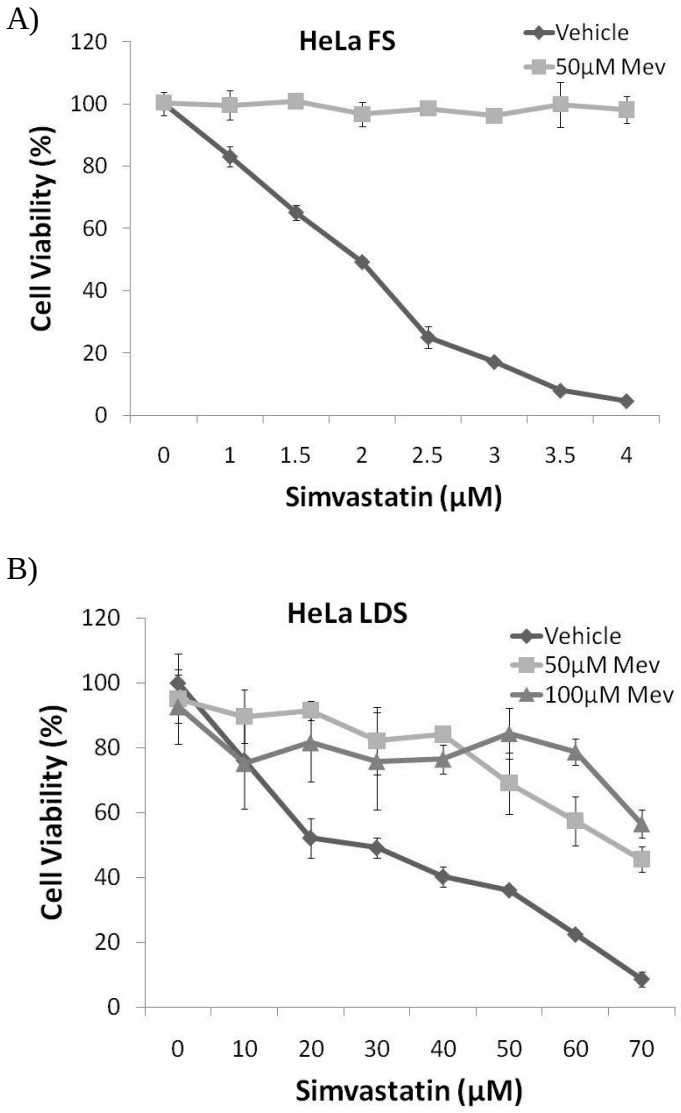


Figure 6.3. Mevalonate rescues statin induced cell death under both FS and LDS conditions. HeLa-PHGL cells were cultured in the presence of increasing concentrations of Simvastatin under either (A) FS or (B) LDS conditions, in the absence or presence of mevalonate at the indicated concentrations. Experiments were performed in triplicate and error bars represent ± SD. Significance of mevalonate rescue was measured using Student's t-Test ($p<0.05$).

***Inhibition of the SREBP pathway enhances statin sensitivity in HeLa-PHGL cells***

Culturing cells under LDS conditions confers a resistance to statin-mediated cell death in HeLa-PHGL cells, and the data shown indicate that the mechanism underlying this relates to a SREBP-mediated increase in HMGCR expression. Thus, in the absence of this feed-forward SREBP mediated increase in HMGCR, the sensitivity of the cells to statin mediated cytotoxicity would be expected to increase. To investigate this possibility, a panel of known inhibitors of the SREBP pathway were first screened to identify the most potent as measured by reducing HMGCR reporter expression and the effect of such inhibitors on statin mediated cytotoxicity was evaluated. The compounds screened were 25-OHC, cholesterol and also a more recently identified regulator of SREBP activation called betulin. Betulin is a naturally occurring compound derived from birch bark, and has been shown to negatively regulate SREBP by promoting binding of INSIG by SCAP. 19-OHC was used as a negative control oxysterol as it has been reported that 19-OHC does not to bind SCAP or INSIG, and does not affect SREBP cleavage. 19-OHC has been used in previous studies as a suitable control for SREBP feedback inhibition studies. The stable HeLa-PHGL cell line was treated with increasing concentrations of each inhibitory compound. The maximal repression of HMGCR promoter activity was achieved using 25-OHC at 1 µg/ml and cholesterol at 10 µg/ml under LDS conditions (5-fold and 5.5-fold, respectively) (Figure 6.4A and 6.4B). Betulin was less effective at reducing HMGCR promoter readout, with a maximum decrease of 1.8-fold achieved in LDS prior to any cell death occurring (Figure 6.4C). No significant decrease in luciferase reporter readout was observed for betulin under FS conditions at non toxic concentrations. Unexpectedly, these dose-response screens yielded surprising results for 19-OHC. This oxysterol was included as a negative

control but the results indicate that 19-OHC displays a dose-dependent regulation of the HMGCR promoter at higher concentrations (Figure 6.4D). A concentration of 1 µg/ml 19-OHC resulted in a 1.15 and 1.34-fold decrease in luciferase reporter readout under FS and LDS conditions, respectively. Based on these results, 25-OHC, cholesterol and betulin were brought forward to the next stage of experiments. 19-OHC was also brought forward with a view to identifying if this oxysterol was indeed having an effect on SREBP activation and that the results observed here were not due to some regulatory effect outside of SREBP activation.

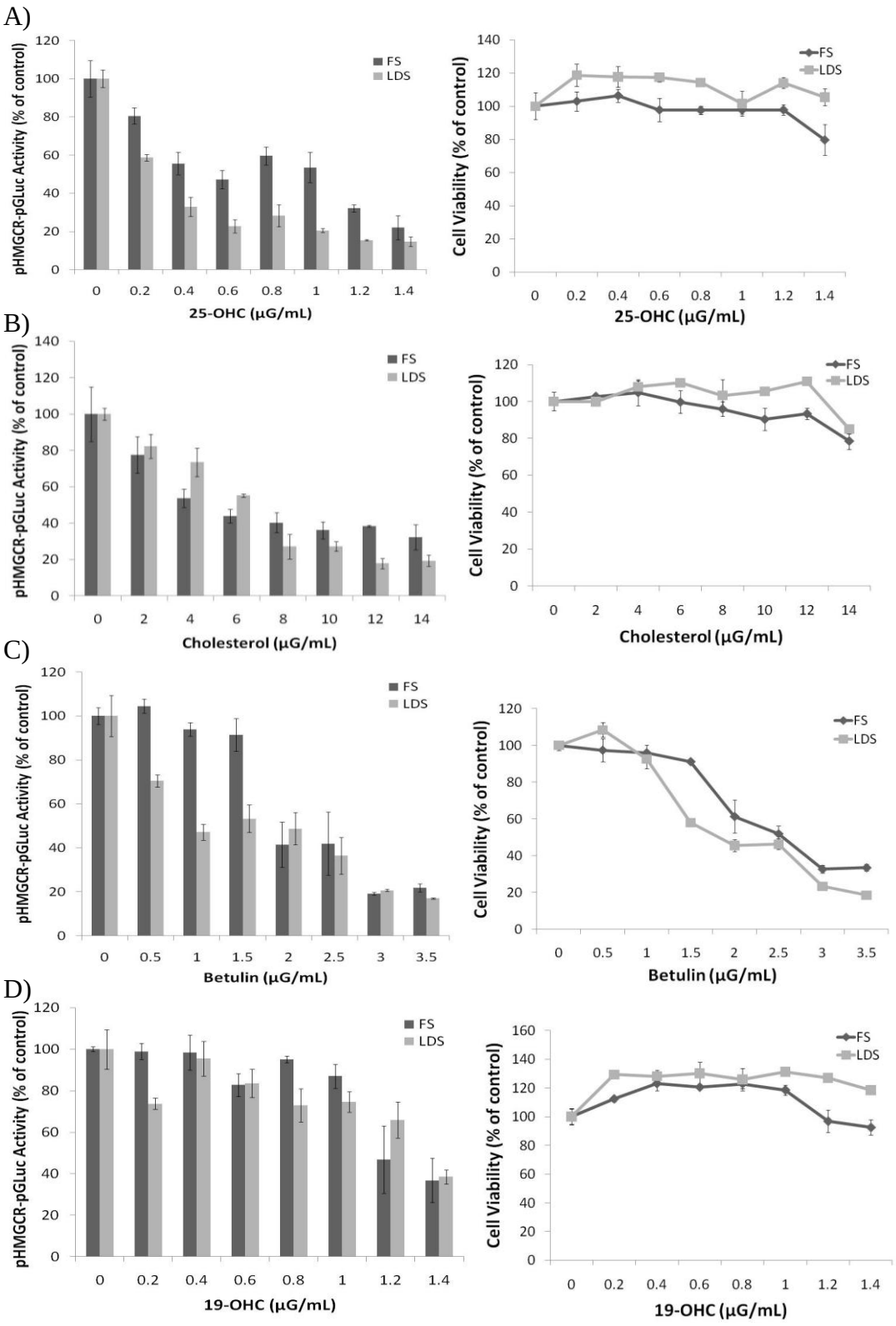


Figure 6.4. Inhibitors of SREBP processing. Increasing concentrations of a panel of SREBP processing inhibitors were incubated with the HeLa-PHGL cell line and secreted luciferase activity was measured 48 hours after addition of 25-OHC, Cholesterol, Betulin or 19-OHC. Cell viability was measured for the same experiments using the MTT assay. All sterols, with the exception of cholesterol, were prepared in EtOH. Cholesterol was prepared in MβCD as described in methods.

To investigate the hypothesis that blocking the induction of SREBP activity would increase the sensitivity of HeLa-PHGL cells to statin induced cytotoxicity, cells were cultured in the presence or absence of an SREBP inhibitor, in the presence of increasing concentrations of statin. The inhibitor chosen was 25-OHC as this was deemed the most potent with respect to inhibition of SREBP activation (Figure 6.4). ED 50s were calculated for HeLa-PHGL cells for simvastatin and atorvastatin in the absence and presence of 1μg/ml 25-OHC (Figure 6.5 and Table 6.1). The presence of 25-OHC reduced the ED50 for cells grown in FS treated with simvastatin from 2.5 μM to 1.5 μM (Figure 6.5A) and reduced the ED50 for cells grown in LDS treated with simvastatin from 25 μM to 2 μM (Figure 6.5B). Similarly, the presence of 25-OHC reduced the ED50 for cells grown in FS treated with atorvastatin from 7 μM to 3 μM (Figure 6.5C) and reduced the ED50 for cells grown in LDS treated with atorvastatin from 30 μM to 3 μM (Figure 6.5D). Thus the presence of 25-OHC significantly improved the cytotoxic effect of both statins under FS and LDS culture conditions, and for both statins the maximum enhancing effect of 25-OHC was observed for statin-treated cells cultured under LDS conditions.

Addition of exogenous mevalonate (50 μM) rescued cells from the enhancing effect of the 25-OHC on simvastatin treated cells (Figure 6.5E) Mevalonate rescue was considered to be similar for atorvastatin and as such, mevalonate rescue of cells treated with atorvastatin and 25OHC was not performed. Mevalonate rescue restored HeLa-PHGL cell viability in cells treated with simvastatin and 25-OHC to within the range of simvastatin alone treated cells. The presence of 1 μg/ml 25-OHC is sufficient to reduce SREBP luciferase reporter readout approximately 5-fold (Figure 6.4A). The ability of mevalonate to rescue cell cytotoxicity in the presence of simvastatin plus 25-OHC indicates that the basal level of SREBP pathway activity

which remains in the presence of 25-OHC permits sufficient expression of cholesterogenic genes to utilise this exogenous mevalonate to produce essential isoprenoids and sterols required to maintain cell viability.

Betulin significantly inhibited SREBP readout in the initial screen (Figure 6.4C) and therefore was also investigated for its effectiveness in enhancing simvastatin cytotoxicity. Incubation of HeLa-PHGL cells with simvastatin in the presence of betulin under LDS conditions reduced the $ED_{50}$ 1.4 fold compared to cells treated with simvastatin alone (Figure 6.6). Betulin was less effective than 25-OHC at reducing the $ED_{50}$ of simvastatin-mediated cytotoxicity for cells cultured in LDS, only reducing the $ED_{50}$ from 35 µM to 25 µM (Figure 6.6). This is consistent with betulin having less effect on SREBP processing, as measured by luciferase reporter readout compared to that achieved with 25-OHC (Figure 6.4A vs. 6.4C). The presence of betulin was sufficient to significantly improve the cytotoxicity induced by simvastatin overall compared to HeLa-PHGL cells treated with simvastatin alone, as measured by two-way ANOVA (p=1.78E-11).

Cholesterol also significantly inhibited SREBP readout in the initial screen (Figure 6.4B) and therefore was investigated for its effectiveness in enhancing simvastatin cytotoxicity. Co-incubation of cholesterol with simvastatin decreased the statin $ED_{50}$ from 25 µM to 1.25 µM (Figure 6.7A). The presence of cholesterol significantly improved the cytotoxicity induced by simvastatin overall compared to HeLa-PHGL cells treated with simvastatin alone, as measured by two-way ANOVA (p=9.28E-18).While this finding is consistent with the hypothesis, 25-OHC did not behave as expected in this experiment (Figure 6.7A). This can be explained by the following: unlike 25-OHC, cholesterol requires transport across the plasma membrane, and

methyl-β-cyclodextrin (MβCD) is a commonly used vehicle. Therefore, cholesterol was prepared as a sterol-MβCD complex and 25-OHC was prepared in the same way as a positive control, as described under materials and methods. Measurement of SREBP/HMGCR luciferase reporter activity in response to each sterol with or without MβCD indicated that 25-OHC/MβCD was less effective at lowering SREBP reporter readout below that of the vehicle treated control compared to 25-OHC alone (Figure 6.7B). However, the data indicate that this decreased effect of 25-OHC is due to the presence of MβCD alone causing a 2-fold increase in SREBP reporter readout compared to vehicle treated control. The 25-OHC/MβCD complexes do significantly reduce SREBP reporter activity below that of MβCD alone (Figure 6.7B). Cholesterol/ MβCD is capable of reducing SREBP reporter readout below the levels of vehicle treated control, despite the increase caused by MβCD. Thus cholesterol is potentially a stronger inhibitor of SREBP processing than 25-OHC. However, further experiments focused on 25-OHC as data interpretation is clearer and the effects of cholesterol may be confounded by the effects of MβCD.

19-OHC was also investigated for its effectiveness in enhancing the cytotoxicity of simvastatin. 19-OHC had less of an inhibitory effect on the SREBP luciferase reporter compared to 25-OHC (Figure 6.4A vs. 6.4D). However, this oxysterol was brought forward with a view to further characterising if 19-OHC was indeed have some regulatory effect on the SREBP pathway. Interestingly, co-treatment of HeLa-PHGL cells with simvastatin and 19-OHC in LDS yielded a similar enhancement of statin mediated cytotoxicity to that observed with simvastatin and 25-OHC co-treatment. Incubation of HeLa-PHGL cells with simvastatin in the presence of 19-OHC reduced the simvastatin $ED_{50}$ in LDS to 3 μM compared to that of 25 μM for simvastatin alone (Figure 6.8). 19-OHC significantly improved the cytotoxicity

induced by simvastatin overall compared to HeLa-PHGL cells treated with simvastatin alone, as measured by two-way ANOVA (p=1E-14). The concentration of 19-OHC used here was 1 µg/mL. The SREBP luciferase reporter readout for the 19-OHC dose-response indicated that higher concentrations of 19-OHC may have been used (Figure 6.4D). The 1 µg/mL concentration of 19-OHC was chosen to match the concentration used for 25-OHC. 19-OHC has been used in previous studies as a negative control for 25-OHC. Using these two oxysterols at the same concentration would allow for direct comparison between the effects seen with 19-OHC to those seen with 25-OHC. The slightly reduced effect of 19-OHC compared to 25-OHC on enhancing simvastatin $ED_{50}$ in HeLa-PHGL cells cultured under LDS conditions is consistent with the reduced inhibitory effect of 19-OHC on SREBP processing compared to that achieved with the same concentration of 25-OHC (Figure 6.4A vs. 6.4D).

Table 6.1. Statin ED50 values for HeLa-PHGL cell line.

| $ED_{50}$ (µM) | | | | |
|---|---|---|---|---|
| | FS | FS+25-OHC | LDS | LDS+25-OHC |
| Simvastatin | 2.5 | 1.5 | 25 | 2 |
| Atorvastatin | 7 | 3 | 30 | 3 |

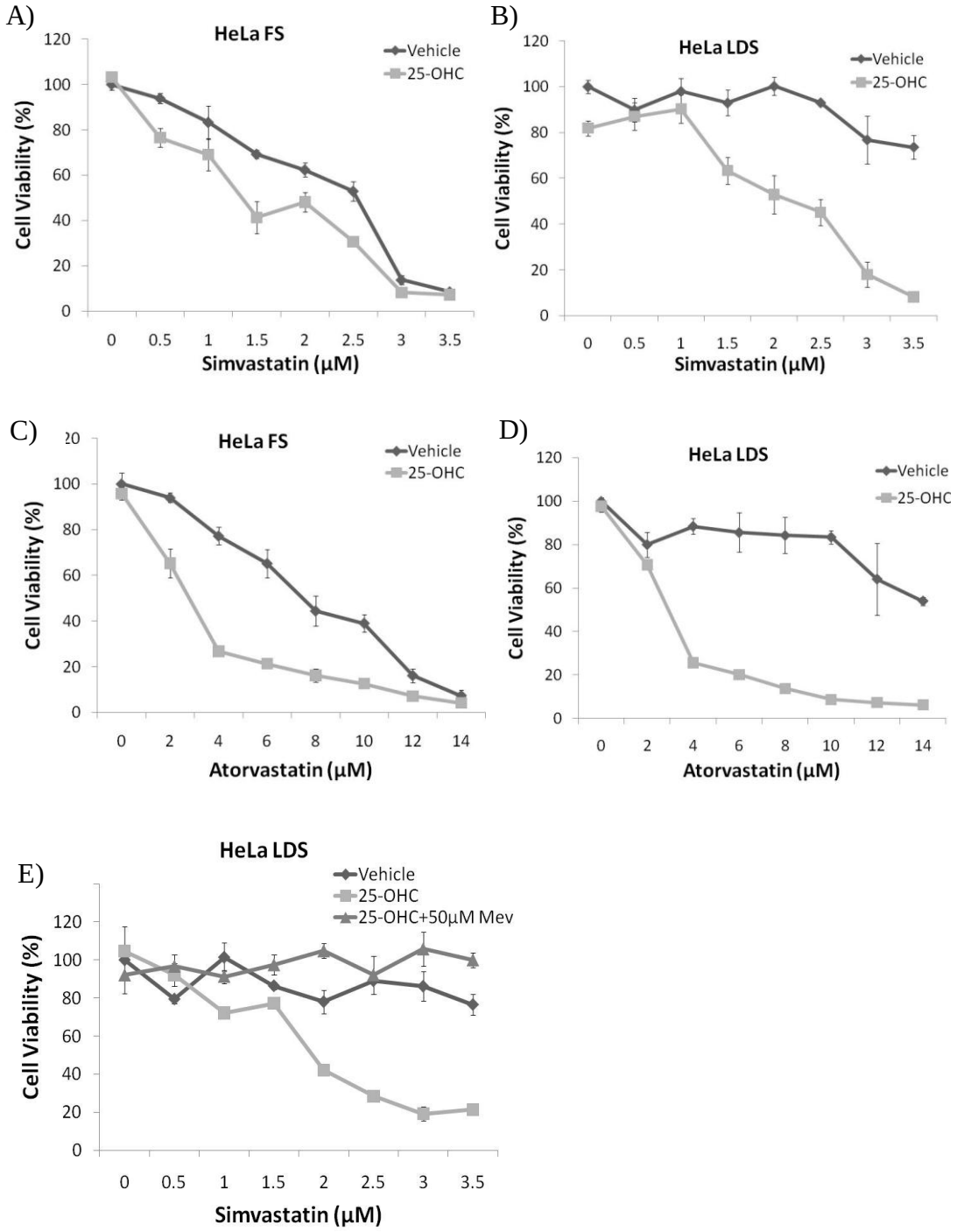


Figure 6.5. Inhibition of SREBP activity with 25-OHCenhances statin-induced cytotoxicity. HeLa-PHGL cells were incubated with increasing concentrations of either Simvastatin(A, B,) or Atorvastatin(C, D) under FS or LDS conditions, in the absence or presence of 25-OHC (1µg/ml) and cell viability was measured using the MTT assay E) Cells were incubated with increasing concentrations of simvastatin in the absence or presence of 25-OHC (1µg/ml) or 25-OHC (1µg/ml) plus mevalonate (50 µM). Experiments were performed in triplicate and error bars represent ± SD.

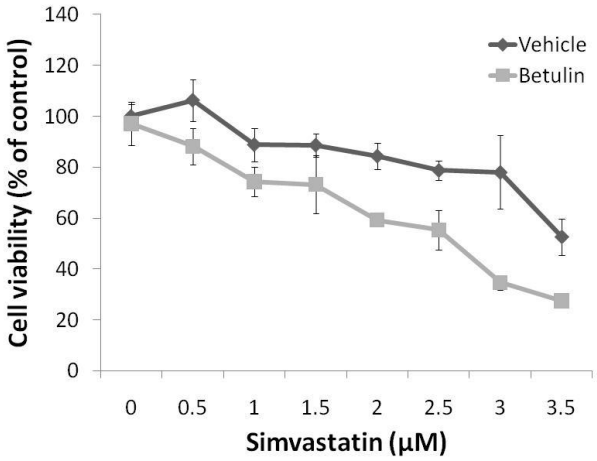


Figure 6.6. Inhibition of the SREBP pathway with betulin enhances statin-mediated cytotoxicity, HeLa-PHGL cells were incubated with increasing concentrations of simvastatin in the absence or presence of 1 µg/ml Betulin. Cell viability was measured using MTT assay. Experiments were performed in triplicate and error bars represent ± SD. Significance of enhancement of statin induced cytotoxicity was measured using two-way ANOVA ($p<0.05$).

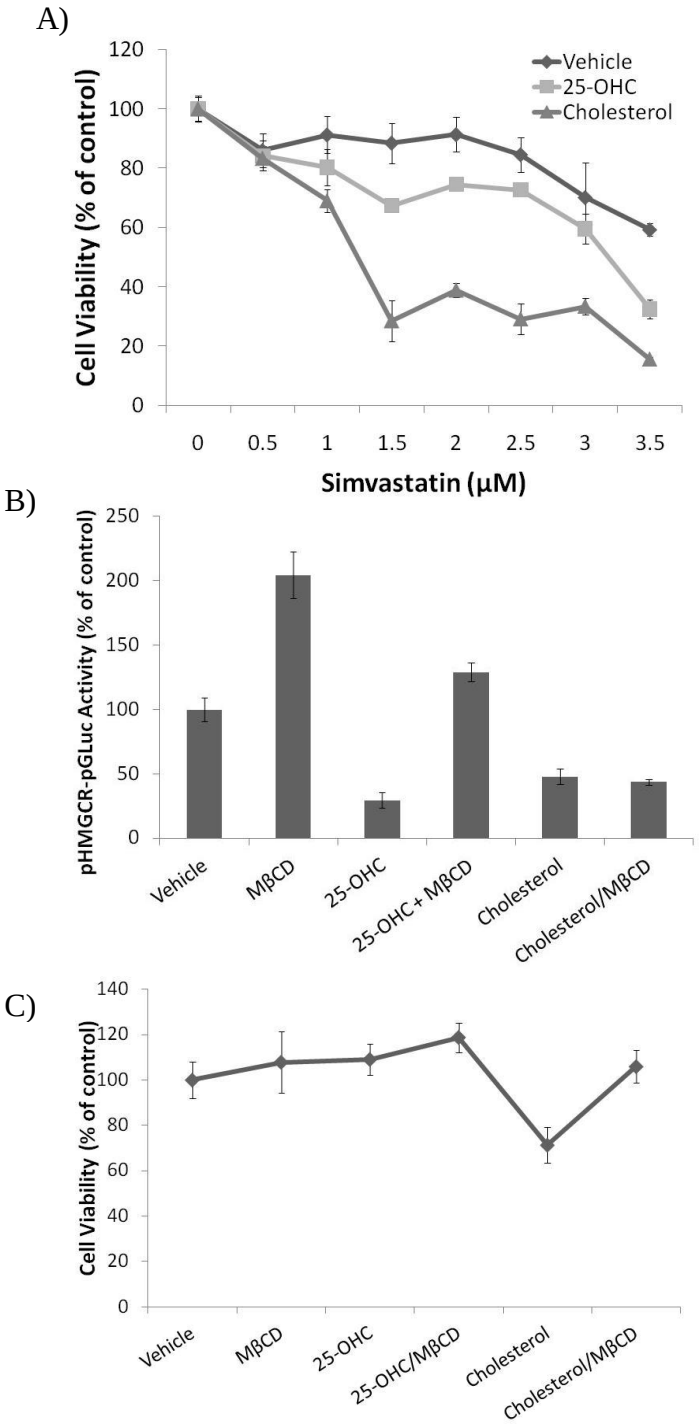


Figure 6.7. Cholesterol enhances statin-mediated cytotoxicity. (B)HeLa-PHGL cells were incubated with increasing concentrations of simvastatin in the absence or presence of 10 µg/ml cholesterol/ MβCD or 1 µg/ml 25-OHC/MβCD for 48 hours. Cell viability was measured using MTT assay (C) HeLa-PHGL cells were incubated with the indicated sterols either alone or complexed with MβCD (25-OHC(1 µg/ml); cholesterol (10 µg/ml)).(D) Cell viability in response to the indicated sterol alone or sterol/ MβCD complexes, measured using MTT assay. Experiments were performed in triplicate and error bars represent ± SD. Significance of enhancement of statin induced cytotoxicity was measured using two-way ANOVA ($p<0.05$).

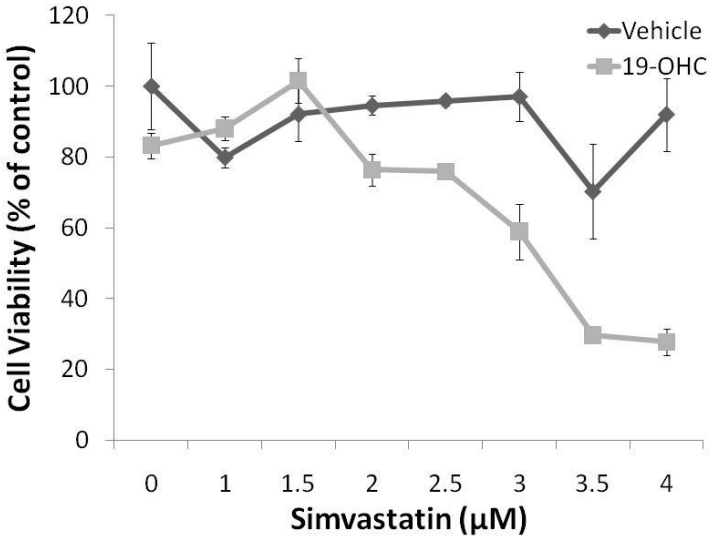


Figure 6.8. 19-OHC enhances statin-mediated cytotoxicity, HeLa-PHGL cells were incubated with increasing concentrations of simvastatin in the absence or presence of 1 µg/ml 19-OHC. Cell viability was measured using MTT assay. Experiments were performed in triplicate and error bars represent ± SD. Significance of enhancement of statin induced cytotoxicity was measured using two-way ANOVA ($p<0.05$).

***Inhibition of the SREBP pathway enhances statin sensitivity in HeLa-PHGL cells through preventing statin-mediated increases in nSREBP2 and HMGCR levels***

The previous results show that 25-OHC was the most effective agent of the panel tested at reducing the $ED_{50}$ for simvastatin. Therefore, 25-OHC was used extensively in subsequent experiments on statin cytotoxicity. 19-OHC was also further investigated with respect to its association with SREBP processing and enhancement of statin efficacy in reducing cell viability.

To further investigate that the oxysterols are enhancing statin-mediated cell death through blocking of SREBP mediated increases in HMGCR, the levels of HMGCR and SREBP2 proteins in HeLa-PHGL cells were analysed by immunoblot. Cells were cultured with simvastatin in the presence and absence of either 25-OHC or 19-OHC, in both FS and LDS culture conditions. Western blot analysis showed that cells cultured in the presence of simvastatin alone under FS conditions increased the levels of both HMGCR and nSREBP2 at the protein level (Figure 6.9, more sensitive exposure; lane 1 vs. 2). This increase in both HMGCR and nSREBP2 was completely blocked in the presence of simvastatin plus 25-OHC in FS (Figure 6.9, lane 2 vs. 3). The presence of 19-OHC (1μg/ml) did not significantly affect the levels of nSREBP2 produced in FS (Figure 6.9, SREBP2 more sensitive exposure; lane 2 vs. 4). This is consistent with the low inhibitory effect of 1μg/ml 19-OHC on the SREBP luciferase reporter (Figure 6.4D). Interestingly, the presence of 19-OHC completely blocked the statin-induced increase in HMGCR in FS (Figure 6.9, lane 2 vs. 4). This data suggests that 19-OHC is having a greater effect on HMGCR stability than on repressing nSREBP levels.

Similar results were observed for HeLa-PHGL cells cultured under LDS conditions. In the presence of simvastatin alone under LDS conditions, the levels of HMGCR

and nSREBP2 were both increased (Figure 6.9, lane 5 vs. 6). This increase in both HMGCR and nSREBP2 was completely blocked in the presence of simvastatin plus 25-OHC in FS (Figure 6.9, lane 6 vs. 7). The presence of 19-OHC (1μg/ml) did not significantly affect the levels of nSREBP2 produced in LDS (Figure 6.9, lane 6 vs. 8). This is consistent with the low inhibitory effect that 1μg/ml 19-OHC has on the SREBP luciferase reporter under LDS conditions also (Figure 6.4D). Consistent with the findings in FS, the presence of 19-OHC completely blocked the statin-induced increase in HMGCR in LDS (Figure 6.9, lane 6 vs. 8). This data further suggests that 19-OHC is having a greater effect on HMGCR stability than on repressing nSREBP2 levels.

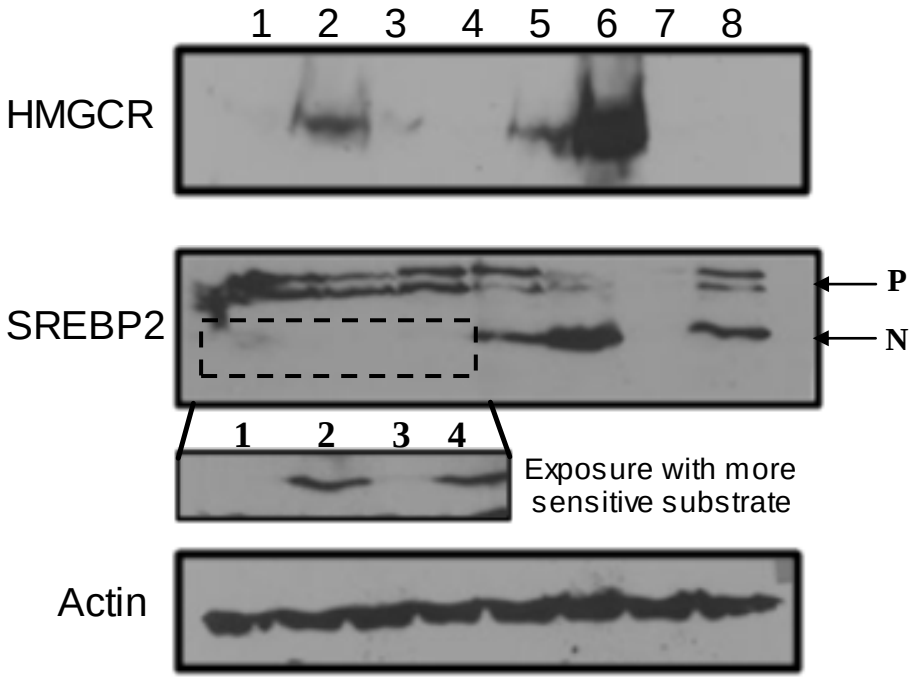


Figure 6.9. Western blot analysis of HMGCR and SREBP2 in HeLa-PHGL cells treated with simvastatin in the absence and presence of oxysterols. Cells were cultured for 24 hours with 0.5 µM simvastatin in FS or 10 µM simvastatin in LDS in the presence and absence of either 25-OHC (1 µg/ml) or 19-OHC (1 µg/ml). All culture conditions contained 50 µM mevalonate to maintain cell viability. Lanes: 1-4; FS, Lanes: 5-8; LDS. Lanes: 1 and 5; Vehicle, 2 and 6; Simvastatin, 3 and 7; Simvastatin+25-OHC, 4 and 8; Simvastatin+19-OHC. P= SREBP2 precursor protein, N= nSREBP2

***Over-expression of constitutively active nSREBP2 partially rescues cell death induced by combined statin and oxysterol treatment in HeLa-PHGL cells***

The results indicate that the oxysterol enhancement of statin mediated cytotoxicity is via repression of SREBP processing. If this is the case, the enhancement effect should be reversed if the activation domain of SREBP2 (nSREBP2) is supplied *in trans*. To test this, cells were transfected with nSREBP2 which is constitutively active and is not subject to the regulation of the SREBP precursor protein as it lacks the transmembrane and regulatory domains. Expression of the nSREBP2 in transfected cells was confirmed by immunoblotting in the presence and absence of 25-OHC (Figure 6.10A). Over-expression of nSREBP2 increases the SREBP luciferase reporter readout 1.42-fold (42% increase) compared to empty vector ($p=0.0285$) following a 48-hour incubation period (Figure 6.10B). The presence of 25-OHC results in a 3.35-fold decrease in luciferase reporter readout ($p=3.05E-04$). While over-expression of nSREBP2 fails to restore this 25-OHC mediated decrease in luciferase reporter activity back to control levels, it does restore it 1.85-fold which corresponds to 47% rescue, which is similar to the activation achieved by nSREBP2 in the absence of 25-OHC ($p=0.0066$) (Figure 6.10B). Another possible explanation for this limited rescue of nSREBP2 in the presence of 25-OHC possibly lies in the transient transfection of the over-expression plasmid. The HeLa-PHGL cell line was used and thus all cells contain the luciferase reporter plasmid. The 25-OHC treatment affects all cells present, and its effects are active following the 48 hour incubation period on day four. However, the over-expression plasmid lacks a mammalian origin of replication and so is not replicated with every cell division. Thus, taking into account the doubling time of HeLa is approximately 24 hours, one would expect only approximately one quarter of the final cell population to express nSREBP2 on day 4 following transient transfection of the over-expression plasmid

on day 2. The level of nSREBP2 rescue in the presence of 25-OHC observed in Figure 6.10B is consistent with this explanation. Nonetheless, over-expression of nSREBP2 was capable of significantly, although not completely, reverting the oxysterol enhanced statin cytotoxicity back towards the more resistant phenotype, as compared by two-way ANOVA (statin vs. statin+25-OHC+EV, p=3.07E-32; statin vs. statin+25-OHC+nSREBP2,p=8.22E-23) (Figure 6.10C). It is noteworthy that the rescue up to 1μM simvastatin is a 40% rescue, back up to 100% viability, and that this 40% rescue is maintained right up 3μM. The lack of capability of nSREBP2 to rescue up to 100% viability is likely attributable to the activation capacity of nSREBP2 alone in the presence of 25-OHC without any statin present, as shown in figure 6.10B.

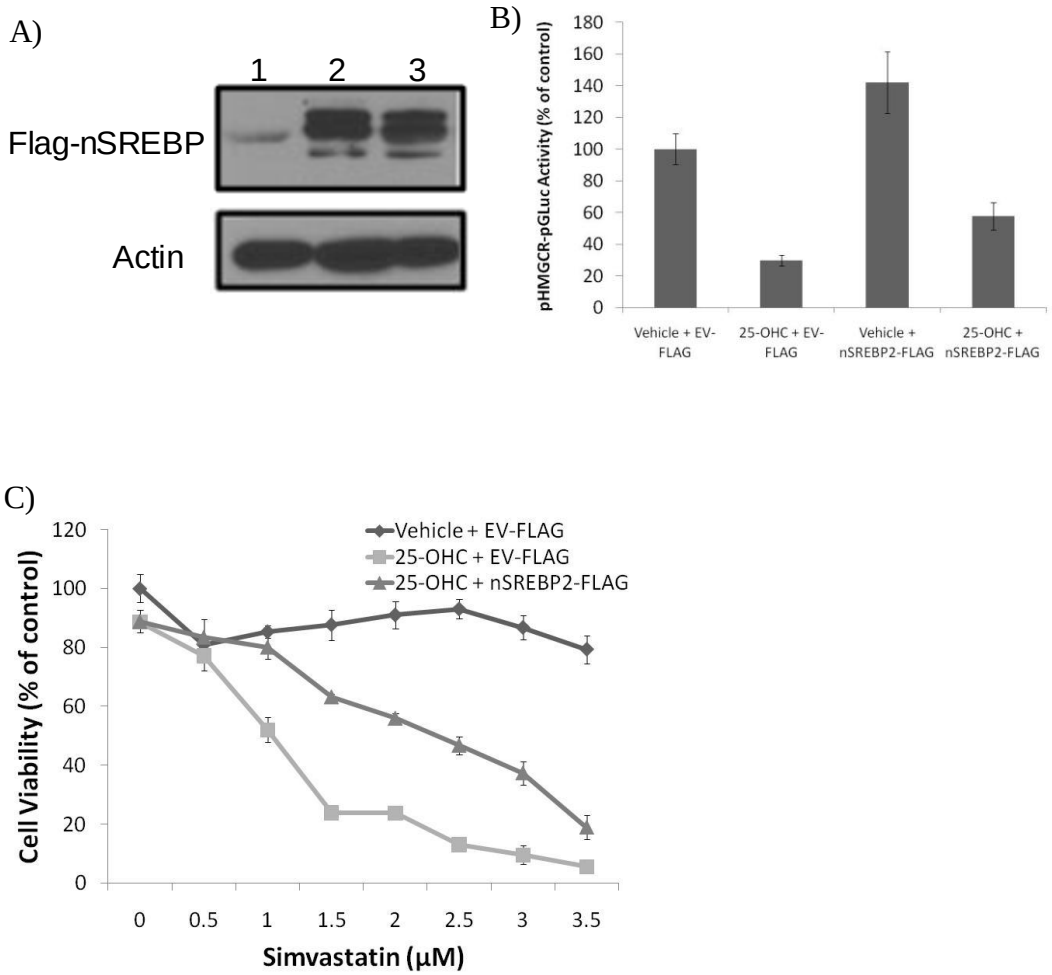


Figure 6.10. Over expression of constitutively active nSREBP2 partially rescues cell death induced by simvastatin plus 25-OHC. (A) Immunoblot of over-expressed Flag-nSREBP2 in HeLa-PHGL cells: lane 1, empty vector; lane 2, Flag nSREBP2; lane 3, Flag nSREBP2 plus 25-OHC. (B) Luciferase readout from the HeLa-PHGL stable cell line transfected with Flag-nSREBP2 +/- 25-OHC (1 µg/ml). (C) HeLa-PHGL cells were transfected with empty vector or Flag and treated with increasing concentration of simvastatin. Cell viability was measured by MTT. Experiments were performed in triplicate and error bars represent ± SD. Significance of SREBP luciferase reporter activation or repression were measured using Student's t-Test ($p<0.05$). Significance of enhancement or rescue of statin induced cytotoxicity was measured using two-way ANOVA ($p<0.05$).

***HeLa-PHGL cells co-treated with statin and oxysterol undergo apoptosis***

Statins are known to induce apoptosis in a variety of cell lines, including HeLa cells. In previous experiments the effect of statins and oxysterol on HeLa-PHGL cells has been measured using the MTT assay which measures cell viability and cell proliferation. While this assay is a standard assay for cytotoxicity, it was important to confirm by a separate means that apoptosis was occurring in the cells treated with statin alone or with statin plus oxysterol. Propidium iodide (PI) is a common fluorescent dye used to measure cellular DNA content and facilitates cell cycle analysis using FACS. PI fluorescence is proportional to the DNA content of the cell. As apoptotic cells are characterised by fragmented DNA, this method can also be used to identify cells undergoing apoptosis (Nicoletti et al. 1991). Thus FACS analysis of PI labelled DNA was used here to compare the extent of apoptosis induction by simvastatin in cells grown in FS or in LDS in the presence and absence of 25-OHC. 4 µM simvastatin has been previously shown to be sufficient to kill all HeLa-PHGL cells cultured under FS conditions following a 48 hour incubation period while 4 µM simvastatin has no effect on HeLa-PHGL cells under LDS conditions.

For analysis of apoptosis, HeLa-PHGL cells were cultured with 4 µM simvastatin for 24 hours to allow induction of apoptosis, either in the absence or presence of 25-OHC. Cells were then harvested and stained with PI for analysis by FACS. Using PI staining with FACs analysis normal cells display characteristic peaks corresponding to diploid (2n) or tetraploid (4n) DNA content while apoptotic cells can be distinguished by increased fluorescence detected below these peaks (sub-$G_1$, <2n) due the presence of fragmented DNA. For HeLa-PHGL cells cultured with 4 µM simvastatin under FS conditions, the sub-G1 population increases by 49.4%

compared to the untreated control (Figure 6.11A and 6.11B). Conversely under LDS conditions, 4 µM simvastatin increases the sub-G1 population by only 7.2% compared to the untreated control (Figure 6.11C and 6.11D). However cells cultured under LDS conditions with 4 µM simvastatin in the presence of 1 µg/ml 25-OHC display a 55.3% increase in the sub-G1 population compared to cells treated with 25-OHC alone (Figure 6.11E and 6.11F). This data demonstrates that the level of fragmented DNA in the sub-G1 population (which is indicative of apoptosis) is at similar levels for simvastatin treated cells cultured in FS conditions and in LDS conditions with 25-OHC. This is consistent with the previous MTT data.

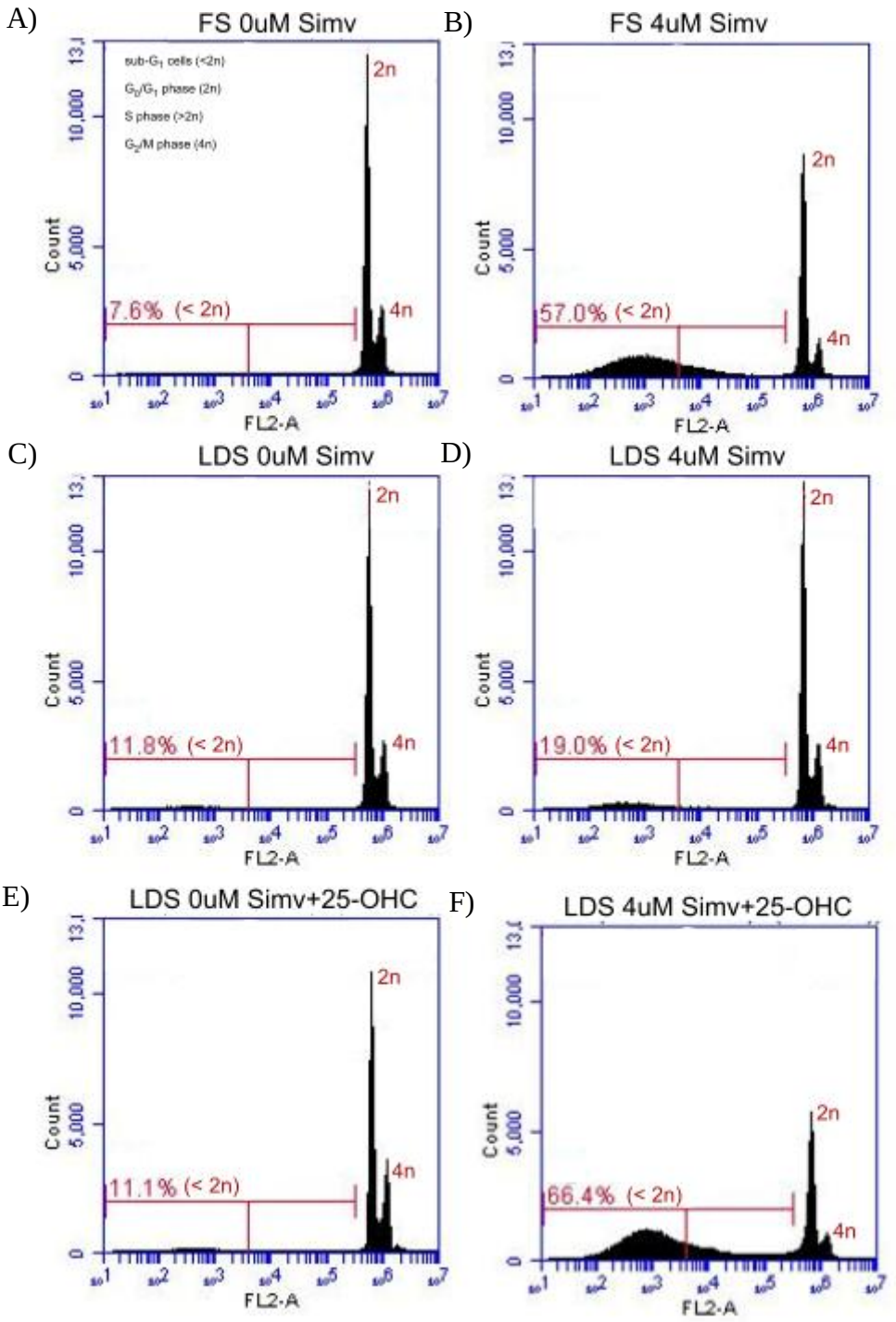


Figure 6.11. Measurement of apoptosis induced by simvastatin in FS conditions and LDS conditions in the absence and presence of 25-OHC. Cells were cultured in FS or LDS conditions in the presence of the indicated compounds for 24 hours. Cells were then harvested, permeabilised using ethanol, and DNA was stained using PI as described under materials and methods. Cells were then analysed by FACS. A, FS conditions without simvastatin; B, FS conditions with 4 µM simvastatin; C, LDS conditions without simvastatin; D, LDS conditions with 4 µM simvastatin; E, LDS conditions with 1 µg/ml 25-OHC F, LDS conditions with 4 µM simvastatin and 1 µg/ml 25-OHC.

***Investigation of oxysterol-mediated SREBP feedback and statin cytotoxicity in a panel of cancer cell lines***

Cell lines derived from other cancer types were tested to see if they had similar oxysterol-mediated SREBP feedback and statin cytotoxicity to HeLa-PHGL cells. Dose-response curves for simvastatin treated A-498 (kidney carcinoma), DU-145 (prostate carcinoma), MeWo (malignant melanoma), MCF-7 (breast adenocarcinoma), HepG2 (hepatocellular carcinoma), KYSE-70 (oesophageal squamous cell carcinoma) and HT-29 *(*Colorectal adenocarcinoma) cell lines were determined for both FS and LDS conditions (Figure 6.12A). Two-way ANOVA analysis revealed that A-498, DU-145 and MCF-7 cell lines did not have significantly different dose-responses to simvastatin under FS and LDS conditions (p=0.973, 0.126 and 0.401, respectively) while MeWo, HepG2, KYSE-70 and HT-29 cell lines had significantly different dose-responses to simvastatin under FS and LDS conditions (p=1.55E-06, 3.22E-09, 0.045 and 4.71E-33, respectively). The dose response curves were then used to calculate the $ED_{50}$ values for each cell line (Figure 6.12B). The $ED_{50}$ values varied widely across the cell lines tested from 5 µM to 50 µM in FS and from 16 µM to 69 µM in LDS reflecting different sensitivities across the cancer cell lines to statin induced cytotoxicity. In agreement with the two-way ANOVA analysis of the cell line dose-response curves, A-498, DU-145 and MCF-7 cell lines did not display significant difference in their simvastatin $ED_{50}$ values in FS and LDS (p=0.219, p=0.172, p=0.079, respectively (student's t-test)), while KYSE-70, HepG2, MeWo and HT-29 cell lines were significantly different in FS vs. LDS (p=9.37E-04, p=1.51E-03, p=0.034 and p=9.41E-06, respectively).

To investigate if the cell lines displayed a sterol regulated feedback response of the SREBP pathway, each cell line (A-498, DU-145, MeWo, MCF-7, HepG2, KYSE-70 and HT-29) was transiently transfected with the SREBP luciferase reporter plasmid promHMGCR-GLuc. To achieve this, transfection for each of the cell lines required optimisation. Luciferase activity of a constitutively active luciferase reporter plasmid, pCMV-GLuc, was used to compare the transfection efficiency achieved using three commercial transfection reagents; Lipofectamine 2000, TurboFect and Xtremegene (Figure 6.13). Maximal transfection efficiency was achieved using Lipofectamine 2000 for A-498, KYSE-70, and MeWo and Xtremegene for DU-145, HT-29, and MCF-7. For HeLa-PHGL there was no significant difference observed across the three transfection reagents used, and thus TurboFect was used due to simplicity of use and cost effectiveness. The levels of transfection of HepG2 with Xtremegene and TurboFect were 9.08-fold and 3.96-fold higher than HeLa-PHGL cells respectively and the TurboFect method was deemed sufficient for use with the HepG2 cells. The results indicated that a 1:2 ratio of plasmid DNA to transfection reagent (µg:µl) was optimal in all cases. The optimal transfection conditions were then used to transiently transfect each cell line with promHMGCR-pGLuc and the cell lines were screened for a sterol feedback response using the SSLR method described in chapter 4.

The cell lines A-498, DU-145, MeWo and MCF-7 did not display any decrease in luciferase reporter activity in response to increasing concentrations of 25-OHC (data not shown), and thus were not followed up any further for the purpose of this investigation. However, the lack of a sterol feedback response in these cells lines is interesting and merits further investigation. The cell lines KYSE-70, HepG2 and HT-29, however, did display a decrease in SREBP luciferase reporter activity in response

to 25-OHC, thus confirming that sterol regulated feedback is present in these cell lines (Figure 6.14). Interestingly, HT-29 and KYSE-70 displayed significantly different responses to oxysterol induced cytotoxicity under FS compared to LDS conditions. HT-29 and KYSE-70 cells were more sensitive when cultured in LDS (Figure 6.14A and 6.14C). In contrast, HepG2 cells displayed a similar response to oxysterol induced cytotoxicity under both FS and LDS conditions (Figure 6.14B). Based on the presence of a sterol feedback response in these cell lines, HT-29, KYSE-70 and HepG2 were further investigated to see if co-treatment of simvastatin with 25-OHC would reduce the statin $ED_{50}$ for these cell lines.

A)

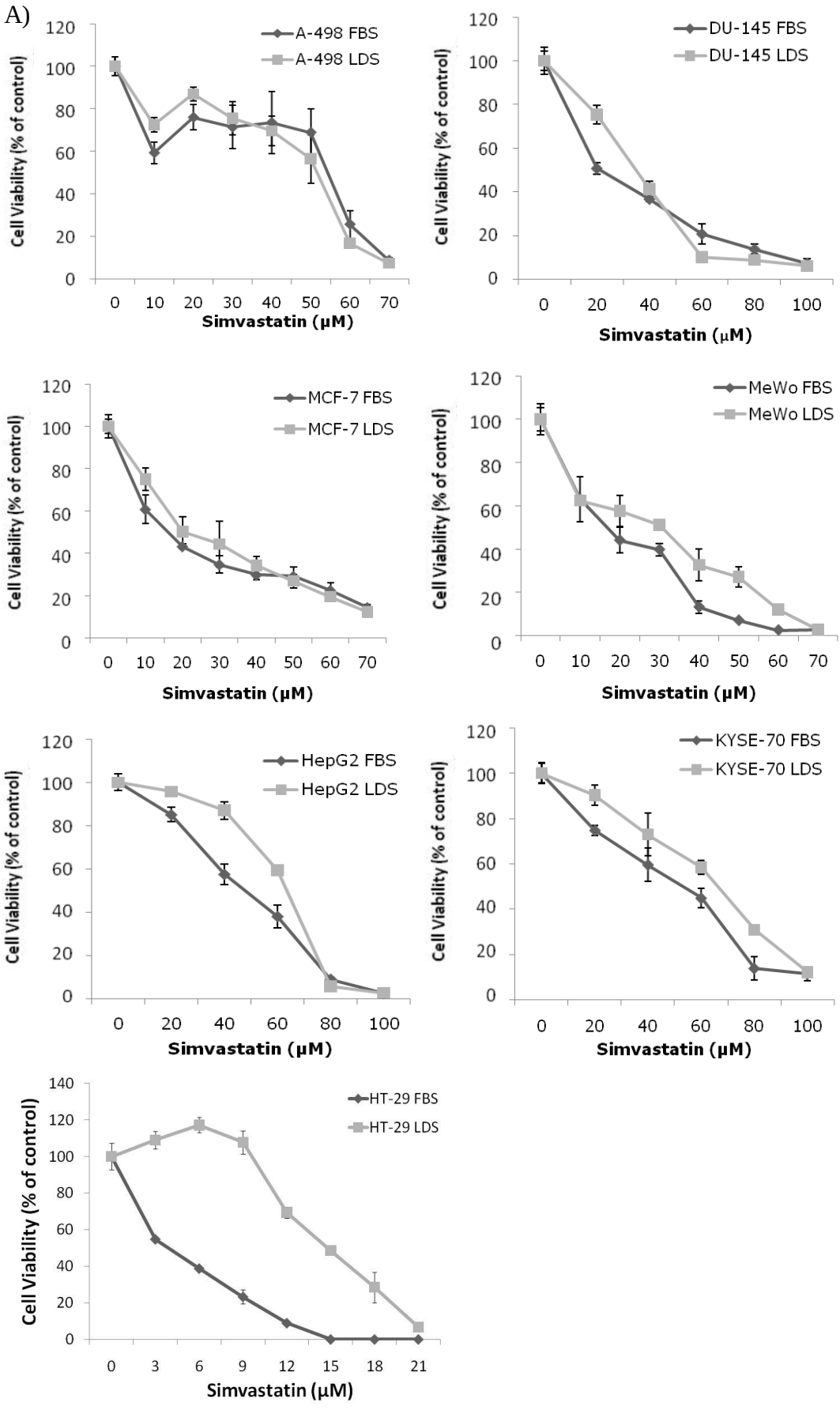
A-498 FBS
A-498 LDS
Cell Viability (% of control)
Simvastatin (µM)
DU-145 FBS
DU-145 LDS
Cell Viability (% of control)
Simvastatin (µM)
MCF-7 FBS
MCF-7 LDS
Cell Viability (% of control)
Simvastatin (µM)
MeWo FBS
MeWo LDS
Cell Viability (% of control)
Simvastatin (µM)
HepG2 FBS
HepG2 LDS
Cell Viability (% of control)
Simvastatin (µM)
KYSE-70 FBS
KYSE-70 LDS
Cell Viability (% of control)
Simvastatin (µM)
HT-29 FBS
HT-29 LDS
Cell Viability (% of control)
Simvastatin (µM)

B)

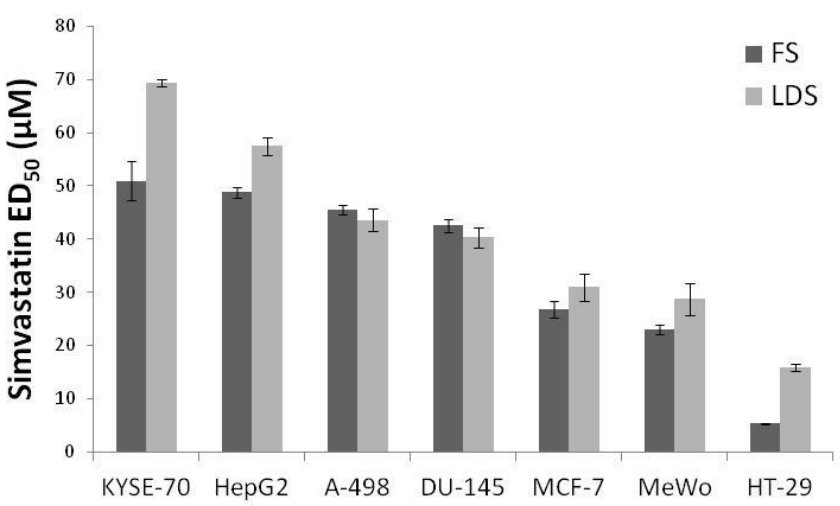


Figure 6.12. Simvastatin cell viability dose-response curves for a panel of cancer cell lines under FS and LDS conditions. A) All cell lines were cultured in the presence of increasing concentrations of simvastatin under FS and LDS conditions for 48 hours. Cell viability was assessed using MTT assay. B) Simvastatin ED50 of the different cell lines under FS and LDS conditions.

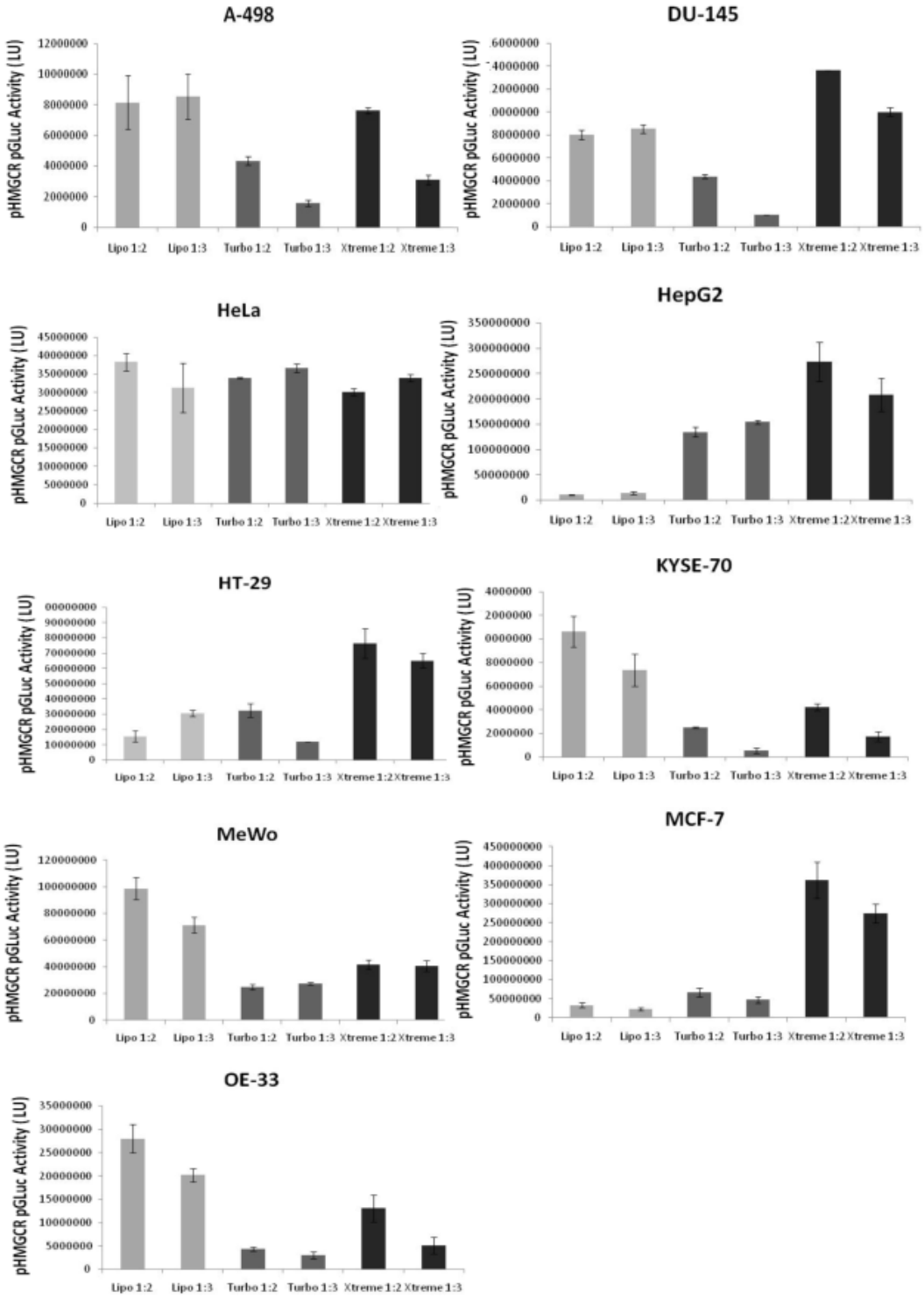


Figure 6.13. Optimising transfection of cell lines. Cells were transfected according to manufacturers guidelines for Lipofectamine 2000 (Lipo ) TurboFect (Turbo ) or Xtremegene (Xtreme ) transfection reagents. The amount of pCMV-GLuc reporter plasmid transfected was kept constant at 0.5 µG and the transfection reagents were used at either 1:2 or 1:3 (µG/ µL) ratios. Transfection efficiency was assessed by measuring luciferase enzyme activity. Transfections were performed in triplicate. Error bars represent ±SD.

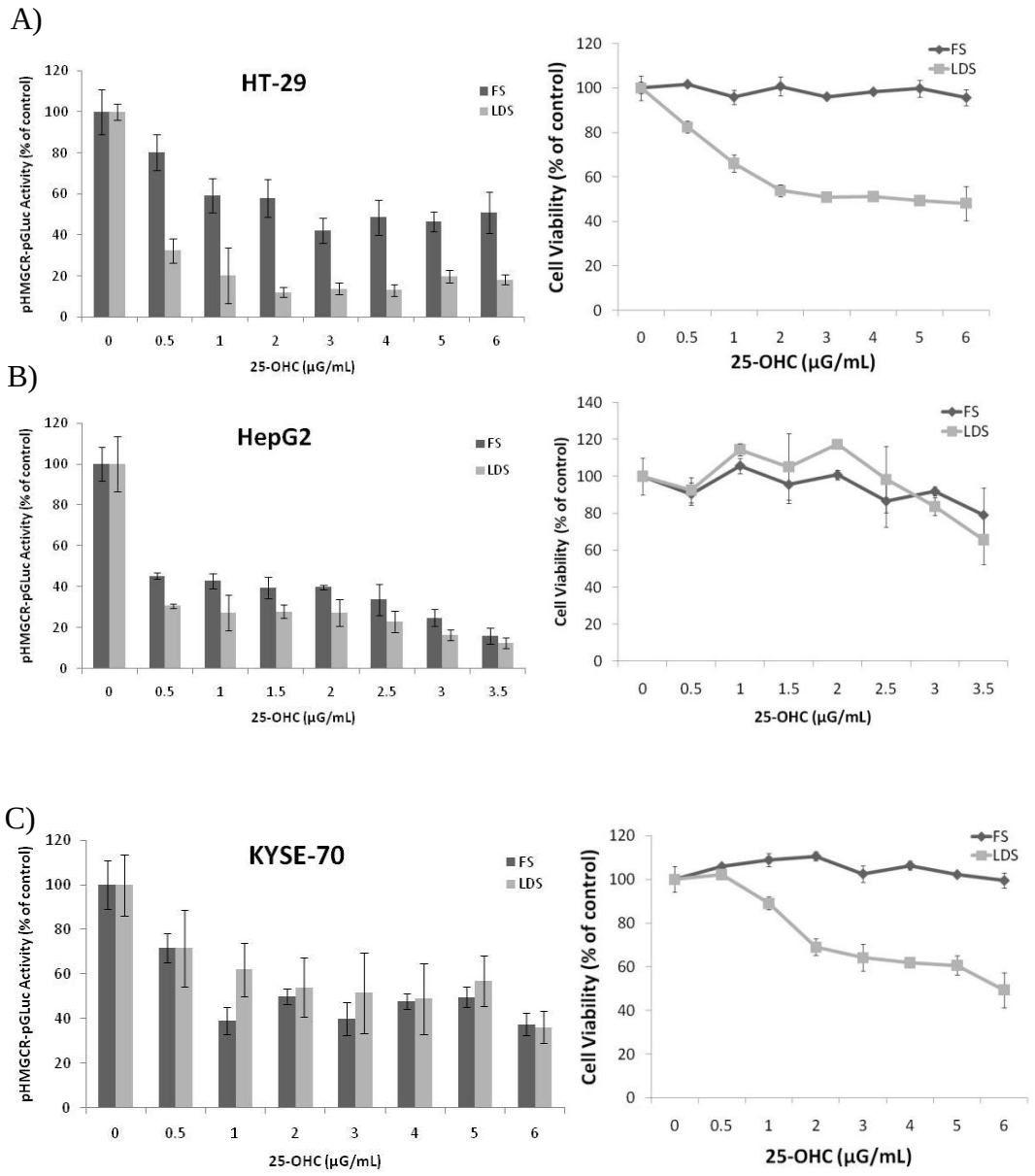


Figure 6.14. SREBP feedback response to 25-OHC treatment in cell lines. Cells were incubated in the presence of increasing concentrations of 25-OHC under both FS and LDS conditions. Media was sampled after 48 hours and assayed for secreted luciferase activity. Cell viability was measured using MTT assay.

***Investigation of inhibition of the SREBP pathway and statin sensitivity in HT29, HEPG2, KYSE70 cells***

The effect of co-treatment of 25-OHC or 19-OHC and statins in enhancing cancer cell death was investigated and yielded mixed results. For HT-29 cells cultured in FS conditions, co-treatment of simvastatin with either 25-OHC or 19-OHC reduced the $ED_{50}$ 6-fold from 6μM to less than 1μM (Figure 6.15A). The presence or absence of 25-OHC and 19-OHC on statin cytotoxicity was compared. The presence of 25-OHC and 19-OHC significantly enhances the cytotoxicity caused by increasing concentrations of simvastatin in FS, (p=1.87E-26 and p=1.78E-26, respectively (two way ANOVA)). Analysis of the SREBP activation readout using the HMGCR promoter luciferase reporter in the same experiment showed that 25-OHC and 19-OHC reduced SREBP readout 3 fold and 2.8 fold respectively (Figure 6.15B). This indicates that the enhancement of statin-mediated cell death is due to the inhibitory effects that 25-OHC and 19-OHC have on HMGCR promoter activation. HMGCR promoter activation is significantly repressed by both 25-OHC and 19-OHC in the presence of increasing statin concentrations. Thus, this confirms that there is an active SREBP-feedback response in the HT-29 cell line. However, when cells were cultured in LDS rather than FS conditions and were treated with simvastatin in the presence and absence of oxysterols, the same degree of oxysterol enhancement of statin $ED_{50}$ did not occur ($ED_{50}$=15 μM for all in LDS) (Figure 6.15A and 6.15C) although analysis of the dose-response curves by two-way ANOVA indicated that the presence of 25-OHC did significantly improve the overall cytotoxicity induced with increasing concentrations of simvastatin (p=0.0012) compared to conditions where 25-OHC was absent, while no difference was observed with 19-OHC (p=0.491). Analysis of the SREBP activation readout using the HMGCR promoter luciferase of the same experiment indicates that the lack of simvastatin cytotoxicity

enhancement may by the oxysterols is likely to be to the much lower inhibitory effect of the oxysterols on HMGCR promoter activity under LDS conditions compared to FS (Figure 6.15B and 6.15D). In LDS conditions, 25-OHC reduced the luciferase reporter readout 1.26-fold while 19-OHC reduced it 1.34-fold. These differences were not significant over conditions where the 25-OHC and 19-OHC were absent ($p=0.179$ and $p=0.115$, respectively (student's t test)).

Immunoblot analysis of HT-29 cells revealed an induction of both SREBP2 and HMGCR in response to statin treatment in FS conditions (Figure 6.16, lane 2). This induction is inhibited by both 25-OHC and 19-OHC, although to a lesser extent by 19-OHC (Figure 6.16, lane 3, 4). By contrast, there is a substantial level of induction of both HMGCR and SREBP2 under LDS conditions in the presence of simvastatin (Figure 6.16, lane 6). Again this induction is inhibited by 25-OHC and to a lesser extent by 19-OHC. Overall the levels of induction or repression of SREBP correlate with the levels of HMGCR detected and correlate with the statin cytotoxicity observed in the absence and presence of the sterols under FS conditions. Under LDS conditions, the trend remained the same. However, while the 25-OHC repressed SREBP2 expression to background levels, the levels of HMGCR were not repressed accordingly.

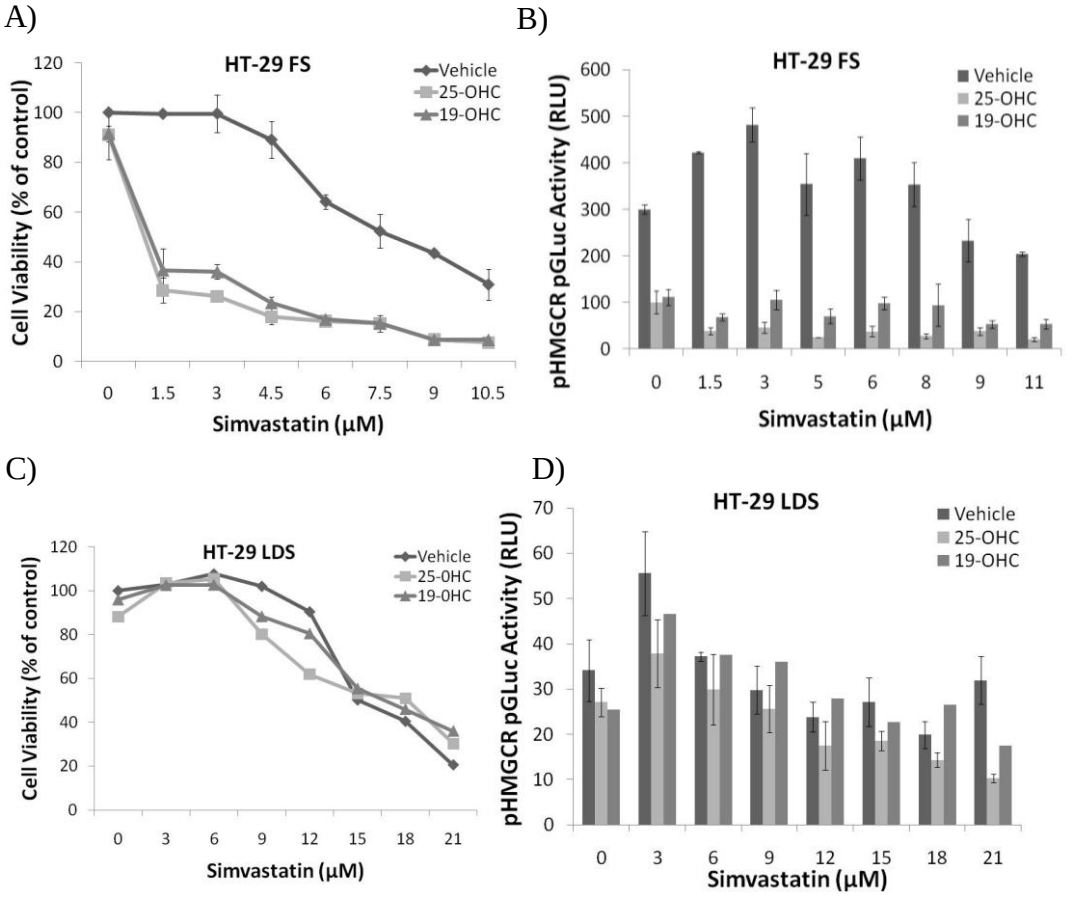


Figure 6.15. Analysis of the effect of oxysterols on cell viability and SREBP readout in HT-29 cells grown in FS or LDS conditions. Cells were cultured in the presence of increasing amounts of simvastatin in the absence or presence of oxysterols under both FS and LDS conditions. Cell viability was measured using MTT assay (A and C). Media was sampled after 48 hrs and assayed for secreted luciferase (B and D).

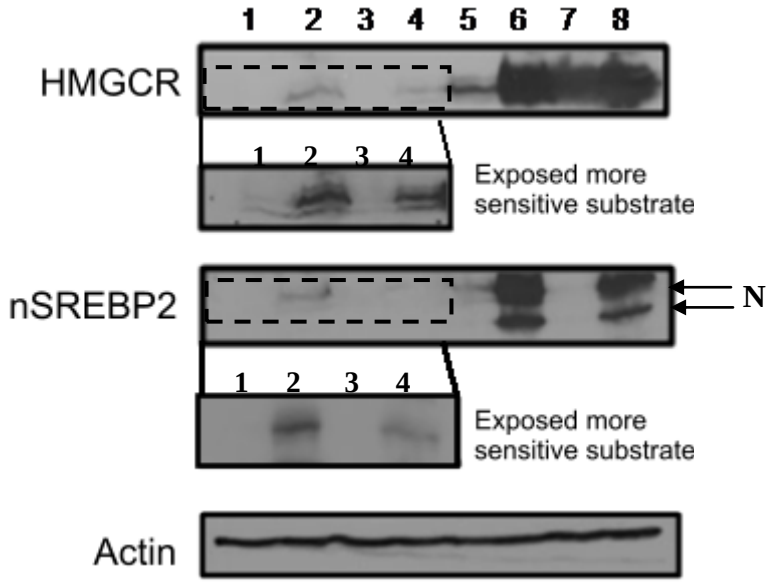


Figure 6.16. Western blot analysis of HMGCR and SREBP2 in HT-29 cells treated with simvastatin in the absence and presence of oxysterols. Cells were cultured for 24 hours with 1µM simvastatin in FS or 3 µM simvastatin in LDS in the presence and absence of 25-OHC (FS=3 µg/ml, LDS=0.25 µg/ml) or 19-OHC (FS=3 µg/ml, LDS=0.25 µg/ml). 50 µM mevalonate was included in the growth media to maintain cell viability. FS conditions lanes 1-4 and LDS conditions lanes 5-8. Lanes 1-8: vehicle, simvastatin, simvastatin plus 25-OHC FS, simvastatin plus 19-OHC, vehicle, simvastatin, simvastatin plus 25-OHC, simvastatin+ plus 19-OHC respectively. N= nSREBP2

The effect of co-treatment of oxysterols and statins in enhancing cancer cell death was next investigated for HepG2 cells. Co-treatment of HepG2 cells with simvastatin and 25-OHC significantly improved the $ED_{50}$ 2.3-fold from 35µM to 15 µM in the $ED_0$-$ED_{50}$ region of the graph. However, this was not sustained across the whole dose response range, and did not affect the simvastatin concentration required to decrease cell viability 100%, which remained at approximately 100 µM (Figure 6.17A). 19-OHC had a similar, but slightly less effect than 25-OHC (Figure 6.17A, 17C). SREBP/HMGCR luciferase reporter readout analysis for the same experiment indicated that19-OHC reduced the luciferase reporter readout 1.53-fold compared to the 2.12-fold decrease achieved with 25-OHC (Figure 6.17B). In the presence of simvastatin, overall repression of luciferase reporter activity remained statistically significant for 25-OHC and 19-OHC compared to statin alone, as compared by two-way ANOVA (p=6.37E-14 and p=6E-07, respectively). A similar effect was seen in for HepG2 cells co-treated with simvastatin and oxysterols under LDS conditions (Figure 6.17C). 25-OHC and 19-OHC significantly enhanced simvastatin induced cytotoxicity overall in LDS conditions, as compared by two-way ANOVA (p=1.36E-07 and p=0.005, respectively). However, consistent with what was observed for HepG2 under FS conditions this enhancement was observed at lower simvastatin doses but not at higher ones. Analysis of the SREBP readout luciferase reporter activity for the same experiment showed a 4.41-fold decrease achieved with 25-OHC and a 1.63-fold decrease achieved with 19-OHC (p=1.19E-04 and p=0.002, respectively). In the presence of simvastatin, overall repression of luciferase reporter activity remained statistically significant for 25-OHC and 19-OHC compared to statin alone, as measured by two-way ANOVA(p=5.11E-20 and p=1.09E-10, respectively). Consistent with results from HeLa-PHGL and HT-29, the level of

SREBP luciferase reporter repression achieved with each oxysterol was related to the level of oxysterol enhancement of the statin effect on cell viability. Immunoblot analysis of HMGCR and SREBP2 protein levels indicated that there was an increase in both proteins in response to simvastatin treatment, and that the increase was higher under LDS conditions (Figure 6.18, lane 2, 6). This is consistent with what was seen in HeLa-PHGL and HT-29 cells, but was unexpected as unlike the HeLa-PHGL and HT-29 cells, HepG2 cells have the same simvastatin $ED_{50}$ in both FS and LDS conditions. The presence of 25-OHC completely prevented the statin-mediated increase in both HMGCR and nSREBP2, with 19-OHC having a lesser effect, under both FS and LDS conditions (Figure 6.18, lane 3, 4, 7, 8).

A similar set of experiments were carried out on KYSE-70 cells and results were very similar to results with HepG2. Co-treatment of KYSE-70 cells with simvastatin and 25-OHC reduced the $ED_{50}$ 5.2-fold from 58 µM to 10 µM in FS conditions (Figure 6.19A). However, the 50% decrease in cell viability achieved with 10 µM simvastatin in the presence of either 25-OHC or 19-OHC does not decrease any further from 10 µM up to 40 µM simvastatin. Similar to HepG2 cells, 25-OHC and 19-OHC significantly enhanced simvastatin induced cytotoxicity overall in FS conditions over simvastatin alone (p=1.5E-10 and p=3.52E-11, respectively (two-way ANOVA)). Analysis of the SREBP luciferase readout for the same experiment showed that 25-OHC and 19-OHC reduced secreted luciferase with 19-OHC having a stronger effect than 25-OHC (Figure 6.19B). For KYSE-70 cells co-treated with simvastatin and oxysterols under LDS conditions, similar results were observed. 25-OHC significantly enhanced simvastatin induced cytotoxicity overall in LDS conditions, (p=0.02 (two-way ANOVA)) while 19-OHC did not have a significantly enhancing effect (p=0.113) (Figure 6.19C). Analysis of the SREBP luciferase

reporter activity for the same experiment indicated that the 19-OHC was only marginally effective in inducing SREBP feedback by comparison with 25-OHC in KYSE-70 cells under LDS conditions (Figure 6.19D) and explains why the 19-OHC did not significantly enhance simvastatin cytotoxicity under these conditions.

In the presence of simvastatin, overall repression of luciferase reporter activity remained statistically significant for 25-OHC and 19-OHC compared to statin alone ($p=1.9E-09$ and $p=1E-05$, respectively (two-way ANOVA). However, consistent with what was observed for HepG2 under LDS conditions the enhancement of simvastatin induced cytotoxicity by 25-OHC was not sustained across the whole dose response range, and did not affect the concentration required to decrease cell viability to 100% levels, Consistent with results from HeLa-PHGL, HT-29 and HepG2, the level of SREBP luciferase reporter repression achieved with each oxysterol correlated with the level of oxysterol enhancement of the statin effect on cell viability.

Immunoblot analysis of HMGCR and SREBP2 protein levels indicated that there was an increase in both proteins in response to simvastatin treatment, and that the increase was substantially higher under LDS conditions (Figure 6.20, lane 2, 6). This is consistent with what was seen in HeLa-PHGL, HT-29 and HepG2 cells. The presence of 25-OHC completely prevented the statin-mediated increase in both HMGCR and nSREBP2, with 19-OHC having a lesser effect under FS and practically no effect under LDS conditions (Figure 6.20, lane 3, 4, 7, 8).

Overall, the data from the analysis of the simvastatin cytotoxicity in HepG2 and KYSE-70 in the presence and absence of oxysterols suggest that the simvastatin cell viability effects at lower doses are via HMGCR inhibition and that this is enhanced

by oxysterol induced reduction of HMGCR while the loss of cell viability at higher statin concentrations appears to be by a different mechanism since the oxysterols are ineffective at the higher statin concentrations. To further explore this idea, the ability of mevalonate to rescue the statin-mediated cell death in HT-29, HepG2 and KYSE-70 cell lines was investigated. Full rescue of statin-mediated cytotoxicity in the three cell lines occurred when 100 μM mevalonate was included in the growth media (50 μM mevalonate had and intermediate to full rescue effect depending on the cell line) (Figure 6.21) at or under simvastatin concentration of 40 to 60 μM. However, when the simvastatin concentration were higher than this, mevalonate rescue was no longer effective indicating that the decrease in cell viability at the higher statin concentration are likely to be due to statin effects outside of HMGCR inhibition.

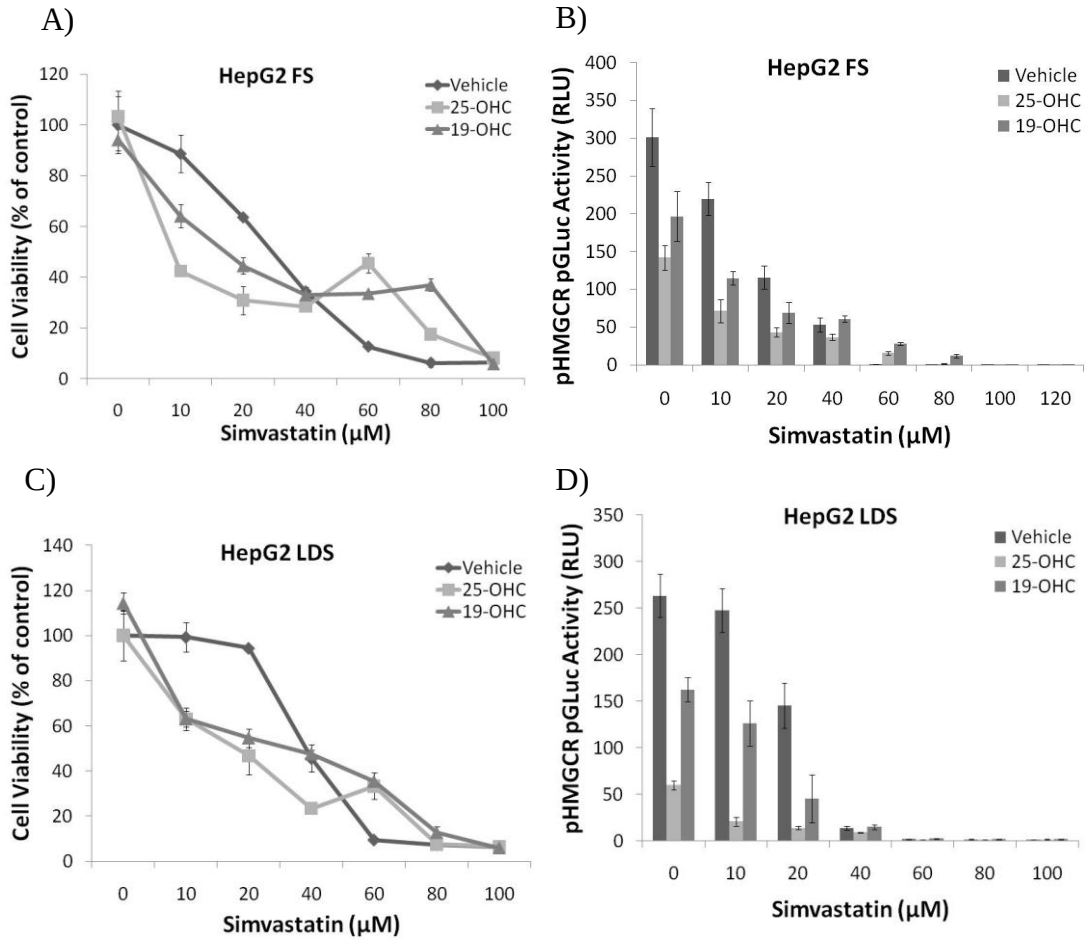


Figure 6.17. Analysis of the effects of oxysterols on simvastatin cytotoxicity under both FS and LDS culture conditions in HepG2 cells. Cells were cultured in the presence of increasing simvastatin concentrations under both FS and LDS conditions. Cells were co-treated with or without 25-OHC (2 µg/ml) or 19-OHC (2 µg/ml) as indicated. Cell viability was measured using MTT assay (A and C). Media was sampled after 48 hrs and assayed for secreted luciferase (B and D).

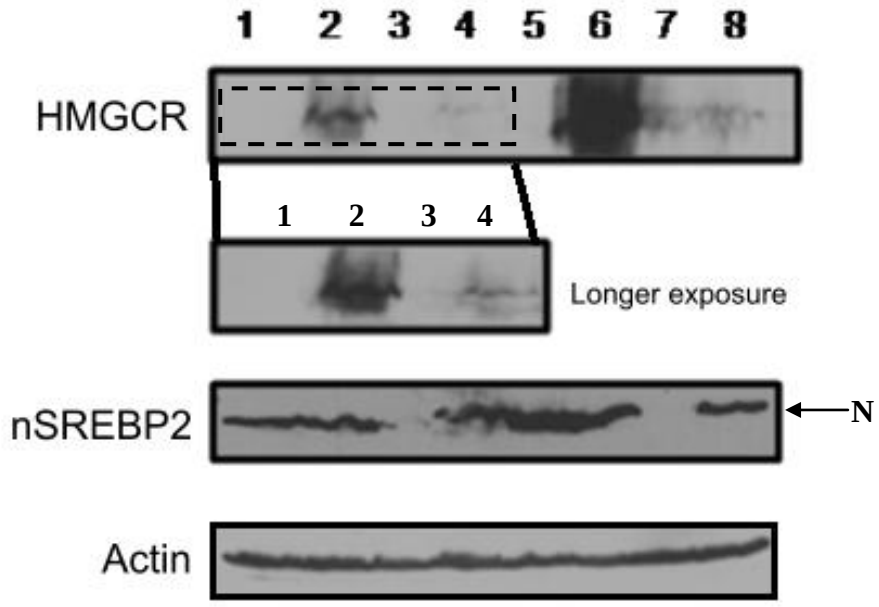


Figure 6.18. Western blot analysis of HMGCR and SREBP2 in HepG2 cells treated with simvastatin in the absence and presence of oxysterols. Cells were cultured for 24 hours with 10 µM simvastatin in FS or 10 µM simvastatin in LDS in the presence and absence of 25-OHC (2 µg/ml) or 19-OHC (2 µg/ml). 50 µM mevalonate was included in the growth media to maintain cell viability. FS conditions lanes 1-4 and LDS conditions lanes 5-8.Lanes 1-8, Vehicle, Simvastatin, Simvastatin plus 25-OHC, Simvastatin plus 19-OHC, Vehicle, Simvastatin LDS, Simvastatin plus 25-OHC LDS and Simvastatin plus 19-OHC respectively. N=nSREBP2.

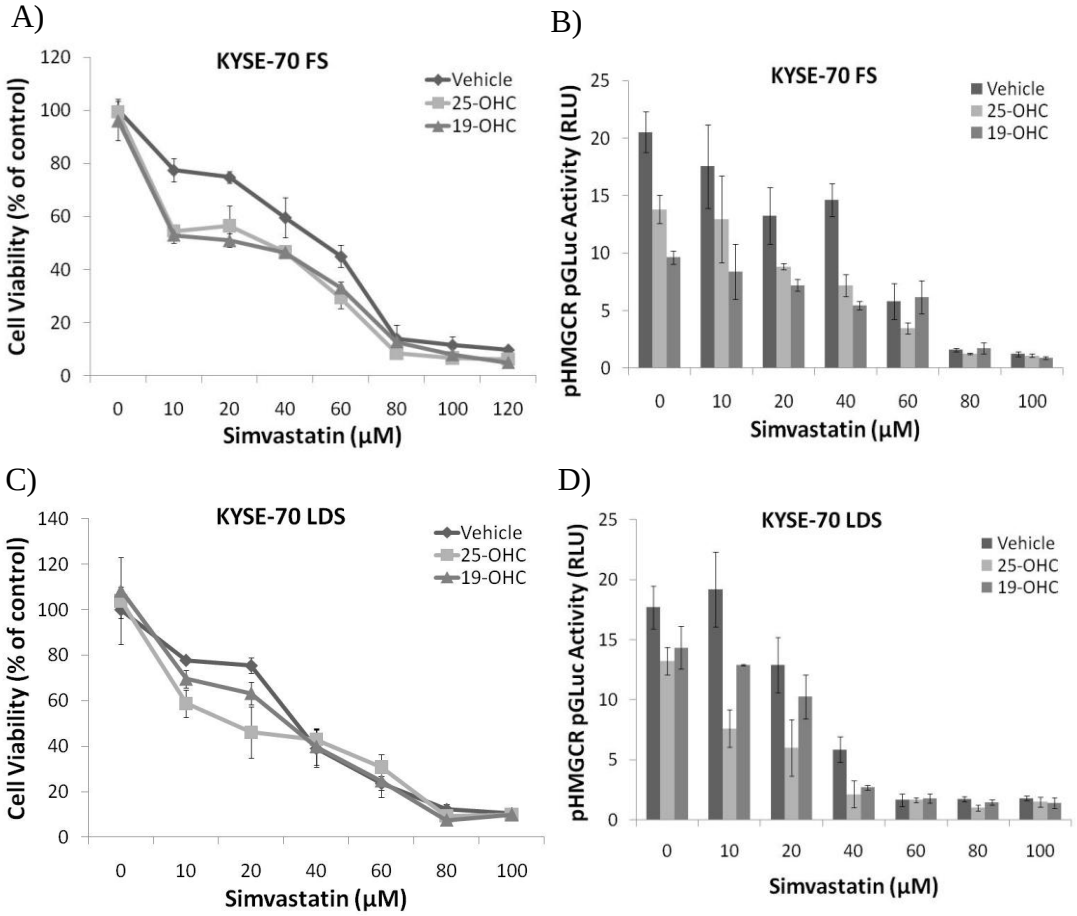


Figure 6.19. Analysis of the effect of oxysterols on cell viability and SREBP readout in KYSE-70 cells grown in FS or LDS conditions. Cells were cultured in the presence of increasing amounts of simvastatin in the absence or presence of oxysterols (FS=5 µg/ml, LDS=0.5 µg/ml) under both FS and LDS conditions. Cell viability was measured using MTT assay (A and C). Media was sampled after 48 hrs and assayed for secreted luciferase (B and D).

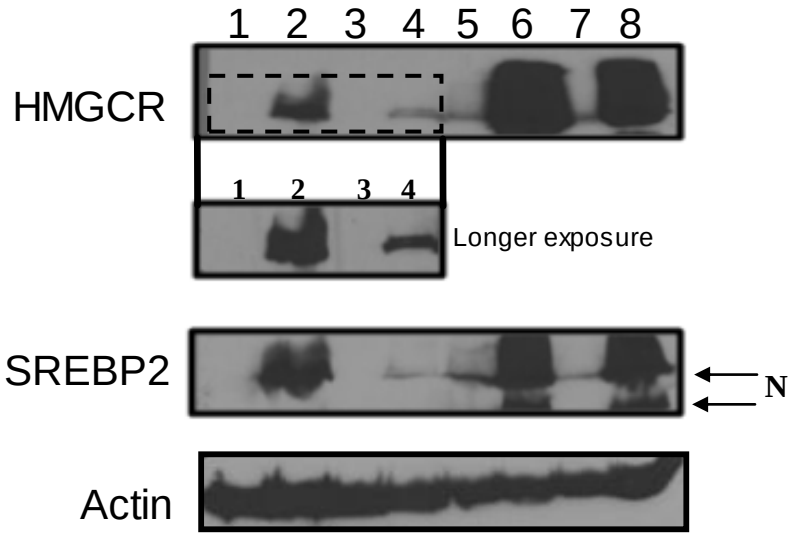


Figure 6.20. Western blot analysis of HMGCR and SREBP2 in KYSE-70 cells treated with simvastatin in the absence and presence of oxysterols. Cells were cultured for 24 hours with 10 µM simvastatin in FS or 10 µM simvastatin in LDS in the presence and absence of 25-OHC or 19-OHC (FS=5 µg/ml, LDS=0.5 µg/ml). 50 µM mevalonate was included in the growth media to maintain cell viability. FS conditions lanes 1-4 and LDS conditions lanes 5-8.Lanes 1-8, Vehicle, Simvastatin, Simvastatin plus 25-OHC, Simvastatin plus 19-OHC, Vehicle, Simvastatin LDS, Simvastatin plus 25-OHC LDS and Simvastatin plus 19-OHC respectively. N=nSREBP2.

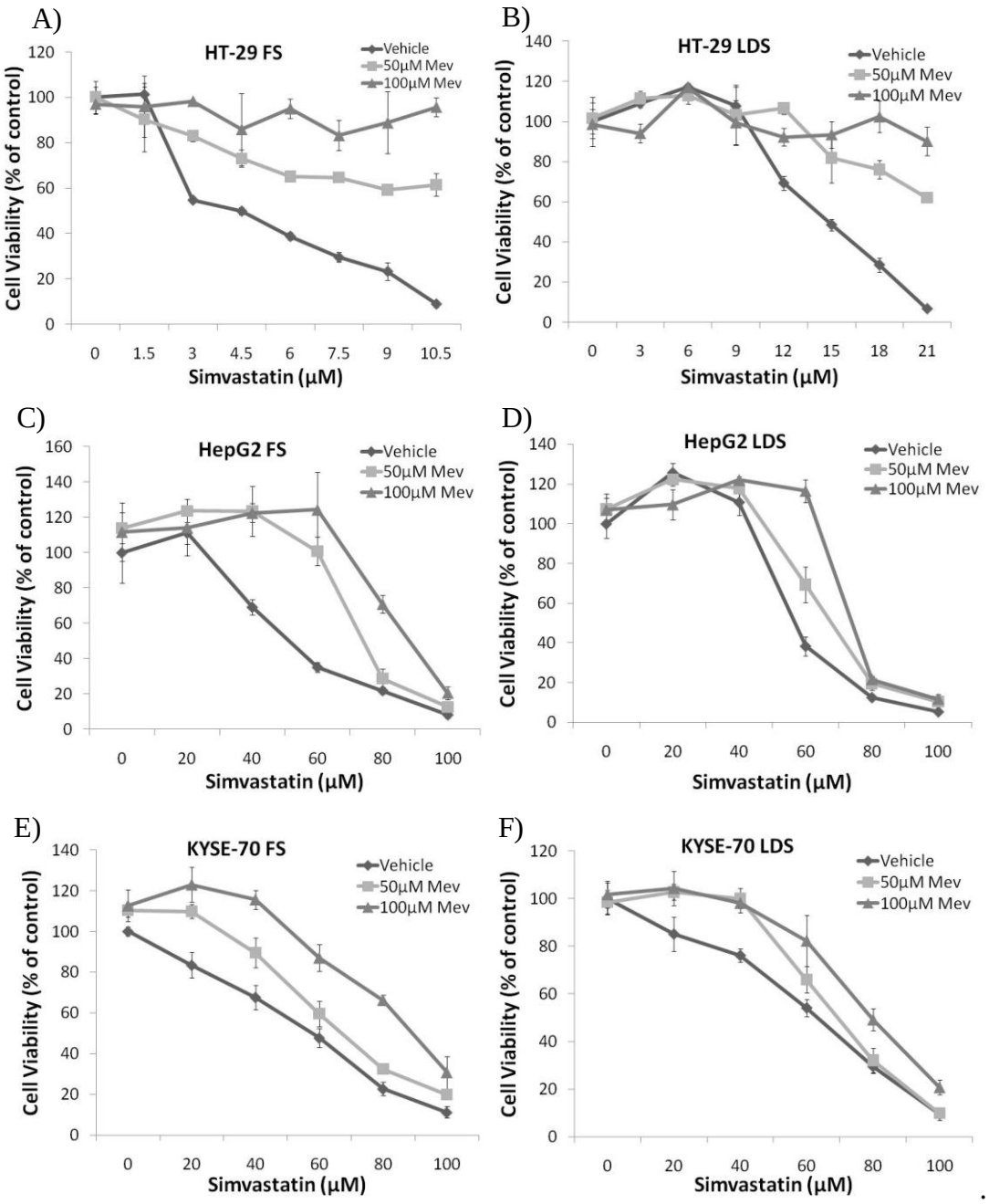


Figure 6.21. Mevalonate rescue of statin treated HT-29, HepG2 and KYSE-70 cells under FS and LDS culture conditions. Cells were incubated with increasing concentrations of simvastatin in the presence and absence of 50 μM or 100 μM mevalonate over a 48 hour period. Cell viability was measured using the MTT assay.

## Discussion

The work described in this chapter tested the hypothesis that preventing the SREBP-mediated activation of cholesterogenic genes that occurs upon statin treatment would reduce the level of the HMGCR gene and protein expression, which in turn would reduce the effective statin concentration required to induce cancer cell apoptosis via mevalonate starvation and consequently improve the chemotherapeutic potential of the statins.

Initially the investigation involved looking at the effect of statin cytotoxicity in HeLa-PHGL cells in full vs. lipid depleted serum. Interestingly, HeLa-PHGL cells grown in LDS were significantly more resistant to statin induced cytotoxicity than when grown in FS. This response was observed with both a naturally occurring statin simvastatin (12.5-fold difference) and a synthetic statin atorvastatin (4.3-fold difference). Simvastatin and atorvastatin are the two most commonly used statins on the market used for the treatment of high cholesterol related disease. The differences in efficacy between simvastatin and atorvastatin in inducing cytotoxicity were not unexpected because although statins all target the active site of HMGCR, they differ in their pharmacokinetic properties (Schachter 2004). This result of an increased resistance to statin cytotoxicity in LDS has not been seen previously. Despite the extensive amount of research on statins, all previous work on statin cytotoxicity has been focused on cells in FS. The simplest explanation for this is that cholesterol is depleted in LDS. Therefore cells in LDS would be expected to have increased SREBP processing and therefore increased transcription of downstream SREBP target genes including HMGCR (Nohturfft et al. 1999; Vallett et al. 1996). Analysis of SREBP/HMGCR luciferase reporter readout confirmed that there was a direct relationship between the level of readout and resistance to statin. The cytotoxicity of

statins has been reported to be due to HMGCR inhibition limiting the production of essential mevalonate derived protein modification substrates including geranylgeranyl pyrophosphate and farnesyl pyrophosphate (Stancu & Sima 2001). Consistent with the cytotoxicity being related to SREBP/HMGCR down-regulation, mevalonate rescued the cells from statin induced cytotoxicity, with full rescue occurring in FS and rescue ranging from 60-90% occurring in LDS. The difference in rescue is likely linked to the higher statin concentration required to achieve cytotoxicity in LDS compared to FS. For these higher concentrations of statin, it is likely that cytotoxicity for a large part is due to HMGCR inhibition but that other mechanism(s) may also be involved.

These findings show that increasing HMGCR levels increases resistance to statin cytotoxicity and suggest that a strategy whereby agents are used to reduce HMGCR would increase the cytotoxicity of statins and increase their potential for use as chemotherapeutic agents. In this work three previously characterised sterol feedback response agents that decrease SREBP processing were evaluated (cholesterol, 25-OHC and betulin) and 19-OHC was used as a negative control. Using the SREBP/HMGCR luciferase reporter assay, cholesterol and 25-OHC were highly effective in reducing reporter readout, and betulin was less effective. Interestingly, 19-OHC was found to have an effect on SREBP/HMGCR luciferase reporter readout, whereas previous reports all show that 19-OHC does not interact with INSIG or SCAP and is commonly used as a negative control (Sun et al. 2005; Radhakrishnan et al. 2007a). Consistent with previous reports, use of 19-OHC in the same concentration range as 25-OHC had little effect on SREBP/HMGCR luciferase reporter readout, with the effect of 19-OHC only being observed at higher concentrations.

The statin cytotoxic effects were significantly enhanced when used in combination with cholesterol or 25-OHC and to a lesser extent with betulin. In LDS, 25-OHC and cholesterol reduced the simvastatin ED50 by 12.5-fold and 20-fold, respectively, while betulin reduced it only 1.4-fold. This is consistent with betulin having less of an effect on SREBP/HMGCR luciferase reporter readout. Clinical trials to date using statin as chemotherapeutic have used statin treatment regimes in the order of 40-80mg/day, which translates into low serum concentrations (Solomon & Freeman 2008). Low serum concentrations may be only partially effective in inducing cell death, while *in vitro* studies show micromolar concentrations are required to achieve significant cancer cell death. The work reported here provides a potential solution to achieving higher cell death with lower statin concentrations, namely by co–administration with 25-OHC or cholesterol. One interesting prospect not investigated here is whether a combination of cholesterol and 25-OHC would give further enhancement of statin cytotoxicity. The justification for this is that cholesterol binds SCAP and 25-OHC binds INSIG and promotes degradation of HMGCR (Radhakrishnan et al. 2007a). The reason that the combination treatment, and indeed cholesterol itself was not followed up here was that the cyclodextrin delivery vehicle (MβCD) for cholesterol had an effect on increasing SREBP/HMGCR luciferase reporter readout. This is not unexpected as other cyclodextrins are used to deplete cellular membranes of cholesterol (Christian et al. 1997). This depletion in cholesterol would cause an increase in SREBP/HMGCR luciferase reporter readout. This limitation could be circumvented by using LDL-cholesterol but this was not available for this work.

Given that 19-OHC unexpectedly had a repressive effect on SREBP/HMGCR luciferase reporter readout, it was investigated further. The results show that at

similar concentrations (1µg/ml) it is comparable with 25-OHC with respect to enhancing statin cytotoxicity. This was a surprising finding as at this concentration 19-OHC has a very small effect on SREBP/HMGCR luciferase reporter readout in the region of 10% reduction. These results indicate that 19-OHC may not be exerting its effect by suppression of HMGCR transcription at this concentration. More insight into the mechanism by which 19-OHC works was provided by immunoblot analysis, which is discussed below.

While the SREBP/HMGCR luciferase reporter readout is a measure of SREBP transcription activity and HMGCR promoter activity, analysis of HMGCR and SREBP at the protein level is required for a comprehensive analysis of these proteins under the different conditions studied (Figure 6.9). Consistent with the SREBP/HMGCR luciferase reporter readout and the statin resistance of the HeLa-PHGL cells in LDS, immunoblot analysis showed that both nSREBP2 and HMGCR were higher in LDS compared to FS. In the presence of simvastatin HMGCR and nSREBP2 were induced to a very high level in HeLa-PHGL cells in LDS compared to FS, further explaining the significant resistance of HeLa-PHGL cells to the simvastatin cytotoxicity. 25-OHC was very effective in reducing both HMGCR and nSREBP2 in both FS and LDS, presumably reflecting its ability to prevent SREBP processing and stimulate degradation of HMGCR.

The results with 19-OHC were somewhat surprising. At the concentration used 19-OHC only had small effect on SREBP/HMGCR luciferase reporter readout compared to 25-OHC, but was as effective as 25-OHC in enhancing the cytotoxic effect of simvastatin. The immunoblot analysis offers an explanation for this as it demonstrates that 19-OHC causes a partial reduction nSREBP2 but fully reduces

HMGCR. This indicates that 19-OHC is less effective than 25-OHC in repressing SREBP processing but is very effective in promoting HMGCR degradation. Previous reports on 19-OHC have only investigated 19-OHC binding to SCAP or INSIG and this was shown to be negative at the concentration used (Radhakrishnan et al. 2007a). Thus this work has shed new light on a common dietary oxysterol and indicates that it is a novel regulator of HMGCR protein stability.

The results indicate that the mechanism by which 25-OHC enhances statin cytotoxicity is mediated by its effect on preventing SREBP processing. This was confirmed by the processed form of SREBP2 (nSREBP2) rescuing the cell from the enhanced statin cytotoxicity in the presence of 25-OHC. The rescue observed using nSREBP2 was about 40%. The lack of capability of nSREBP2 to rescue up to 100% viability is likely to be partially accounted for by the fact that all of the cells contain the luciferase construct and 25-OHC treatment affects 100% of the cells. However nSREBP2 is transiently transfected into the cells and the transfection is not likely to have surpassed more than 80%.

Statins are known to induce apoptosis in a variety of cell lines (Cafforio et al. 2005; Clendening, Aleksandra Pandyra, et al. 2010; Wächtershäuser et al. 2001; Glynn et al. 2008). The MTT assay used here for the majority of experiments measures mitochondrial dehydrogenase activity which is a measure of respiring cells. Thus the MTT assay is a measure of cell viability and cell proliferation. While this assay is a standard assay for cytotoxicity, FACS analysis of PI-stained DNA confirmed that induction of apoptosis was occurring at a high level with simvastatin in FS and with the simvastatin combination with 25-OHC in LDS, and was consistent with the MTT data.

The oxysterol enhancement of statin cytotoxicity worked very successfully using HeLa cells. However, cancers are very heterogeneous and it was important to investigate other cancer cell lines to determine if they responded the same way as the HeLa cells. The cell lines investigated reflected a number of different cancer types. Investigation of the statin induced cytotoxicity in these cell lines showed a broad range of $ED_{50}$ concentrations. Statin sensitivity differs in HeLa cells in FS vs. LDS. The cell lines KYSE-70, HepG2 and HT-29 were similar to HeLa in this respect while no significant difference was observed with the other cell lines (A-498, DU-145, MCF-7 and MeWo). To explore this difference further, all cell lines were tested for the presence of a sterol feedback response. This response was present in the cell lines which showed different statin sensitivity in FS vs. LDS, while it was absent in the other cell lines.

Loss of sterol feedback was reported very early on in liver cancer models, although sterol feedback remains present in HepG2 cell line (Siperstein & Fagan 1964). The sterol feedback response has been investigated the most with respect to prostate cancer. Absence of a sterol feedback response has previously been reported for DU-145 and PC-3 cells, and deregulated processing of SREBPs is associated with progression to androgen-independence (Chen & Hughes-Fulford 2001; Ettinger et al. 2004b). However, a conflicting report shows the presence of a sterol feedback response in PC-3 and LNCaP prostate cancer cell lines, although DU-145 cells were not investigated in this study (Krycer et al. 2009). Whether the sterol feedback response is intact in other cancer cell lines has not been investigated. The absence of this response would be advantageous to the cancer cell as it ensures a consistent high level supply of mevalonate and other essential sterol intermediates to support persistent cell growth. The absence of a sterol feedback response in the cell lines

shown here is interesting and indicates that this may be a regular feature in cancer. The analysis here did not give any insight into the mechanism underlying the absence of the sterol feedback response and was not pursued in this work. It would be interesting to determine if this lack of feedback correlates with a more aggressive cancer phenotype, however this aspect was not pursued here.

The sterol feedback response was evident in HT-29, HepG2 and KYSE-70 but the response differed between the cell lines. HT-29 were unusual in several respects by comparison with HeLa cells. Like HeLa, HT-29 cells were more resistant to statin cytotoxicity in LDS vs. FS and they exhibited sterol feedback response in FS conditions. However in LDS conditions, HT-29 cells were highly sensitive to cytotoxicity induced by 25-OHC. The reason for this increased sensitivity to oxysterol cytotoxicity seen here compared to in HeLa is unclear.

In FS, enhancement of statin cytotoxicity with 25-OHC in HT-29 cells was significant and correlated with the reduction of SREBP/HMGCR luciferase reporter readout by 25-OHC. Enhancement of statin cytotoxicity with 25-OHC in HT-29 in LDS was also investigated, but because of the heightened sensitivity to 25-OHC induced cytotoxicity, a low concentration of 25-OHC or 19-OHC was used. This concentration was not sufficient to reduced the SREBP/HMGCR luciferase reporter readout (Figure 6.15D), and the inclusion of this concentration of the oxysterols had little impact in enhancing the statin cytotoxicity (Figure 6.15C). Immunoblot analysis of HT-29 in FS was as expected with respect to HMGCR and nSREBP2. Both were increased in response to statin and this increase was blocked by 25-OHC with 19-OHC being less effective. The result from the immunoblot analysis of HT-29 in LDS was surprising. The nSREBP2 and HMGCR were substantially elevated

in response to statin, however the presence of the low amount of 25-OHC decreased nSREBP2 to background levels but had only a minor effect on HMGCR levels. Given that nSREBP2 is virtually absent, SREBP/HMGCR luciferase reporter readout should be highly suppressed but this was not the case (Figure 6.15D). This indicates in LDS conditions that the sterol feedback response in HT-29 is intact with respect to SREBP processing but that SREBP2 regulation of HMGCR is uncoupled at the transcriptional level, as evidenced by the SREBP/HMGCR luciferase reporter readout. There is also the possibility that HMGCR protein stability is also being deregulated. The implication of this finding is that certain cancers may be able to adapt to changing dietary conditions with respect to HMGCR regulation and further investigations will be necessary to explore the different HMGCR response in FS vs. LDS.

HepG2 did not exhibit any difference to 25-OHC induced cytotoxicity between FS and LDS and the sterol feedback response in relation to 25-OHC and 19-OHC was evident in both culture conditions. The oxysterols enhance statin cytotoxicity at low to medium concentrations of simvastatin in both FS and LDS, but at higher statin concentrations in FS and LDS, the oxysterols appeared to have a slightly protective effect. The reasons for this are unclear but given that high statin concentrations are used, it is possible that the cytotoxicity induced at the higher concentrations is due to a mechanism(s) outside of HMGCR inhibition, especially as the statin cytotoxicity at higher concentrations was only rescued to a limited extent with mevalonate (Figure 6.21C and 6.21D). Immunoblot analysis of HMGCR and nSREBP2 in HepG2 cells in FS and LDS in the presence or absence of oxysterol yielded somewhat similar to HeLa cells, in that 25-OHC blocked the statin induced increase in HMGCR and nSREBP2. Also similar to HeLa, 19-OHC had a minor effect on nSREBP2 but

reduced HMGCR to background levels. This supports the idea discussed earlier that 19-OHC is primarily affecting the stability of HMGCR protein. Overall, the enhancing effects of oxysterols on statin cytotoxicity observed in HepG2 at lower statin concentrations are consistent with the enhancing effects of oxysterols seen in HeLa, and seen in HT-29 in FS only. However, further investigation is required to elucidate the mechanism(s) of statin cytotoxicity at higher statin concentrations.

The response of KYSE-70 cells was similar to HepG2 in FS, in that the oxysterols enhance statin cytotoxicity at low to medium concentrations of simvastatin but to a lesser extent at the higher statin concentrations. Also similar to HepG2, the statin cytotoxicity at higher concentrations was only rescued to a limited extent with mevalonate in KYSE-70 (Figure 6.21E and 6.21F). This supports the idea that the cytotoxic effects of statins are not limited to inhibition of HMGCR at higher concentrations. In LDS, the KYSE-70 cells were more similar to HT-29 in that they had an increased sensitivity to cytotoxicity induced by 25-OHC, which meant that a low concentration of 25-OHC or 19-OHC was used to investigate oxysterol enhancement of statin cytotoxicity with in LDS. This concentration used was not sufficient to reduced the SREBP/HMGCR luciferase reporter readout (Figure 6.19D), and the inclusion of this concentration of the oxysterols had little impact in enhancing the statin cytotoxicity in LDS (Figure 6.19C). Immunoblot analysis in KYSE-70 for simvastatin and 25-OHC was as expected in FS, with 25-OHC reducing both nSREBP2 and HMGCR. However, the 19-OHC appeared to behave differently in the FS compared to HepG2 and HeLa, as nSREBP2 processing was reduced to almost the same extent as with 25-OHC while HMGCR was also substantially reduced. The results for KYSE-70 in LDS were more surprising. 25-OHC reduced both nSREBP2 and HMGCR substantially yet the HMGCR reduction

was not well reflected in the statin cytotoxicity results in the presence of 25-OHC. The response to 19-OHC in LDS was almost absent. This was very different to 25-OHC and also different to what was observed in FS. Overall, the enhancing effects of oxysterols on statin cytotoxicity observed in KYSE-70 in FS are consistent with the enhancing effects of oxysterols seen in HeLa and HepG2, and in HT-29 in FS only. Similar to HepG2, due to the limited rescue of mevalonate on statin cytotoxicity in KYSE-70, further investigation is required to elucidate the mechanism(s) of statin cytotoxicity at higher statin concentrations.

The results presented here show that different cancer cell lines have related yet different responses to statin induced cytotoxicity and enhancing of statin cytotoxicity with oxysterol. Results in HeLa, HT-29, HepG2 and KYSE-70 show that lowering statin sensitivity using oxysterols is a valid approach in FS conditions. However, the different responses of the cell lines in LDS indicate that dietary influences may have a significant impact on the efficacy of this approach. The results presented here give significant new insight into the potential use of statins as anticancer agents and indicate approaches to enhance their efficacy. Further elucidation of the mechanisms underlying the deregulated response in cells where the feedback is absent and in cells where the feedback is altered in LDS conditions will provide additional insights and progress towards using statins as anticancer agents.

# Chapter 7
General Discussion

The SREBP family of transcription factors are central to regulating *de novo* cholesterol and fatty acid biosynthesis. The aims of this thesis were to gain further insight into the regulatory aspects surrounding SREBP processing and also to investigate the potential of exploiting the SREBP pathway in the treatment of cancer.

The interaction between SCAP and SREBP is essential for both SREBP protein stability and in regulating SREBP processing. The interaction has been localised to the respective CTDs of each protein, but has not been elucidated. Mapping the exact binding site of the SREBP CTDs within SCAP would give valuable insight into the control and regulation of SREBP processing and would shed light on the regulation surrounding differential activation of SREBP1 and SREBP2. The knowledge could also contribute to development of an inhibitor of the SREBP-SCAP interaction. Inhibiting this interaction has major relevance to disease including cancer as blocking the interaction could enhance cell killing. Blocking this interaction could also reduce lipid biosynthesis and prove beneficial in the treatment of obesity. Significant obstacles were encountered in purifying recombinant SREBP CTDs and limited the prospect of mapping the site on SCAP to which SREBP1 and SREBP2 bind. Preliminary peptide array analysis using $SREBP2_{CTD}$-$His_6$ identified peptides in $SCAP_{CTD}$ that could potentially be key in the interaction. However, these results were not reproduced in a repeat peptide array. The reason for this is not clear but may be related to the difficulty in preparing good quality native SREBP. However, peptide array analysis using $SREBP1_{CTD}$-$His_6$ identified multiple amino acid stretches in $SCAP_{CTD}$ that could potentially be key in the interaction, and these were reproduced in a repeat peptide array. Attempts to narrow down the $SREBP1_{CTD}$-$His_6$ binding site in SCAP further using alanine scanning arrays of the identified amino acid stretches were unsuccessful for reasons unknown. Mutagenesis of these

candidate residues in the context of the full length SCAP protein is required to assess their impact on the SCAP-SREBP interaction. Due to the limitations presented in preparing good quality native SREBP, time constraints did not permit these functional studies to be performed within the scope of this thesis.

PGRMC1 was clearly identified as interacting directly with SCAP and INSIG1 by Suchanek et al in 2005 using photo cross-linking of proteins and this prompted an investigation of PGRMC1s influence on SREBP reported in this thesis, in particular with respect to regulation of SREBP processing. Investigation of PGRMC1 as a putative regulator of SREBP processing indicated that it did not have any effect under the conditions tested here that could be attributed to direct regulation of SREBP processing,. However, while the results indicated that PGRMC1 did not affect SREBP processing, and P4 did not appear to impact on this, our studies did highlight novel roles for both PGRMC1 and SCAP in mediating cytotoxic actions of P4 under lipid depleted conditions as at high concentrations of P4 LDS protected against cell killing whereas the protection was absent in the presence of over-expressed PRGMC1 or SCAP. A role for SCAP in P4-induced cytotoxicity is a novel finding, and suggests a role for SCAP in cell response to P4 in addition to its role in SREBP processing. These novel findings in relation to P4 were not followed up within the scope of the aims of this thesis, but the significance of this finding merits further investigation.

INSIG1 is a well characterised protein with respect to its role in negative regulation of both SREBP processing and HMGCR protein stability. However, there are two INSIG1 isoforms produced from INSIG1 mRNA through the use of two alternative in-frame translational start sites. The work presented on INSIG1 sought to

investigate the reason for the evolutionary conservation of the two in-frame start sites present within the INSIG1 transcript, and to discern the functional significance of the generation of two INSIG1 isoforms through alternate translation start sites. The results indicate that the presence of the two start sites is highly conserved among vertebrates and is also present in the fission yeast homolog, Ins-1. Conservation of the Kozak sequence surrounding the two start sites suggests translation initiation in other vertebrate species is likely to occur similarly to the human INSIG1scenario. The results presented indicate that there are no significant functional differences between the two human INSIG1 isoforms with respect to the current known functions of INSIG1 protein, but novel function(s) of the isoforms could not be ruled out. Bioinformatic analysis suggested a possible regulatory mechanism surrounding isoform expression involving ribosome stalling, but confirmation of such regulation remains to be established. However, without a functional difference between the two isoforms, the significance of having such a regulation is unclear.

During the course of this research, 19-OHC was identified as a novel negative regulator of SREBP processing and HMGCR protein stability. The ability of 19-OHC to decrease HMGCR at the protein level was achieved at concentrations below that required to inhibit of SREBP processing and HMGCR promoter activity. The action of 19-OHC is different than cholesterol with respect to SREBP feedback as the latter does not affect HMGCR stability. The action of 19-OHC is similar to 25-OHC in that it promotes degradation of HMGCR and at higher concentrations reduces SREBP activity to a certain extent. The data suggests that its efficacy in promoting degradation of HMGCR is similar to 25-OHC but its efficacy in reducing SREBP processing is lower. In previous reports 19-OHC has been used as a control for 25-OHC, the results presented here show that 19-OHC is not suitable as a control

for 25-OHC or other oxysterols affecting HMGCR stability or SREBP processing. Further characterisation of 19-OHC with respect to INSIG-mediated regulation of SREBP processing and HMGCR degradation is necessary to confirm that it is working in a similar manner to 25-OHC. 19-OHC is reported as a common oxysterol found in cholesterol-rich foods, however how 19-OHC is produced remains unknown and a functional role for 19-OHC has not been reported. Regulation of cholesterol biosynthesis by 19-OHC adds to the knowledge on oxysterol and dietary regulation of SREBP processing. It would be interesting to see if 19-OHC would also function similarly to other oxysterols in other manners, such as in LXR signalling.

One of the most interesting findings in this thesis is that targeted inhibition of SREBP processing is a viable means of enhancing statin cytotoxicity and thus lowering the statin concentration required to kill cancer cells. The potential use of statins as anti-cancer agents is limited by the high concentrations of statins required to induce cell death. The results presented here indicate that the inherent ability of statins to increase their own target HMGCR contributes significantly to this resistance to statin cytotoxicity. Previous studies whereby HMGCR was targeted post-transcriptionally with tocotrienols showed that lowering HMGCR protein had synergistic effects with statin in inducing cytotoxicity. In the approach presented a superior effect was considered achievable since targeted inhibition of SREBP2 processing would reduce HMGCR at both mRNA and protein levels, but would also prevent essential cholesterol uptake through preventing the statin-associated increase in LDLR. Although not assessed in the work presented here, inhibition of SREBP processing could also negatively impact on the expression of other genes essential to cancer cell survival, such as FASN.

The finding that half of the cancer cell lines screened here displayed an increased resistance to statin cytotoxicity under lipid depleted conditions has important implications for considering the impact of diet on both clinical trials for potential use of statins as anti-cancer agents but also in interpreting the data from epidemiology studies investigating links between cancer incidence and the use of statins.

The finding that the other half of the cancer cell lines screened here displayed a lack of sterol feedback response in SREBP processing is consistent with reports for a subset of AML and prostate cancers so far. However, this finding suggests that evading this feedback response is a more common event than previously expected and now extends to cell lines from breast, renal and melanoma cancer types. Deregulation of the SREBP pathway is presumably advantageous to cancer cell survival as it provides a sustained increase in mevalonate levels. Understanding the mechanisms underlying this deregulation is important to consider with respect to the potential use of statins as anti-cancer agents. While cell lines lacking a feedback response were not explored in the current investigation, oxysterols may also be capable of enhancing statin cytotoxicity in these cell lines, by promoting HMGCR degradation, but this remains to be investigated.

Another key finding from this research is that mevalonate does not rescue cytotoxicity induced at higher concentrations of statins in the cancer cell lines screened (40-100 μM dose range). This would suggest that statin cytotoxicity is occurring via a mechanism outside of mevalonate limitation at higher concentrations and thus is independent of HMGCR activity. This is an important finding with respect to the potential use of statins as anti-cancer agents as understanding the mechanism of cytotoxicity is important for drug development and in understanding

potential side effects. Thus further investigation of the mechanisms underlying statin cytotoxicity at high concentrations is necessary.

Overall, the work presented here supports the potential use of statins as anti-cancer agents and has raised some important issues for consideration for the use of statins in this context. This work has also presented targeted inhibition of SREBP processing as a viable method of lowering statin doses required for cancer cell death. However this work has also highlighted that this approach may be limited if the statin induced cytotoxicity is not caused by inhibition of HMGCR.

***Summary of Thesis Achievements***

The first aim of this thesis was to investigate the possibility that SREBP1 and SREBP2 bound distinct sites within the CTD of SCAP through mapping their interaction sites. Progress in bringing this aim to completion was limited by difficulties in obtaining high quality purified $SREBP_{CTD}$ proteins. However, significant steps were taken towards achieving this aim by identifying candidate SREBP binding residues within $SCAP_{CTD}$. Interestingly, the preliminary results presented in this thesis suggest that SREBP1 and SREBP2 may actually bind to a common site within the CTD of SCAP. The residues identified here require follow up by SDM within the full length SCAP protein and functional analysis with respect to their role in binding SREBP.

The second aim of this thesis was to further characterise proteins which interact with the SCAP:SREBP complex with respect to their roles in regulating SREBP activation and cholesterol biosynthesis. Two proteins were investigated; PGRMC1 and INSIG1. The results presented in this thesis indicate that PGRMC1 does not regulate SREBP processing. However, the experiments performed have highlighted a potential role for both PGRMC1 and SCAP in mediating the cytotoxic action of progesterone under lipid depleted conditions, which merits follow up investigation.

INSIG1 has two protein isoforms produced through the use of two in-frame translational start sites. The aim was to investigate if the isoforms served different purposes with respect to the two known functions of INSIG1, which are negative regulation of SREBP processing and HMGCR protein stability under high sterol conditions. The results presented in this thesis conclude that the two isoforms of INSIG1 are not produced to differentially mediate the functions of INSIG1 in

response to sterols as both isoforms were individually capable of inhibiting SREBP processing and promoting HMGCR degradation.

The final aim of this thesis was to investigate inhibition of SREBP processing as a means to lower the concentration of statin required to induce cancer cell death. The results presented in this thesis show that inhibition of SREBP processing using sterols is a viable method to enhance statin induced cancer cell death and thus lower the statin concentration required to achieve cancer cell death. This has important implications for the use of statins as a chemotherapeutic drug since their use is currently limited by inability to achieve serum concentrations high enough to achieve cancer cell death. Lowering the effective cytotoxic concentration of statins may also limit adverse side effects which are associated with high statin doses. The work from this thesis has also highlighted a number of key issues which require consideration for the use of statins as a chemotherapeutic, including a) the potential influence of diet as a number of cancer cell lines were found to be more resistant to statin induced cell death in lipid depleted conditions, and b) that high concentratons of statins may be inducing cell death by mechanism(s) outside of inhibiting the catalytic activity of HMGCR.

Overall, the work presented in this thesis has contributed to the knowledge base surrounding regulation of SREBP proteins and has offered a means to further the use of statins as a chemotherapeutic drug through manipulation of the SREBP pathway.

# Bibliography

Adams, C.M. et al., 2004. Cholesterol and 25-hydroxycholesterol inhibit activation of SREBPs by different mechanisms, both involving SCAP and Insigs. *Journal of Biological Chemistry*, 279(50), pp.52772–80.

Adams, C.M., Goldstein, J.L. & Brown, M.S., 2003. Cholesterol-induced conformational change in SCAP enhanced by Insig proteins and mimicked by cationic amphiphiles. *PNAS*, 100(19), pp.10647–10652.

Adams, D.R., Ron, D. & Kiely, P. a, 2011. RACK1, A multifaceted scaffolding protein: Structure and function. *Cell communication and signaling : CCS*, 9(1), p.22.

Adams, D.R., Ron, D. & Kiely, P.A., 2011. RACK1 , A multifaceted scaffolding protein : Structure and function. *Cell Communication and Signaling*, 9(1), p.22.

Ahmed, I.S. et al., 2010. Progesterone Receptor Membrane Component 1 ( Pgrmc1 ): A Heme-1 Domain Protein That Promotes Tumorigenesis and Is Inhibited by a Small Molecule □. *Journal of Pharmacology and Experimental Therapeutics*, 333(2), pp.564–573.

Alakurtti, S. et al., 2006. Pharmacological properties of the ubiquitous natural product betulin. *European journal of pharmaceutical sciences*, 29(1), pp.1–13. Available at: http://www.ncbi.nlm.nih.gov/pubmed/16716572

Alberts, A. et al., 1980. Mevinolin: A highly potent competitive inhibitor of hydroxymethylglutaryl-coenzyme A reductase and a cholesterol-lowering agent. *Proceedings of the National Academy of Sciences of the United States of America*, 77(7), pp.3957–3961.

Alsheikh-Ali, A. a et al., 2008. Statins, low-density lipoprotein cholesterol, and risk of cancer. *Journal of the American College of Cardiology*, 52(14), pp.1141–7. Available at: http://www.ncbi.nlm.nih.gov/pubmed/18804740

Altmann, S.W. et al., 2004. Niemann-Pick C1 Like 1 Protein Is Critical for Intestinal Cholesterol Absorption. *Science*, 303, pp.1200–1204.

Amemiya-kudo, M. et al., 2002. Transcriptional activities of nuclear SREBP-1a , -1c , and -2 to different target promoters of lipogenic and cholesterogenic genes. *Journal of Lipid Research*, 43, pp.1220–1235.

Aronow, W.S., 2013. Treatment of Hypercholesterolemia. *Journal of Clinical and Experimental Cardiology*, pp.1–8.

Aye, I.L.M.H. et al., 2010. Placental ABCA1 and ABCG1 transporters efflux cholesterol and protect trophoblasts from oxysterol induced toxicity. *Biochimica et biophysica acta*, 1801(9), pp.1013–24.

Ball, L.J. et al., 2005. Recognition of proline-rich motifs by protein-protein-interaction domains. *Angewandte Chemie (International ed. in English)*, 44(19), pp.2852–69.

Banker, D.E. et al., 2004. Cholesterol synthesis and import contribute to protective cholesterol increments in acute myeloid leukemia cells. *Blood*, 104(6), pp.1816–24.

Baulieu, E. & Schumacher, M., 2000. Progesterone as a neuroactive neurosteroid, with special reference to the effect of progesterone on myelination. *Steroids*, 65(10-11), pp.605–12.

Bien, C.M. & Espenshade, P.J., 2010. Sterol Regulatory Element Binding Proteins in Fungi : Hypoxic Transcription Factors Linked to Pathogenesis. *Eukaryotic Cell*, 9(3), pp.352–359.

Bistolas, N. et al., 2005. Cytochrome P450 biosensors-a review. *Biosensors & bioelectronics*, 20(12), pp.2408–23.

Björkhem-Bergman, L., Lindh, J.D. & Bergman, P., 2011. What is a relevant statin concentration in cell experiments claiming pleiotropic effects? *British journal of clinical pharmacology*, 72(1), pp.164–5.

Bocci, G. et al., 2005. Fluvastatin synergistically enhances the antiproliferative effect of gemcitabine in human pancreatic cancer MIAPaCa-2 cells. *British journal of cancer*, 93(3), pp.319–30.

Bonetti, P.O. et al., 2003. Statin effects beyond lipid lowering — are they clinically relevant ? *European Heart Journal*, 24, pp.225–248.

Boudreau, D.M., Yu, O. & Johnson, J., 2010. Statin use and cancer risk: a comprehensive review. *Expert opinion on drug safety*, 9(4), pp.603–21.

Bressler, J. et al., 2009. The INSIG2 rs7566605 genetic variant does not play a major role in obesity in a sample of 24,722 individuals from four cohorts. *BMC medical genetics*, 10, p.56.

Brown, A.J. et al., 2002a. Cholesterol addition to ER membranes alters conformation of SCAP, the SREBP escort protein that regulates cholesterol metabolism. *Molecular cell*, 10(2), pp.237–45.

Brown, A.J. et al., 2002b. Cholesterol addition to ER membranes alters conformation of SCAP, the SREBP escort protein that regulates cholesterol metabolism. *Molecular cell*, 10(2), pp.237–45.

Brown, M. et al., 1978. Induction of 3-Hydroxy-3-methylglutaryl Coenzyme A Reductase Activity in Human Fibroblasts Incubated with Compactin ( ML-236B ), A Competitive Inhibitor of the Reductase. *Journal of Biological Chemistry*, 253, pp.1121–1128.

Brown, M., Dana, S. & Goldstein, J., 1973. Regulation of 3-Hydroxy-3-Methylglutaryl Coenzyme A Reductase Activity in Human Fibroblasts by Lipoproteins. *Proceedings of the National Academy of Sciences of the United States of America*, 70(7), pp.2162–2166.

Brown, M. & Goldstein, L., 1999. A proteolytic pathway that controls the cholesterol content of membranes , cells , and blood. *Proceedings of the National Academy of Sciences of the United States of America*, 96(September), pp.11041–11048.

Brown, M.S. & Goldstein, J.L., 1986. A receptor-mediated pathway for cholesterol homeostasis. *Science*, 232(4746), pp.34–47.

Brown, M.S. & Goldstein, J.L., 2004. A tribute to Akira Endo , discoverer of a " Penicillin " for cholesterol. *Atherosclerosis Supplements*, 5, pp.13–16.

Brown, M.S. & Goldstein, J.L., 2009. Cholesterol feedback: from Schoenheimer's bottle to Scap's MELADL. *Journal of lipid research*, 50 Suppl(50), pp.S15–27.

Browning, D.R.L. & Martin, R.M., 2007. Statins and risk of cancer: a systematic review and metaanalysis. *International journal of cancer*, 120(4), pp.833–43. Available at: http://www.ncbi.nlm.nih.gov/pubmed/17131313

Burg, J.S. et al., 2009. Insig Regulates HMG-CoA Reductase by Controlling Enzyme Phosphorylation in Fission Yeast. *Cell Metabolism*, 8(6), pp.522–531.

Burkhardt, R. et al., 2008. Common SNPs in HMGCR in micronesians and whites associated with LDL-cholesterol levels affect alternative splicing of exon13. *Arteriosclerosis, thrombosis, and vascular biology*, 28(11), pp.2078–84.

Cafforio, P. et al., 2005. Statins activate the mitochondrial pathway of apoptosis in human lymphoblasts and myeloma cells. *Carcinogenesis*, 26(5), pp.883–891.

Cahill, M. a, 2007. Progesterone receptor membrane component 1: an integrative review. *The Journal of steroid biochemistry and molecular biology*, 105(1-5), pp.16–36.

Calleros, L. et al., 2009. Oncogenic Ras, but not (V600E)B-RAF, protects from cholesterol depletion-induced apoptosis through the PI3K/AKT pathway in colorectal cancer cells. *Carcinogenesis*, 30(10), pp.1670–7.

Campbell, M.J. et al., 2006. Breast cancer growth prevention by statins. *Cancer research*, 66(17), pp.8707–14.

Candido, J. & Hagemann, T., 2013. Cancer-related inflammation. *Journal of clinical immunology*, 33 Suppl 1(November 2012), pp.S79–84.

Chan, K.K.W., Oza, A.M. & Siu, L.L., 2003. The Statins as Anticancer Agents. *Clinical Cancer Research*, 9, pp.10–19.

Chan, T. et al., 2013. Statin use and the risk of esophageal cancer : a case-control study. *InformaHealthcare; Original Research*, pp.293–298.

Chatterjee, S. et al., 2009. Identification of Novel Genes and Pathways Regulating SREBP Transcriptional Activity. *PLoS ONE*, 4(4), p.e5197.

Che, Y. et al., 2012. Differential regulation of HMG-CoA reductase and Insig-1 by enzymes of the ubiquitin- proteasome system. *Molecular Biology of the Cell*, 23, pp.4484–4495.

Chen, S. et al., 2004. Interaction of Gbeta/gamma with RACK1 and other WD40 repeat proteins. *Journal of Molecular and Cellular Cardiology*, 37, pp.399–406.

Chen, Y. & Hughes-Fulford, M., 2001. Human prostate cancer cells lack feedback regulation of low-density lipoprotein receptor and its regulator, SREBP2. *International journal of cancer*, 91(1), pp.41–5.

Cheng, Z. et al., 2004. Crystal structure of Ski8p , a WD-repeat protein with dual roles in mRNA metabolism and meiotic recombination. *Protein Science*, 13, pp.2673–2684.

Christenson, L.K. et al., 1998. Oxysterol Regulation of Steroidogenic Acute Regulatory Protein Gene Expression : Structural Specificity And Transcriptional And Posttranscriptional Actions. *Journal of Biological Chemistry*, 273, pp.30729–30735.

Christian, A. et al., 1997. Use of cyclodextrins for manipulating cellular cholesterol content. *Journal of lipid research*, 38, pp.2264–2272.

Cichewicz, R.H. & Kouzi, S. a, 2004. Chemistry, biological activity, and chemotherapeutic potential of betulinic acid for the prevention and treatment of cancer and HIV infection. *Medicinal research reviews*, 24(1), pp.90–114.

Clarke, P.R. & Hardie, D.G., 1990. Regulation of HMG-CoA reductase: identification of the site phosphorylated by the AMP-activated protein kinase in vitro and in intact rat liver. *The EMBO journal*, 9(8), pp.2439–46.

Clendening, J.W., Pandyra, Aleks, et al., 2010. Dysregulation of the mevalonate pathway promotes transformation. *PNAS*, 107(34), pp.15051–15056.

Clendening, J.W., Pandyra, Aleksandra, et al., 2010. Exploiting the mevalonate pathway to distinguish statin-sensitive multiple myeloma. *Blood*, 115(23), pp.4787–97.

Craven, R.J., 2008. PGRMC1: a new biomarker for the estrogen receptor in breast cancer. *Breast cancer research : BCR*, 10(6), p.113.

Cronin, M. et al., 2010. Orally Administered Bifidobacteria as Vehicles for Delivery of Agents to Systemic Tumors. *The American Society of Gene and Cell Therapy*, 18(7), pp.1397–1407.

Crudden, G., Chitti, R.E. & Craven, R.J., 2006. Hpr6 ( Heme-1 Domain Protein ) Regulates the Susceptibility of Cancer Cells to Chemotherapeutic Drugs. *The Journal of Pharmacology and Experimental Therapeutics*, 316(1), pp.448–455.

Dale, K.M. et al., 2006. Statins and Cancer Risk. *Journal of American Medical Association*, 295(1), pp.74–80.

Davis, H.R. et al., 2004. Niemann-Pick C1 Like 1 (NPC1L1) is the intestinal phytosterol and cholesterol transporter and a key modulator of whole-body cholesterol homeostasis. *Journal of Biological Chemistry*, 279(32), pp.33586–92.

DeBose-Boyd, R. a, 2008. Feedback regulation of cholesterol synthesis: sterol-accelerated ubiquitination and degradation of HMG CoA reductase. *Cell research*, 18(6), pp.609–21.

DeBose-Boyd, R. a et al., 1999. Transport-dependent proteolysis of SREBP: relocation of site-1 protease from Golgi to ER obviates the need for SREBP transport to Golgi. *Cell*, 99(7), pp.703–12.

Demierre, M.-F. et al., 2005. Statins and cancer prevention. *Nature reviews. Cancer*, 5(12), pp.930–42. Available at:

Diczfalusy, U., 2013. On the formation and possible biological role of 25-hydroxycholesterol. *Biochimie*, 95(3), pp.455–60.

Difilippantonio, S. et al., 2003. Gene expression profiles in human non-small and small-cell lung cancers. *European Journal of Cancer*, 39(13), pp.1936–1947.

Du, X. et al., 2006. Involvement of Akt in ER-to-Golgi Transport of SCAP / SREBP : A Link between a Key Cell Proliferative Pathway and Membrane Synthesis. *Molecular Biology of the Cell*, 17(June), pp.2735–2745.

Duncan, E.A. et al., 1997a. Cleavage Site for Sterol-regulated Protease Localized to a Leu-Ser Bond in the Lumenal Loop of Sterol Regulatory Element Binding Protein-2. *Journal of Biological Chemistry*, 272(19), pp.12778–12785.

Duncan, E.A. et al., 1997b. Cleavage Site for Sterol-regulated Protease Localized to a Leu-Ser Bond in the Lumenal Loop of Sterol Regulatory Element Binding Protein-2. *Journal of Biological Chemistry*, 272(19), pp.12778–12785.

Duncan, E.A. et al., 1998. Second-site Cleavage in Sterol Regulatory Element-binding Protein Occurs at Transmembrane Junction as Determined by Cysteine Panning Second-site Cleavage in Sterol Regulatory Element-binding Protein

Occurs at Transmembrane Junction as Determined by Cystei. *Journal of Biological Chemistry*, 273, pp.17801–17809.

Dyer, B.W. et al., 2000. A Noncommercial Dual Luciferase Enzyme Assay System for Reporter Gene Analysis. *Analytical Biochemistry*, 282, pp.158–161.

Eberlé, D. et al., 2004. SREBP transcription factors: master regulators of lipid homeostasis. *Biochimie*, 86(11), pp.839–48.

Edwards, P. a et al., 2000. Regulation of gene expression by SREBP and SCAP. *Biochimica et biophysica acta*, 1529(1-3), pp.103–13.

Egan, A. & Colman, E., 2011. Weighing the benefits of high-dose simvastatin against the risk of myopathy. *The New England journal of medicine*, pp.2011–2013.

Engelking, L.J. et al., 2004. Overexpression of Insig-1 in the livers of transgenic mice inhibits SREBP processing and reduces insulin-stimulated lipogenesis. *The Journal of clinical investigation*, 113(8), pp.1168–1175.

Engelking, L.J. et al., 2005. Schoenheimer effect explained — feedback regulation of cholesterol synthesis in mice mediated by Insig proteins. *The Journal of clinical investigation*, 115(9), pp.2489–2498.

Escobar, C., Echarri, R. & Barrios, V., 2008. Relative safety profiles of high dose statin regimens. *Vascular Health and Risk Management*, 4(3), pp.525–533.

Espenshade, P.J., Li, W. & Yabe, D., 2002. Sterols block binding of COPII proteins to SCAP , thereby controlling SCAP sorting in ER. *PNAS*, 99(18), pp.11694–11699.

Ettinger, S.L. et al., 2004a. Dysregulation of Sterol Response Element-Binding Proteins and Downstream Effectors in Prostate Cancer during Progression to Androgen Independence *Cancer Research*, pp.2212–2221.

Ettinger, S.L. et al., 2004b. Dysregulation of Sterol Response Element-Binding Proteins and Downstream Effectors in Prostate Cancer during Progression to Androgen Independence *Cancer Research*, 64, pp.2212–2221.

Fan, F. & Wood, K. V, 2007. Bioluminescent Assays for High-Throughput Screening. *ASSAY and Drug Development Technologies*, 5(1), pp.127–136.

Fan, J. & Watanabe, T., 2003. Inflammatory reactions in the pathogenesis of atherosclerosis. *Journal of atherosclerosis and thrombosis*, 10(2), pp.63–71.

Feleszko, W. et al., 2000. Lovastatin Potentiates Antitumor Activity and Attenuates Cardiotoxicity of Doxorubicin in Three Tumor Models in Mice. *Clinical Cancer Research*, 6, pp.2044–2052.

Feleszko, W. et al., 1998. Original Paper Potentiated Antitumour E V ects of Cisplatin and Lovastatin Against MmB16 Melanoma in Mice. *European Journal of Cancer*, 34(3), pp.406–411.

Feramisco, J.D., Goldstein, J.L. & Brown, M.S., 2004. Membrane Topology of Human Insig-1 , a Protein Regulator of Lipid Synthesis *Journal of Biological Chemistry*, 279, pp.8487–8496.

Frangioni, J. & Neel, B., 1993. Solubilisation and Purification of Enzymatically Active Glutathione S-Transferase (pGEX) Fusion Proteins. *Analytical Biochemistry*, 210, pp.179–187.

Garcia-Higuera, I. et al., 1996. Folding of proteins with WD-repeats: comparison of six members of the WD-repeat superfamily to the G protein beta subunit. *Biochemistry*, 35(44), pp.13985–94.

Garenc, C., Julien, P. & Levy, E., 2010. Oxysterols in biological systems: the gastrointestinal tract, liver, vascular wall and central nervous system. *Free radical research*, 44(1), pp.47–73.

Gbelcová, H. et al., 2008. Differences in antitumor effects of various statins on human pancreatic cancer. *International journal of cancer*, 122(6), pp.1214–21.

Ge, L. et al., 2011. Flotillins play an essential role in Niemann-Pick C1-like 1-mediated cholesterol uptake. *Proceedings of the National Academy of Sciences of the United States of America*, 108(2), pp.551–6.

Gérard, P. et al., 2004. Gnotobiotic rats harboring human intestinal microbiota as a model for studying cholesterol-to-coprostanol conversion. *Federation of European Microbiological Societies*, 47, pp.337–343.

Glynn, S. a et al., 2008. The 3-hydroxy-3-methylglutaryl-coenzyme A reductase inhibitors, simvastatin, lovastatin and mevastatin inhibit proliferation and invasion of melanoma cells. *BMC cancer*, 8, p.9.

Goldstein, J., Helgeson, J. & Brown, S., 1979. Inhibition of cholesterol synthesis with compactin renders growth of cultured cells dependent on the low density lipoprotein receptor. *Journal of Biological Chemistry*, 254, pp.5403–5409.

Goldstein, J.L. & Brown, M.S., 2009. The LDL Receptor. *Journal of the American Heart Association*, 29, pp.431–438.

Goldstein, J.L., Debose-boyd, R.A. & Brown, M.S., 2006. Protein Sensors for Membrane Sterols. *Cell*, 124, pp.35–46.

Gong, Y., Lee, J.N., Brown, M.S., et al., 2006. Juxtamembranous aspartic acid in Insig-1 and Insig-2 is required for cholesterol homeostasis. *Proceedings of the National Academy of Sciences of the United States of America*, 103(16), pp.6154–9.

Gong, Y., Lee, J.N., Lee, P.C.W., et al., 2006a. Sterol-regulated ubiquitination and degradation of Insig-1 creates a convergent mechanism for feedback control of cholesterol synthesis and uptake. *Cell Metabolism*, 3(January), pp.15–24.

Gong, Y., Lee, J.N., Lee, P.C.W., et al., 2006b. Sterol-regulated ubiquitination and degradation of Insig-1 creates a convergent mechanism for feedback control of cholesterol synthesis and uptake. *Cell Metabolism*, 3(January), pp.15–24.

Gorin, A., Gabitova, L. & Astsaturov, I., 2012. Regulation of cholesterol biosynthesis and cancer signaling. *Current opinion in pharmacology*, 12(6), pp.710–6.

Graaf, M.R. et al., 2004. The risk of cancer in users of statins. *Journal of clinical oncology*, 22(12), pp.2388–94.

Hager, M.H., Solomon, K.R. & Freeman, M.R., 2006a. The role of cholesterol in prostate cancer. *Current Opinion in Clinical Nutrition and Metabolic Care*, 9, pp.379–385.

Hager, M.H., Solomon, K.R. & Freeman, M.R., 2006b. The role of cholesterol in prostate cancer. *Current opinion in clinical nutrition and metabolic care*, 9(4), pp.379–85.

Hanahan, D. & Weinberg, R.A., 2011. Review Hallmarks of Cancer : The Next Generation. *Cell*, 144(5), pp.646–674.

Hand, R. a & Craven, R.J., 2003. Hpr6.6 protein mediates cell death from oxidative damage in MCF-7 human breast cancer cells. *Journal of cellular biochemistry*, 90(3), pp.534–47.

Hawk, M.A. et al., 1996. Inhibition of lung tumor cell growth in vitro and mouse lung tumor formation by lovastatin. *Cancer Letters*, 109, pp.217–222.

Heemers, H. et al., 2001. Androgens Stimulate Lipogenic Gene Expression in Prostate Cancer Cells by Activation of the Sterol Regulatory Element-Binding Protein Cleavage Activating Protein/Sterol Regulatory Element-Binding Protein Pathway. *Molecular Endocrinology*, 15(10), pp.1817–1828.

Heemers, H. et al., 2004. Identification of an androgen response element in intron 8 of the sterol regulatory element-binding protein cleavage-activating protein gene allowing direct regulation by the androgen receptor. *The Journal of biological chemistry*, 279(29), pp.30880–7.

Heemers, H. V, Verhoeven, G. & Swinnen, J. V, 2006. Androgen activation of the sterol regulatory element-binding protein pathway: Current insights. *Molecular endocrinology*, 20(10), pp.2265–77.

Hegarty, B.D. et al., 2005. Distinct roles of insulin and liver X receptor in the induction and cleavage of sterol regulatory element- binding protein-1c. *PNAS*, 102(3), pp.791–796.

Higgins, D et al., 1994. CLUSTAL W: improving the sensitivity of progressive multiple sequence alignment through sequence weighting, position-specific gap penalties and weight matrix choice. *Nucleic Acids Res*, 22, pp.4673–4680.

Ho, C.K.M. & Strauss III, J.F., 2004. Activation of the control reporter plasmids pRL-TK and pRL-SV40 by multiple GATA transcription factors can lead to aberrant normalization of transfection efficiency. *BMC Biotechnology*, 5, pp.1–5.

Holstein, S. a & Hohl, R.J., 2001. Interaction of cytosine arabinoside and lovastatin in human leukemia cells. *Leukemia research*, 25(8), pp.651–60.

Hoppe, T., Rape, M. & Jentsch, S., 2001. Membrane-bound transcription factors : regulated release by RIP or RUP. *Current Opinion in Cell Biology*, 13, pp.344–348.

Horton, J.D. et al., 1998. Activation of Cholesterol Synthesis in Preference to Fatty Acid Synthesis in Liver and Adipose Tissue of Transgenic Mice Overproducing Sterol Regulatory Element-Binding Protein-2. *The Journal of clinical investigation*, 101(11), pp.2331–2339.

Horton, J.D. et al., 2003. Combined analysis of oligonucleotide microarray data from transgenic and knockout mice identifies direct SREBP target genes. *PNAS*, 100(21), pp.12027–12032.

Horton, J.D., Goldstein, J.L. & Brown, M.S., 2002a. SREBPs : activators of the complete program of cholesterol and fatty acid synthesis in the liver. *The Journal of clinical investigation*, 109(9), pp.1125–1131.

Horton, J.D., Goldstein, J.L. & Brown, M.S., 2002b. SREBPs : activators of the complete program of cholesterol and fatty acid synthesis in the liver. *The Journal of Clinical Investigation*, 109(9), pp.1125–1131.

Hua, X. et al., 1993a. SREBP-2 , a second basic-helix-loop-helix-leucine zipper protein that stimulates transcription by binding to a sterol regulatory element. *Proceedings of the National Academy of Sciences of the United States of America*, 90(December), pp.11603–11607.

Hua, X. et al., 1993b. SREBP-2 , a second basic-helix-loop-helix-leucine zipper protein that stimulates transcription by binding to a sterol regulatory element. *Proceedings of the National Academy of Sciences of the United States of America*, 90(December), pp.11603–11607.

Hua, X. et al., 1996. Sterol resistance in CHO cells traced to point mutation in SREBP cleavage-activating protein. *Cell*, 87(3), pp.415–26.

Hua, X. et al., 1995. Structure of the human gene encoding sterol regulatory element binding protein-1 (SREBF1) and localization of SREBF1 and SREBF2 to chromosomes 17p11.2 and 22q13. *Genomics*, 25(3), pp.667–73.

Huang, W.-C. et al., 2012. Activation of androgen receptor, lipogenesis, and oxidative stress converged by SREBP-1 is responsible for regulating growth and progression of prostate cancer cells. *Molecular cancer research*, 10(1), pp.133–42.

Hughes, A.L. et al., 2007. Dap1/PGRMC1 binds and regulates cytochrome P450 enzymes. *Cell metabolism*, 5(2), pp.143–9.

Hughes, A.L., Todd, B.L. & Espenshade, P.J., 2005. SREBP Pathway Responds to Sterols and Functions as an Oxygen Sensor in Fission Yeast. *Cell*, 120, pp.831–842.

Ibrahim, N. et al., 2000. Pitfall of an internal control plasmid: response of Renilla luciferase (pRL-TK) plasmid to dihydrotestosterone and dexamethasone. *Biotechniques*, (4), pp.782–4.

Ikonen, E., 2008. Cellular cholesterol trafficking and compartmentalization. *Nature reviews. Molecular cell biology*, 9(2), pp.125–38.

Istvan, E.S. & Deisenhofer, J., 2001. Structural mechanism for statin inhibition of HMG-CoA reductase. *Science*, 292(5519), pp.1160–4.

Iuliano, L., 2011. Pathways of cholesterol oxidation via non-enzymatic mechanisms. *Chemistry and physics of lipids*, 164(6), pp.457–68.

Ivanov, I.P. et al., 2010. Initiation context modulates autoregulation of eukaryotic translation initiation factor 1 ( eIF1 ). *PNAS*, 107(42), pp.18056–18060.

Jain, M.K. & Ridker, P.M., 2005. Anti-inflammatory effects of statins: clinical evidence and basic mechanisms. *Nature reviews. Drug discovery*, 4(12), pp.977–87.

Jakóbisiak, M. et al., 1991. Cell cycle-specific effects of Lovastatin. *PNAS*, 88(May), pp.3628–3632.

Jamroz-wiśniewska, A., Wójcicka, G. & Horoszewicz, K., 2007. Liver X receptors ( LXRs ). Part II : Non-lipid effects , role in pathology , and therapeutic implications Receptory wątrobowe X ( LXR ). *Postepy Hig Med Dosw. (online)*, 61, pp.760–785.

Jo, Y. et al., 2011. Sterol-induced degradation of HMG CoA reductase depends on interplay of two Insigs and two ubiquitin ligases, gp78 and Trc8. *PNAS*, 108(51), pp.2–7.

Johnson, T.E. et al., 2004. Statins induce apoptosis in rat and human myotube cultures by inhibiting protein geranylgeranylation but not ubiquinone. *Toxicology and applied pharmacology*, 200(3), pp.237–50.

Joy, T.R. & Hegele, R.A., 2009. Statin-related myopathy. *Annals of Internal Medicine*, 150, pp.858–868.

Kamisuki, S. et al., 2009. A small molecule that blocks fat synthesis by inhibiting the activation of SREBP. *Chemistry & biology*, 16(8), pp.882–92.

Karlson, P., 1969. Terpenoids in Insects. *Proceedings of the Biochemical Society*, p.26.

Kast-woelbern, H.R. et al., 2004. Rosiglitazone Induction of Insig-1 in White Adipose Tissue Reveals a Novel Interplay of Peroxisome Proliferator-activated Receptor γ and Sterol Regulatory Element-binding Protein in the Regulation of Adipogenesis. *Journal of Biological Chemistry*, 279, pp.23908–23915.

Kikuchi, T., Nagata, Y. & Abe, T., 1997. In vitro and in vivo antiproliferative effects of simvastatin , an HMG-CoA reductase inhibitor , on human glioma cells. *Journal of Neuro-Oncology*, 34, pp.233–239.

Kim, J. et al., 1998. Nutritional and Insulin Regulation of Fatty Acid Synthetase and Leptin Gene Expression through ADD1/SREBP1. *Journal of Clinical Investigation*, 101(1), pp.1–9.

Kita, T., Brown, M.S. & Goldstein, J.L., 1980. Feedback Regulation of 3-Hydroxy-3-Methylglutaryl Coenzyme A Reductase in Livers of Mice Treated with Mevinolin , a Competitive Inhibitor of the Reductase. *The Journal of clinical investigation*, 66(November), pp.1094–1100.

Korn, B.S. et al., 1998. Blunted feedback suppression of SREBP processing by dietary cholesterol in transgenic mice expressing sterol-resistant SCAP(D443N). *The Journal of clinical investigation*, 102(12), pp.2050–60.

Kornblau, S.M. et al., 2007. Blockade of adaptive defensive changes in cholesterol uptake and synthesis in AML by the addition of pravastatin to idarubicin + high-dose Ara-C: a phase 1 study. *Blood*, 109(7), pp.2999–3006.

Kozak, M., 1987. An analysis of 5' non-coding sequences from 699 vertebrate messenger RNAs. *Nucleic Acids Res*, (15), pp.8125–8148.

Kozak, M., 1989. Circumstances and Mechanisms of Inhibition of Translation by Secondary Structure in Eucaryotic mRNAs. , 9(11).

Kozak, M., 1986. Influences of mRNA secondary structure on initiation by eukaryotic ribosomes. *Proceedings of the National Academy of Sciences of the United States of America*, 83(9), pp.2850–4.

Kozak, M., 1999. Initiation of translation in prokaryotes and eukaryotes. *Gene*, 234, pp.187–208.

Krauss, R.M. et al., 2008. Variation in the 3-hydroxyl-3-methylglutaryl coenzyme a reductase gene is associated with racial differences in low-density lipoprotein cholesterol response to simvastatin treatment. *Circulation*, 117(12), pp.1537–44.

Kruit, J. et al., 2005. Increased Fecal Neutral Sterol Loss Upon Liver X Receptor Activation Is Independent of Biliary Sterol Secretion in Mice. *Gastroenterology*, 128, pp.147–156.

Krycer, J.R. et al., 2010. The Akt-SREBP nexus: cell signaling meets lipid metabolism. *Trends in endocrinology and metabolism*, 21(5), pp.268–76.

Krycer, J.R., Kristiana, I. & Brown, A.J., 2009. Cholesterol homeostasis in two commonly used human prostate cancer cell-lines, LNCaP and PC-3. *PloS one*, 4(12), p.e8496.

Kwak, B. et al., 2000. Statins as a newly recognized type of immunomodulator. *Nature medicine*, 6(12), pp.1399–402.

Lakkis, F.G. & Billiar, T.R., 2013. Molecular analysis of transplant rejection: marching onward. *The Journal of experimental medicine*, 210(11), pp.2147–9.

Lange, Y. et al., 2008. Effectors of rapid homeostatic responses of endoplasmic reticulum cholesterol and 3-hydroxy-3-methylglutaryl-CoA reductase. *The Journal of biological chemistry*, 283(3), pp.1445–55.

Larsen, S. et al., 2013. Simvastatin effects on skeletal muscle: relation to decreased mitochondrial function and glucose intolerance. *Journal of the American College of Cardiology*, 61(1), pp.44–53.

Law, M.R., Wald, N.J. & Rudnicka, A.R., 2002. Quantifying effect of statins on low density lipoprotein cholesterol , ischaemic heart disease , and stroke : systematic review and meta-analysis. *BMJ*, 326, pp.1423–1427.

Lee, J. & Ye, J., 2004. Proteolytic Activation of Sterol Regulatory Element-binding Protein Induced by Cellular Stress through Depletion of Insig-1. *Journal of Biological Chemistry*, 279(43), pp.45257–45265.

Lee, J.N., Gong, Y., et al., 2006. Proteasomal degradation of ubiquitinated Insig proteins is determined by serine residues flanking ubiquitinated lysines. *PNAS*, 103(13), pp.9–14.

Lee, J.N., Song, B., et al., 2006. Sterol-regulated Degradation of Insig-1 Mediated by the Membrane-bound Ubiquitin Ligase gp78. *Journal of Biological Chemistry*, 281, pp.39308–39315.

Lee, J.N. et al., 2008. Unsaturated Fatty Acids Inhibit Proteasomal Degradation of Insig-1 at a Postubiquitination Step. *Journal of Biological Chemistry*, 283, pp.33772–33783.

Li, A.C. & Glass, C.K., 2004. PPAR- and LXR-dependent pathways controlling lipid metabolism and the development of atherosclerosis. *Journal of lipid research*, 45(12), pp.2161–73.

Li, H.Y. et al., 2003. Cholesterol-modulating agents kill acute myeloid leukemia cells and sensitize them to therapeutics by blocking adaptive cholesterol responses. *Blood*, 101(9), pp.3628–3634.

Li, X. et al., 2014. Fatostatin Displays High Antitumor Activity in Prostate Cancer by Blocking SREBP-Regulated Metabolic Pathways and Androgen Receptor Signaling. *Molecular cancer therapeutics*, ePub ahead.

Li, Y. et al., 2010. Betulin induces mitochondrial cytochrome c release associated apoptosis in human cancer cells. *Molecular carcinogenesis*, 49(7), pp.630–40.

Li, Y., Wang, D. & Chiang, J., 1990. Regulation of cholesterol 7 alpha-hydroxylase in the liver. Cloning,sequencing, and regulation of cholesterol 7 alpha-hydroxylase mRNA. *Journal of Biological Chemistry*, 265(20), pp.12012–12019.

Li, Y.C. et al., 2006. Elevated levels of cholesterol-rich lipid rafts in cancer cells are correlated with apoptosis sensitivity induced by cholesterol-depleting agents. *The American journal of pathology*, 168(4), pp.1107–18; quiz 1404–5.

Lindgren, V. et al., 1985. Human genes involved in cholesterol metabolism: chromosomal mapping of the loci for the low density lipoprotein receptor and 3-hydroxy-3-methylglutaryl-coenzyme A reductase with cDNA probes. *Proceedings of the National Academy of Sciences of the United States of America*, 82(24), pp.8567–71.

Liscum, L., 2000. Niemann-Pick type C mutations cause lipid traffic jam. *Traffic (Copenhagen, Denmark)*, 1(3), pp.218–25.

Liscum, L. & Munn, N.J., 1999. Intracellular cholesterol transport. *Biochimica et biophysica acta*, 1438(1), pp.19–37.

Liu, Y. et al., 2014. Association between statin use and colorectal cancer risk: a meta-analysis of 42 studies. *Cancer causes & control*, 25(2), pp.237–49.

Lordan, S., Mackrill, J.J. & O'Brien, N.M., 2009. Oxysterols and mechanisms of apoptotic signaling: implications in the pathology of degenerative diseases. *The Journal of nutritional biochemistry*, 20(5), pp.321–36.

Lösel, R.M. et al., 2008. Progesterone receptor membrane component 1--many tasks for a versatile protein. *Steroids*, 73(9-10), pp.929–34.

Loughran, G. et al., 2012. Stringency of start codon selection modulates autoregulation of translation initiation factor eIF5. *Nucleic acids research*, 40(7), pp.2898–906.

Luckman, S.P. et al., 1998. Nitrogen-Containing Bisphosphonates Inhibit the Mevalonate Pathway and Prevent Post-Translational Prenylation of GTP-Binding Proteins , Including Ras. *Journal of Bone and Mineral Research*, 13(4), pp.581–589.

Lutz, R.J. et al., 1992. Nucleoplasmic localization of prelamin A : Implications for prenylation-dependent lamin A assembly into the nuclear lamina. *Proceedings of the National Academy of Sciences of the United States of America*, 89, pp.3000–3004.

Ma, X. et al., 2009. NO-1886 up-regulates Niemann-Pick C1 protein (NPC1) expression through liver X receptor alpha signaling pathway in THP-1 macrophage-derived foam cells. *Cardiovascular drugs and therapy*, 23(3), pp.199–206.

Mansouri, M.R. et al., 2008. Alterations in the expression, structure and function of progesterone receptor membrane component-1 (PGRMC1) in premature ovarian failure. *Human molecular genetics*, 17(23), pp.3776–83.

Marquart, T.J. et al., 2010. miR-33 links SREBP-2 induction to repression of sterol transporters. *PNAS*, 107(27), pp.12228–12232.

Matsuda, M. et al., 2001. SREBP cleavage-activating protein (SCAP) is required for increased lipid synthesis in liver induced by cholesterol deprivation and insulin elevation. *Genes & development*, 15(10), pp.1206–16.

May, O., 2008. Mediating Cholesterol Homeostasis through SREBP-2 / LDLR / PCSK9 Signalling. *Cayman Chemical*, March.

Mclean, K.J., Hans, M. & Munro, A.W., 2012. Cholesterol , an essential molecule : diverse roles involving cytochrome P450 enzymes. *Biochemical Society Transactions*, 79, pp.587–593.

Medina, M.W. et al., 2008. Alternative splicing of 3-hydroxy-3-methylglutaryl coenzyme A reductase is associated with plasma low-density lipoprotein cholesterol response to simvastatin. *Circulation*, 118(4), pp.355–62.

Medina, M.W. & Krauss, R.M., 2009. The role of HMGCR alternative splicing in statin efficacy. *Trends in cardiovascular medicine*, 19(5), pp.173–7.

Metherall, J.E., Waugh, K. & Li, H., 1996. Progesterone Inhibits Cholesterol Biosynthesis in Cultured Cells. *Journal of Biological Chemistry*, 271(5), pp.2627–2633.

Meyer, C. et al., 1996. Purification and partial sequencing of high-affinity progesterone-binding site(s) from porcine liver membranes. *European journal of biochemistry / FEBS*, 239(3), pp.726–31.

Mifsud, W. & Bateman, A., 2002. Membrane-bound progesterone receptors contain a cytochrome b5-like ligand-binding domain. *Genome biology*, 3(12), p.RESEARCH0068.

Miller, W.L., 1988. Molecular biology of steroid hormone synthesis. *Endocrine reviews*, 9(3), pp.295–318.

Min, L. et al., 2005. Molecular identification of adrenal inner zone antigen as a heme-binding protein. *The FEBS journal*, 272(22), pp.5832–43.

Mir, S.U.R. et al., 2012. Elevated progesterone receptor membrane component 1/sigma-2 receptor levels in lung tumors and plasma from lung cancer patients. *International journal of cancer. Journal international du cancer*, 131(2), pp.E1–9.

Miraglia, L., King, F. & Damoiseaux, R., 2001. Seeing the light; luminescent reporter gene assays. *Comb Chem High Throughput Screen*, 14(8), pp.648–657.

Miserez, A.R. et al., 2002. Sterol-regulatory element-binding protein (SREBP)-2 contributes to polygenic hypercholesterolaemia. *Atherosclerosis*, 164(1), pp.15–26. Available at: http://www.ncbi.nlm.nih.gov/pubmed/12119189.

Mohn, K.L. et al., 1991. The Immediate-Early Growth Response in Regenerating Liver and Insulin-Stimulated H-35 Cells : Comparison with Serum-Stimulated 3T3 Cells and Identification of 41 Novel Immediate-Early Genes. *Molecular and Cellular Biology*, 11(1), pp.381–390.

Motamed, M. et al., 2011. Identification of luminal Loop 1 of Scap protein as the sterol sensor that maintains cholesterol homeostasis. *The Journal of biological chemistry*, 286(20), pp.18002–12.

Mucci, L. a & Stampfer, M.J., 2014. Mounting evidence for prediagnostic use of statins in reducing risk of lethal prostate cancer. *Journal of clinical oncology*, 32(1), pp.1–2.

Mullauer, F.B., Kessler, J.H. & Medema, J.P., 2009. Betulin is a potent anti-tumor agent that is enhanced by cholesterol. *PloS one*, 4(4), p.e1.

Nagoshi, E. et al., 1999. Nuclear import of sterol regulatory element-binding protein-2, a basic helix-loop-helix-leucine zipper (bHLH-Zip)-containing transcription factor, occurs through the direct interaction of importin beta with HLH-Zip. *Molecular biology of the cell*, 10(7), pp.2221–33.

Nagoshi, E.M.I. & Yoneda, Y., 2001. Dimerization of Sterol Regulatory Element-Binding Protein 2 via the Helix-Loop-Helix-Leucine Zipper Domain Is a

Prerequisite for Its Nuclear Localization Mediated by Importin Beta. *Molecular and Cellular Biology*, 21(8), pp.2779–2789.

Nakajima, T. et al., 1999a. Genomic structure and chromosomal mapping of the human sterol regulatory element binding protein (SREBP) cleavage-activating protein (SCAP) gene. *Journal of human genetics*, 44(6), pp.402–7.

Nakajima, T. et al., 1999b. Genomic structure and chromosomal mapping of the human sterol regulatory element binding protein (SREBP) cleavage-activating protein (SCAP) gene. *Journal of human genetics*, 44(6), pp.402–7.

Nakajima, Y.N. et al., 2004. cDNA Cloning and Characterization of a Secreted Luciferase from the Luminous Japanese Ostracod , Cypridina noctiluca. *Biosci. Biotechnol. Biochem*, 68(3), pp.565–570.

Needham, M. & Mastaglia, F.L., 2014. Statin myotoxicity : A review of genetic susceptibility factors. *Neuromuscular Disorders*, 24(1), pp.4–15.

Neer, N. et al., 1994. The ancient regulatory-protein family of WD-repeat proteins. *Nature*, 371, pp.297–300.

Nei, M. & Kumar, S., 2000. *Molecular Evolution and Phylogenetics*,

Nelson, E.R. et al., 2013. 27-Hydroxycholesterol links hypercholesterolemia and breast cancer pathophysiology. *Science*, 342(6162), pp.1094–8.

Nicoletti, I. et al., 1991. A rapid and simple method for measuring thymocyte apoptosis by propidium iodide staining and flow cytometry. *Journal of Immunological Methods*, 139(2), pp.271–279.

Nie, A.Y. et al., 2006. Predictive Toxicogenomics Approaches Reveal Underlying Molecular Mechanisms of Nongenotoxic Carcinogenicity. *Molecular Carcinogenesis*, 45(August 2005), pp.914–933.

Nielsen, S.F., Nordestgaard, B.G. & Bojesen, S.E., 2012. Statin use and reduced cancer-related mortality. *The New England journal of medicine*, 367(19), pp.1792–802.

Nohturfft, A. et al., 1999. Sterols regulate cycling of SREBP cleavage-activating protein ( SCAP ) between endoplasmic reticulum and Golgi. *Proceedings of the National Academy of Sciences of the United States of America*, 96(September), pp.11235–11240.

Nohturfft, A., Brown, M.S. & Goldstein, J.L., 1998. Sterols regulate processing of carbohydrate chains of wild-type SREBP cleavage-activating protein (SCAP), but not sterol-resistant mutants Y298C or D443N. *Proceedings of the National Academy of Sciences of the United States of America*, 95(22), pp.12848–53.

Nölte, I. et al., 2000. Localization and topology of ratp28, a member of a novel family of putative steroid-binding proteins. *Biochimica et biophysica acta*, 1543(1), pp.123–30.

O Brien, N.M. et al., 2000. Biological Effects of Dietary Cholesterol Oxidation Products. *Irish Journal of Agriculture and Foods Research*, 39(2), pp.265–273.

Olkkonen, V.M., Béaslas, O. & Nissilä, E., 2012. Oxysterols and Their Cellular Effectors. *Biomolecules*, 2(4), pp.76–103.

Ory, D.S., 2004. The niemann-pick disease genes; regulators of cellular cholesterol homeostasis. *Trends in cardiovascular medicine*, 14(2), pp.66–72.

Otaegui-Arrazola, A. et al., 2010. Oxysterols: A world to explore. *Food and chemical toxicology*, 48(12), pp.3289–3303.

Pai, J.T., Brown, M.S. & Goldstein, J.L., 1996. Purification and cDNA cloning of a second apoptosis-related cysteine protease that cleaves and activates sterol regulatory element binding proteins. *Proceedings of the National Academy of Sciences of the United States of America*, 93(11), pp.5437–42.

Parker, B. a, Gregory, S.M., et al., 2013. A randomized trial of coenzyme Q10 in patients with statin myopathy: rationale and study design. *Journal of clinical lipidology*, 7(3), pp.187–93.

Parker, B. a, Capizzi, J. a, et al., 2013. Effect of statins on skeletal muscle function. *Circulation*, 127(1), pp.96–103.

Peet, D.J. et al., 1998. Cholesterol and bile acid metabolism are impaired in mice lacking the nuclear oxysterol receptor LXR alpha. *Cell*, 93(5), pp.693–704.

Pelton, K., Freeman, M.R. & Solomon, K.R., 2012. Cholesterol and prostate cancer. *Current opinion in pharmacology*, 12(6), pp.751–9.

Peluso, J.J. et al., 2005. Expression and function of PAIRBP1 within gonadotropin-primed immature rat ovaries: PAIRBP1 regulation of granulosa and luteal cell viability. *Biology of reproduction*, 73(2), pp.261–70.

Peluso, J.J. et al., 2013. Plasminogen activator inhibitor 1 RNA-binding protein interacts with progesterone receptor membrane component 1 to regulate progesterone's ability to maintain the viability of spontaneously immortalized granulosa cells and rat granulosa cells. *Biology of reproduction*, 88(1), p.20.

Peluso, J.J. et al., 2010. Progesterone inhibits apoptosis in part by PGRMC1-regulated gene expression. *Molecular and cellular endocrinology*, 320(1-2), pp.153–61.

Peluso, J.J. et al., 2006. Progesterone membrane receptor component 1 expression in the immature rat ovary and its role in mediating progesterone's antiapoptotic action. *Endocrinology*, 147(6), pp.3133–40.

Peluso, J.J., 2011. Progesterone signaling mediated through progesterone receptor membrane component-1 in ovarian cells with special emphasis on ovarian cancer. *Steroids*, 76(9), pp.903–909.

Peluso, J.J., Liu, X., et al., 2008. Regulation of ovarian cancer cell viability and sensitivity to cisplatin by progesterone receptor membrane component-1. *The Journal of clinical endocrinology and metabolism*, 93(5), pp.1592–9.

Peluso, J.J., Lodde, V. & Liu, X., 2012. Progesterone regulation of progesterone receptor membrane component 1 (PGRMC1) sumoylation and transcriptional activity in spontaneously immortalized granulosa cells. *Endocrinology*, 153(8), pp.3929–39.

Peluso, J.J., Romak, J. & Liu, X., 2008. Progesterone receptor membrane component-1 (PGRMC1) is the mediator of progesterone's antiapoptotic action in spontaneously immortalized granulosa cells as revealed by PGRMC1 small interfering ribonucleic acid treatment and functional analysis of PGRMC1 mutations. *Endocrinology*, 149(2), pp.534–43.

Peng, Y. et al., 1997. Cloning , Human Chromosomal Assignment , and Adipose and Hepatic Expression of the CL-6 / INSIG1 Gene. *Genomics*, 43, pp.278–284.

Poli, G., Biasi, F. & Leonarduzzi, G., 2013. Oxysterols in the pathogenesis of major chronic diseases. *Redox biology*, 1(1), pp.125–130.

Prinz, V. & Endres, M., 2011. Statins and stroke: prevention and beyond. *Current opinion in neurology*, 24(1), pp.75–80.

Qin, X. et al., 2008. Peroxisome Proliferator-Activated Receptor-delta Induces Insulin-Induced Gene-1 and Suppresses Hepatic Lipogenesis in Obese Diabetic Mice. *Hepatology*, 48(2), pp.432–441.

Quesney-huneeus, V., Wiley, M.H. & Siperstein, M.D., 1979. Essential role for mevalonate synthesis in DNA replication. *Proceedings of the National Academy of Sciences of the United States of America*, 76(10), pp.5056–5060.

Radhakrishnan, A. et al., 2004. Direct binding of cholesterol to the purified membrane region of SCAP: mechanism for a sterol-sensing domain. *Molecular cell*, 15(2), pp.259–68.

Radhakrishnan, A. et al., 2007a. Sterol-regulated transport of SREBPs from endoplasmic reticulum to Golgi : Oxysterols block transport by binding to Insig. *PNAS*, 104(16), pp.6511–6518.

Radhakrishnan, A. et al., 2007b. Sterol-regulated transport of SREBPs from endoplasmic reticulum to Golgi: oxysterols block transport by binding to Insig. *Proceedings of the National Academy of Sciences of the United States of America*, 104(16), pp.6511–8.

Radhakrishnan, A. et al., 2008. Switch-like control of SREBP-2 transport triggered by small changes in ER cholesterol: a delicate balance. *Cell metabolism*, 8(6), pp.512–21.

Rao, S. et al., 1999. Lovastatin-mediated G1 arrest is through inhibition of the proteasome, independent of hydroxymethyl glutaryl-CoA reductase. *Proceedings of the National Academy of Sciences of the United States of America*, 96(14), pp.7797–802.

Ravid, T. et al., 1999. Impaired Regulation of 3-Hydroxy-3-methylglutaryl-Coenzyme A Reductase Degradation in Lovastatin-resistant Cells. *Journal of Biological Chemistry*, 274(41), pp.29341–29351.

Rawson, R.B. et al., 1999. Failure to Cleave Sterol Regulatory Causes Cholesterol Auxotrophy in Chinese Hamster Ovary Cells with Genetic Absence of SREBP Cleavage-activating Protein Failure to Cleave Sterol Regulatory Element-binding Proteins ( SREBPs ) Causes Cholesterol Auxotroph. *Journal of Biological Chemistry*, 274, pp.28549–28556.

Rayner, K.J. et al., 2010. MiR-33 contributes to the regulation of cholesterol homeostasis. *Science*, 328, pp.1570–3.

Raza, F.S. et al., 2001. Identification of the rat adrenal zona fasciculata/reticularis specific protein, inner zone antigen (IZAg), as the putative membrane progesterone receptor. *European journal of biochemistry / FEBS*, 268(7), pp.2141–7.

Reddy, B.S. et al., 2006. Prevention of azoxymethane-induced colon cancer by combination of low doses of atorvastatin, aspirin, and celecoxib in F 344 rats. *Cancer research*, 66(8), pp.4542–6.

Ren, D. et al., 1996. Mechanism of cholesterol reduction to coprostanol by Eubacterium coprostanoligenes ATCC 51222. *Steroids*, 61(33-40).

Renault, L. et al., 1998. The 1.7A crystal structure of the regulator of chromosome condensation (RCC1) reveals a seven-bladed propeller. *Letters to Nature*, 392(March), pp.97–101.

Repa, J.J. et al., 2002. Regulation of ATP-binding cassette sterol transporters ABCG5 and ABCG8 by the liver X receptors alpha and beta. *The Journal of biological chemistry*, 277(21), pp.18793–800.

Retey, J. et al., 1970. A Probable Intermediate in the Enzymic Reduction of 3-Hydroxy-3-methylglutaryl Coenzyme A. *Eur. J. Biochem.*, 15, pp.72–76.

Rétey, J. et al., 1970. A probable intermediate in the enzymic reduction of 3-Hydroxy-3-methylglutaryl CoenzymeA. *European Journal of Biochemistry*, 15, pp.72–76.

Rilling, H. et al., 1993. Differential Prenylation of Proteins as a Function of Mevalonate Concentration in CHO cells. *Archives of biochemistry and biophysics*, 301(2), pp.210–215.

Rodal, S.K. et al., 1999. Extraction of cholesterol with methyl-beta-cyclodextrin perturbs formation of clathrin-coated endocytic vesicles. *Molecular biology of the cell*, 10(4), pp.961–74.

Rodríguez-Carmona, E. et al., 2010. Isolation of cell-free bacterial inclusion bodies. *Microbial cell factories*, 9(71), pp.1–9.

Rome, S. et al., 2008. Microarray analyses of SREBP-1a and SREBP-1c target genes identify new regulatory pathways in muscle. *Physiological genomics*, 34(3), pp.327–37.

Rozman, D. et al., 1996. Structure and mapping of the human lanosterol 14alpha-demethylase gene (CYP51) encoding the cytochrome P450 involved in cholesterol biosynthesis; comparison of exon/intron organization with other mammalian and fungal CYP genes. *Genomics*, 38(3), pp.371–81.

Rudling, M.J. et al., 1990. Low Density Lipoprotein Receptor Activity in Human Intracranial Tumors and Its Relation to the Cholesterol Requirement. *Cancer Research*, 50, pp.483–487.

Russell, D.W., 2003. The Enzymes, Regulation and Genetics of Bile Acid Synthesis. *Annual Reviews Biochemistry*, 72, pp.137–174.

Rzeski, W. et al., 2009. Betulin elicits anti-cancer effects in tumour primary cultures and cell lines in vitro. *Basic & clinical pharmacology & toxicology*, 105(6), pp.425–32.

Sacks, F. et al., 1996. The Effect Of Pravastatin On Coronary Events After Myocardial Infarction In Patients With Average Cholesterol Levels. *The New England journal of medicine*, 335(14), pp.1001–1009.

Saitou, N. & Nei, M., 1987. The neighbor-joining method: A new method for reconstructing phylogenetic trees. *Molecular Biology and Evolution*, 4, pp.406–425.

Sakai, J., 1995. Hairpin Orientation of Sterol Regulatory Element-binding Protein-2 in Cell Membranes as Determined by Protease Protection. *Journal of Biological Chemistry*, 270(49), pp.29422–29427.

Sakai, J. et al., 1997. Identification of complexes between the COOH-terminal domains of sterol regulatory element-binding proteins (SREBPs) and SREBP

cleavage-activating protein. *The Journal of biological chemistry*, 272(32), pp.20213–21.

Sakai, J. et al., 1996. Sterol-regulated release of SREBP-2 from cell membranes requires two sequential cleavages, one within a transmembrane segment. *Cell*, 85(7), pp.1037–46.

Sakakura, Y. et al., 2001. Sterol Regulatory Element-Binding Proteins Induce an Entire Pathway of Cholesterol Synthesis. *Biochemical and Biophysical Research Communications*, 286, pp.176–183.

Sato, R. et al., 1994. Assignment of the membrane attachment, DNA binding, and transcriptional activation domains of sterol regulatory element-binding protein-1 (SREBP-1). *The Journal of biological chemistry*, 269(25), pp.17267–73.

Sato, R. et al., 1996. Sterol-dependent Transcriptional Regulation of Sterol Regulatory Element-binding Protein-2. *Journal of biological chemistry*, 271(43), pp.26461–26464.

Savage, G.P., Dutta, P.C. & Rodriguez-Estrada, M.T., 2002. Cholesterol oxides: their occurrence and methods to prevent their generation in foods. *Asia Pacific journal of clinical nutrition*, 11(1), pp.72–8.

Schachter, M., 2004. Chemical , pharmacokinetic and pharmacodynamic properties of statins : an update. *Fundamental and Clinical Pharmacology*, 19, pp.117–125.

Schagat, T., Paguio, A. & Kopish, K., 2007. Normalizing Genetic Reporter Assays Approaches and Considerations for Increasing Consistency and Statistical Significance. *Promega Cell Notes*, (17), pp.9–12.

Sebti, S.M. & Hamilton, A.D., 2000. Farnesyltransferase and geranylgeranyltransferase I inhibitors in cancer therapy : important mechanistic and bench to bedside issues. , 9, pp.2767–2782.

Sever, N. et al., 2003a. Accelerated Degradation of HMG CoA Reductase Mediated by Binding of Insig-1 to Its Sterol-Sensing Domain. *Molecular cell*, 11, pp.25–33.

Sever, N. et al., 2003b. Accelerated Degradation of HMG CoA Reductase Mediated by Binding of Insig-1 to Its Sterol-Sensing Domain. *Molecular Cell*, 11, pp.25–33.

Shea-eaton, W.K. et al., 2014. Sterol Regulatory Element Binding Protein-1a Regulation of the Steroidogenic Acute Regulatory Protein Gene *. *Endocrinology*, 142(4), pp.1525–1533.

Sheng, Z. et al., 1995. Independent regulation of sterol regulatory element binding proteins 1 and 2 in the hamster liver. *Proceedings of the National Academy of Sciences of the United States of America*, 92(February), pp.935–938.

Sherf, B.B.A. et al., 1996. Dual-Luciferase TM Reporter Assay : An Advanced Co-Reporter Technology Integrating Firefly and Renilla Luciferase Assays. *Promega Notes*, 2(57).

Shimano, H., Shimomura, I., et al., 1997. Elevated levels of SREBP-2 and cholesterol synthesis in livers of mice homozygous for a targeted disruption of the SREBP-1 gene. *The Journal of clinical investigation*, 100(8), pp.2115–24.

Shimano, H., Horton, J.D., et al., 1997. Isoform 1c of sterol regulatory element binding protein is less active than isoform 1a in livers of transgenic mice and in cultured cells. *The Journal of clinical investigation*, 99(5), pp.846–54.

Shimomura, I. et al., 1997. Differential expression of exons 1a and 1c in mRNAs for sterol regulatory element binding protein-1 in human and mouse organs and cultured cells. *The Journal of clinical investigation*, 99(5), pp.838–45.

Simons, K. & Ikonen, E., 2000. How Cells Handle Cholesterol. *Science*, 290(5497), pp.1721–1726.

Simons, K. & Toomre, D., 2000. Lipid rafts and signal transduction. *Nature reviews. Molecular cell biology*, 1(1), pp.31–9.

Singh, P. et al., 2013. Cholesterol biosynthesis and homeostasis in regulation of the cell cycle. *PloS one*, 8(3), p.e58833.

Singh, S. et al., 2013. Statins are associated with a reduced risk of hepatocellular cancer: a systematic review and meta-analysis. *Gastroenterology*, 144(2), pp.323–32.

Siperstein, M.D., 1972. The Relationship of Cholesterol Biosynthesis to Cancer. *Transactions of the American Clinical and Climatological Association*, pp.156–164.

Siperstein, M.D. & Fagan, V.M., 1964. Deletion of the Cholesterol-negative Feedback System in Liver Tumors. *Cancer Research*, 24, pp.1108–1115.

Sleijfer, S. et al., 2005. The potential of statins as part of anti-cancer treatment. *European Journal of Cancer*, 41, pp.516–522.

Smith, T.F., 2008. Diversity of WD-repeat proteins. *Sub-cellular biochemistry*, 48, pp.20–30.

Smith, T.F. et al., 1999. The WD repeat: a common architecture for diverse functions. *Trends in biochemical sciences*, 24, pp.181–5.

Solaas, K. et al., 2000. Subcellular organization of bile acid amidation in human liver : a key issue in regulating the biosynthesis of bile salts. *Journal of Lipid Research*, 41, pp.1154–1162.

Solomon, K.R. & Freeman, M.R., 2008. Do the cholesterol-lowering properties of statins affect cancer risk ? *Cell*, (March), pp.113–121.

Song, B.-L., Sever, N. & DeBose-Boyd, R. a, 2005. Gp78, a membrane-anchored ubiquitin ligase, associates with Insig-1 and couples sterol-regulated ubiquitination to degradation of HMG CoA reductase. *Molecular cell*, 19(6), pp.829–40.

Song, J. et al., 2004. Letter to the Editor : Hypothetical protein At2g24940 . 1 from Arabidopsis thaliana has a cytochrome b5 like fold. *Journal of Biomolecular NMR*, 30, pp.215–218.

Stancu, C. & Sima, a, 2001. Statins: mechanism of action and effects. *Journal of cellular and molecular medicine*, 5(4), pp.378–87.

Stark, W.W. et al., 1998. Inhibiting geranylgeranylation blocks growth and promotes apoptosis in pulmonary vascular smooth muscle cells. *The American journal of physiology*, 275(1 Pt 1), pp.L55–63.

Stocco, D.M., 2001. StAR protein and the regulation of steroid hormone biosynthesis. *Annual Reviews Physiology*, 63(1), pp.193–213.

Stormshak, F. & Bishop, C. V, 2008. Estrogen and progesterone signaling: genomic and nongenomic actions in domestic ruminants. *Journal of animal science*, 86(2), pp.299–315.

Strömstedt, M., Rozman, D. & Waterman, M.R., 1996. The ubiquitously expressed human CYP51 encodes lanosterol 14 alpha-demethylase, a cytochrome P450 whose expression is regulated by oxysterols. *Archives of biochemistry and biophysics*, 329(1), pp.73–81.

Subtil, A. et al., 1999. Acute cholesterol depletion inhibits clathrin-coated pit budding. *Proceedings of the National Academy of Sciences of the United States of America*, 96(12), pp.6775–80.

Suchanek, M., Radzikowska, A. & Thiele, C., 2005. Photo-leucine and photo-methionine allow identification of protein-protein interactions in living cells. *Nature Methods*, (March), pp.1–7.

Sun, L. et al., 2007. Sterol-regulated transport of SREBPs from endoplasmic reticulum to Golgi : Insig renders sorting signal in Scap inaccessible to COPII proteins. *PNAS*, 104(16), pp.6519–6526.

Sun, L.-P. et al., 2005. Insig required for sterol-mediated inhibition of Scap/SREBP binding to COPII proteins in vitro. *The Journal of biological chemistry*, 280(28), pp.26483–90.

Sun, L.-P. et al., 2007. Sterol-regulated transport of SREBPs from endoplasmic reticulum to Golgi: Insig renders sorting signal in Scap inaccessible to COPII proteins. *Proceedings of the National Academy of Sciences of the United States of America*, 104(16), pp.6519–26.

Swamy, M. V et al., 2006. Chemoprevention of familial adenomatous polyposis by low doses of atorvastatin and celecoxib given individually and in combination to APCMin mice. *Cancer research*, 66(14), pp.7370–7.

Swanson, K.M. & Hohl, R.J., 2006. Anti-cancer therapy: targeting the mevalonate pathway. *Current cancer drug targets*, 6(1), pp.15–37.

Tamura, K. et al., 2007. Molecular Evolutionary Genetics Analysis (MEGA) software version 4.0. *Molecular Biology and Evolution*, 24, pp.1596–1599.

Tang, J.-J. et al., 2011. Inhibition of SREBP by a small molecule, betulin, improves hyperlipidemia and insulin resistance and reduces atherosclerotic plaques. *Cell metabolism*, 13(1), pp.44–56.

Tao, H. et al., 2010. Purifying natively folded proteins from inclusion bodies using sarkosyl, Triton X-100, and CHAPS. *BioTechniques*, 48(1), pp.61–4.

Tatidis, L., Gruber, a & Vitols, S., 1997. Decreased feedback regulation of low density lipoprotein receptor activity by sterols in leukemic cells from patients with acute myelogenous leukemia. *Journal of lipid research*, 38(12), pp.2436–45.

Tatsuno, I. et al., 1997. Geranylgeranylpyrophosphate , a Metabolite of Mevalonate , Regulates the Cell Cycle Progression and DNA Synthesis in Human Lymphocytes. *Biochemical and Biophysical Research Communications*, 382(241), pp.376–382.

Thomas, C. et al., 2008. Targeting bile-acid signalling for metabolic diseases. *Nature reviews. Drug discovery*, 7(8), pp.678–93.

Tobert, J.A., 2003. LOVASTATIN AND BEYOND : The History of the HMG-CoA reductase inhibitors. *Nature Reviews Drug Discovery*, 2(July), pp.517–526.

Vallett, S.M. et al., 1996. A Direct Role for Sterol Regulatory Element Binding Protein in Activation of Reductase Gene A Direct Role for Sterol Regulatory Element Binding Protein in Activation of 3-Hydroxy-3-methylglutaryl Coenzyme A Reductase Gene. *Journal of Biological Chemistry*, 271(21), pp.12247–12253.

Vaughan, C.J., Gotto, A.M. & Basson, C.T., 2000. The Evolving Role of Statins in the Management of Atherosclerosis. *Journal of the American College of Cardiology*, 35(1), pp.1–10.

Verhaegen, M. & Christopoulos, T.K., 2002. Recombinant Gaussia Luciferase. Overexpression, Purification , and Analytical Application of a Bioluminescent Reporter for DNA Hybridization. *Analytical Chemistry*, 74(17), pp.4378–4385.

Voegtli, W.C., Madrona, a Y. & Wilson, D.K., 2003. The structure of Aip1p, a WD repeat protein that regulates Cofilin-mediated actin depolymerization. *The Journal of biological chemistry*, 278(36), pp.34373–9.

Wächtershäuser, a, Akoglu, B. & Stein, J., 2001. HMG-CoA reductase inhibitor mevastatin enhances the growth inhibitory effect of butyrate in the colorectal carcinoma cell line Caco-2. *Carcinogenesis*, 22(7), pp.1061–7.

Wang, J. et al., 2013. Statin use and risk of lung cancer: a meta-analysis of observational studies and randomized controlled trials. *PloS one*, 8(10), p.e77950.

Wang, L.-J. & Song, B.-L., 2012. Niemann-Pick C1-Like 1 and cholesterol uptake. *Biochimica et biophysica acta*, 1821(7), pp.964–72.

Wang, X. et al., 1994. SREBP-1, a membrane-bound transcription factor released by sterol-regulated proteolysis. *Cell*, 77(1), pp.53–62.

Wilkinson, M.J., Laffin, L.J. & Davidson, M.H., 2014. Overcoming toxicity and side-effects of lipid-lowering therapies. *Best Practice & Research Clinical Endocrinology & Metabolism*, pp.1–14.

Wilson, J.D., 1961. The effect of dietary fatty acids on coprostanol excretion bv the rat. *Journal of lipid research*, 2(4), pp.350–356.

Wilson, M.D. & Rudel, L.L., 1994. Review of cholesterol absorption with emphasis on dietary and biliary cholesterol. *Journal of lipid research*, 35(6), pp.943–55.

Wójcicka, G. et al., 2007. Liver X receptors ( LXRs ). Part I : Structure , function , regulation of activity , and role in lipid metabolism Receptory wątrobowe X ( LXR ). Część I : Budowa , funkcja , regulacja aktywności i znaczenie w metabolizmie lipidów. *Postepy Hig Med Dosw. (online)*, 61, pp.736–759.

Wong, W. et al., 2002. HMG-CoA reductase inhibitors and the malignant cell: the statin family of drugs as triggers of tumor-specific apoptosis. *Leukemia*, 16(September 2001), pp.508–519.

Wu, C., Kawasaki, K., et al., 2007. Preparation of Biotinylated Cypridina Luciferase and Its Use in Bioluminescent Enzyme Immunoassay. *Analytical Chemistry*, 79(4), pp.1634–1638.

Wu, C., Suzuki-ogoh, C. & Ohmiya, Y., 2007. Dual-reporter assay using two secreted luciferase genes. *Biotechniques*, 42(3), pp.2–3.

Wurdinger, T. et al., 2008. A secreted luciferase for ex vivo monitoring of in vivo processes. *Nature Methods*, 5(2), pp.171–173.

Xu, J. et al., 1999. Sterol Regulatory Element Binding Protein-1 Expression Is Suppressed by Dietary Polyunsaturated Fatty Acids : A Mechanism For The Coordinate Suppression Of Lipogenic Genes By Polyunsaturated Fats. *Journal of Biological Chemistry*, 274, pp.23577–23583.

Yabe, D., Brown, M.S. & Goldstein, J.L., 2002. Insig-2 , a second endoplasmic reticulum protein that binds SCAP and blocks export of sterol regulatory element-binding proteins. *PNAS*, 99(20), pp.12753–12758.

Yang, J. et al., 1994. Sterol-resistant transcription in CHO cells caused by gene rearrangement that truncates SREBP-2. *Genes and Development*, pp.1910–1919.

Yang, T. et al., 2002. Crucial Step in Cholesterol Homeostasis : Sterols Promote Binding of SCAP to INSIG-1 , a Membrane Protein that Facilitates Retention of SREBPs in ER. *Cell*, 110, pp.489–500.

Yang, T., Goldstein, J.L. & Brown, M.S., 2000. Overexpression of membrane domain of SCAP prevents sterols from inhibiting SCAP.SREBP exit from endoplasmic reticulum. *The Journal of biological chemistry*, 275(38), pp.29881–6.

Ye, J. et al., 2000. ER Stress Induces Cleavage of Membrane-Bound ATF6 by the Same Proteases that Process SREBPs. *Molecular Cell*, 6(6), pp.1355–1364.

Ye, J. & Debose-boyd, R.A., 2011. Regulation of Cholesterol and Fatty Acid Synthesis. *Cold Spring Harbour Perspectives in Biology*, 3, pp.1–13.

Yellaturu, C.R., Deng, X., Cagen, L.M., et al., 2009. Insulin Enhances Post-translational Processing of Nascent SREBP-1c by Promoting Its Phosphorylation and Association with COPII Vesicles. *Journal of Biological Chemistry*, 284(12), pp.7518–7532.

Yellaturu, C.R., Deng, X., Park, E.A., et al., 2009. Insulin Enhances the Biogenesis of Nuclear Sterol Regulatory Element-binding Protein ( SREBP ) -1c by Posttranscriptional Down-regulation of Insig-2A and Its Dissociation from SREBP Cleavage-activating Protein ( SCAP )-SREBP-1c Complex. *Journal of Biological Chemistry*, 284(46), pp.31726–31734.

Yi, X. et al., 2014. Statin use is associated with reduced risk of haematological malignancies: evidence from a meta-analysis. *PloS one*, 9(1), p.e87019.

Yokomizo, A. et al., 2011. Statins reduce the androgen sensitivity and cell proliferation by decreasing the androgen receptor protein in prostate cancer cells. *The Prostate*, 71(3), pp.298–304.

Yokoyama, C. et al., 1993. SREBP-1, a basic-helix-loop-helix-leucine zipper protein that controls transcription of the low density lipoprotein receptor gene. *Cell*, 75(1), pp.187–197.

Yoshikawa, T. et al., 2010. Activated Receptor ( PPAR ) alpha and Liver X Receptor ( LXR ) in Nutritional Regulation of Fatty Acid Metabolism . I . PPARs Suppress Sterol Regulatory Element Binding Protein-1c Promoter through Inhibition of LXR Signaling. *Molecular Endocrinology*, 17(7), pp.1240–1254.

Yu, C.-Y. et al., 2014. HNRNPA1 regulates HMGCR alternative splicing and modulates cellular cholesterol metabolism. *Human molecular genetics*, 23(2), pp.319–32.

Yu, L., 2008. The Strucutre and Function of Niemann-Pick C1-like Protein. *Current opinion in lipidology*, 19(3), pp.263–269.

Zhang, K. et al., 2006. Endoplasmic reticulum stress activates cleavage of CREBH to induce a systemic inflammatory response. *Cell*, 124(3), pp.587–99. A

Zhang, X.-L. et al., 2013. Statin use and risk of kidney cancer: a meta-analysis of observational studies and randomized trials. *British journal of clinical pharmacology*, 77(3), pp.458–65.

Zhang, X. et al., 2013. Statin use and risk of bladder cancer: a meta-analysis. *Cancer causes & control*, 24(4), pp.769–76.

Zhang, Y. et al., 2013. Point mutation in luminal loop 7 of Scap protein blocks interaction with loop 1 and abolishes movement to Golgi. *The Journal of biological chemistry*, 288(20), pp.14059–67.

Zhou, Q. & Liao, J., 2010. Pleiotropic effects of satins: basic research and clinical perspectives. *Circulation Journal*, 74(5), pp.818–826.

Zhuang, L. et al., 2005. Cholesterol targeting alters lipid raft composition and cell survival in prostate cancer cells and xenografts. *Journal of Clinical Investigation*, 115(4), pp.959–968.

Zhuang, L. et al., 2002. Cholesterol-rich Lipid Rafts Mediate Akt-regulated Survival in Prostate Cancer Cells. *Cancer Research*, 62, pp.2227–2231.

# Appendix 1

A single secreted luciferase-based gene reporter assay.
Barriscale, KA, O'Sullivan, SA, McCarthy, TV.
*Analytical Biochemistry* 453 (2014) 44–49